UNIVERSIDADE DE BRASÍLIA
INSTITUTO DE BIOLOGIA
DEPARTAMENTO DE GENÉTICA E MORFOLOGIA
PROGRAMA DE PÓS-GRADUAÇÃO EM BIOLOGIA ANIMAL

DIEGO SOUSA MOURA

O USO DE CARBONO MICRO/NANOESTRUTURADO HÍBRIDO NA REMEDIAÇÃO DE ECOSSISTEMAS AQUÁTICOS CONTAMINADOS POR FÁRMACOS PSICOTRÓPICOS UTILIZANDO O PEIXE-ZEBRA COMO BIOSSENSOR.

Brasília
2019

UNIVERSIDADE DE BRASÍLIA
INSTITUTO DE BIOLOGIA
DEPARTAMENTO DE GENÉTICA E MORFOLOGIA
PROGRAMA DE PÓS-GRADUAÇÃO EM BIOLOGIA ANIMAL

DIEGO SOUSA MOURA

O USO DE CARBONO MICRO/NANOESTRUTURADO HÍBRIDO NA REMEDIAÇÃO DE ECOSSISTEMAS AQUÁTICOS CONTAMINADOS POR FÁRMACOS PSICOTRÓPICOS UTILIZANDO O PEIXE-ZEBRA COMO BIOSSENSOR.

Tese apresentada ao curso de Pós-graduação em Biologia Animal da Universidade de Brasília – UnB como requisito para obtenção do título de doutor.
Orientador: Prof. Dr. Cesar Koppe Grisolia
Co-orientador: Prof. Dr. Rhaul de Oliveira

Brasília
2019

BANCA EXAMINADORA

_____

Prof. Dr. Cesar Koppe Grisolia (Universidade de Brasília – UnB)
Presidente da banca avalidora

_____

Prof. Dr. Sacha Braun Chaves (Universidade de Brasília – UnB)
Membro externo ao programa

_____

Prof. Dra. Aline Pic-Taylor (Universidade de Brasília – UnB)
Membro interno vinculado ao programa PPG BioAni

_____

Prof. Dr. Paulo Cesar de Morais (Universidade Católica de Brasília – UCB)
Membro externo

Brasília
2019

RESUMO

Os tratamentos convencionais aplicados na água têm em geral, boa capacidade de retenção de substâncias, entretanto, muitas moléculas químicas com potencial risco ecológico têm passado diariamente pelos sistemas tradicionais de tratamento. Os Carbonos Micro/Nanoestruturado Híbridos (CMNH) têm ganhado destaque por possuírem propriedades elétricas, mecânicas e térmicas únicas, os quais podem ser aplicados em vários campos industriais. Poucos estudos com essas nanoestruturas focam em remediação de ecossistemas aquáticos contaminados por fármacos psicotrópicos. Objetivo: avaliar a interação de duas nanoestruturas carbonáceas (Carvão Ativado (CA) e CMNH) com um fármaco constantemente detectado em matrizes ambientais, fluoxetina (FLX), utilizando o peixe-zebra como biossensor. As nanoestruturas foram caracterizadas por: Espalhamento Dinâmico de Luz (EDL), Microscopia Eletrônica de Varredura (MEV) com espectroscopia de raios X por dispersão de energia (EDS) acoplado e Espectroscopia Infravermelho com Transformada de Fourier (FTIR). Os testes de embriotoxicidade para avaliação da interação entre fármaco e nanoestruturas foram conduzidos de acordo com a OECD nº236. Analises de Cromatografia Liquida de Alta Resolução (HPLC) e FTIR foram realizadas para avaliar a saturação e o tipo de interação entre os compostos, respectivamente. Os resultados dos testes de embriotoxicidade mostraram que há interação entre a FLX e as nanoestruturas carbonáceas. Observou-se uma diminuição significativa dos efeitos subletais e letalidade na mistura entre os compostos quando comparados ao controle positivo. As análises de HPLC mostraram que o CMNH adsorveram mais moléculas do fármaco quando comparados ao CA, além disso, o FTIR mostrou que a ligação entre as nanoestruturas e o fármaco é do tipo π-π. Conclui-se que o peixe-zebra é um bom biossensor; os CMNH levam vantagem como elementos filtrantes em comparação ao CA; carbonos nanoestruturados são eficientes na remoção de moléculas presentes em ecossistemas aquáticos contaminados por fármacos.

Palavras-chave: *Danio rerio*; descontaminação aquática; nanomateriais; ecotoxicologia, tratamento de água.

ABSTRACT

Conventional treatments applied to water have generally good retention capacity, however, many chemical molecules with potential ecological risk have been daily passed through traditional treatment systems. The Hybrid Micro / Nanostructured Carbon (HMNH) have gained prominence because they have unique electrical, mechanical and thermal properties, which can be applied in various industrial fields. Few studies with these nanostructures focus on remediation of aquatic ecosystems contaminated by psychotropic drugs. Aim: to evaluate the interaction of two carbonaceous nanostructures (Activated Charcoal (AC) and HMNC) with a drug constantly detected in environmental matrices, fluoxetine (FLX), using the zebrafish as biosensor. The nanostructures were characterized by: Dynamic light scattering (DLS), Scanning Electron Microscopy (SEM) with coupled energy dispersive X-ray spectroscopy (EDS) and Fourier Transform Infrared Spectroscopy (FTIR). Embryotoxicity tests to evaluate the interaction between drug and nanostructures were conducted according to OECD nº236. High Resolution Liquid Chromatography (HPLC) and FTIR analyzes were performed to evaluate the saturation and the type of interaction between the compounds, respectively. The results of the embryotoxicity tests showed that there is interaction between the FLX and the carbonaceous nanostructures. There was a significant decrease in sublethal effects and lethality in the mixture between the compounds when compared to the positive control. HPLC analysis showed that CMNH adsorbed more drug molecules when compared to AC, in addition, FTIR showed that the bond between the nanostructures and the drug is of the π-π type. It is concluded that the zebrafish is a good biosensor; HMNC take advantage as filter elements compared to AC; and Nanostructured carbons are effective at removing molecules present in drug-contaminated aquatic ecosystems..

Keywords: *Danio rerio*; aquatic decontamination; nanomaterials; ecotoxicology, water treatment.

Sumário

Lista de figuras

Agradecimentos

Venho por meio desta agradecer a todas as pessoas que me ajudaram de forma indireta e direta para a realização dessa tese de doutorado. Em especial, quero agradecer a Deus e a minha família por todo apoio que tive nas horas difíceis (os obstáculos não foram fáceis de superar). Quero agradecer a Universidade de Brasília – UnB por me proporcionar uma boa formação, com um ótimo corpo docente e excelentes laboratórios. Quero agradecer o Prof. Dr. Cesar Koppe Grisolia por me ensinar a ser um pesquisador e um cidadão comprometido com a sociedade (o tenho como um pai). Quero agradecer a melhor equipe do mundo - laboratório G-Tox (sem vocês não seria possível realizar a coleta dos dados e a escrita dos artigos). Quero agradecer os meus pais, Antônio Filho Moura Guedes e Maria Ivonete de Sousa Moura. Essa vitória não minha é de vocês! Quero agradecer a minha esposa, Thaís Rocha de Miranda, e os meus filhos: Mateus Rocha Moura e Heloísa Rocha Moura (vocês são a razão da minha vida). Quero agradecer o Prof. Dr. Rhaul de Oliveira (você é um ser iluminado – devo muito a você, obrigado por fazer parte da minha vida). Quero agradecer os professores, Dr. Maurício Rosolen e Dra. Elaine Matsubara, muitíssimo obrigado pelas orientações ao longo do período de doutoramento, aprendi e aprendo muito com vocês! Quero agradecer o Prof. Dr. Sebastião e a futura doutora Isis Szlachetka (vocês são fantásticos!). Muito obrigado por abrirem as portas do laboratório para realizarmos as caracterizações das nanoestruturas carbonáceas! Quero agradecer os melhores amigos que a vida acadêmica pôde me dar (Marcia Oliveira, Nicholas Serafim e o professor Dr. André Villacis)! Quero agradecer a excelente parceria do Bryan, Thaty e Larissa (continuem sempre com essa garra – vocês são ótimos pesquisadores). Quero agradecer a população brasileira por ter investido na minha formação (acredito que dei o

retorno que se espera de um doutorando – publicando artigos e ajudando jovens com projetos de iniciação científica). Quero agradecer a CAPES, CNPq, FAP-DF, FINATEC pelo fomento a pesquisa.

Lista de abreviações

AC – *Activated carbon* ou no português **CA -** carvão ativado

BET - Brunauer, Emmett, Teller

BPP – Bupropiona

CAT – Catalase

CBZ - Carbamazepina

CNTs – *Carbon Nanotubes* (nanotubos de carbono)

CVD - *Chemical Vapor Deposition* (deposição de vapor químico)

DLS - *Dynamic Light Scattering* (Espalhamento dinâmico de luz)

EDS - Energy Dispersive X-ray Spectroscopy (espectroscopia de raios X por dispersão de energia)

ETE – Estações de tratamento de esgoto

FET – *Fish Embryo Toxicity FET test* (teste de embriotoxicidade)

FLX – Fluoxetina

FTIR - *Fourier Transform Infrared Spectroscopy* (Espectroscopia de Infravermelho por Transformada de Fourier)

GST - Glutationa S-Transferase

HMNC – *Hibrid MicroNanoestrutured Carbon* ou no português **CMNH** - carbono micronanoestruturado híbrido.

HPLC - *High Performance Liquid Chromatography* (Cromatografia Liquida de Alta Performance)

LDH – Lactato Desidrogenase

MEV – Microscopia Eletrônica de Varredura

Estrutura da tese

Esta tese de doutorado está dividida em 3 capítulos, (1) potencial risco ecológico dos fármacos no ambiente aquático e formas de remoção dessas substâncias químicas utilizando nanoestruturas carbonáceas, (2) Resultados em formato de artigo científico (remediação aquática); (3) conclusão e por fim anexos e apêndices (artigos publicados em colaboração).

Mais detalhadamente o texto pode ser dividido da seguinte forma:

Capítulo 01 – Contextualização e objetivos da tese: nesse capítulo é apresentada a problemática dos poluentes emergentes (fármacos) além da necessidade do desenvolvimento de tecnologias eficientes no controle ambiental. São também apresentados os objetivos do presente projeto.

Capítulo 02 – Resultados: nesse capítulo é apresentado o artigo "*CNTs coated charcoal as a hybrid composite material: adsorption of Fluoxetine probed by zebrafish embryos and its potential for environmental remediation*", que foi publicado na revista "*Chemosphere*". Fator de impacto: 5.108 (2018), Qualis A1 (Capes).

Capítulo 03 – Conclusão: Nesse capítulo é apresentada a conclusão da tese de doutorado.

Anexos e apêndices: Nesse capítulo é apresentada a declaração da comissão de ética no uso animal do instituto de ciências biológicas da universidade de Brasília – UnB, protocolo nº100226/2014 e artigos publicados em colaboração ao longo do período de doutoramento. Os artigos científicos foram publicados nas seguintes revistas indexadas: *Comparative Biochemistry and Physiology, Part C* (fator de impacto: 2.697);

Ecotoxicology and Environmental Safety (fator de impacto: 4.527) e *Chemosphere* (fator de impacto: 5.108). *Journal of Environmental Chemical Engineering*, CiteScore: 4.09 (2018); *Journal of Ethnopharmacology*, fator de impacto: 3.414 (2018) e *Acta Limnologica Brasiliensia*, fator de impacto: 0.18 (2018).

Capítulo 01 – Introdução: contextualização e objetivos da tese

Tese de Doutorado

2019

---

1. Introdução

1.1. Contextualização

A água doce de boa qualidade é de extrema importância para a manutenção das mais variadas populações e sustentabilidade dos ciclos do planeta. Atualmente devido ao ritmo acelerado da industrialização e aumento populacional, a contaminação dos recursos hídricos tem ocorrido globalmente. Vale ressaltar que a demanda por água nos últimos anos aumentou significativamente nos setores: agrícola, industrial e doméstico, consumindo: 70%, 22% e 8%, da água doce disponível, respectivamente, o que consequentemente resulta na geração de grandes quantidades de águas residuais (Helmer *et al*. 1997; Lehr and DeMarre 1980; Nemerrow 1978) podendo conter vários tipos poluentes emergentes.

Bogardi *et al*., (2012) alertam que garantir a qualidade dos recursos hídricos é um dos maiores desafios do milênio para a humanidade. Nos últimos anos, os produtos farmacêuticos têm recebido crescente atenção por serem na maioria das vezes químicos

bioativos em matrizes ambientais (Kümmerer, *2009*). Baseado em amplas revisões sobre o destino final dos fármacos, na Figura 1 é apresentada algumas importantes rotas de contaminação aquática (Kümmerer 2009; Monteiro and Boxall 2010; Pauwels and Verstraete 2006).

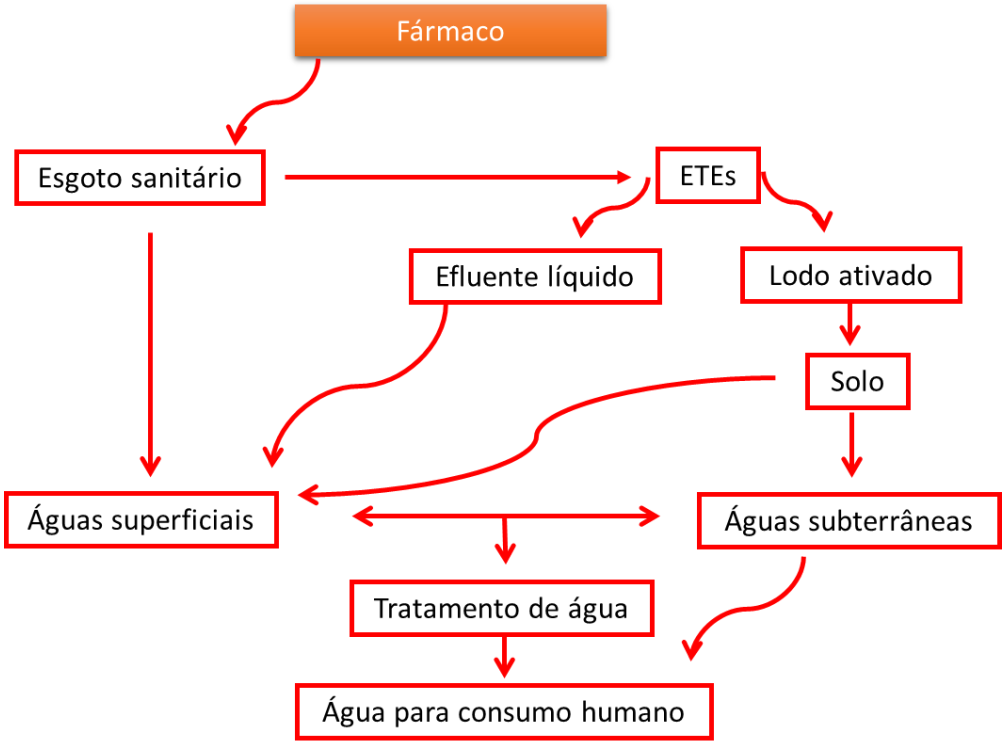

Figura 1. Principais rotas de contaminação de ecossistemas aquáticos por fármacos. ETEs – Estações de tratamento de esgoto.

Estes compostos e seus metabólitos bioativos são continuamente introduzidos no ambiente aquático, onde são detectados em concentrações residuais (gama entre ng/L^{-1} – µg/L^{-1}) (Tim Aus *et al*., 2015), podendo tornar-se pseudo-persistentes. Normalmente esse tipo de poluição surge de variadas formas, como: (1) emissão dos locais de produção (exemplo: indústria); (2) do descarte direto de medicamentos em excesso (residências domésticas e hospitais); (3) excreção via urina ou fezes após a administração de

medicamentos (humanos ou animais); (4) tratamentos de água (exemplo: piscicultura); (5) entre outros.

A função principal de uma Estação de Tratamento de Esgoto (ETE) é reduzir a carga orgânica lançada no corpo d'água receptor, entretanto, moléculas inalteradas ou metabólitos de produtos farmacêuticos tem persistido devido à sua eliminação incompleta (permanecendo entre 60-90% dessas substâncias mesmo após as ações de: biodegradação, desconjugação, adsorção e fotodegradação) (Jones, Lester, and Voulvoulis 2005).

Embora que para muitos fármacos os efeitos agudos e crônicos sobre organismos não-alvos ainda estejam pouco elucidados, alguns trabalhos têm abordado que essas moléculas liberadas no meio ambiente podem trazer toxicidade para organismos de qualquer nível trófico. Exemplo: hormônios sintéticos, como o etinil estradiol, causam feminização em populações de peixes (Jobling et al. 1998), antibióticos desencadeiam o aumento de genes de resistência em bactérias (Allen *et al*. 2010). Antinflamatórios, como o diclofenaco, causam hepatotoxicidade em aves e peixes (Triebskorn et al. 2004). Antihelmintos, como as ivermectinas, são extremamente tóxicas para artrópodes edáficos (Sanderson *et al*., 2007). Fármacos psicotrópicos, como o oxazepam, podem modular o comportamento de peixes, interferindo em seu nado, alimentação, fuga de predadores e reprodução (Brodin *et al*. 2013).

Ainda no contexto dos fármacos psicotrópicos, vale destacar que na presente tese, nos anexos e apêndices, é possível visualizar alguns artigos publicados em revistas indexadas ao longo do período de doutoramento, como exemplo o artigo intitulado: *Exposure to low concentration of fluoxetine affects development, behaviour and*

acetylcholinesterase activity of zebrafish embryos. No referido, Farias *et al*., (2018) avaliaram os efeitos toxicológicos da fluoxetina (FLX) (antidepressivo que atua inibindo a recaptação de serotonina / parâmetros: sobrevivência, desenvolvimento, comportamento e marcadores bioquímicos neuronais) utilizando embriões de peixe-zebra como organismo modelo. Os autores observaram efeitos significativos sobre a atividade locomotora (alterações comportamentais) e atividade da acetilcolinesterase (AChE) (alterações bioquímicas), ≥ 0,88 e 6 µg / L, respectivamente, tais concentrações de efeito estão próximas das encontradas em águas superficiais, assim, os autores sugerem que a FLX é neurotóxica para os estágios iniciais de vida do peixe-zebra.

Seguindo a mesma linha de desenho experimental, o artigo intitulado: *Exposure to dilute concentrations of bupropion affects zebrafish early life stages*. Franco *et al*., (2019), ao estudarem os efeitos toxicológicos da bupropiona (BPP) (antidepressivo que atua inibindo da recaptação de noradrenalina e dopamina) observaram que concentrações a partir de 7300 ug / L provocaram alterações no equilíbrio dos embriões eclodidos (técnica utilizada: *Fish Embryo Toxicity* FET *test*). A análise comportamental (equipamento: Zebrabox) mostrou que a bupropiona afetou o comportamento locomotor do peixe-zebra, diminuindo a atividade dos organismos expostos a concentração de 0,6 ug / L, aumentando a atividade em 8,8 e 158 ug / L e diminuindo a atividade em 50000 ug / L. A análise bioquímica mostrou um aumento da atividade da AChE em 158 e 2812 ug / L, um aumento na atividade da Glutationa S-Transferase (GST) nas concentrações mais altas, alteração na atividade da Catalase (CAT) e aumento do Lactato desidrogenase (LDH) em 0,6; 2812 e 50000 ug / L, assim os autores puderam concluir que a BPP afeta

os estágios iniciais de vida do peixe-zebra em concentrações que podem ser encontradas nas matrizes ambientais.

Santos *et al*., (2018), no artigo intitulado: *Chronic effects of carbamazepine on zebrafish: Behavioral, reproductive and biochemical endpoints* ao estudarem os efeitos toxicológicos crônicos da carbamazepina (CBZ) utilizando organismos adultos de peixe-zebra como modelo biológico (parâmetros analisados: comportamento alimentar, taxa de crescimento, número de ovos fecundados / viabilidade, alterações histológicas nas gônadas femininas e biomarcadores associados às defesas antioxidantes (atividades da - CAT e GST); neurotransmissor (atividade da AChE) e metabolismo (LDH)), observaram que a viabilidade dos ovos foi significativamente prejudicada; houve alterações nos estágios foliculares das gônadas femininas; houve alterações bioquímicas nas referidas enzimas em concentrações ambientalmente relevantes. Os autores destacaram graves preocupações com os riscos colocados pelos resíduos de CBZ para as populações de peixes.

Baseado em todo o contexto de poluição aquática e ao entender a água como um recurso cada vez mais escasso e essencial para o bem-estar humano e do meio ambiente, fazem-se necessários métodos mais eficientes no controle da poluição de águas residuais, superficiais e subterrâneas.

1.1.1. Nanomateriais como adsorventes para tratamento de água

Atualmente existem várias técnicas destinadas ao tratamento de águas residuais, como: extração por solvente, micro e ultrafiltração, sedimentação e separação por gravidade, flotação, precipitação, coagulação, oxidação, evaporação, destilação, osmose

reversa, adsorção, troca iônica, eletrodiálise, eletrólise, etc. Dentre as técnicas mencionadas vale destacar a "adsorção", pois pode remover uma ampla gama de poluentes orgânicos, inorgânicos e biológicos, solúveis e insolúveis; pode recuperar fontes para fins de água potável; é de fácil operação e há disponibilidade de uma ampla gama de agentes adsorventes. Entretanto, apesar dos adsorventes possuírem várias vantagens os mesmos possuem certas limitações, como: não conseguir um bom *status* a níveis comerciais; um único adsorvente não é capaz de remover todos os tipos de poluentes (normalmente um adsorvente é selecionado baseado nos tipos de poluentes que ele pode adsorver) (Huang *et al*., 2011), entre outras.

Sanady. M *et al*., (1995) em um estudo comparativo de tecnologias de tratamento de água definiram o seguinte ranking de custo-benefício: (1) adsorção; (2) evaporação; (3) aeróbica; (4) anaeróbica; (5) troca iônica; (6) eletrodiálise; (7) micro e ultrafiltração; (8) osmose reversa; (9) precipitação; (10) destilação; (11) oxidação; e por fim (12) extração por solvente. Baseado nesses resultados a "adsorção" poderá ser a principal técnica de tratamento de água em um futuro próximo.

Para qualquer processo de adsorção, um adsorvente com grande área superficial, volume de poros e funcionalidades adequadas é a chave para o sucesso. Atualmente, há o desenvolvimento de muitos materiais porosos destinados a remoção de poluentes do ar, água e solo (exemplos: carvão ativado, zeólitos, óxidos mesoporosos, polímeros, entre outros) (Ngah, Teong, and Hanafiah 2011; Wang and Peng 2010; Yi 2004). Dentre esses vários desenvolvimentos, os adsorventes à base de carbono, incluindo: carvão ativado, nanotubos de carbono, fulerenos e grafeno, tem se destacado por apresentarem alta

capacidade de adsorção e estabilidade térmica (G. P. Rao, Lu, and Su 2007; Ren et al. 2011; Seymour et al. 2012).

Atualmente o carvão ativado é o principal adsorvente mais utilizado no mundo para purificação de água e ar em escala industrial (Yu et al., 2016). Para uma melhor compreensão da utilização do carvão ativado a Figura 2 mostra um desenho esquemático de sua estrutura morfológica.

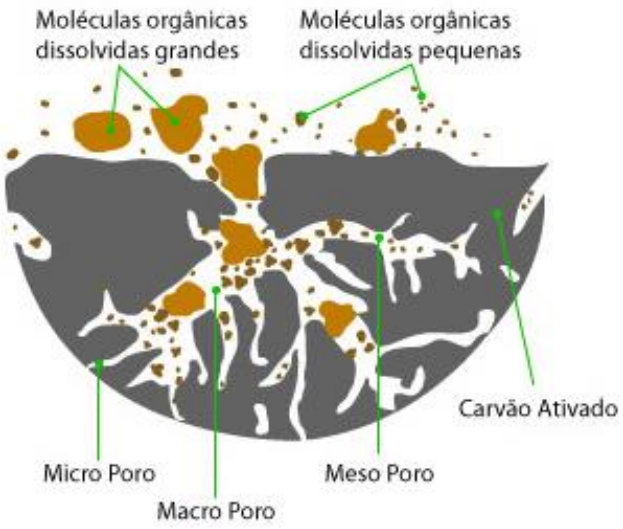

Figura 2. Desenho esquemático de um carvão ativado evidenciando sua estrutura morfológica. *Fonte: Google imagens*.

O carvão ativado é constituído por três tipos de volume de poros: (1) macroporos, (2) mesoporos e (3) microporos. A função dos **macroporos** é facilitar a entrada de moléculas químicas no carvão ativado; os **mesoporos** tem como função o "transporte" e os **microporos** tem como função a adsorção de substâncias. Em resumo, as moléculas são difundidas nos poros do carvão ativado, que aderem às superfícies internas. Vale ressaltar que nem todas as moléculas são adsorvidas igualmente na área superficial do carvão ativado (existem graus de afinidade por diferentes substâncias químicas -

exemplo: maior interação por impurezas que tenham carbono como base e menor afinidade por compostos como o sódio, nitratos, etc.). Ademais, moléculas de menor peso molecular se difundem mais profundamente (resultando em um maior domínio de área superficial (havendo mais ligações químicas) quando comparadas a moléculas de maior peso molecular) (Yu et al., 2016).

A produção de carvão ativado pode ser dividida em três etapas: (1) pré-tratamento de matérias-primas (ex: madeira, carvão, ossos, caroços de frutas, etc); (2) carbonização em baixa temperatura e (3) ativação. Existem dois tipos de ativação: **ativação física:** que é a ativação da matéria-prima após a carbonização, temperatura entre 800 - 1000 °C - normalmente em ambiente anaeróbico (Laine., Calafat, and M. 1989; Wigmans 1989); e **ativação química:** que é a adição de produtos químicos às matérias-primas para posterior aquecimento sob a proteção de um gás inerte; os processos de carbonização e ativação são realizados simultaneamente (Mohammad-Khah e Ansari, 2009).

Atualmente a ativação química tornou-se o principal método para produção de carvão ativado de alto desempenho devido ao curto tempo de ativação, reação de ativação facilmente controlável e grande área de superfície específica, quando comparadas às técnicas de ativação física (Ahmadpour and Do, 1996).

Existem diferentes tipos de carvão ativado de acordo com suas propriedades físico-químicas (por exemplo: tamanho de partícula e distribuição de tamanho de poros, área de superfície, densidade aparente) e a capacidade de adsorção depende dessas propriedades. A distribuição dos grupos funcionais na superfície do carvão ativado é responsável pelas interações com os contaminantes. O mecanismo de adsorção é

controlado por interações do tipo Van der Walls com contaminantes apolares e para contaminantes polares a interação é do tipo eletrostática entre a superfície de carvão ativado.

Apesar do carvão ativado possuir inúmeras vantagens o valor elevado do custo para sua manufatura, dificuldades de reativação, necessidade de um maior tempo de contato para obter uma boa adsorção, entre outros (El Gamal et al. 2018; Mccreary and Snoeyink 2014; Yoon et al. 2008) tem incitado pesquisadores a criarem novas formas de desenvolvimento. A nanotecnologia é uma ciência multidisciplinar que nos últimos anos tem desenvolvido muitas nanoestruturas carbonáceas (incluindo o carvão ativado) e tem proporcionado novas alternativas para o tratamento de águas residuais (Jusoh, Su, and Noor 2007; Tratnyek and Johnson 2006; Vaseashta et al. 2007; Zhang 2003). Um exemplo tem sido os nanotubos de carbono que possuem grande área superficial ativa; bom controle em relação ao volume e distribuição de tamanho de poros; têm boa capacidade de adsorção e alta eficiência de adsorção em comparação com carvão ativado granular convencional que possui algumas limitações.

1.1.1.1. Nanotubos de carbono

Desde a descoberta dos nanotubos de carbono e suas variadas aplicações, como exemplo: aplicação em energia (Kolpak 2011), adsorção (Calvaresi and Zerbetto, 2014), distribuição de fármacos (Yang et al., 2009), tem sido um grande desafio projetar esses adsorventes a um custo menor pois a produção em larga escala ainda é inviável economicamente.

Os nanotubos de carbono são alótropos de carbono e estes podem apresentar diversas formas estruturais do elemento carbono (Figura 3). Basicamente os nanotubos de carbono apresentam a forma cilíndrica (formato de tubo). De acordo com Endo *et al*., (2005), os nanotubos de carbono possuem três formas: (1) nanotubos de carbono de parede única (com diâmetro típico do tubo de aproximadamente 0,4 - 2nm (Ajayan, 1999; Hong et al., 2005)); (2) de parede dupla e (3) multi-paredes (estes consistem em cilindros concêntricos com espaçamento entre camadas de 0,34 nm com um diâmetro de 2 a 25 nm (Ajayan, 1999)). Vale destacar que as definições dos formatos dos nanotubos são determinadas pelo número de camadas grafíticas da estrutura cilíndrica (Yu et al 2016). Ademais, além do diâmetro e comprimento (que frequentemente excede a ordem nanométrica), a quiralidade (ângulo entre os hexágonos e o eixo do nanotubo) é outro parâmetro chave na organização dos nanotubos de carbono (Ajayan, 1999).

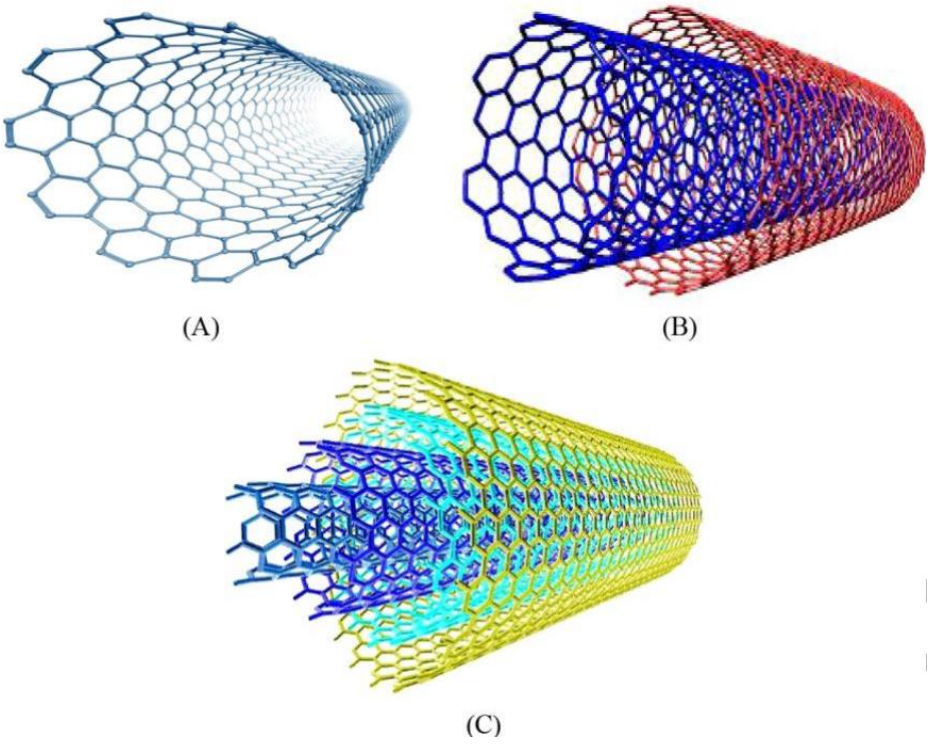

Figura 3. Diferenças morfológicas dos nanotubos de carbono. (A) - nanotubos de carbono de parede única. (B) - nanotubos de carbono de parede dupla. (C) - nanotubos de carbono multi-paredes. Fonte: Rafique *et al*., (2016).

A literatura tem mostrado que a capacidade de adsorção de nanotubos de carbono depende dos grupos funcionais de sua superfície e da natureza do adsorbato. Por exemplo: a acidez superficial em nanotubos (por grupos: carboxílico, lactônico e fenólico) favorece a adsorção de compostos químicos polares – interações químicas (X. Wang, Lu, and Xing 2008). Por outro lado, a não-funcionalização superficial em nanotubos favorece uma maior afinidade por compostos apolares (exemplo: hidrocarbonetos aromáticos policíclicos) – interações físicas (Stafiej and Pyrzynska 2008). Além disso, a capacidade de adsorção de nanotubos de carbono é efetiva em uma ampla faixa de pH (Santhosh et al. 2016).

Embora a manufatura dos nanotubos de carbono ainda seja mais cara em comparação com o carvão ativado convencional, sua adsorção e ciclos de dessorção são mais eficientes. Atualmente, existem três principais métodos de produção de nanotubos de carbono (Andrews et al. 2002; Charlier 2007; Dai 2002; Thostenson, Ren, and Chou 2001), que são: (1) **descarga por arco elétrico**, (2) **ablação a laser** (nessas duas técnicas a sintetize é através da vaporização de amostras de grafite) e (3) **deposição de vapor químico** (o vapor contendo carbono é passado sobre o catalisador (nanopartículas metálicas, como: níquel, cobalto, ferro) mantido em temperatura constante em um forno).

Vale ressaltar que dependendo da forma de síntese os nanotubos de carbono podem apresentar algum grau de toxicidade a organismos não-alvos devido à presença de catalisadores metálicos, enquanto os nanotubos de carbono funcionalizados quimicamente até o momento não demonstraram toxicidade (Chen and Wang 2006).

Muitos estudos têm mostrado o quão valem os esforços para o desenvolvimento de nanotubos. Por exemplo: Ji *et al*. (2010) em um estudo analítico avaliando a interação entre nanotubos de carbono a compostos monoaromáticos (fenol e nitrobenzeno) e antibióticos (sulfametoxazol, tetraciclina e tilosina) em soluções aquosas observaram que após a modificação dos nanotubos de parede única e multi-paredes com KOH a área de superfície específica foi aumentada de 410,7 m^2/g para 652,8 m^2/g e de 157,3 m^2/g para 422,6 m^2/g, respetivamente. E consequentemente, a adsorção dos solutos do teste foi aumentada de 2-3 vezes em nanotubos de parede única e de 3-8 vezes em multi-paredes. Além disso, os nanotubos de carbono ativados mostraram reversibilidade de adsorção aprimorada para os compostos monoaromáticos selecionados, em comparação com os homólogos intocados.

Cho, Huang, and Schwab (2011) ao estudarem as interações entre ibuprofeno e triclosan sobre nanotubos de carbono relataram que a adsorção dos referidos compostos em nanotubos de carbono de parede única foi mais forte quando comparados aos nanotubos de carbono multi-paredes devido à maior área superficial específica. Além disso, os autores baseados nos resultados da isoterma de adsorção confirmaram que a química da superfície dos nanotubos, as propriedades químicas dos adsorbatos e a química da solução aquosa (pH, força iônica, ácido fúlvico) desempenham papel importante na adsorção.

Lu and Chiu (2006) ao avaliarem a adsorção de zinco (II) com nanotubos de carbono purificados com soluções de hipoclorito de sódio observaram que as propriedades dos nanotubos (como: pureza, estrutura e natureza da superfície) foram melhoradas. Os autores observaram que a purificação removeu os catalisadores metálicos e carbono amorfo dos nanotubos tornando as nanoestruturas mais hidrofílicas e adequados para a adsorção de Zn^{2+}. Os potenciais zeta dos nanotubos de carbono purificados foram mais negativos que os de nanotubos sem purificação devido à presença de grupos funcionais negativos na superfície. Um estudo comparativo na adsorção de Zn^{2+} entre nanotubos de carbono de parede única, multi-paredes e carvão ativado comercial em pó também foi realizado. As capacidades máximas de adsorção do Zn^{2+} calculadas pelo modelo de *Langmuir*, foram: 43,66; 32,68 e 13,04 mg/g^{-1}, respectivamente, em uma faixa de concentração inicial de 10-80 mg/l^{-1} de Zn^{2+}. Os autores observaram que a cinética de adsorção de Zn^{2+} nos nanotubos de carbono foi relativamente rápida (60 min). Por fim, os autores baseados no curto tempo de contato necessário para atingir o equilíbrio, bem como a alta capacidade de adsorção, sugerem

que os nanotubos de carbono de parede única e multi-paredes possuem aplicações altamente potenciais para a remoção de Zn^{2+} da água.

Sotelo *et al*., (2012) ao avaliarem as interações do atenolol, cafeína, diclofenaco, isoproturona e efluente de estação de tratamento municipal com três materiais carbonáceos: (1) carvão ativado, (2) nanotubos de carbono multi-paredes e (3) nanofibras de carbono, chegaram a importantes conclusões, como: todas as nanoestruturas carbonáceas mostraram-se eficientes na remoção dos referidos fármacos; a capacidade de adsorção dessas nanoestruturas em soluções individuais é maior quando comparado ao desempenho das mesmas em águas residuais reais, sugerindo que o material orgânico natural de fundo tem um impacto no processo de adsorção; a influência da temperatura no processo de adsorção é mais apreciável em carvão ativado do que em nanotubos de carbono multi-paredes ou nanofibras de carbono; os nanotubos de carbono multi-paredes e nanofibras de carbono podem ser adsorventes alternativos no tratamento de água entretanto, os autores ressaltam que trabalhos adicionais devem investigar o desempenho e custo operacional desses materiais.

Chatterjee, Lee, and Wooa (2010) ao avaliarem a eficiência de adsorção de esferas de hidrogel de quitosana com nanotubos de carbono multi-paredes impregnados em sua superfície para remoção do “corante vermelho congo” observaram que a referida modificação tornou as esferas mais densas e porosas. A adsorção do corante nas esferas modificadas foi altamente dependente do pH. A capacidade máxima de adsorção foi de 450,4 mg/g^{-1}. Os valores obtidos a partir de modelos cinéticos de primeira e segunda ordem e o modelo de difusão intra-partícula mostraram que a taxa de transferência de massa foi bastante aumentada pela adição dos nanotubos.

Não há dúvidas de que os nanotubos de carbono possuem grande potencial como adsorventes superiores para remoção de várias substâncias químicas em soluções aquosas e diante o contexto de poluição aquática a prioridade atual é desenvolve-los para aumentar ainda mais sua capacidade de adsorção e eficiência de remoção para realizar o controle efetivo de poluentes ambientais a um custo relativamente baixo.

1.1.1.2. Grafeno e derivados

O grafeno, considerado o material mais fino do universo, pode ser visto como a unidade de construção de importantes alótropos de carbono, como: **grafite** que é um empilhamento de camadas de grafeno, **nanotubos de carbono** que é uma laminação de uma ou mais camadas de grafeno, **fulerenos** que é um envolvimento de uma camada de grafeno, entre outros (Geim and Novoselov., 2007).

O grafeno é composto de uma única camada de átomos de carbono (hibridização sp^2) dispostos em uma estrutura hexagonal (Novoselov et al., 2004) ligados entre si por meio de ligações co0m outros três átomos de carbono vizinhos (ligações d covalentes) proporcionando alta estabilidade mecânica (Zhu et al., 2010). Além disso, o grafeno também possui grandes valores de mobilidade intrínseca de aproximadamente 200.000 $cm^2\ V^{-1}\ s^{-1}$, área superficial teórica de 2630 m^2/g^{-1}, transmitância óptica de aproximadamente 97,7% para uma única folha de grafeno, módulo de Young de aproximadamente 1 TPa e condutividade de aproximadamente $5000Wm^{-1}$ (que é resultante do tipo de hibridização dos átomos de carbono presentes em sua estrutura) (Carbon et al. 2010; Neto 2009; C. N. R. Rao et al. 2009; Zhu et al. 2010). Para uma melhor compreensão a figura 4 mostra a estrutura morfológica de uma folha de grafeno.

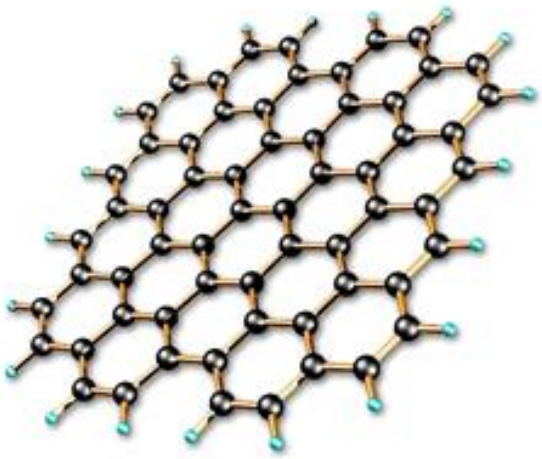

Figura 4. Estrutura morfológica do grafeno. *Fonte: Google imagens*.

Baseado nessas excelentes propriedades muitas pesquisas tem focado no uso desse alótropo de carbono em muitos campos da tecnologia, incluindo: eletrocatálise, detecção de DNA, microscopia eletrônica de alta resolução, eletrônica e eletrônica flexível, bio-cultura para dessalinização (Kemp et al., 2013) e tem sido considerada uma alternativa frente aos nanotubos de carbono por possuírem dois planos basais disponíveis para adsorção de variados tipos de poluentes (C. N. R. Rao et al. 2009; Sitko, Zawisza, and Malicka 2013; J. Zhao et al. 2014), diferentemente dos nanotubos de carbono que suas paredes internas não são acessíveis pelos adsorbatos (Sitko, Zawisza, and Malicka 2013).

Atualmente, os quatro principais métodos de obtenção de grafeno, são: (1) esfoliação mecânica, (2) esfoliação química, (3) deposição de vapor químico e (4) crescimento epitaxial (Neto 2009; C. N. R. Rao et al. 2009; Zhu et al. 2010; Kim et al., 2009; Li et al., 2009). Vale destacar que a esfoliação mecânica é considerada a técnica de melhor custo/benefício dentre as mencionadas devido ao baixo custo relativo, elevado

rendimento, possibilidade de obtenção de grafenos multi-camadas e fácil processabilidade (Santhosh et al. 2016).

Apesar das grandes aplicações em variados campos tecnológicos o grafeno ainda é considerado um material caro para produção em larga escala. Nesse contexto, as aplicações baseadas em óxido de grafeno oferecem possibilidades mais realistas em comparação com o grafeno puro devido ao menor custo de manufatura. O óxido de grafeno é um grupo funcional de grafeno que contém oxigênio e apresenta uma alta densidade de grupos funcionais (como: carboxila, hidroxila, carbonila e epóxi) em sua rede de carbono (Perreault, Fariaa, and Elimelech 2015); conferindo-lhes um caráter hidrofílico (suspensões estáveis em soluções aquosas) e alta reatividade (G. Zhao et al. 2011). Um ponto relevante ao compararmos o óxido de grafeno aos nanotubos de carbono é que o primeiro pode ser facilmente sintetizado através da esfoliação química do grafite, sem o uso de aparelhos complexos ou catalisadores metálicos, ou seja, há obtenção materiais isentos de resíduos de catalisadores e sem necessidade de muitos passos de purificação.

Muitos estudos têm demonstrado os potenciais de aplicações do grafeno e seus derivados como importantes adsorventes. Por exemplo: Cai and Larese-Casanova (2014) compararam o poder de adsorção de três importantes carbonáceos (1) óxido de grafeno (2) nanotubos de carbono multi-paredes e (3) carvão ativado granulado. A fármaco psicotrópico utilizado como adsorbato foi a carbamazepina. Os autores observaram que a cinética de adsorção do composto químico em óxido de grafeno foi rápida e reversível com a lavagem em álcool, o que é consistente com interações p – p. O óxido de grafeno

de maior área superficial (771 m^2/g^{-1}) superou o carvão ativado granulado e os nanotubos de carbono multi-paredes na adsorção da carbamazepina.

Huang *et al*., (2011) em um estudo comparando o desempenho de adsorção de Pb (II) por grafeno e óxido de grafeno demonstraram a importância dos grupos funcionais constituintes do óxido de grafeno. Os autores observaram que o alto teor de oxigênio disponíveis para interagirem com os íons metálicos fazia com que o óxido de grafeno fosse mais eficiente que o grafeno cristalino evidenciando a aplicabilidade dessas nanoestruturas.

Lateefa A. Al-Khateeb (2014) ao avaliarem a remoção de aspirina, paracetamol e cafeína em solução aquosa por nanoplaquetas de grafeno de área superficial de 635,2 m^2/g^{-1} observaram que ao modularem o processo de adsorção em diferentes fatores ambientais (como: pH, temperatura, dureza da água, etc) observaram que as capacidades de adsorção para aspirina, cafeína e paracetamol, foram: 12,98 mg/g-1; 19,72 mg/g-1 e 18,07 mg/g-1, respectivamente. Os autores concluíram que a maioria dos compostos farmacêuticos poderiam ser removidos usando apenas 10 mg, com um tempo de 10 min, a temperatura de 296 K em soluções com pH de 8,0. Assim, as nanoplaquetas de grafeno podem ser usadas para remoção de aspirina, paracetamol e cafeína da água da torneira, água residual e água do mar com alta eficiência.

Baseado nesses estudos e nos principais desafios encontrados para produção em larga escala dessa tecnologia de remoção de contaminantes aquáticos. É possível em um futuro próximo a utilização das mesmas em refis de filtros domésticos, auxilio em estações de tratamento de água potável, composição de equipamentos hospitalares, etc.

1.1.1.3. Uso do peixe-zebra como organismo modelo

O peixe-zebra (Figura 5) é um pequeno teleósteo, com tamanho médio de: 3-4 cm, de água doce da família Cyprinidae, natural da Ásia (Tailândia, Índia, Paquistão, Bangladesh, Nepal e Myanmar). Esta espécie é onívora (alimenta-se principalmente de fitoplâncton e microinvertebrados). São ovíparos e possui um tempo médio de vida entre 2-5 anos (USEPA 2015; Rico 2007; OECD 2013).

Figura 5. *Danio rerio* (popularmente: peixe-zebra ou paulistinha). Fonte: google imagens.

Atualmente o peixe-zebra é um organismo consolidado como modelo experimental em diversas áreas da ciência, como: genética, biologia do desenvolvimento, comportamento, toxicologia e neurociências (Vascotto et al. 1997; Nishimura et al. 2015). Dentre as vantagens em utiliza-lo, destacam-se: (i) a facilidade no cultivo de todos os estágios de vida em laboratório; (ii) baixo custo de cultivo (iii) alta performance reprodutiva com desova abundante; (iv) os embriões são translúcidos, permitindo avaliação do desenvolvimento embrionário e teratologias; (v) tamanho pequeno, que permite o cultivo em espaços reduzidos, (vi) seu genoma já foi sequenciado permitindo o desenvolvimento de estudos filogenéticos (Broughton et al. 2001) e estudos genéticos

comparados com seres humanos (Dooley 2000) (vii) estudos sobre o desenvolvimento de diversos sistemas, órgãos e patologias relacionadas são realizados utilizando adultos e embriões de peixe-zebra como modelo experimental (Dodd et al. 2000; Ackermann & Paw 2003), (viii) no âmbito das ciências ambientais, há também muitos trabalhos comportamentais de exposição desta espécie a diversos pesticidas, fármacos entre outros xenobióticos (Levin & Chen 2004; Swain et al. 2004; Serra et al. 1999).

Kimmel, B. *et al* (1995), descreveram uma série de etapas relacionadas ao desenvolvimento embrionário do peixe-zebra, definindo sete grandes períodos de embriogênese: (1) o zigoto, (2) clivagem, (3) blástula, (4) gástrula, (5) segmentação, (6) faríngula, (7) e os períodos de incubação (eclosão). Estas divisões destacam os principais processos de desenvolvimento que ocorrem durante os três primeiros dias após a fertilização (Figura 6) (Kimmel C et al. 1995)**.**

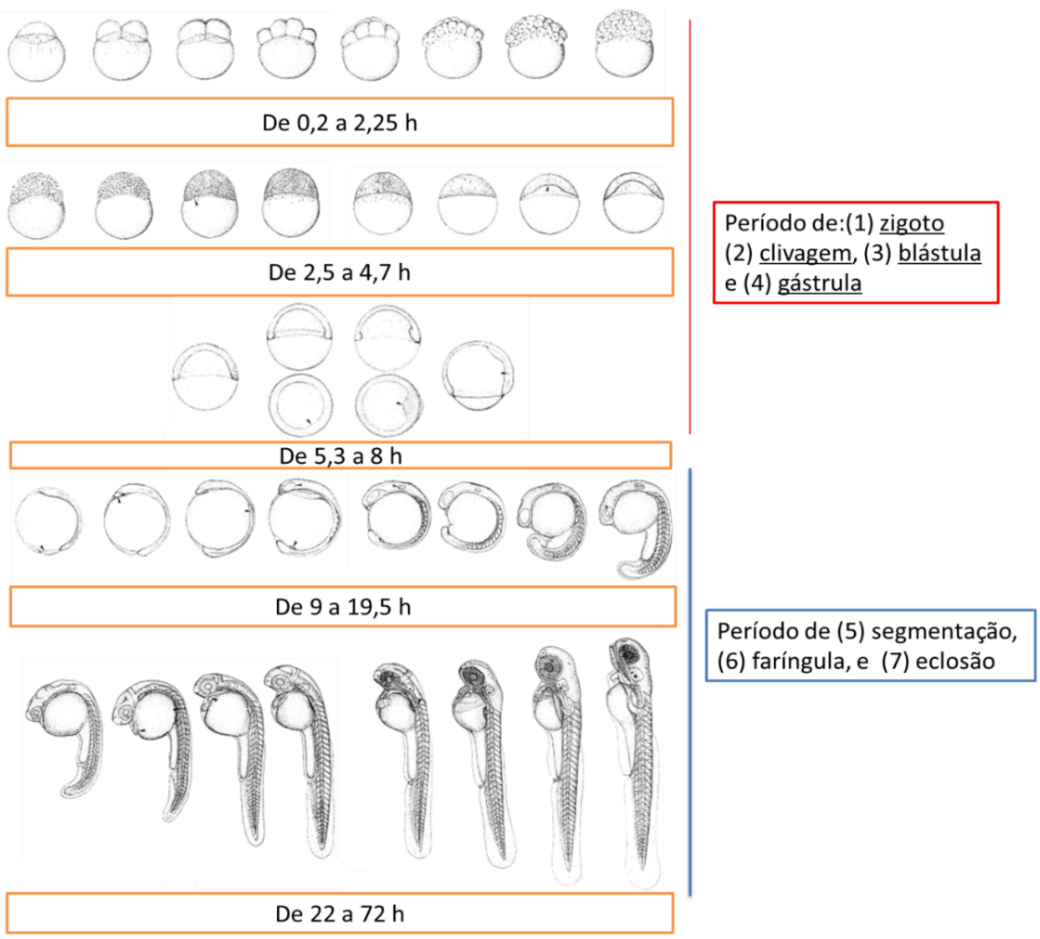

Figura 6. Desenvolvimento embrionário do peixe-zebra adaptado de Kimmel, B *et al*., (1995).

Atualmente, essas definições de períodos embriogênicos servem de base para testes de embriotoxicidade (Ali *et al*. 2014; Andrade 2015).

Em 2013, foi lançado um protocolo de testes embriotoxicológicos agudos com o peixe-zebra (OECD nº 236 2013). O princípio do teste é baseado na utilização de ovos fertilizados expostos a uma substância química. Mais detalhadamente, a exposição é realizada em microplacas de 24 poços com dois ml de cada concentração sendo que as soluções testes são preparadas com a água de cultivo de peixe-zebra. Todos os testes de

toxicidade aguda são feitos em triplicata com um total de 60 organismos por concentração. A duração dos testes é de até 96 h.

Na fase de embrião pode ser avaliada a mortalidade antes e após a eclosão (coagulação dos ovos e morte de embriões) e alterações em parâmetros de desenvolvimento embrionário, como: formação do otólito, pigmentação do corpo e olhos, formação dos somitos, presença de batimento cardíaco, separação da cauda do saco vitelino, edema, acúmulo de hemácias, líquido amniótico, absorção do saco vitelino, formação do telencéfalo e eclosão (para uma melhor compreensão a Figura 7 mostra alterações no desenvolvimento). Após a eclosão pode ser avaliado a pigmentação do corpo e olhos, batimento cardíaco, edema, acúmulo de hemácias, absorção do saco vitelino, inflação da bexiga natatória, malformações da cauda, resposta a estímulos mecânicos (equilíbrio, definido como o embrião deitado lateralmente no fundo do poço da microplaca), entre outros.

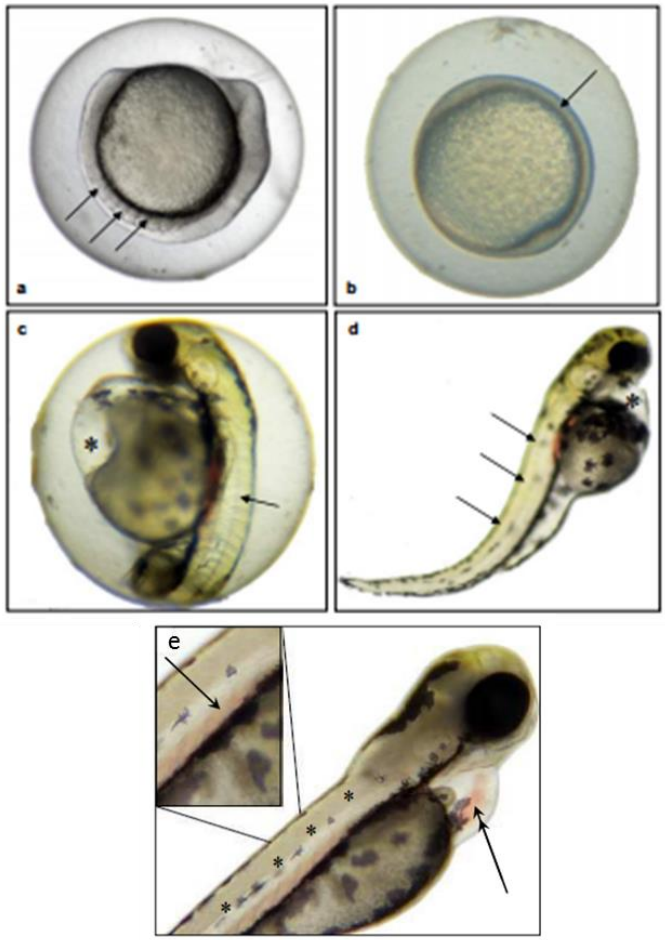

Figura 7. Alterações no desenvolvimento embrionário: (a) desenvolvimento de somitos (24 h) (b) ausência de somitos (24 h) (c) edema pronunciado no saco vitelino e alteração dos somitos (48 h) (d) curvatura anormal da cauda e edema pericárdico (72 h). *Fonte: OECD n.236*.

1.2. Considerações finais

Parece provável que a maioria das águas residuais urbanas estejam contaminadas com compostos químicos (Jones et al., 2005). Isso afeta a qualidade da água e o abastecimento de água potável e pode constituir um potencial risco para os ecossistemas e o bem-estar humano e animal a longo prazo (Klavarioti et al., 2009).

A nanotecnologia tem sido responsável por grandes avanços para humanidade, e na presente tese vários agentes adsorventes (*alótropos de carbono*) são revisados tendo como foco a retenção de micropoluentes. Nota-se que apesar dessas nanoestruturas serem uma alternativa promissora aos métodos convencionais de tratamento de água a maioria dessas ainda não estão prontas para produção em larga escala devido a alguns desafios técnicos (por exemplo: valor de manufatura (custo-benefício), configuração do sistema de filtração, preocupações ambientais (como: riscos a organismos não-alvos), entre outros). No capítulo 2 é apresentado os resultados em formato de artigo científico de um novo tipo de nanoestrutura carbonácea “o carbono micro/nanoestruturado híbrido”. Esse material híbrido é constituído por um substrato micrométrico que interage eletronicamente com os nanotubos de carbono que são cultivados diretamente em suas superfícies. Neste tipo de compósito, os nanotubos de carbono estão ligados a uma superfície de um material muito mais densa e podem ser facilmente contidos por máscaras, papel de filtro, etc., diferentes do que estão na forma de material particulado. Baseado nos resultados obtidos do presente trabalho o carbono micro/nanoestruturado híbrido apresenta grande potencial no tratamento de água e remediação aquática e pode ser mais uma alternativa aos métodos convencionais.

Referências bibliográficas

Ackermann, G E, and B H Paw. 2003. "Zebrafish: A Genetic Model for Vertebrate Organogenesis and Human Disorders." *Frontiers in bioscience: a journal and virtual library* 8: d1227-53.

Ahmadpour, A., and D. D. Do. 1996. "The Preparation of Active Carbons from Coal by Chemical and Physical Activation." *Carbon* 34(4): 471–79.

Ajayan, P M. 1999. "Nanotubes from Carbon." *Chemical Review* 99(7): 14. http://pubs.acs.org/doi/full/10.1021/cr970102g.

Ali, Shaukat, Jeffrey Aalders, and Michael K Richardson. 2014. "Teratological Effects of a Panel of Sixty Water-Soluble Toxicants on Zebrafish Development." *Zebrafish* 11(2): 129–41. http://www.ncbi.nlm.nih.gov/pubmed/24650241.

Allen, Heather K. *et al*. 2010. "Call of the Wild: Antibiotic Resistance Genes in Natural Environments." *Nature Reviews Microbiology* 8(4): 251–59. http://dx.doi.org/10.1038/nrmicro2312.

Andrade, Thayres de Sousa. 2015. "EFFECTS OF ENVIRONMENTAL FACTORS ON THE TOXICITY OF PESTICIDES TO ZEBRAFISH EMBRYOS." Universidade de Aveiro. http://hdl.handle.net/10773/4335.

Andrews, R, D Jacques, D L Qian, and T Rantell. 2002. "Multiwall Carbon Nanotubes: Synthesis and Application." *Accounts of Chemical Research* 35(12): 1008–17.

Aus der Beek, Tim *et al*. 2015. "Pharmaceuticals in the Environment - Global Occurrences and Perspectives." *Environmental Toxicology and Chemistry*: n/a-n/a. http://doi.wiley.com/10.1002/etc.3339.

Bogardi, Janos J. *et al*. 2012. "Water Security for a Planet under Pressure: Interconnected Challenges of a Changing World Call for Sustainable Solutions." *Current Opinion in Environmental Sustainability* 4(1): 35–43.

Brandão, F. P. *et al*. 2013. "Short-Term Effects of Neuroactive Pharmaceutical Drugs on a Fish Species: Biochemical and Behavioural Effects." *Aquatic Toxicology* 144–145: 218–29.

Brodin, T, J Fick, M Jonsson, and J Klaminder. 2013. "Dilute Concentrations of a Psychiatric Drug Alter Behavior of Fish from Natural Populations." *Science (New York, N.Y.)* 339(6121): 814–15. http://www.ncbi.nlm.nih.gov/pubmed/23413353.

Broughton, Richard E *et al*. 2001. "The Complete Sequence of the Zebrafish (Danio Rerio) Mitochondrial Genome and Evolutionary Patterns in Vertebrate Mitochondrial DNA." *Genome Research* 11: 1958–67.

Cai, Nan, and Philip Larese-Casanova. 2014. "Sorption of Carbamazepine by

Commercial Graphene Oxides: A Comparative Study with Granular Activated Carbon and Multiwalled Carbon Nanotubes." *Journal of Colloid and Interface Science* 426: 152–61. http://dx.doi.org/10.1016/j.jcis.2014.03.038.

Calvaresi, Matteo, and Francesco Zerbetto. 2014. "Atomistic Molecular Dynamics Simulations Reveal Insights into Adsorption, Packing, and Fluxes of Molecules with Carbon Nanotubes." *Journal materials chemistry*.

Carbon, H, Matthew J.; Allen, Vincent C.; Tung, and Richard B Kaner. 2010. "A Review of Graphene." *Chemical Review* 110: 132–45.

Charlier, Jean-christophe. 2007. "Electronic and Transport Properties of Nanotubes." 79(June): 677–732.

Chatterjee, Sudipta, Min W. Lee, and Seung H. Wooa. 2010. "Adsorption of Congo Red by Chitosan Hydrogel Beads Impregnated with Carbon Nanotubes." *Bioresource Technology* 101(6): 1800–1806. http://dx.doi.org/10.1016/j.biortech.2009.10.051.

Chen, Changlun, and Xiangke Wang. 2006. "Adsorption of Ni(II) from Aqueous Solution Using Oxidized Multiwall Carbon Nanotubes." *Industrial and Engineering Chemistry Research* 45(26): 9144–49.

Cho, Hyun-hee, Haiou Huang, and Kellogg Schwab. 2011. "Effects of Solution Chemistry on the Adsorption of Ibuprofen and Triclosan onto Carbon Nanotubes." : 12960–67.

Dai, Hongjie. 2002. "Carbon Nanotubes : Synthesis , Integration , and Properties." : 1035–44.

Dodd, a, P M Curtis, L C Williams, and D R Love. 2000. "Zebrafish: Bridging the Gap between Development and Disease." *Human molecular genetics* 9(16): 2443–49.

Dooley, K. 2000. "Zebrafish: A Model System for the Study of Human Disease." *Current Opinion in Genetics & Development* 10(3): 252–56. http://www.sciencedirect.com/science/article/pii/S0959437X00000745.

Endo, M. 2005. "Biochemistry: Role of PQQ as a Mammalian Enzyme Cofactor?" *Nature* 433(7025): E10.

El Gamal, Maisa *et al*. 2018. "Bio-Regeneration of Activated Carbon: A Comprehensive Review." *Separation and Purification Technology* 197(January): 345–59.

Geim, A. K., and K. S. Novoselov. 2007. "The Rise of Graphene." *Nature Publishing Group* 6: 183–91.

Helmer, Richard *et al*. 1997. *Water Pollution Control - A Guide to the Use of Water Quality Management Principles*. 2nd editio. eds. Richard Helmer and Ivanildo Hespanhol. London: Behaf of the United Nations Environment Programme, the

Water Supply & Sanitation Collaborative Council and the World Health Organization.

Hong, Byung Hee *et al*. 2005. "Extracting Subnanometer Single Shells from Ultralong Multiwalled Carbon Nanotubes." 102(40).

Huang, Zheng-hong *et al*. 2011. "Adsorption of Lead (II) Ions from Aqueous Solution on Low-Temperature Exfoliated Graphene Nanosheets." (Ii): 7558–62.

Ji, Liangliang *et al*. 2010. "Adsorption of Monoaromatic Compounds and Pharmaceutical Antibiotics on Carbon Nanotubes Activated by KOH Etching." *Environmental Science and Technology* 44(16): 6429–36.

Jobling, Susan *et al*. 1998. "Widespread Sexual Disruption in Wild Fish." *Environ Sci Technol* 32(17): 2498–2506. https://pubs.acs.org/doi/pdf/10.1021/es9710870.

Jones, Oliver A, John N Lester, and Nick Voulvoulis. 2005. "Pharmaceuticals: A Threat to Drinking Water?" *TRENDS in Biotechnology* 23(4): 163–67.

Jusoh, Ahmad, Lam Su, and M J M M Noor. 2007. "A Simulation Study of the Removal Efficiency of Granular Activated Carbon on Cadmium and Lead." 206(May 2006): 9–16.

Kemp, K Christian *et al*. 2013. "Environmental Applications Using Graphene Composites : Water Remediation and Gas Adsorption." : 3149–71.

Kim, Keun Soo *et al*. 2009. "Large-Scale Pattern Growth of Graphene Films for Stretchable Transparent Electrodes." *Nature* 457(7230): 706–10. http://dx.doi.org/10.1038/nature07719.

Kimmel C, B *et al*. 1995. "Stages of Embryonic Development of the Zebrafish." *Developmental Dynamics* 203(3): 253–310. http://doi.wiley.com/10.1002/aja.1002030302.

Klavarioti, Maria, Dionissios Mantzavinos, and Despo Kassinos. 2009. "Removal of Residual Pharmaceuticals from Aqueous Systems by Advanced Oxidation Processes." *Environment International* 35(2): 402–17. http://dx.doi.org/10.1016/j.envint.2008.07.009.

Kolpak, Alexie M. 2011. "Azobenzene-Functionalized Carbon Nanotubes As High-Energy Density Solar Thermal Fuels." : 3156–62.

Kümmerer, Klaus. 2009. "The Presence of Pharmaceuticals in the Environment Due to Human Use--Present Knowledge and Future Challenges." *Journal of environmental management* 90(8): 2354–66.

Lateefa A. Al-Khateeb, Sitah Almotiry, Mohamad Abdel Salam. Adsorption of pharmaceutical pollutants onto graphene nanoplatelets. Chemical Engineering Journal 248 (2014) 191–199.

Laine., J., A. Calafat, and Labady M. 1989. “Preparation and Characterization of Activated Carbons from Coconut Shell Impregnated with Phosphoric Acid.” *Carbon* 27(2): 191–95.

Lehr, T.E.G.J.H., and J. Pettyjohn DeMarre. 1980. *Domestic Water Treatment*. ed. McGraw-Hill Book Company. New York.

Levin, Edward D., and Elaine Chen. 2004. “Nicotinic Involvement in Memory Function in Zebrafish.” *Neurotoxicology and Teratology* 26(6 SPEC. ISS.): 731–35.

Li, Xuesong *et al*. 2009. “Transfer of Large-Area Graphene Films for High-Performance Transparent Conductive Electrodes.” *Nano Letters* 9(12): 4359–63.

Lu, Chungsying, and Huantsung Chiu. 2006. “Adsorption of Zinc(II) from Water with Purified Carbon Nanotubes.” *Chemical Engineering Science* 61(4): 1138–45.

Mccreary, J, and L Snoeyink. 2014. “Granular Activated Carbon in Water Treatment Author (s): John J . McCreary and Vernon L . Snoeyink Source : Journal (American Water Works Association), Vol . 69 , No . 8 , Esthetics and Facilities Designs (August 1977), Pp . 437-444 Stable URL : Htt.” 69(8): 437–44.

Mohammad-Khah, A., R. Ansari, A. Mohammad-Khah, and R. Ansari. 2009. “Activated Charcoal: Preparation, Characterization and Applications: A Review Article.” *International Journal of ChemTech Research* 1(4): 859–64.

Monteiro, Sara C., and Alistair B A Boxall. 2010. “Occurrence and Fate of Human Pharmaceuticals in the Environment.” *Reviews of Environmental Contamination and Toxicology* 202: 53–154.

Nemerrow, N.L. 1978. *Industrial Water Pollution: Origins, Characteristics, and Treatment*. ed. Addison-Wesley Publishing Company. Massachusetts.

Neto, A H Castro. 2009. “The Electronic Properties of Graphene.” 81(March).

Ngah, W S Wan, L C Teong, and M A K M Hanafiah. 2011. “Adsorption of Dyes and Heavy Metal Ions by Chitosan Composites : A Review.” *Carbohydrate Polymers* 83(4): 1446–56. http://dx.doi.org/10.1016/j.carbpol.2010.11.004.

Nishimura, Yuhei *et al*. 2015. “Pharmacological Profiling of Zebrafish Behavior Using Chemical and Genetic Classification of Sleep-Wake Modifiers.” *Frontiers in Pharmacology* 6(NOV): 1–21.

Novoselov, K. S. *et al*. 2004. “Electric Field Effect in Atomically Thin Carbon Films.” *Science (New York, N.Y.)* 306(October): 666–70.

OECD. 2013. “Test No. 236: Fish Embryo Acute Toxicity (FET) Test.” *OECD Guidelines for the Testing of Chemicals, Section 2, OECD Publishing* (July): 1–22.

Pauwels, B., and Willy Verstraete. 2006. “The Treatment of Hospital Wastewater: An

Appraisal.” *Journal of Water and Health* 4(4): 405–16.

Perreault, François, Andreia Fonseca de Fariaa, and Menachem Elimelech. 2015. “Environmental Applications of Graphene-Based Nanomaterial.” *Chemical Society reviews*. 10.1039/C5CS00021A.

Rafique, Irum, Ayesha Kausar, Zanib Anwar, and Bakhtiar Muhammad. 2016. “Exploration of Epoxy Resins, Hardening Systems, and Epoxy/Carbon Nanotube Composite Designed for High Performance Materials: A Review.” *Polymer - Plastics Technology and Engineering* 55(3): 312–33.

Rao, C N R, A K Sood, K S Subrahmanyam, and A Govindaraj. 2009. “Graphene : The New Two-Dimensional Nanomaterial Angewandte.” : 7752–77.

Rao, Gadupudi Purnachadra, Chungsying Lu, and Fengsheng Su. 2007. “Sorption of Divalent Metal Ions from Aqueous Solution by Carbon Nanotubes : A Review.” 58: 224–31.

Ren, Xuemei, Changlun Chen, Masaaki Nagatsu, and Xiangke Wang. 2011. “Carbon Nanotubes as Adsorbents in Environmental Pollution Management : A Review.” *Chemical Engineering Journal* 170(2–3): 395–410. http://dx.doi.org/10.1016/j.cej.2010.08.045.

Rico, Eduardo Pacheco. 2007. NeuroToxicology “Influência Do Metanol E Do Etanol Sobre a Atividade E a Expressão Gênica Das Ectonucleotidases E Acetilcolinestrase Em.” Universidade Federal Rio Grande do Sul.

Sanady, I.S.M.C. 1995. “Health Damage Due to Pollution in Hungary, in: Proceedings of the Rome Symposium, International Association of Hydrological Sciences, Wallingford.” In Oxfordshire, UK.

Sanderson, Hans *et al*. 2007. “Assessment of the Environmental Fate and Effects of Ivermectin in Aquatic Mesocosms.” *Aquatic Toxicology* 85(4): 229–40.

Santhosh, Chella *et al*. 2016. “Role of Nanomaterials in Water Treatment Applications: A Review.” *Chemical Engineering Journal* 306: 1116–37. http://dx.doi.org/10.1016/j.cej.2016.08.053.

Serra, E. L., C. C. Medalha, and R. Mattioli. 1999. “Natural Preference of Zebrafish (Danio Rerio) for a Dark Environment.” *Brazilian Journal of Medical and Biological Research* 32(12): 1551–53.

Seymour, Megan B *et al*. 2012. “Characterization of Carbon Nano-Onions for Heavy Metal Ion Remediation.”

Sitko, Rafal, Beata Zawisza, and Ewa Malicka. 2013. “Trends in Analytical Chemistry Graphene as a New Sorbent in Analytical Chemistry.” *Trends in Analytical Chemistry* 51: 33–43. http://dx.doi.org/10.1016/j.trac.2013.05.011.

Sotelo, José L *et al*. 2012. “Journal of Environmental Science and Health , Part B : Adsorption of Pharmaceutical Compounds and an Endocrine Disruptor from Aqueous Solutions by Carbon Materials Adsorption of Pharmaceutical Compounds and an Endocrine Disruptor from Aqueous Solutions By.” *Journal of Environmental Science and Health* Part B(47): 640–652.

Stafiej, Anna, and Krystyna Pyrzynska. 2008. “Solid Phase Extraction of Metal Ions Using Carbon Nanotubes.” 89: 29–33.

Swain, Holly a., Chris Sigstad, and Frank M. Scalzo. 2004. “Effects of Dizocilpine (MK-801) on Circling Behavior, Swimming Activity, and Place Preference in Zebrafish (Danio Rerio).” *Neurotoxicology and Teratology* 26(6 SPEC. ISS.): 725–29.

Thostenson, Erik T, Zhifeng Ren, and Tsu-wei Chou. 2001. “Advances in the Science and Technology of Carbon Nanotubes and Their Composites : A Review.” 61: 1899–1912.

Tratnyek, Paul G, and Richard L Johnson. 2006. “Nanotechnologies for Among the Many Applications of Nanotechnology That Have Environmental.” 1(2): 44–48.

Triebskorn, R. *et al*. 2004. “Toxic Effects of the Non-Steroidal Anti-Inflammatory Drug Diclofenac: Part II. Cytological Effects in Liver, Kidney, Gills and Intestine of Rainbow Trout (Oncorhynchus Mykiss).” *Aquatic Toxicology* 68(2): 151–66.

USEPA. 2015. *US Environmental Protection Agency: ECOTOXicology Knowledgebase (ECOTOX)*. Washington, D.C. http://cfpub.epa.gov/ecotox/ (September 1, 2015).

Vascotto, S G, Y Beckham, and G M Kelly. 1997. “The Zebrafish’s Swim to Fame as an Experimental Model in Biology.” *Biochemistry and cell biology = Biochimie et biologie cellulaire* 75(5): 479–85.

Vaseashta, A, M Vaclavikova, S Vaseashta, and G Gallios. 2007. “Nanostructures in Environmental Pollution Detection , Monitoring , and Remediation.” 8: 47–59.

Wang, Shaobin, and Yuelian Peng. 2010. “Natural Zeolites as Effective Adsorbents in Water and Wastewater Treatment.” 156: 11–24.

Wang, Xilong, Jialong Lu, and Baoshan Xing. 2008. “Sorption of Organic Contaminants by Carbon Nanotubes : Influence of Adsorbed Organic Matter.” *Environ Sci Technol* 42: 3207–12.

Wigmans, T. 1989. “INDUSTRIAL ASPECTS OF PRODUCTION OF ACTIVATED CARBONS.” *Carbon* 27(i): 13–22.

Yang, Dong *et al*. 2009. “Hydrophilic Multi-Walled Carbon Nanotubes Decorated with Magnetite Nanoparticles as Lymphatic Targeted Drug Delivery Vehicles W.” (C): 4447–49.

Yi, Younghun Kim; Jongheop. 2004. “Advances in Environmental Technologies via the Application of Mesoporous Materials.” *J. Ind. Eng. Chem* 10: 41–51.

Yoon, Ki Young, Jeong Hoon Byeon, Chul Woo Park, and Jungho Hwang. 2008. “Antimicrobial Effect of Silver Particles on Bacterial Contamination of Activated Carbon Fibers.” *Environmental Science & Technology* 42(4): 1251–55. http://pubs.acs.org/doi/abs/10.1021/es0720199.

Yu, Fei, Yong Li, Shen Han, and Jie Ma. 2016. “Adsorptive Removal of Antibiotics from Aqueous Solution Using Carbon Materials.” *Chemosphere* 153: 365–85. http://dx.doi.org/10.1016/j.chemosphere.2016.03.083.

Zhang, Wei Xian. 2003. “Nanoscale Iron Particles for Environmental Remediation: An Overview.” *Journal of Nanoparticle Research* 5(3–4): 323–32.

Zhao, Guixia *et al*. 2011. “Few-Layered Graphene Oxide Nanosheets As Superior Sorbents for Heavy Metal Ion Pollution Management.” : 10454–62.

Zhao, Jian, Zhenyu Wang, Jason C White, and Baoshan Xing. 2014. “Graphene in the Aquatic Environment : Adsorption , Dispersion , Toxicity and Transformation Graphene in the Aquatic Environment : Adsorption , Dispersion , Toxicity and Transformation.”

Zhu, By Yanwu *et al*. 2010. “Graphene and Graphene Oxide : Synthesis , Properties , and Applications.” : 3906–24.

1.3. Objetivo geral

Analisar a toxicidade de fármacos psicotrópicos e nanoestruturas carbonáceas híbridas incluindo seus efeitos letais e subletais para peixes (embriões de *Danio rerio*), e num segundo momento, avaliar as possíveis interações utilizando o referido modelo animal como biossensor e técnicas analíticas numa proposta de remediação aquática.

Observação: Os fármacos selecionados, foram: fluoxetina, carbamazepina e bupropiona (artigos publicados em colaboração). Os fármacos foram selecionados por sua constante detecção em ecossistemas aquáticos e pelo potencial risco ecológico.

1.4. Objetivos específicos

a) Caracterizar as nanoestruturas carbonáceas híbridas utilizando metodologias já consolidadas, como: Espalhamento dinâmico de luz (DLS) (condutividade e carga do material); cromatografia líquida de alta eficiência (HPLC) (saturação), Espectroscopia de infravermelho por transformada de Fourier (FTIR) (avaliar os grupos funcionais que compõem a amostra), Microscopia Eletrônica de Varredura (MEV) (estrutura morfológica).

b) Determinar os efeitos letais e subletais nos princípios ativos (controle fármacos) e das nanoestruturas (controle nanoestruturas) por meio de testes de embriotoxicidade com *D. rerio*.

c) Avaliar a interação entre as nanoestruturas carbonáceas e um fármaco psicotrópico utilizando embriões de *D. rerio* como biossensores e

posteriormente utilizar técnicas analíticas para comprovação da interação.

Obs: Dentre os fármacos testados na primeira etapa do presente trabalho a fluoxetina foi o composto selecionado para os testes de interações com as nanoestruturas carbonáceas devido a elevada detecção ambiental e toxicidade.

Capítulo 2. Resultados em formato de artígo científico

Tese de doutorado

2019

Neste capítulo são apresentados os resultados da presente pesquisa em formato de artigo científico. O presente estudo foi publicado na revista "Chemosphere", fator de impacto: 5.108 (2018). Qualis A1.

2.1. Resultados (artigo científico)

Chemosphere 230 (2019) 369–376

Contents lists available at ScienceDirect

Chemosphere

journal homepage: www.elsevier.com/locate/chemosphere

CNTs coated charcoal as a hybrid composite material: Adsorption of fluoxetine probed by zebrafish embryos and its potential for environmental remediation.

Diego Sousa-Moura [a, **], Elaine Yoshiko Matsubara [c, *], Irvin Bryan Machado Ferraz [a], Rhaul de Oliveira [a], Ísis Oliveira Szlachetka [b], Sebastião William da Silva [b], Níchollas Serafim Camargo [a], José Maurício Rosolen [c], Cesar Koppe Grisolia [a], Marcia Cristina Oliveira da Rocha [a]

[a] Universidade de Brasília, Instituto de Ciências Biológicas, Departamento de Genética & Morfologia, Brasília, DF, Brazil
[b] Universidade de Brasília, Laboratório de Física Aplicada, Instituto de Física, Brasília, DF, Brazil
[c] Universidade de São Paulo, FFCLRP - Departamento de Química, Ribeirão Preto, SP, 14040901, Brazil

HIGHLIGHTS

- HMNC and AC are practically non-toxic to zebrafish embryos: LC_{50} (96 h) ≥ 1000 mg.L^{-1}.
- HMNC adsorbs fluoxetine molecules more effectively than AC.
- Fluoxetine interacts with HMNC and is less available to early embryo development stages.
- Embryos exposed to HMNC and unexposed embryos behave similarly.

ARTICLE INFO

Article history:
Received 12 February 2019
Received in revised form
2 May 2019
Accepted 2 May 2019
Available online 10 May 2019

Handling Editor: David Volz

Keywords:
Danio rerio
Carbonaceous materials
Remediation agent
Hybrid micro/nanocomposite

ABSTRACT

Although traditional water treatment systems can remove various substances from wastewater, these conventional systems fail to remove many chemical molecules that pose potential ecological and health risks. Carbon nanotubes (CNTs) appear attractive to adsorption of many substances, but CNTs adsorbed with toxic substances becomes a nanocomposite still more toxic. Here, we employ zebrafish embryos as biosensor to examine how a hybrid micro/nanostructured carbonaceous material (HMNC) derived from a combination of activated carbon (AC) with hydrophilic carbon nanotubes (CNTs) can remediate wastewater contaminated with the pharmaceutical fluoxetine hydrochloride (FLX). AC and HMNC are practically non-toxic to zebrafish embryos (LC_{50} > 1000 mg.L^{-1}). HMNC addition to culture medium containing FLX significantly reduces sublethal effects and lethality. Interaction between FLX and HMNC involves chemical adsorption such that embryo co-exposure to HMNC adsorbed with FLX in the range of concentrations evaluated herein does not elicit any behavioral changes in zebrafish.

1. Introduction

Inefficient fluoxetine hydrochloride (FLX) removal by conventional water treatment and the consequent broad distribution of this drug in the environment (Aus der Beek et al., 2015) make the development of more efficient water treatment methods and of materials that can be incorporated into water treatment plants an urgent matter.

Activated carbon (AC) can remove many pharmaceutically active compounds from water, so it plays an important role in remediating water containing emerging contaminants. Different kinds of AC exist depending on their physicochemical properties (e.g., particle size, pore size distribution, surface area, and bulk density). The functional groups distribution on the AC surface determines how AC interacts with contaminants. Adsorption is controlled by van der

* Corresponding author.
** Corresponding author.
E-mail addresses: diegosousa.12@gmail.com (D. Sousa-Moura), elainematsubara@yahoo.com (E.Y. Matsubara).

https://doi.org/10.1016/j.chemosphere.2019.05.019
0045-6535/

Waals interactions between AC and non-polar contaminants or electrostatic interactions between the charged AC surface and polar contaminants. However, AC has disadvantages, including difficult reactivation and need for longer contact with the contaminant for adsorption to occur (Yoon et al., 2008; Mccreary and Snoeyink, 2014; El Gamal et al., 2018). Thus, carbon nanomaterials have been studied as alternative to improve micropollutant removal in water (Cho et al., 2011; Sotelo et al., 2012).

Several carbon nanomaterials have been studied for micropollutant removal (Cho et al., 2011; Sotelo et al., 2012; Ji et al., 2010). In this context, carbon nanotubes (CNTs) have been claimed as one of the most promising remediation materials for their large specific surface area, high porosity, high selectivity, numerous adsorption sites, short intraparticle diffusion distance, and tunable pore size, not to mention that they can engage in desirable interactions with countless contaminants and can be produced on a large scale. In spite of CNTs can be potentially applied in water remediation, their similarities with asbestos and their possible cyto- and genotoxic effects (Franchi et al., 2012) have raise concerns. Various studies have shown that CNTs impact terrestrial and aquatic organisms negatively (Lam et al., 2004; Warheit et al., 2004; Donaldson et al., 2006; Templeton et al., 2006; Roberts et al., 2007; Smith et al., 2007). In aquatic environment the CNTs when combined with toxic adsorbents become indeed a harmful element, and this has been recently observed as well as to case of fluoxetine combined with MWCNTs (Yan et al., 2018). Furthermore, there exist additional drawbacks concerning the practical usage of particulate CNTs in water treatment. First, it is hard to obtain hydrophilic CNTs at low costs. Second, using renewable resources to obtain hydrophilic CNTs is difficult because raw CNTs are predominantly hydrophobic. Finally, ensuring that all the nanomaterial will be well exposed to contaminants while avoiding the deleterious CNT-toxic adsorbent release into the aquatic environment is a challenging task.

To overcome the challenges associated with effective commercial use of CNTs in water treatment, here we propose the use of a hybrid micro/nanostructured material (HMNC) consisting of granular active charcoal or active carbon (AC) covered with hydrophilic CNTs grown directly on the AC surface. HMNCs are composites that allow the physicochemical properties of CNTs to be explored as a result of the amount and type of constituents and of the electronic interactions between them. In this kind of hybrid composite material, CNT coating bind to the surface of a dense and micrometric material and can be easily captured by masks, filter paper, etc., which is not possible with free CNTs (a low-density particulate material). HMNCs can be composed of many kinds of micrometric matrixes such as carbon fiber non-woven, charcoal, and bone charcoal and have been little studied in the context of water treatment (Gonçales et al., 2011; Zhang et al., 2009).

We then use zebrafish embryos as biosensor to evaluate how AC or HMNC interacts with FLX. Zebrafish is a small teleost (3–4 cm) belonging to the freshwater fish family Cyprinidae. This fish species is often employed as a model to assess the ecotoxicity of metals, pesticides, pharmaceuticals, and other substances (Kanungo et al., 2014) because the fish are small and undergo rapid external development. Several studies have suggested that acute toxicity measured by using zebrafish embryos (Fish Embryo Toxicity (FET) test –– OECD n. 236) provides similar sensitivity as compared to the adult fish (Lammer et al., 2009). The FET test offers advantages: it requires small volumes of test solutions, consequently generating less waste; the species used in the test are easy to obtain within a short period; and mortality as well as alterations in embryo development can be easily measured (OECD, 2013). To date, zebrafish have not been used as biosensor to check HMNC toxicity to non-target species, and the use of HMNC as adsorbent of psychotropic drugs has not been evaluated to verify whether these composites can be considered as a novel material for application in water treatment and environmental remediation.

2. Materials and methods

2.1. Fluoxetine and activated carbon

Fluoxetine was purchased from C&C pharmaceutical industry (CAS number: 54910-89-3, empirical formula $C_{17}H_{18}F_3NO$). Activated carbon (AC) derived from carbonization of eucalyptus was provided by AlphaCarbo Industrial (particle size = 325 mesh).

2.2. Hybrid micro/nanostructured carbonaceous material

The composite material studied in the present work was synthetized as described previously in detail in Matsubara et al. (2016) and Rosolen et al. (2006). AC was used as a micrometric carbonaceous material. Briefly, AC was submitted to a chemical vapor deposition (CVD) method; alcohol and Co/Mn particles (1:1) were employed as carbon source and catalyst, respectively, to obtain AC covered with CNTs, referred to as hybrid micro/nanostructured carbonaceous material (HMNC) hereafter.

2.3. Samples characterization

The surface charge (zeta potential) was determined by DLS experiments using the Zetasizer Nano ZS apparatus. Samples morphology was assessed by Scanning Electron Microscopy (SEM) using a Zeiss-EVO 50 scanning electron microscope. Energy-dispersive X-ray spectroscopy (EDS) was carried out with the IXRF Systems 500 digital processing for compositional characterization. Specific surface area (SSA) was determined by using the Brunauer, Emmett, Teller (BET) method at 77K and the Quantachrome NOVA 1200 equipment (with N_2). Before the BET experiments, the samples were dried at 150 °C and under reduced pressure for 3 h. The FTIR experiments were performed using a Bruker spectrometer (model Vertex 70). The spectra were recorded using potassium bromide (KBr) pressed pellet containing ~1% w/w of the investigated sample. The measurements were averaged over 96 scans, which were taken at a resolution of 4 cm^{-1} from 400 to 4000 cm^{-1}. The background signal was averaged over 96 scans before each measurement.

2.4. Zebrafish (Danio rerio) embryo culture

This research project was approved by the Ethics Committee on Animal Research of the Institute of Biological Science of the University of Brasilia under protocol number n. 100226/2014.

Zebrafishes were raised in an aquatic facility (ZebTec - Tecniplast, Italy) with a photoperiod cycle of 12:12 h (light:dark) in aquariums under reverse osmosis and activated carbon filtered water. The water parameters were strictly controlled: temperature was maintained at 27.0 ± 1 °C, conductivity at 650 ± 100 μS/cm, pH at 7.0 ± 0.5 and dissolved oxygen ≥95% saturation. These conditions were maintained in all the performed tests. Zebrafish eggs were collected immediately after natural mating, rinsed in water, and checked under a stereomicroscope (Stereoscopic Zoom Microscope – Stemi 2000, Zeiss, Germany). The unfertilized eggs and those showing cleavage irregularities or injuries were discarded.

2.5. Fish embryo toxicity (FET) test

Fish embryo toxicity test was based on the OECD guideline Protocol 236 “Fish Embryo Toxicity” (FET) test (Braunbeck et al., 2014, OECD, 2013). Zebrafish embryos were exposed to different

treatments (single and mixture exposure) prepared by successive dilutions of a stock solution. The test was performed using 60 eggs per treatment, divided in 3 replicates, selected and distributed in 24-well microplates in the climate chamber (SL-24 Solab Científica, Brazil), 20 wells were filled up with 2 mL of the test solution and four wells with water (internal plate control, as required in the OECD guideline). The test was initiated immediately after fertilization, and it was continued for 96 h. Embryos and larvae were observed daily under a stereomicroscope. Developmental parameters were evaluated in embryos over the test period, using a magnification of × 70 for eggs and × 40 for hatched embryos. Before hatching, the following parameters were evaluated: egg coagulation, otolith formation, general delay in development, eye and body pigmentation, somite formation, heartbeat, oedemas, detachment of the tail-bud from the yolk sac, yolk sac absorption and hatching. After hatching, spine malformation and posture (embryos side-lying in the bottom of the microplate well after mechanical stimulus = behavioral changes) were also evaluated. All parameters were assessed and quantified as observed or not observed.

2.5.1. Single and mixture exposure

Zebrafish embryos were exposed to four different concentrations of AC or HMNC (0, 10, 100, and 1000 mg.L^{-1}, in the absence of FLX – pilot test). The FLX toxicity test was performed at the following five different concentrations: 0, 3.19, 4.33, 7.59 and 18.46 mg.L^{-1} (pilot test). After the single toxicity tests (pilot test), the blend bioassays comprised three groups. Group 1 (or FLX Group) consisted of FLX-exposed embryos (0, 3.19, 4.33, 7.59 and 18.46 mg.L^{-1}). For groups 2 and 3 (FLX@AC and FLX@HMNC, respectively), stock solutions of folded and mixed concentrations were prepared in a ratio of 1:1, namely: 0; 6.38; 8.66; 15.18 and 36.92 mg.L^{-1} of FLX and 20; 200; 2000 mg.L^{-1} of AC (or HMNC). After mixed FLX and AC (or HMNC), the mixture concentration will be half of initial. Thus, the final concentrations of the mixtures are: 0, 3.19, 4.33, 7.59 and 18.46 mg.L^{-1} of FLX, and 10, 100 and 1000 mg.L^{-1} of AC (or HMNC). Fig. 1 illustrates the experimental tests with negative control (0 mg.L^{-1}), control of carbonaceous materials (10, 100 and 1000 mg.L^{-1}), single toxicity of the FLX group and their respective mixtures (FLX@AC and FLX@HMNC). The test was performed using 60 eggs per treatment, divided in 3 replicates (20 eggs per replicate and four wells with water (internal plate control, as required in the OECD guideline). The same parameters described in the previous section were analyzed and quantified as observed or not observed.

2.6. High performance liquid chromatography analysis

FLX stock solutions at 2, 10, 20, 30, 40, 50, 80, and 100 mg.L^{-1} concentrations were prepared in the same solvent proportion as the mobile phase and diluted to half of the initial concentration using AC or HMNC 2000 mg.L^{-1} solution to evaluate AC or HMNC saturation. The final concentrations were 1; 5; 10; 15; 20; 25; 40 and 50 mg.L^{-1} of FLX and 1000 mg.L^{-1} of AC or HMNC. Analyses were performed in triplicate; 1 mL was used per replicate at 26 ± 1 °C. The final solutions were kept under stirring, light, and at room temperature for 20 min. Then, they were filtered through a syringe-driven Millex filter (0.22 μm, 13-mm pore) and analyzed by HPLC.

To determine FLX remaining in the medium, the method adapted from Sabbioni et al., (2004) was used. The standard curve was obtained by using a Shimadzu-Prominence high performance liquid chromatograph comprising an online degasser (DGU 20A5 model), a solvent delivery unit (LC-20AT model), an auto sample injector (SIL-20 AHT model), a column oven (20A), an UV-VIS detector (SPD-20A model), and a controller (CBM-20A). The column consisted of C-18-ODS (M) reverse phase CLC (150 mm × 4.6 mm and 5-μm particle size). To construct the standard curve, FLX solutions at concentrations ranging between 1 and 50 mg.L^{-1} were prepared in 35:65 (v/v) phosphate buffer pH 3.0 and acetonitrile. The isocratic method was used. The mobile phase consisted of 35:65 (v/v) phosphate buffer pH 3.0 and acetonitrile at a flow rate of 1 mL min^{-1}. The detection wavelength was set at 228 nm, and the injection volume was 20 μL. The oven temperature was maintained

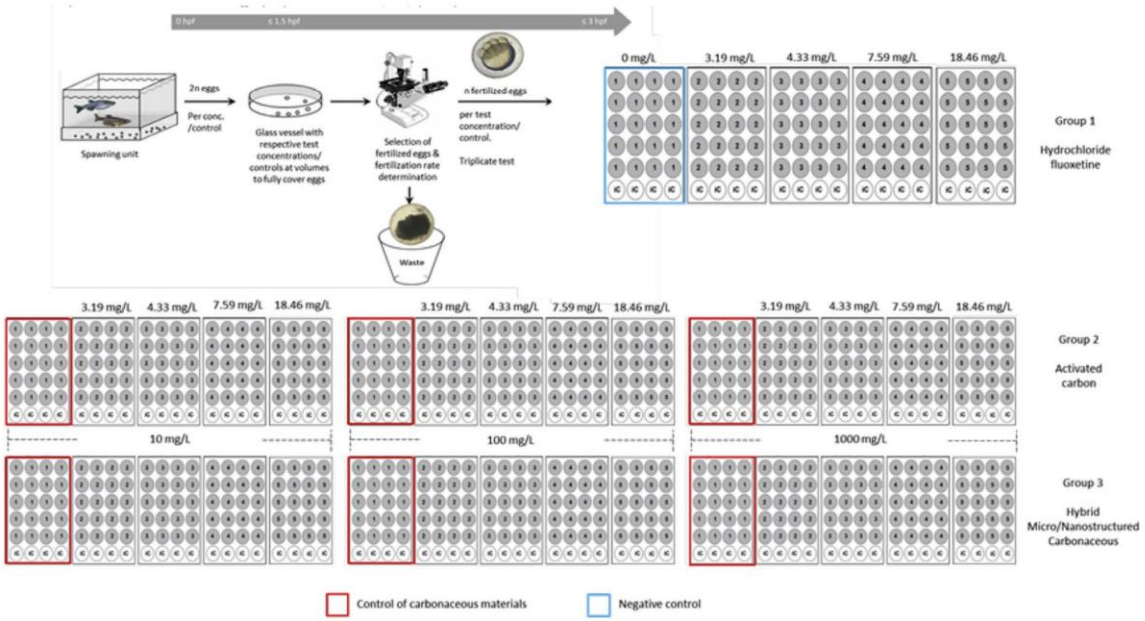

Fig. 1. Experimental embryo toxicity tests, adapted from OECD protocol no. 236.1–5: concentrations of the tested substances; IC: internal control. Group 1: Fluoxetine (FLX); Group 2: Activated Carbon + Fluoxetine (FLX@AC); and Group 3: Hybrid Micro/Nanostructured Carbonaceous Material + Fluoxetine (FLX@HMNC).

at 30 °C. Data were collected and processed with the LC solution software (Shimadzu, Tokyo, Japan).

2.7. Statistical analysis

The effective concentrations (LC_{50} and EC_{50}) to mortality and to behavior change (loss of equilibrium) were calculated using a two-parameter Logistic model. All analyses were performed using the Rstudio statistical package (R Core Team (2018)).

3. Results and discussion

3.1. Morphology of AC and HMNC

AC is a cheap adsorbent extensively studied in the literature and employed in water treatment, and for this reason it is the material chosen to be combined with CNTs. Nevertheless, it is also particularly interesting to preparation of HMNC because its surface is excellent to the incorporation of catalyst used to the CNT growth. Carbonaceous materials, as AC are also attractive to HMNC synthesis since they do not react with catalyst during the CVD methodology used to prepare them Fig. 2 shows SEM pictures of AC with average particle size of 500 μm, whereas Fig. 3 reveals that CNTs cover all the surface of the AC micrometric particles, producing the HMNC. EDS compositional analysis (not shown here) demonstrates that carbon and oxygen predominate in both AC and HMNC, in agreement with the literature (Bansal and Goyal, 2005). AC and HMNC SSA values are 329.4 and 266.0 $m^2 g^{-1}$, respectively, as determined from BET N_2 isotherms. Although CNTs are well known for their large surface area, the lower HMNC SSA as compared to AC is due to blockade of AC pores by CNTs. It is worth to remember that the AC surface is composes by large cavities or holes and small particles of charcoal (inserted in Fig. 2). During the process of the Mn/Co catalyst incorporation on the AC's surface (to CNTs' growth synthesis) these small particles are probably removed. The Mn/Co catalyst precursor salt is expected to penetrate in all large cavities as well as in a fraction of AC's mesopores and micropores too. This could explain the decrease of specific surface area after the AC surface coating with CNTs. In the HMNC, CNTs are found in whole surface of HMNC and inside of the cavities.

DLS measurements allowed determining zeta potential for the carbonaceous nanostructures before and after adsorption with fluoxetine. The values of potential for CA and HMNC pure are $\xi = -30.4 \pm 0.2$ mV and $\xi = -14.3 \pm 0.2$ mV, respectively. After adsorption, these values increased to $\xi = 9.99 \pm 0.2$ mV and $\xi = 16.8 \pm 0.2$ mV, respectively. The positive results of the ξ values indicate the carbonaceous nanostructures were loaded successfully and suggest that fluoxetine adsorption on CNT is probably chemical. Adsorption of FLX on single-walled carbon nanotubes has been studied by simulation and suggests that there exist a charge transfer between FLX and CNTs (Shahabi and Tavakol, 2017). For the case of MWCNTs is still not clear the presence of eventual charge transfer between the MWCNTs and FLX. In supplementary materials is show the he FTIR spectra of free FLX and of FLX adsorbed onto the nanostructure's AC and HMNC (Fig. S1a, ii and iv) do not reveal any significant changes in the FLX vibrational energies. On the other hand, the shifts in the aromatic ring vibration modes and the unchanged behavior of the CF_3 and C-O-C modes suggest that FLX adsorbs onto the carbonaceous nanostructures through π-π interaction. Similar results are found in the literature. The hypothesis that considers π-π interaction agrees with the changes in the AC and HMNC zeta potential values from negative (before FLX adsorption) to positive (after FLX adsorption).

3.2. Biological tests and HPLC analysis

Zebrafish have been widely used in ecotoxicological assessments. In the present study, the embryos present normal development in control medium as well as in carbonaceous adsorbent materials (AC or HMNC), which agrees with previous studies described by Kimmel et al. (1995). The maximum mortality is 3% for the entire test period. We were unable to determine LC_{50} or EC_{50} (sublethal parameters) for HMNC because they are above the highest concentration tested herein (1000 $mg.L^{-1}$).

Literature studies have focused on showing how carbonaceous nanostructures affect non-target species of different trophic levels. However, most of these studies, especially studies on vertebrates, report sublethal effects, generating a knowledge gap about lethality. Additionally, Lovern and Klaper, (2006) pointed out that nanomaterial toxicity depends on the methodology that was used to manufacture them. Therefore, establishing a toxicity pattern is difficult Yu et al. (2016). Zhu et al. (2007) evaluated the toxicity of a carbonaceous nanostructure, C_{60} (fullerene), to zebrafish embryos and observed that the nanomaterial is not toxic at concentrations of up to 50 $mg.L^{-1}$, but the authors were not able to calculate LC_{50} or EC_{50}. Nevertheless, when they evaluated C_n (other fullerene forms), they observed effects on hatching, embryo development, and mortality. Moreover, Cherukuri et al. (2006) assessed the toxicity of CNTs modified with Pluronic to rabbits (intravenous administration), but they did not identify sublethal effects. In contrast, Ye et al. (2009) verified cellular death, morphological changes, ROS, and expression of interleukin-8 (IL-8) genes when they investigated evaluating CNTs dispersed by Pluronic F_{68}. Here, the absence of lethal or sublethal effects on zebrafish embryos shows that AC and HMNC are not toxic to the fish. In our previous study, MWCNTs were tested in zebrafish for cyto- or genotoxicity. The lack of cyto-

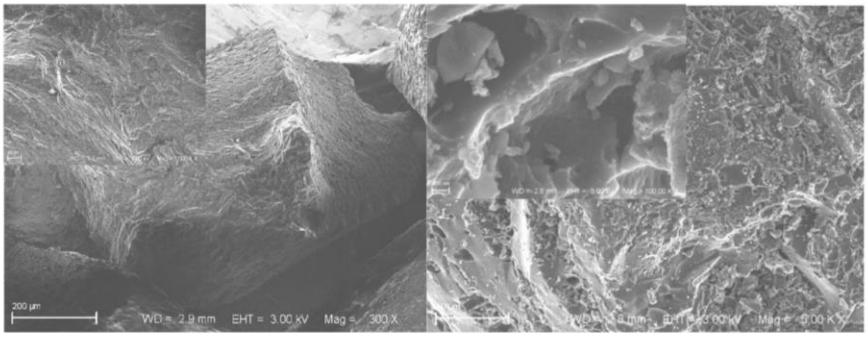

Fig. 2. SEM images of Activated Carbon (AC) at different magnifications.

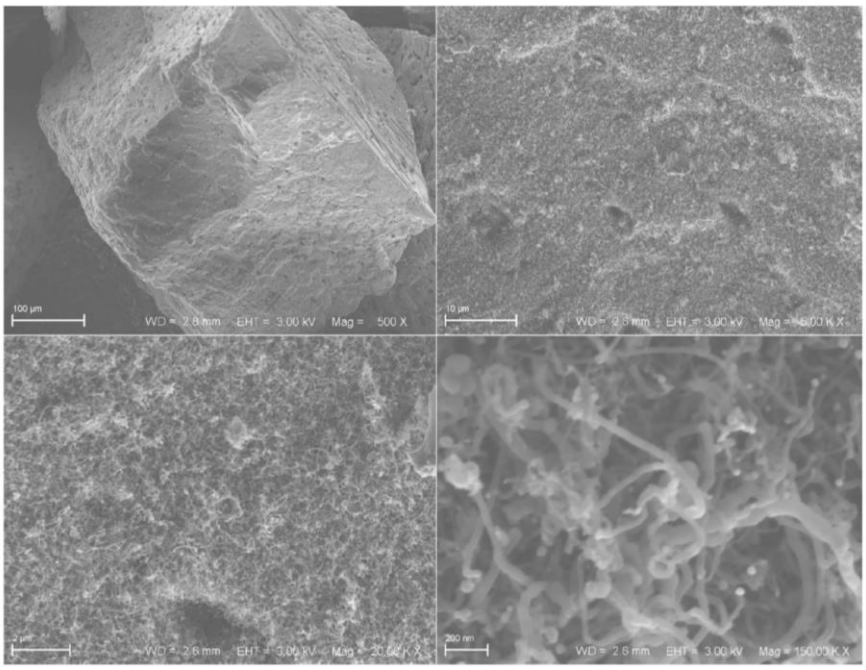

Fig. 3. SEM images of Hybrid Micro/Nanostructured Carbonaceous Material (HMNC) at different magnifications.

genotoxicity and reactivity encouraged more refined studies with purposes for using this nanomaterial in remediation processes Souza Filho et al. (2014).

The lethality results obtained with control FLX (LC_{50} 96 h = 6.32 mg.L^{-1}) can be compared to literature studies. For example, Nakamura et al. (2008) evaluated FLX effects on *Oryzias latipes* fish and determined LC_{50} 96 h = 5.5 mg.L^{-1}. Brooks et al. (2003) assessed the FLX environmental risk to selected benthic and pelagic toxicity test organisms, to obtain LC_{50} 168 h = 0.89 mg.L^{-1} for *Pimephales promelas* fish. Henry and Black (2008) achieved LC_{50} 168 h = 0.56 mg.L^{-1} for the adverse FLX effects on *Gambusia affinis* fish. Alsop and Wood (2013) conducted a study on zebrafish, to find lower acute FLX toxicity: LC_{50} 96 h = 0.25 mg.L^{-1}.

Table 1 lists the LC_{50} values for the positive control (FLX) and for FLX in the presence of different concentrations of carbonaceous adsorbents (AC or HMNC).

For AC or HMNC at 10 mg.L^{-1}, LC_{50} is around 34% higher for HMNC. In the case of AC or HMNC at 100 mg.L^{-1}, LC_{50} is approximately 6.5% higher for AC. A tenfold increase in AC concentration raises LC_{50} by 38.6%, whereas a tenfold increase in HMNC concentration raises LC_{50} by only 1.1%. Therefore, a lower HMNC concentration provides optimal results in terms of LC_{50}. In other words, HMNC 10 mg.L^{-1} is equivalent to AC 100 mg.L^{-1}, which represents an advantage of HMNC over AC when it comes to minimizing zebrafish embryo mortality.

FLX@AC 1000 mg.L^{-1} and FLX@HMNC 1000 mg.L^{-1} had *no mortality effect*, so we were no able to calculate LC_{50}. Fig. 4 shows an overview of the embryo toxicological results.

Although LC_{50} is higher for AC 100 mg.L^{-1} as compared to HMNC 100 mg.L^{-1}, HMNC does not elicit any behavioral changes in the organism, whereas mortality in the presence of FLX at 4.33, 7.59, and 18.46 mg.L^{-1} is 5%, 10%, and 100%, respectively.

Serotonin (5-HT) is one of the most important and ubiquitous neurotransmitters in the animal kingdom (Azmitia, 1999). In aquatic organisms, the serotonergic system (the FLX action site) plays a fundamental role in their behavior: social, food demand, and motor responses (Lillesaar et al., 2007; Mennigen et al., 2010). Studies have shown that aquatic organisms exposed to FLX concentrations display altered behavior (Airhart et al., 2007; Prieto, 2012). We evaluated behavioral changes (equilibrium) in hatched embryos after 96 h of exposure to different samples at different concentrations. Fig. 5 shows that approximately 80% of the organisms exposed to 4.33 mg.L^{-1} of FLX are altered. Almost all the organisms exposed to FLX 7.59 mg.L^{-1} died (only n = 2 live organisms in 60 - these data was not showed in Fig. 5). In this case, the only two remaining hatching embryos present behavioral changes, which means 100% behavior change. We were not able to measure behavioral changes in the organisms exposed to FLX 18.46 mg.L^{-1}, because they were all dead at 96 h.

Less than 20% and 2% of the organisms exposed to FLX 4.33 mg.L^{-1}@AC 10 mg.L^{-1} and FLX 4.33 mg.L^{-1}@AC 100 mg.L^{-1}, respectively, have altered behavior. These data reveals a dose-dependent response, as it was detected less behavioral changes when AC concentration increases.

To FLX 7.59 mg.L^{-1}@AC 10 mg.L^{-1}, AC maintains approximately 50% of living organisms, but all of them had changes in the balance. Besides of, it was observed behavioral changes amount to 10% in

Table 1
Lethal concentrations in mg.L^{-1} (±standard error) of Fluoxetine (FLX) and mixtures of Fluoxetine + Hybrid Micro/Nanostructured Carbonaceous Material (FLX@HMNC) and Fluoxetine + Activated Carbon (FLX@AC) used in the zebrafish embryo toxicity tests.

Treatment	LC_{50} (96 h)	Model (R^2)
FLX	5.20 ± 0.19	Logistic - two parameters (0.98)
FLX@AC 10 mg.L^{-1}	7.54 ± 0.31	Logistic - two parameters (0.99)
FLX@AC 100 mg.L^{-1}	11.25 ± 0.71	Logistic - two parameters (0.98)
FLX@HMNC + 10 mg.L^{-1}	10.08 ± 0.60	Logistic - two parameters (0.98)
FLX@HMNC + 100 mg.L^{-1}	10.52 ± 0.65	Logistic - two parameters (0.99)

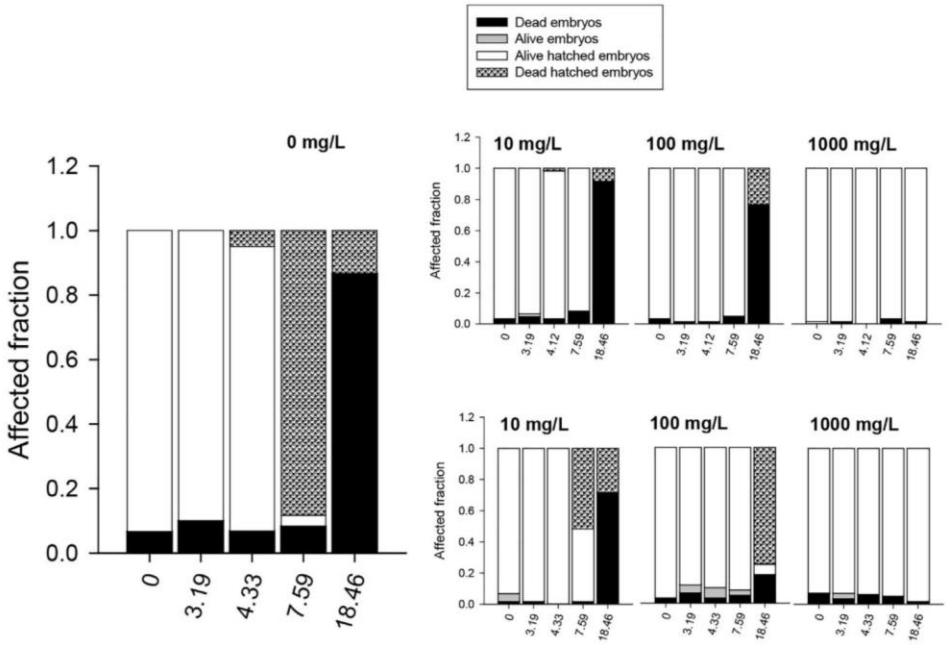

Fig. 4. Overview of the embryotoxicity studies after 96-h exposure to different treatments. Letter "a" represents the Fluoxetine (FLX) treatment. Letters "b", "c", and "d" corresponds to the different treatments with Fluoxetine + Hybrid Micro/Nanostructured Carbonaceous Material (FLX@HMNC), whereas letters "e", "f", and "g" refer to the different treatments with Fluoxetine + Activated Carbon (FLX@AC).

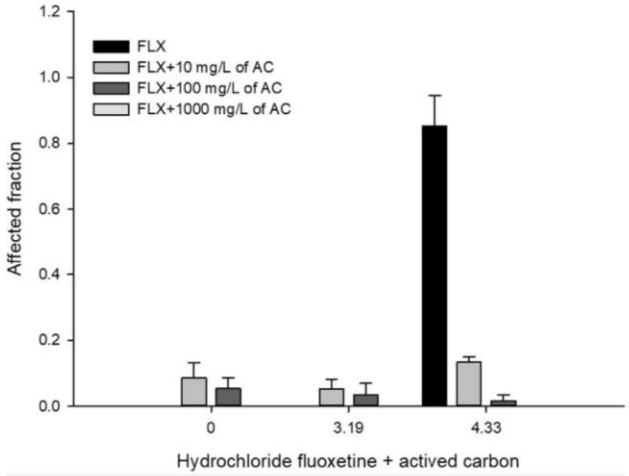

Fig. 5. Bar graph (±standard error) of the behavioral changes at 96 h of exposure to Fluoxetine (FLX) and FLX@Activated Carbon (FLX@AC).

FLX 7.59 mg.L^{-1}@AC 100 mg.L^{-1}. In addition, less than 7% of the organisms (n = 4) are alive in FLX 18.46 mg.L^{-1}@AC 100 mg.L^{-1}, and all of them had changes in equilibrium. Table 2 shows the effect concentrations (EC_{50}) for organisms exposed to FLX and FLX@10 mg.L^{-1} of AC.

Table 2
Effect concentrations in mg.L^{-1} (±standard error) of Fluoxetine (FLX) and mixtures of Fluoxetine + Activated Carbon (FLX@AC) used in the zebrafish embryo toxicity tests. It was not possible to determine an EC_{50} value for organisms exposed to FLX@100 and 1000 mg.L^{-1} of AC.

Treatment	EC_{50} (96 h)	Model (R^2)
FLX	4.22 ± 0.39	Logistic - two parameters (0.98)
FLX@AC 10 mg.L^{-1}	7.89 ± 0.67	Logistic - two parameters (0.99)

FLX@HMNC does not modify organism's behavior. The results described point out a higher interaction between FLX and HMNC; that is, HMNC is a better FLX adsorbent as compared to AC. This HMNC adsorptive property allows good zebrafish embryo development in medium containing lower FLX concentration because a greater amount of the drug is adsorbed onto the HMNC surface.

Zebrafish embryos are a good and efficient biosensor to prove the effects of FLX adsorption onto AC or HMNC. Despite its lower SSA, HMNC at low concentrations (10 mg.L^{-1}) adsorbs FLX more efficiently than AC. This is because AC and HMNC establish different electronic interactions with FLX. In the HMNC composite, the presence of CNTs covering the AC surface creates new properties or improves existing properties. The CNTs contain defects and functional groups originating from the synthesis process (Rosolen et al., 2006; Matsubara, 2010), which favor interaction with the FLX amine group and make the FLX molecules less bioavailable to the zebrafish embryos. At high concentrations (100 mg.L^{-1}), HMNC can adsorb more FLX molecules than AC, which explains the absence of behavioral changes in zebrafish embryos in the presence of FLX@HMNC. This result reinforces the data obtained for HMNC in water: despite bearing CNTs, the highest HMNC concentration in the absence of FLX is not toxic to the zebrafish. This is because CNTs are in the form of a micro/nanostructured hybrid and not in the form of free particulates. Fig. 6 represents how HMNC may have acted.

To confirm this assertion, we measured the amount of free FLX in the medium after contact with the carbonaceous adsorbent by the HPLC technique. We analyzed the different FLX, AC, HMNC, FLX@AC, and FLX@HMNC concentrations of used in embryo toxicity tests were analyzed to find the saturation point of the two carbonaceous adsorbent materials. We constructed a calibration curve on the basis of HPLC peak areas for several FLX concentrations, to obtain the standard curve with the following equation

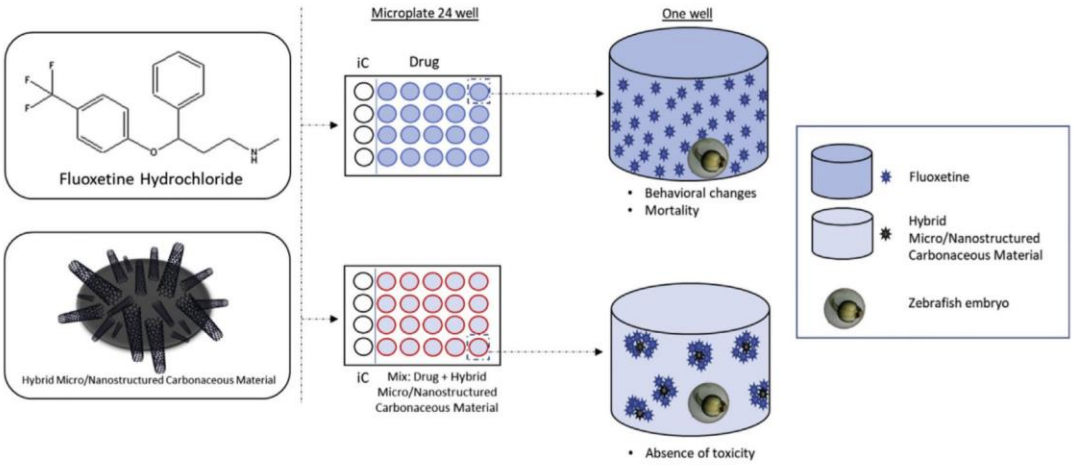

Fig. 6. Scheme of the interactions between Fluoxetine hydrochloride and Hybrid Micro/Nanostructured Carbonaceous Material. iC: internal control.

$Y = 454725*X + 7501$ and R^2 of 0.9998. We used this standard curve in subsequent studies.

Fig. 7 depicts the rate of FLX adsorption onto HMNC and AC during the tests. Fig. 7 - gray color, shows that AC 1000 mg.L^{-1} only removes lower FLX concentrations (between 1 and 10 mg.L^{-1}) from the medium. When the FLX concentration increases, AC becomes saturated. Consequently, some FLX molecules remain free in the medium and are detected by the equipment. Fig. 7 – black color, demonstrates that HMNC can adsorb higher FLX quantities. Saturation starts only at higher FLX concentrations (>40 mg.L^{-1}), when HPLC detects approximately 2% of the FLX in the medium. Lastly, FTIR spectra were performed on the precipitates of FLX@AC and FLX@HMNC samples washed with methanol. The spectra obtained are typical of the carbonaceous nanostructures as prepared, and show no evidence of FLX onto micro/nanostructured surface, as can be seen in Fig. S2 (Supplementary material). Thus, confirming that FLX was successfully desorbed and the regeneration of the adsorbent is feasible.

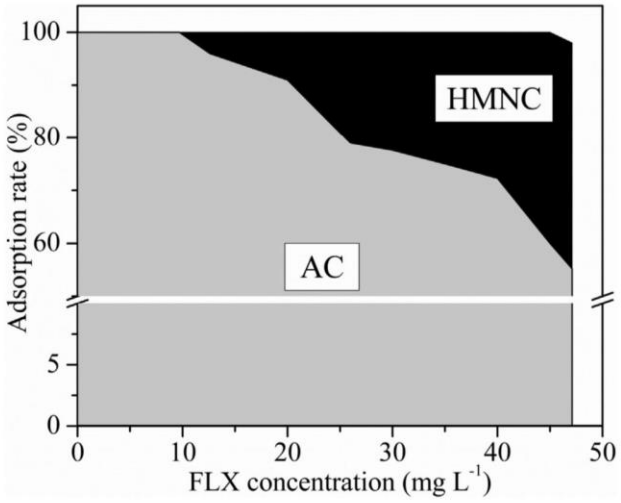

Fig. 7. (gray) Adsorption rate of various fluoxetine concentrations onto Activated Carbon 1000 mg.L^{-1}; (black) Adsorption rate of various fluoxetine concentrations onto Hybrid Micro/Nanostructured Carbonaceous Material 1000 mg.L^{-1}.

4. Conclusion

Here, we show a decrease in FLX sublethal and lethal effects on zebrafish embryos in the presence of carbonaceous adsorbent materials (AC and HMNC). The results indicate that zebrafish embryos are a good biosensor to analyze how HMNC and AC affect FLX adsorption.

HMNC and AC present low toxicity to zebrafish embryos, with LC_{50} above 1000 mg.L^{-1}, but the use of HMNC for FLX adsorption is more advantageous. The presence of CNTs on the AC surface in HMNC elicits electronic interactions that modify the properties of both AC and CNTs, giving rise to a hybrid material. The use of a hybrid composite material (micro/nanostructured carbonaceous material) enables the application of CNTs in environmental remediation without the toxicological effects attributed to carbon nanomaterials. Moreover, this approach allows an easy CNTs recovery.

HMNC proved to be a better FLX adsorbent than AC: HMNC provides the same outcome as AC at tenfold lower concentration (10 mg.L^{-1} versus 100 mg.L^{-1}, respectively) without behavioral changes.

In conclusion, HMNC resulted from a combination of activated carbon and hydrophilic carbon nanotubes can be potentially employed in water treatment or environmental remediation.

Acknowledgments

The authors would like to thank FAPESP (Proc. 2017/04759-2,JMR - Research Grant), CAPES (PROEX –1869/2016, EYM) and CNPq (JMR - Research Grant, DSM - PhD fellowship and CKG - 305741/2015-2 Research Grant). Prof. C.K. Grisolia would like to thank Juliana B.M.F. Vieira (Technical assistance).

Appendix A. Supplementary data

Supplementary data to this article can be found online at https://doi.org/10.1016/j.chemosphere.2019.05.019.

References

Airhart, M.J., et al., 2007. Movement disorders and neurochemical changes in zebrafish larvae after bath exposure to fluoxetine (PROZAC). Neurotoxicol. Teratol. 29 (6), 652–664. https://doi.org/10.1016/j.ntt.2007.07.005.
Alsop, D., Wood, C.M., 2013. Metal and pharmaceutical mixtures: Is ion loss the

mechanism underlying acute toxicity and widespread additive toxicity in zebrafish? Aquat. Toxicol. 140–141, 257–267. https://doi.org/10.1016/j.aquatox.2013.05.021.
Aus der Beek, T., et al., 2015. Pharmaceuticals in the environment - global occurrences and perspectives. Environ. Toxicol. Chem. n/a. -n/a. doi: 10.1002/etc.3339.
Azmitia, E.C., 1999. Serotonin neurons, neuroplasticity, and homeostasis of neural tissue. Neuropsychopharmacology 21, 33S–45S. https://doi.org/10.1016/S0893-133X(99)00022-6 (Woolley 1961.
Bansal, R.C., Goyal, M., 2005. Activated Carbon Adsorption. Taylor & Frances Group LLC, Florida, USA.
Braunbeck, T., et al., 2014. The fish embryo test (FET): Origin, applications, and future. Environ. Sci. Pollut. Control Ser. 22 (21), 16247–16261. https://doi.org/10.1007/s11356-014-3814-7.
Brooks, B.W., et al., 2003. Waterborne and sediment toxicity of fluoxetine to select organisms. Chemosphere 52 (1), 135–142. https://doi.org/10.1016/S0045-6535(03)00103-6.
Cherukuri, P., et al., 2006. Mammalian pharmacokinetics of carbon nanotubes using intrinsic near-infrared fluorescence. Proc. Natl. Acad. Sci. U. S. A 103 (50), 18882–18886. https://doi.org/10.1073/pnas.0609265103.
Cho, Hyun-hee, Huang, Haiou, Schwab, Kellogg, 2011. Effects of Solution Chemistry on the Adsorption of Ibuprofen and Triclosan onto Carbon Nanotubes, pp. 12960–12967.
Donaldson, K., et al., 2006. Carbon nanotubes: A review of their properties in relation to pulmonary toxicology and workplace safety. Toxicol. Sci. 92 (1), 5–22. https://doi.org/10.1093/toxsci/kfj130.
El Gamal, M., et al., 2018. Bio-regeneration of activated carbon: A comprehensive review. Separ. Purif. Technol. 197 (January), 345–359. https://doi.org/10.1016/j.seppur.2018.01.015.
Franchi, L.P., et al., 2012. Citotoxicidade e Genotoxicidade de Nanotubos de Carbono. Quim. Nova 35 (3), 571–580.
Gonçales, V.R., et al., 2011. Micro/nanostructured carbon composite modified with a hybrid redox mediator and enzymes as a glucose biosensor. Carbon 49 (9), 3039–3047.
Henry, T.B., Black, M.C., 2008. Acute and chronic toxicity of fluoxetine (selective serotonin reuptake inhibitor) in western Mosquitofish. Arch. Environ. Contam. Toxicol. 54 (2), 325–330. https://doi.org/10.1007/s00244-007-9018-0.
Ji, L., et al., 2010. Adsorption of monoaromatic compounds and pharmaceutical antibiotics on carbon nanotubes activated by KOH etching. Environ. Sci. Technol. 44 (16), 6429–6436. https://doi.org/10.1021/es1014828.
Kanungo, J., et al., 2014. Zebrafish model in drug safety assessment. Curr. Pharmaceut. Des. 20 (34), 5416–5429. https://doi.org/10.2174/1381612820666140205145658.
Kimmel, C.B., et al., 1995. Stages of embryonic development of the zebrafish. Dev. Dynam. 203 (3), 253–310. https://doi.org/10.1002/aja.1002030302.
Lam, C.W., et al., 2004. Pulmonary toxicity of single-wall carbon nanotubes in mice 7 and 90 days after intractracheal instillation. Toxicol. Sci. 77 (1), 126–134. https://doi.org/10.1093/toxsci/kfg243.
Lammer, E., et al., 2009. Is the Fish Embryo Toxicity Test (FET) with the Zebrafish (Danio rerio) a Potential Alternative for the Fish Acute Toxicity Test? Comparative Biochemistry and Physiology Part C: Toxicology & Pharmacology, vol. 149. Elsevier, pp. 196–209.
Lillesaar, C., et al., 2007. The Serotonergic Phenotype Is Acquired by Converging Genetic Mechanisms within the Zebrafish Central Nervous System. Developmental Dynamics, vol. 236. Wiley Online Library, pp. 1072–1084.
Lovern, S.B., Klaper, R., 2006. Daphnia magna mortality when exposed to titanium dioxide and fullerene (C60) nanoparticles. Environ. Toxicol. Chem./SETAC 25 (4), 1132–1137. https://doi.org/10.1897/05-278r.1.
Matsubara, E.Y., 2010. PhD Thesis. http://www.teses.usp.br/teses/disponiveis/59/59138/tde-24032010-112625/pt-br.php.
Matsubara, E.Y., et al., 2016. Electronic enhancement of hybrid specific capacity of carbon nanotube/bone charcoal composite with Ag nanoparticle decoration. J. Electroanal. Chem. 765, 58–64. https://doi.org/10.1016/j.jelechem.2015.11.020. Elsevier B.V.
Mccreary, J., Snoeyink, L., 2014. Granular activated carbon in water treatment author (s): John J . Mccreary and Vernon L . Snoeyink Source . J. Am. Water Works Assoc. 69 (8), 437–444. Esthetics and Facilities Designs (August 1977).
Mennigen, J.A., et al., 2010. Waterborne Fluoxetine Disrupts Feeding and Energy Metabolism in the Goldfish Carassius auratus. Aquatic Toxicology, vol. 100. Elsevier B.V., pp. 128–137. https://doi.org/10.1016/j.aquatox.2010.07.022
Nakamura, Y., et al., 2008. The effects of pH on fluoxetine in Japanese medaka (Oryzias latipes): Acute toxicity in fish larvae and bioaccumulation in juvenile fish. Chemosphere 70 (5), 865–873. https://doi.org/10.1016/j.chemosphere.2007.06.089.
OECD, 2013. Test No. 236: Fish Embryo Acute Toxicity (FET) Test. OECD Guidelines for the Testing of Chemicals, vol. 2. OECD Publishing, pp. 1–22. https://doi.org/10.1787/9789264203709-en (July).
Prieto, M.J., 2012. Effect of risperidone and fluoxetine on the movement and neurochemical changes of zebrafish. Open J. Med. Chem. 2 (4), 129–138. https://doi.org/10.4236/ojmc.2012.24016.
R Core Team, 2018. R: A Language and Environment for Statistical Computing. R Foundation for Statistical Computing, Vienna. https://www.R-project.org/.
Roberts, A.P., et al., 2007. In vivo biomodification of lipid-coated carbon nanotubes by Daphnia magna. Environ. Sci. Technol. 41 (8), 3028–3029. https://doi.org/10.1021/es062572a.
Rosolen, J.M., et al., 2006. Carbon nanotube/felt composite electrodes without polymer binders. J. Power Sources 162 (1), 620–628. https://doi.org/10.1016/j.jpowsour.2006.06.087.
Sabbioni, C., et al., 2004. A rapid HPLC-DAD method for the analysis of fluoxetine and norfluoxetine in plasma from overdose patients. J. Pharm. Biomed. Anal. 36, 351–356. https://doi.org/10.1016/j.jpba.2004.06.008.
Shahabi, D., Tavakol, H., 2017. DFT, NBO and molecular docking studies of the adsorption of fluoxetine into and on the surface of simple and sulfur-doped carbon nanotubes. Appl. Surf. Sci. 420, 267–275. https://doi.org/10.1016/j.apsusc.2017.05.068.
Smith, C.J., Shaw, B.J., Handy, R.D., 2007. Toxicity of single walled carbon nanotubes to rainbow trout, (Oncorhynchus mykiss): Respiratory toxicity, organ pathologies, and other physiological effects. Aquat. Toxicol. 82 (2), 94–109. https://doi.org/10.1016/j.aquatox.2007.02.003.
Sotelo, José L., et al., 2012. Adsorption of pharmaceutical compounds and an endocrine disruptor from aqueous solutions by carbon materials adsorption of pharmaceutical compounds and an endocrine disruptor from aqueous solutions. J. Environ. Sci. Health, Part B (47), 640–652.
Souza Filho, J., et al., 2014. Evaluation of carbon nanotubes network toxicity in zebrafish (danio rerio) model. Environ. Res. 134, 9–16.
Templeton, R.C., et al., 2006. Life-cycle effects of single-walled carbon nanotubes (SWNTs) on an estuarine meiobenthic copepod. Environ. Sci. Technol. 40 (23), 7387–7393. https://doi.org/10.1021/es060407p.
Warheit, D.B., et al., 2004. Comparative pulmonary toxicity assessment of single-wall carbon nanotubes in rats. Toxicol. Sci. 77 (1), 117–125. https://doi.org/10.1093/toxsci/kfg228.
Yan, Zhenhua, et al., December 2018. Accumulation, metabolite and active defence system responses of fluoxetine in zebrafish embryos: Influence of multiwalled carbon nanotubes with different functional groups. Aquat. Toxicol. 205, 204–212. https://doi.org/10.1016/j.aquatox.2018.10.018.
Ye, S.F., et al., 2009. ROS and NF-Kb Are Involved in Upregulation of IL-8 in A549 Cells Exposed to Multi-Walled Carbon Nanotubes. Biochemical and Biophysical Research Communications, vol. 379. Elsevier Inc., pp. 643–648. https://doi.org/10.1016/j.bbrc.2008.12.137
Yoon, K.Y., et al., 2008. Antimicrobial effect of silver particles on bacterial contamination of activated carbon fibers. Environ. Sci. Technol. 42 (4), 1251–1255. https://doi.org/10.1021/es0720199.
Yu, F., et al., 2016. Adsorptive Removal of Antibiotics from Aqueous Solution Using Carbon Materials. Chemosphere 153, 365–385. https://doi.org/10.1016/j.chemosphere.2016.03.083. Elsevier Ltd.
Zhang, Jiangnan, et al., 2009. Effect of growing CNTs onto bamboo charcoals on adsorption of copper ions in aqueous solution effect of growing CNTs onto bamboo charcoals on adsorption of copper ions in aqueous solution. Carbon (14), 2850–2855.
Zhu, X., et al., 2007. Developmental toxicity in zebrafish (Danio rerio) embryos after exposure to manufactured nanomaterials: Buckminsterfullerene aggregates (nC60) and fullerol. Environ. Toxicol. Chem. 26 (5), 976–979. https://doi.org/10.1897/06-583.1.

Capítulo 3. Conclusão

Tese de doutorado

2019

Nesse capítulo é apresentada a conclusão da tese de doutorado.

3.1. Conclusão.

Tendo em vista que o destino final de vários poluentes emergentes são as matrizes ambientais (principalmente ecossistemas aquáticos) e que a maioria das técnicas de retenção dos mesmos ainda não estão prontas para produção em larga escala devido a alguns desafios técnicos (como: valor de manufatura, configuração do sistema de filtração, preocupações ambientais, entre outros), podemos acentuar o CMNH por ser constituído por um substrato micrométrico (carvão ativado – composto atualmente mais utilizado como agente adsorvente) que interage eletronicamente com os nanotubos de carbono fazendo com que esse material tenha um bom custo benefício além de ter uma melhora considerável em comparação ao carvão ativado "s*ingle*", ademais, os bionsaios de toxicidade aguda apontam que o CMNH é pouco tóxico para embriões de peixe-zebra (CL_{50} > 1000 mg/L). Vale ressaltar que os dados apresentados no artigo mostram que essa nanoestrutura tem potencial para ser utilizada como filtro/ tratamento de água (ver: dados analíticos - HPLC).

Portanto, o CMNH é um bom canditado para o tratamento de água e remediação ambiental e pode ser mais uma alternativa aos métodos convencionais. Estudos devem focar em um sistema recirculante para avaliar o comportamento dessas nanoestruturas na filtração de efluentes industriais e de estações de tratamento de esgoto para uma melhor elucidação.

Anexos e apêndices.

Tese de doutorado

2019

Nos anexos e apêndices são apresentados os artigos publicados em colaboração que estão relacionados com a minha área de expertise (ecotoxicologia clássica utilizando o peixe-zebra como organismo modelo). As revistas indexadas são: Comparative Biochemistry and Physiology, Part C (fator de impacto: 2.697 (2018)); Ecotoxicology and Environmental Safety (fator de impacto: 4.527 (2018)); Chemosphere (fator de impacto: 5.108 (2018); Journal of Environmental Chemical Engineering, CiteScore: 4.09 (2018); Journal of Ethnopharmacology, fator de impacto: 3.414 (2018) e Acta Limnologica Brasiliensia, fator de impacto: 0.18 (2018). Ademais, é apresentada a declaração da comissão de ética no uso animal do instituto de ciências biológicas da universidade de Brasília – UnB, protocolo nº100226/2014.

Comparative Biochemistry and Physiology, Part C 215 (2019) 1–8

Contents lists available at ScienceDirect

Comparative Biochemistry and Physiology, Part C

journal homepage: www.elsevier.com/locate/cbpc

Exposure to low concentration of fluoxetine affects development, behaviour and acetylcholinesterase activity of zebrafish embryos

Natália Oliveira de Farias[a,1], Rhaul Oliveira[a,b,c,*,1], Diego Sousa-Moura[a], Reginaldo Carlyle Silva de Oliveira[a], Maria Augusta Carvalho Rodrigues[a], Thayres Sousa Andrade[a], Inês Domingues[d], Níchollas Serafim Camargo[e,f], Luís Alexandre Muehlmann[e,f], Cesar Koppe Grisolia[a]

[a] Laboratório de Genética Toxicológica, Departamento de Genética e Morfologia, Instituto de Ciências Biológicas, Universidade de Brasília, Asa Norte, 70910-900 Brasília, Distrito Federal, Brazil
[b] Faculdade de Tecnologia, Universidade Estadual de Campinas, UNICAMP, 13484-332 Limeira, São Paulo, Brazil
[c] Programa de Pós-graduação em Toxicologia e Análises Toxicológicas, Faculdade de Ciências Farmacêuticas, Universidade de São Paulo, FCF – USP, 05508-000 Butantã, São Paulo, Brazil
[d] Departamento de Biologia e CESAM, Universidade de Aveiro, Campus Universitário de Santiago, 3810-193 Aveiro, Portugal
[e] Laboratório de Nanobiotecnologia, Departamento de Genética e Morfologia, Instituto de Ciências Biológicas, Universidade de Brasília, Asa Norte, 70910-900 Brasília, Distrito Federal, Brazil
[f] Faculdade da Ceilândia, Universidade de Brasília, 72220-90 Brasília, Distrito Federal, Brazil

ARTICLE INFO

Keywords:
Danio rerio
Embryotoxicity
Pharmaceuticals
Locomotor effects
Neurotoxicity
Fish

ABSTRACT

Fluoxetine (FLX) is a selective serotonin reuptake inhibitor (SSRI) antidepressant widely used in clinics and very often found in environmental samples of urban aquatic ecosystems in concentrations ranging from ng/L to μg/L. Fish populations might be especially susceptible to FLX due to the presence of conserved cellular receptors of serotonin. Neurotoxic effects on fish biota of polluted water bodies may be expected, but there are no sufficient studies in the current literature to elucidate this hypothesis. Batteries of embryo larval assays with zebrafish were performed to evaluate the potential effects of FLX exposure, including environmentally relevant concentrations. Evaluated parameters included survival, development, behaviour and neuronal biochemical markers. Regarding acute toxicity, a 168 h-LC_{50} value of 1.18 mg/L was obtained. Moreover, hatching delay and loss of equilibrium were observed, but at a concentration level much higher than FLX measured environmental concentrations (> 100 μg/L). On the other hand, effects on locomotor and acetylcholinesterase activity (≥ 0.88 and 6 μg/L, respectively) were found at levels close to the maximum reported FLX concentration in surface waters. Altogether, these results suggest that FLX is neurotoxic to early life stages of zebrafish, in a short period of time causing changes in important ecological attributes which can probably be linked from molecular to population level.

1. Introduction

Pharmaceuticals are a highly diverse group of compounds, widely used and not totally eliminated from domestic effluents by current methods of wastewater treatment (Aus Der Beek et al., 2015). Thus, many of them are often detected in surface waters (Hernando et al., 2006). Water contamination by pharmaceuticals has been mainly attributed to the constant discharge of treated or untreated domestic effluents in receiving water bodies (Heberer and Heberer, 2002). Psychiatric drugs are among the most used and detected contaminants in aquatic ecosystems, but their potential risk to aquatic biota is a growing concern, since recent studies have reported behavioural changes in aquatic species, especially fish, exposed to environmentally relevant concentrations of those chemicals (Ford and Fong, 2015).

Discovered in 1975 and approved for commercialization by the Food and Drug Administration (FDA) in 1987, Fluoxetine (FLX) was the first antidepressant used in the treatment of clinical depression (Henry and Black, 2008). Nowadays, FLX is also used in the treatment of major

* Corresponding author at: Instituto de Biologia, Universidade de Brasília, Campus Universitário Darcy Ribeiro, Asa Norte, 70910-900 Brasília, Distrito Federal, Brazil.
E-mail address: rhaul.oliveira@gmail.com (R. Oliveira).
[1] These authors contributed equally to the study.

https://doi.org/10.1016/j.cbpc.2018.08.009
Received 29 May 2018; Received in revised form 28 August 2018; Accepted 31 August 2018
Available online 06 September 2018

depressive disorder, obsessive-compulsive disorder, panic disorder, and bulimia, and has been one of the most heavily prescribed antidepressant drugs worldwide (Stewart et al., 2014). Consequently, FLX has been reported in aquatic environmental samples at concentrations ranging from 0.012 μg/L to 0.93 μg/L (Martínez Bueno et al., 2007; Kolpin et al., 2002; Lister et al., 2009; Metcalfe et al., 2003; Weinberger and Klaper, 2014). Belonging to the group of selective serotonin reuptake inhibitors, this antidepressant is a potent selective inhibitor of the transporter enzyme for serotonin reuptake at the presynaptic membrane, increasing serotonin concentrations at postsynaptic receptor sites (Costagliola et al., 2008).

Unlike other contaminants, pharmaceuticals are designed to trigger a specific therapeutic response in humans (Fent et al., 2006), but many of their molecular targets are also present in other orthologous species (Gunnarsson et al., 2008). Thus, biological effects on non-target organisms might be expected. For instance, FLX has been described as neurotoxic to aquatic organisms, affecting their central nervous system and causing neuroreceptor and neurotransmitter modulation, behavioural changes, reproductive impairment and death (Berg et al., 2013; Weinberger and Klaper, 2014; Weis, 2014). All these biological effects are directly or indirectly related to the drug's designed mode of action to act as an antidepressant for humans. In spite of the increasing number of studies suggesting the potential aquatic environmental risk of psychiatric drugs, standard approaches and endpoints for ecotoxicological assessment of these compounds are not clearly defined, and the link among the observed effects and ecologically relevant parameters remains unclear, especially for fish populations.

Zebrafish (*Danio rerio*) early life stages are widely used as a model organism to assess the toxicity of environmental contaminants in fish populations (Scholz et al., 2008). The species has many advantages, such as a sequenced genome, abundant spawning, rapid embryonic development, transparent embryos and available standard protocols for acute and chronic assessment (ISO, 2007; Prieto et al., 2012; OECD, 2013). Moreover, in the last decade, the assessment of zebrafish behavioural and biochemical neuromarkers (e.g. cholinesterase) has been increasingly used as an endpoint to assess the sub-lethal effects of pollutants, proving to be a sensitive and reliable measure of stress exposure (Domingues et al., 2010; Andrade et al., 2015; Henriques et al., 2015; Klüver, 2015).

In this study, an integrated approach was conducted, using zebrafish embryos to evaluate the short-term toxicity of FLX. The parameters selected, comprising several organizational levels, were: i) mortality; ii) embryo development (including developmental delays and abnormalities); iii) fish behaviour (by measuring locomotor activity) and iv) acetylcholinesterase activity. Obtained data were compared with data from others studies with fish using a SDD analysis. Sub lethal responses, from molecular to population levels are discussed, and links between observed responses and parameters of ecological relevance are proposed.

2. Material and methods

2.1. Chemical

FLX 97% of purity was obtained from C&C Pharmaceutical industry, Amapa, Brazil (CAS Number: 56296-78-7, empirical formula: $C_{17}H_{18}F_3NO$).

2.2. Chromatographic analysis

To confirm the stability of FLX in test conditions, samples from test solutions were analysed using High Performance Liquid Chromatography (HPLC Shimadzu-Prominence). Samples were originally kept in the climate-controlled chamber where all toxicity tests were performed (SL-24 Solab Científica). Stability of FLX in the dilution water and climatic conditions of the tests were evaluated by HLPC, following the method described by Sabbioni et al., 2004 (see details in Suppl. Material-SM1, Fig. S1, Table S1).

2.3. Test organisms

Zebrafish were maintained in aquariums with reverse osmosis and activated carbon filtered water. Fish were raised in an aquatic facility (ZebTec - Tecniplast, Italy) with a photoperiod cycle of 12:12 h (light:dark) at the University of Brasilia (Brazil). The water parameters were strictly controlled: temperature was maintained at 27.0 ± 1 °C, conductivity at 650 ± 100 μS/cm, pH at 7.0 ± 0.5 and dissolved oxygen ≥ 95% saturation. The same water media, with similar physical-chemical parameters, was used to prepare the stock and exposure solutions in all the performed tests.

Zebrafish eggs were collected immediately after natural mating, rinsed in water, and checked under a stereomicroscope (Stereoscopic Zoom Microscope – Stemi 2000, Zeiss, Germany). The unfertilized eggs and those showing cleavage irregularities or injuries were discarded (< 15% of the total number of eggs).

2.4. Fish embryo toxicity (FET) test

Fish embryo toxicity test was based on the OECD guideline Protocol no. 236 "Fish Embryo Toxicity" (FET) test (OECD, 2013) with few adaptations including the extension of time of exposure from 96 h to 168 allowing a better evaluation of locomotor activity. Zebrafish embryos were exposed, immediately after fertilization, to seven different concentrations of FLX (0; 0.01; 0.27; 0.74; 2.02; 5.51; 15.0 mg/L) prepared by successive dilutions of stock solution direct in dilution water. The test was performed in 24-well microplates, 20 wells were filled up with 2 mL of the test solution and four wells with water (internal plate control, as required in the OECD guideline). A total of 60 eggs were used per treatment, divided in three independent replicates. The embryos were selected and distributed individually, one egg per well. The 24-well microplates with exposed embryos were kept in a climate chamber at 26 ± 1 °C and 12 h of light (SL-24 Solab Científica, Brazil). Embryos and larvae were observed daily under a stereomicroscope. Developmental parameters were evaluated in embryos over the test period, using a magnification of × 70 for eggs and × 40 for hatched embryos. Before hatching, the following parameters were evaluated: egg coagulation, otolith formation, general delay in development, eye and body pigmentation, somite formation, heartbeat, oedemas, detachment of the tail-bud from the yolk sac, yolk sac absorption and hatching. After hatching, spine malformation and posture (embryos side-lying in the bottom of the microplate well after mechanical stimulus) were also evaluated. All parameters were assessed and quantified as observed or not observed.

2.5. Sub lethal assays

For locomotor and Acetylcholinesterase activity assays a different range of concentrations were chosen considering both, the results of FET test, previously performed, (NOEC for Loss of equilibrium endpoint = 0.27 mg/L) and the maximum reported FLX concentration in the literature 0.93 μg/L (Bueno et al., 2007). Moreover, for both assays the exposed embryos were kept in a climate chamber at 26 ± 1 °C and 12 h of light.

2.5.1. Locomotor behaviour assay

Immediately after spawning, zebrafish embryos were individually exposed, one embryo per well, in 96-well microplates. The sub-lethal concentrations were 0.0, 0.88, 15.8, 281.2, 500 μg/L of FLX. A total of 48 embryos, divided in three independent replicates of 16, were used per treatment. Locomotor activity was measured at 120, 144 and 168 h, windows of exposure recommend by Padilla et al. (2011). Prior to the assessment of behaviour, dead larvae or larvae that exhibited physical

abnormalities were discarded and not included in the analyses. Larvae movement was evaluated using the Zebrabox (ZEB 478 Viewpoint) tracking system equipped with a 25-frame-per-second infrared camera over a period of 20 min. The zebrafish temperature was maintained stable at 26 ± 1 °C during the reading period. Movement was stimulated by applying light:dark intervals as previously described in Irons et al. (2010). Briefly, the test consisted of acclimating the larvae in the light for 5 min, followed by a 10 min dark period and another 5 min light. Typically, zebrafish larvae show less locomotion during light periods than in the dark. For each replicate, the distance and time moving in 1 min intervals were recorded separately for each dark and light period. The behavioural endpoints measured included the total swimming distance (TSD) moved during each measurement period and the total swimming time (TST) that the larvae displayed movement.

2.5.2. Biomarker analysis

In order to analyse the activity of AChE, a neuroendocrine biomarker, toxicity tests with zebrafish embryos were performed using a range of sub-lethal concentrations, namely 0, 1, 6, 32, 185 and 1053 µg/L of FLX. Tests were performed in 1 L beakers filled up with 500 mL of test solutions and 250 eggs. After 168 h of incubation, 12 pools composed by 15 viable, non-deformed and hatched embryos for each treatment were collected into microtubes with 0.5 mL of K-phosphate buffer (0.1 M, pH 7.4). All samples were frozen in liquid nitrogen and immediately stored at −80 °C until the day of analysis. Prior to AChE enzymatic activity measurement, samples were defrosted on ice, homogenized using a sonicator (Ultrasonic Cleaner 2840D-Odontobras), and refrigerated centrifuged (4 °C) for 20 min at 10,000*g* (Centrifuge Hettich – Mikro 220R). Resulting post-mitochondrial supernatant (PMS) was isolated, and 40 µl of each sample was pipetted in 96-well microplates for enzymatic determinations (Jesus et al., 2013).

AChE activity was determined using acetylthiocholine (ASCh) and propionylthiocoline (PSCh) as substrates, measuring the conjugation product between thiocoline (result of the degradation of ASCh or PSCh) and 5,5-dithiobis-2-nitrobenzoic acid (DTNB) (absorbance increase) at 414 nm, every 20 s, during 05 min, according to the method previously described by Ellman et al. (1961). For the enzymatic determination, 40 µl of PMS and 250 µl of reaction mixture (acetylcholine and propionylcholine (75 mM) and DTNB (10 mM)) in K-phosphate buffer (0.1 M, pH 7.2) were used. Acetylcholinesterase activities were expressed as micromoles of substrate hydrolysed per minute per mg of protein (U).

The protein concentration of samples was quantified using the Bradford Method at 595 nm and γ-globulin as standard (Bradford, 1976). All reactions were performed spectrophotometrically (SpectraMax M2 microplate reader) in quadruplicate.

2.6. Statistical analysis

The effective concentrations (LC_{50} and EC_{50}) were calculated using a four-parameter logistic model. A one-way ANOVA was used to detect the differences between the groups for normally distributed data sets. When data did not pass the Kolmogorov–Smirnov normality test and Levene's homogeneity of variance test, a Kruskal–Wallis test was performed. If significant results were found, Dunnett's or Dunn's test (for parametric or non-parametric data, respectively) was used to detect significant differences between the tested concentrations and the control ($p < 0.05$). All analyses were performed using the Sigma Stat 3.5 statistical package (SPSS, 2004).

2.7. Species sensitivity distribution (SSD)

The SSD was performed with toxicity values (LC_{50}) from the experimental data of the present study and values from indexed articles published in peer reviewed journals (Table S2). Multiple toxicity data for different species of fish were summarized as geometric means. The SSD plot was generated using the U.S. Environmental Protection Agency spreadsheet built over Excel (USEPA, 2018). A logistic curve (log) was fitted to the data using nonlinear regression. The predicted hazardous concentrations for the 5% and 50% most sensitive organisms were estimated (HC_5 and HC_{50}, respectively).

3. Results

3.1. Zebrafish embryo toxicity test

During the 168 h of test, no significant mortality was observed for the control groups. Additionally, control groups showed normal development, as described by Kimmel et al. (1995). The lethal effective concentrations for FLX are summarized in Table S2. FLX showed to

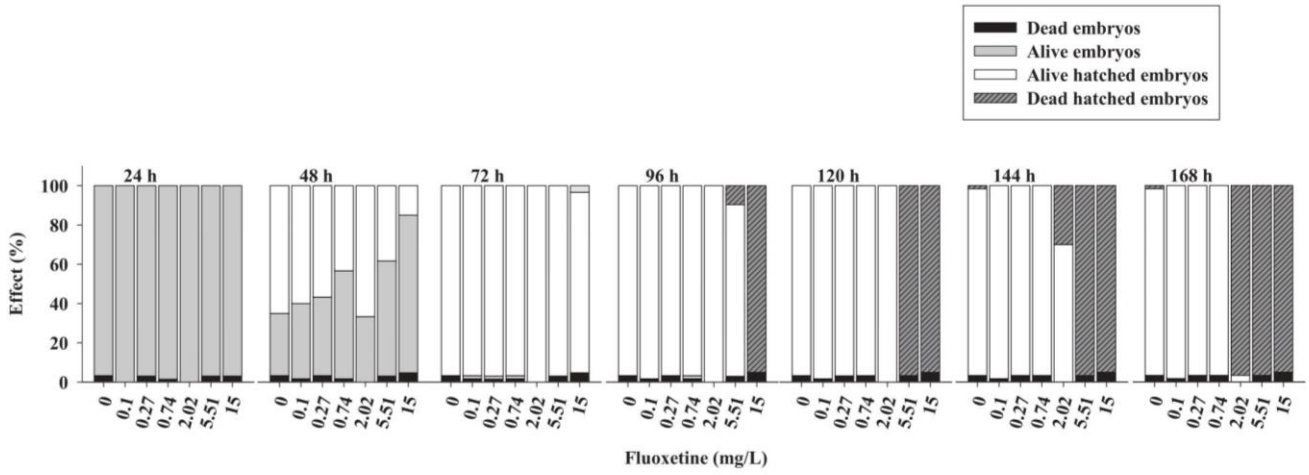

Fig. 1. Overview of zebrafish embryos extended toxicity test after 168 h of exposure to FLX. The proportion of eggs and non-hatched embryos that died are represented by black bars; the proportion of embryos that stayed alive but did not hatch are presented as grey bars; those that hatched as white bars and the proportion of embryos that died after hatch as spotted, dark dashed grey bars.

Table 1
Percentage of hatching for zebrafish embryos during 96 h of exposure to FLX. (A) Normal embryos; (B) Partially hatched embryos[#]; (C) Unhatched embryos.

Fluoxetine (mg/L)	48 h	72 h
0.0	65 (10.4)	100 (0)
0.1	60 (7.6)	98.3 (1.7)
0.3	56.7 (1.7)	98.4 (1.6)
0.7	43.3 (10.9)	98.3 (1.7)
2.0	66.7 (10.9)	100 (0)
5.51	38.3 (1.7)	100 (0)
15	15 (8.7)*	100 (0)

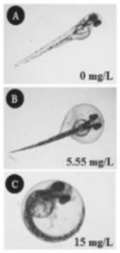

*Asterisks denote statistical significance when compared to control group ($p < 0.05$).
[#]Counted as unhatched embryos for percentage and statistical purposes.

affect embryos' survival only after hatching, as can be observed in Fig. 1. At 96 h no survival was observed at the highest tested concentration. The survival rate of exposed embryos dropped critically after 120 h of exposure with a 168 h-LC_{50} of 1.18 mg/L (Table S2, Fig. 1).

Additionally, FLX significantly affected the development of zebrafish embryos by inhibiting hatching and inducing loss of equilibrium. A dose response inhibition for the hatching time was observed at 48 h of exposure with EC_{50} value of 8.45 mg/L (Table 1). Significant differences in hatching were observed only for the highest tested concentration (15 mg/L, one-way ANOVA: $F_{6,\ 20} = 21.74$; $p < 0.001$). At 48 h, only 15% of the embryos hatched compared to 67% in the control group (Table 1).

The loss of equilibrium is represented by embryos side-lying in the bottom of the microplate well. This phenotype was first observed at 72 h of exposure with significant effect at the highest concentration tested, of 15 mg/L (one-way ANOVA: $F_{6,\ 20} = 38.99$; $p < 0.001$). At 96 h, the concentrations of 2.02 and 5.51 mg/L also affected the loss of equilibrium of hatched embryos (one-way ANOVA: $F_{6,\ 20} = 38.99$; $p < 0.001$). The effects on equilibrium progressively increased until the end of the test, as can be observed in Fig. 2. At 120 h, a loss of equilibrium was still observed at the concentration of 2.02 mg/L (one-way ANOVA: $F_{4,\ 14} = 19.43$; $p < 0.001$). However, all organisms died at the concentration of 5.51 mg/L. The loss of equilibrium remained for this concentration at 144 h and 168 h (one-way ANOVA: $F_{1,\ 10} = 70.32$; $p < 0.001$; one-way ANOVA: $F_{6,\ 20} = 38.99$; $p < 0.001$). A 168 h-EC_{50} of 1.02 mg/L was determined.

3.2. Locomotor behaviour

The Zebrabox results indicated that FLX induced changes in the swimming activity of zebrafish embryos (Fig. 3). Overall, the most pronounced effects were on TSD and TST, especially observed in higher exposure concentrations and intensified in higher exposure time.

FLX exposure caused a significant decrease in the total distance moved (TSD) of the larvae at all tested periods in concentrations ≥15.8 μg/L of FLX (Kruskal-Wallis: $H = 124.362$; $p < 0.001$) Fig. 3A–C. The effects of FLX on the TST are depicted in the Fig. 3D–F. At 120 h, a significant inhibition of TST was observed at lower concentrations (8.8, 15.8 μg/L); however, at the highest concentration (500 μg/L) there was a significant increase in TST (Kruskal-Wallis: $H = 62.276$; $p < 0.001$). At 144 h, a slight increase in the TST was observed at low concentrations, but no statistically significant differences were found in any treatment when compared to the control. (Kruskal-Wallis: $H = 10.299$; $p < 0.067$). At 168 h a significant decrease in TST was observed at the highest tested concentration. (Kruskal-Wallis: $H = 24.565$; $p < 0.001$).

3.3. Biomarkers

The effects of FLX on AChE, using ASCh and PSCh as substrates, are showed in Fig. 4. In general, FLX caused a dose response inhibition in the activity of AChE after 168 h of exposure. AChE was significantly inhibited at concentrations ≥0.006 mg/L when compared to the control group in both assays with ASCh (one-way ANOVA: $F_{5,\ 66} = 8.08$; $p < 0.001$) and PSCh (one-way ANOVA: $F_{5,\ 62} = 5.88$; $p < 0.001$) as substrates.

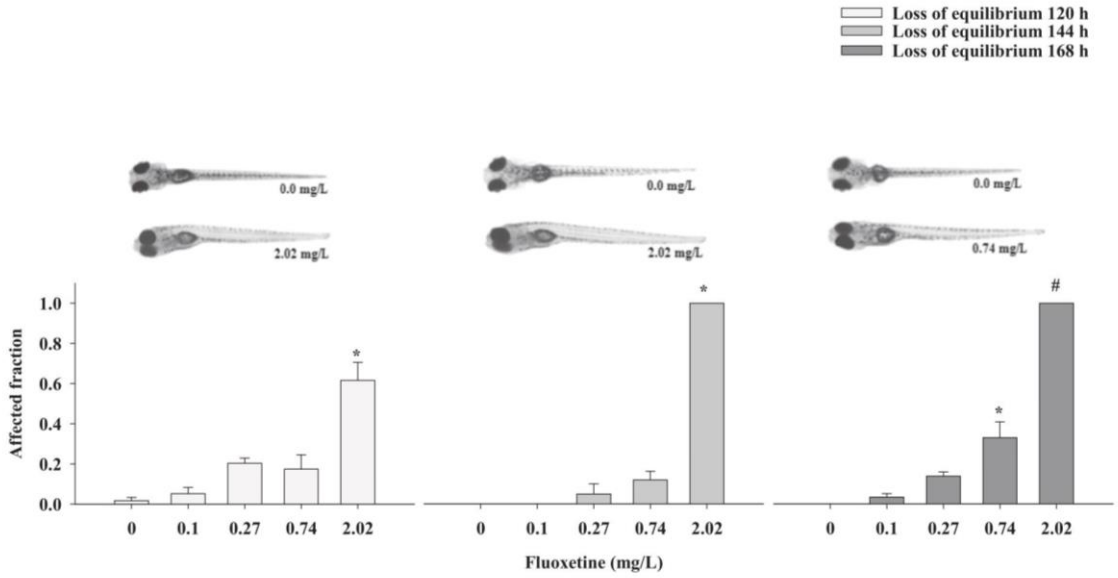

Fig. 2. Effects of FLX on zebrafish equilibrium at 120, 144 and 168 h of exposure (mean value ± standard error). Loss of equilibrium is characterized by the fish side-laying at the bottom of the microplate wells. Asterisks denotes statistical significance ($p < 0.05$), # denotes concentrations where 100% mortality occurred.

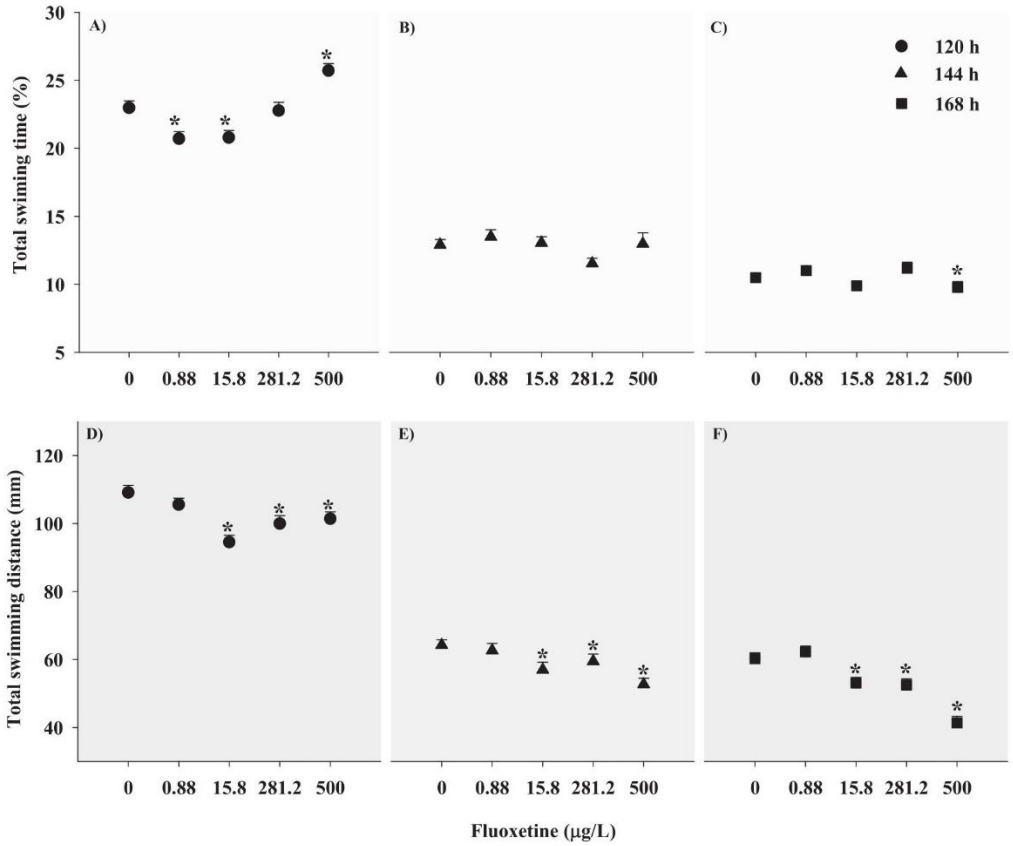

Fig. 3. Total swimming time (TST) and total swimming distance (TSD) travelled after exposure to FLX: (A) TST after 120 h; (B) TST after 144 h; (C) TST after 168 h; (D) TSD after 120 h; (E) TSD after 144 h; (F) TSD after 168 h. Asterisks denote statistical significance when compared to control group ($p < 0.05$).

4. Discussion

FLX had a significant impact on the survival of embryos. Mortality was concentration and time dependent with a 168 h-LC_{50} value of 1.18 mg/L. These results are in line with the findings of other studies (Table S2). LC_{50} values for eight different species of fish gathered from the literature vary from 0.164 to 2 mg/L, and an HC_{50} value of 1000 μg/L was calculated (Fig. 5), similar to the lethal concentration obtained in our study. In a particular study also conducted with zebrafish, a lower acute toxicity of FLX value was found with a 96 h-LC_{50} of 0.25 mg/L (Alsop and Wood, 2013). However, this study was carried out with zebrafish larvae at 4–8 days post fertilization. This developmental stage is more sensitive than embryos, as demonstrated by several previous studies comparing different zebrafish developmental stages (Domingues et al., 2010; Kristofco et al., 2018; Oliveira et al., 2016; Voelker et al., 2007).

Hatching is a critical period of zebrafish embryo development and has been widely used as an endpoint in fish early life stage tests. In this study, hatching was significantly delayed at 48 h in embryos exposed to concentrations above 5.51 mg/L, but among 98 and 100% of the

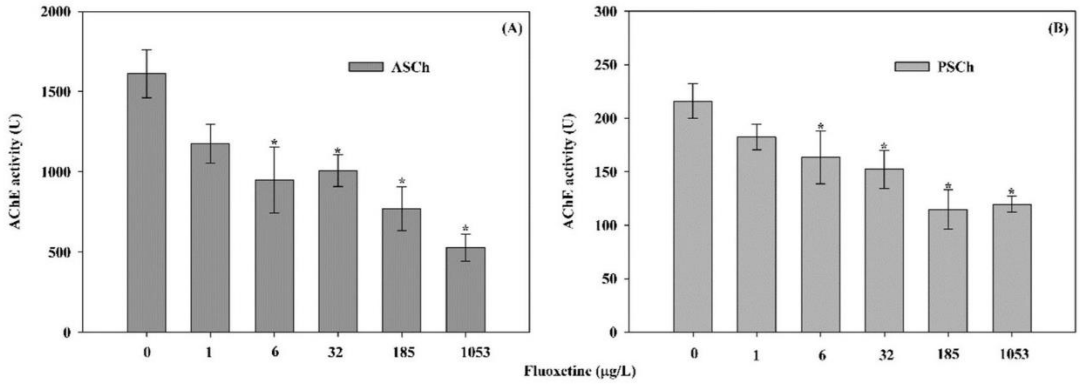

Fig. 4. Fluoxetine effects on cholinesterase activity of zebrafish embryos after 168 h of exposure to FLX (mean values ± standard error). (A) Assay with acetylcholine (ASCh); (B) assay using propionylcholine (PSCh). Asterisks denote statistical significance when compared to control group ($p < 0.05$).

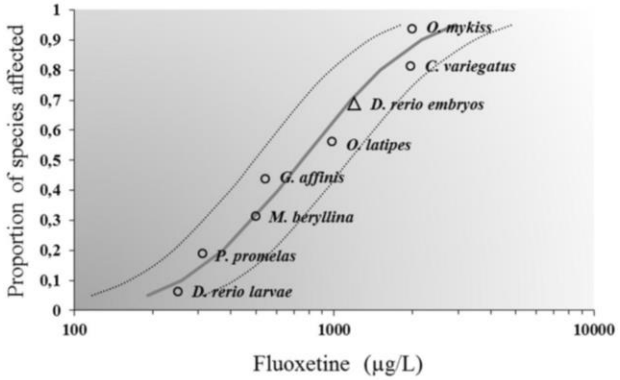

Fig. 5. Species sensitivity distribution (SSD) plot of short-term toxicity data for several fish species versus fluoxetine concentration. Triangle represents own data and the circles other fish species. The dotted line denotes upper and lower limits.

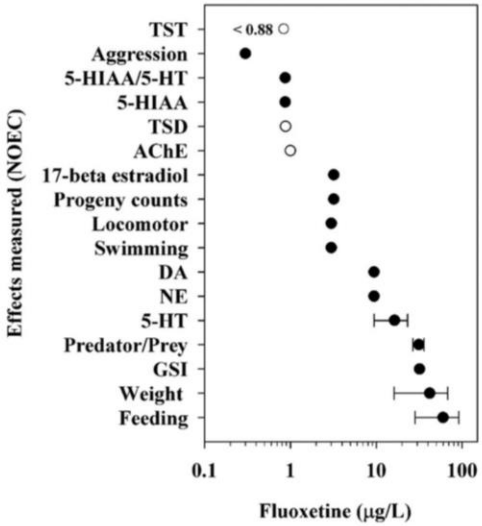

Fig. 6. An overview of No Observed Effect Concentration (NOEC) of fluoxetine on sub-lethal endpoints of different fish species (mean values ± standard error). Abbreviations: TST = Total swimming time, TSD = Total swimming distance, AChE = Acetylcholinesterase, DA = Dopamine, NE = Norepinephrine. Open circles means our own results.

embryos hatched at 72 h observation period. Three main mechanisms are involved in the hatching process of zebrafish: the embryo's movement inside the egg, the activity of the hatching chorionase enzyme and osmotic rupture (Hallare et al., 2005; Schoots et al., 1983). Embryos cannot break the corium barrier if the effects of the chemical on growth or developmental abnormalities are too severe. Although the movement of embryos inside the eggs was not measured in the present study, FLX exposure caused progressive loss of equilibrium of embryos after hatching (Fig. 2). Analysing the earlier locomotor stages, namely spontaneous coiling, evoked coiling, and burst swimming, Airhart et al. (2007) showed no effect of FLX in those parameters at the concentration of 1.42 mg/L. One could speculate that the higher FLX concentrations used in our study (5.51 mg/L) may have caused an inhibition of muscular movements, reducing the ability of the embryo to break the egg shell. However, further studies are necessary to corroborate this hypothesis.

Overall exposure to FLX showed to also impact the locomotor response of hatched organisms. Generally, a significant decrease in TDS was observed at the highest tested concentrations. Our results are in agreement with previous literature investigating the effects of FLX on locomotor behaviour of fish early life stages (Table S3). Airhart et al. (2007) also reported a decrease in swimming activity of zebrafish larvae (1–5 dpf) after exposure to FLX (NOEC of ~700 µg/L). Likewise, Prieto et al. (2012) showed that zebrafish embryos exposed to 15.8 µg/L of FLX exhibited a significant decrease in swimming activity. On the other hand, regarding the parameter TST, a biphasic effect of FLX was observed: very low concentrations caused a decrease, while the highest tested concentration caused an increase. A biphasic effect of the psychiatric drug valproate on zebrafish larvae locomotor activity has also been reported, where low concentrations resulted in hyperactive larvae and high concentrations resulted in hypoactive larvae (Cowden et al., 2012). Maximino et al. (2011) also reported a biphasic effect in a study with zebrafish adults exposed to ethanol, where both anxiety and locomotion patterns were affected at different concentration levels. Biphasic effects of psychiatric drugs are widely described in mammal toxicology, including in humans. Since our results suggest a non-dose response pattern for fish early life stages, further studies might address this topic and the consequences for the risk evaluation of psychiatric drugs in aquatic biota.

Impairment of locomotor behaviour might be related to neurological alterations in neurotransmission mediated by toxic agents. Previous studies (Fig. 6, Table S3), reported that exposure to low concentrations of FLX affected the activity of different neurotransmitters, such as serotonin, dopamine and norepinephrine. A decrease in cholinesterase activity can cause progressive myopathy of skeletal muscles and consequently loss of motility (Tierney, 2011). This may be the case for FLX, as our results showed that exposure to concentrations equal to or above 6 µg/L (Fig. 4) caused a significant inhibition of AChE activity, corroborating the reduced locomotor behaviour profile exhibited by zebrafish larvae (Fig. 3). Our results suggest a link between the decrease of AChE and locomotor activity of hatched embryos, but future measurement of acetylcholine neurotransmitters might be performed to corroborate this hypotheses. Others neurological mechanisms may also be involved in the behaviour alterations caused by FLX exposure. It is already established that serotonin plays an important role in modulating locomotor behaviour in a wide range of vertebrates. Studies conducted in adult teleosts, including zebrafish, have shown an inverse relationship between serotonin levels and spontaneous swimming activity. In the study carried out by Airhart et al. (2007) the reduced locomotor activity observed in zebrafish larvae was correlated with a decrease in two serotonin receptor transcripts (SERT – serotonin transporter protein and 5-HT_{1A} – serotonin 1A receptor transcript) in spinal cord after exposure to FLX. The AChE activity assay is a biochemical, cost-effective technique widely used for toxicity assessment of organophosphorus and carbamate pesticides. Our data suggest a similar sensitivity of cholinergic and serotoninergic markers, suggesting AChE as a viable option for a biomarker for assessing FLX effects.

As shown in Fig. 7, the parameter swimming behaviour is several orders of magnitude more sensitive than developmental parameters and molecular markers reported in this paper. Likewise, when comparing the 'No Observed Effect Concentrations' (NOEC) of several endpoints analysed in other studies from the literature (Fig. 7), swimming behaviour is also the most sensitive parameter. Nonetheless, effects at lower concentrations such as behaviour tend to be disregarded in the current environmental risk assessment practices, which raise a special concern for drugs like FLX (Brodin et al., 2014). Disruption of the developmental process and behaviour alterations caused by these drugs may have negative long-term ecological consequences (Brodin et al., 2014). Therefore, the development of behaviour protocols for the assessment of psychiatric drugs providing parameters that reflect a more realistic exposure scenario could help to improve our knowledge on its effects on aquatic life.

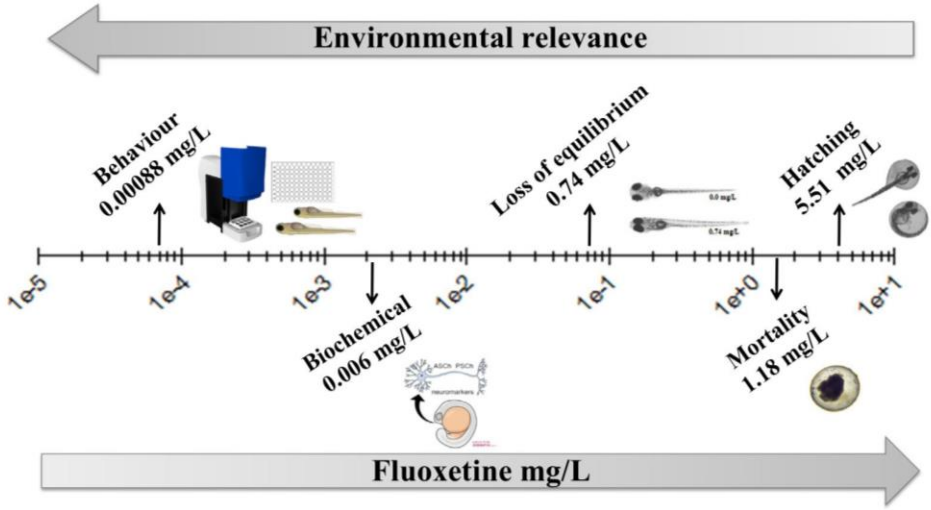

Fig. 7. Comparative sensitivity of measured parameters used in the present study to assess the toxicity of fluoxetine to zebrafish embryos. Values between brackets are LOEC (Lowest Observed Effect Concentrations) and LC_{50} (Lethal concentration 50%) for mortality.

5. Ecological relevance

In general, exposure to environmental chemical compounds does not result in obvious morphological changes, but rather subtle changes at the molecular level, making the effects of exposure difficult to identify and characterize. In fact, our results from the fish embryo toxicity assays demonstrated that FLX is toxic to zebrafish embryos. Exposure to a range of sub-lethal FLX concentrations affected the locomotor activity at environmentally relevant concentrations (0.88 µg/L), with results supported by molecular changes in AChE activity (LOEC < 6 µg/L, Fig. 7). Alterations in swimming behaviour are a particularly important type of response in the ecosystem, since they are related to individual fitness of the organisms and may originate disruption of capability for predator avoidance and feeding, ultimately leading to lower survival rates in the environment (Brodin et al., 2014). Our results are supported by different studies showing that FLX induces alterations in different behavioural traits in exposed fish, such as aggression, predator/prey relationship, feeding, progeny counts, swimming and locomotor activity (Table S3). Adverse effects of FLX on the individual fitness might compromise ecological traits of fish populations such as aggression, boldness, exploration and sociality (Brodin et al., 2014). Thus, altogether, these studies suggest that FLX contamination would cause ecological imbalance in aquatic systems.

6. Conclusion

In summary, FLX caused developmental and neurotoxic effects on zebrafish early life-stages after a short-term exposure. No observed effect concentration for locomotor and acetylcholinesterase activity are in the same range of FLX concentration often detected in environmental samples, suggesting that ecological traits of fish early life stages can be impaired in realistic scenarios of exposure. To improve our findings, future research should focus on toxicity assessment in a chronic exposure scenario at the population level, to unravel how the observed behavioural alterations in the individual fish during early life stages may translate into a direct ecological effect on aquatic communities.

Acknowledgements

The authors are grateful to the Brazilian Ministry of Education and Ministry of Science and Technology of Brazil for the scholarship provided to RO (CNPq BJT-A/PNPD CAPES); DSM for CAPES PhD scholarship. CKG for CNPq research grant 305741/2015-2; NFO and RCS for CNPq PIBIC scholarship. FAPDF for TSA research grant (1250/2016) and project funding call 05/2016 - “Micropoluentes emergentes e o uso da água na Bacia do Paranoá: diagnóstico, identificação de fontes, efeitos tóxicos métodos de remoção e de detecção in situ”.**Ethical standards**

The experiments are in accordance with the current laws of the country in which they were performed. The study was approved by the ethics committee at the University of Brasilia (protocol n.100226/2014).

Conflict of interest

The authors declare that they have no conflict of interest.

Appendix A. Supplementary data

Supplementary data to this article can be found online at https://doi.org/10.1016/j.cbpc.2018.08.009.

References

Airhart, M.J., Lee, D.H., Wilson, T.D., Miller, B.E., Miller, M.N., Skalko, R.G., 2007. Movement disorders and neurochemical changes in zebrafish larvae after bath exposure to fluoxetine (PROZAC). Neurotoxicol. Teratol. 29, 652–664. https://doi.org/10.1016/j.ntt.2007.07.005.

Alsop, D., Wood, C.M., 2013. Metal and pharmaceutical mixtures: is ion loss the mechanism underlying acute toxicity and widespread additive toxicity in zebrafish? Aquat. Toxicol. 140–141, 257–267. https://doi.org/10.1016/j.aquatox.2013.05.021.

Andrade, T.S., Henriques, J.F., Almeida, A.R., Machado, A.L., Koba, O., Giang, P.T., Soares, A.M.V.M., Domingues, I., 2015. Carbendazim exposure induces developmental, biochemical and behavioural disturbance in zebrafish embryos. Aquat. Toxicol. 170, 390–399. https://doi.org/10.1016/j.aquatox.2015.11.017.

Aus Der Beek, T., Weber, F.-A., Bergmann, A., Hickmann, S., Ebert, I., Hein, A., Küster, A., 2015. Pharmaceuticals in the environment - global occurrences and perspectives. Environ. Toxicol. Chem. 35, 823–835. https://doi.org/10.1002/etc.3339.

Berg, C., Backström, T., Winberg, S., Lindberg, R., Brandt, I., 2013. Developmental exposure to fluoxetine modulates the serotonin system in hypothalamus. PLoS One 8. https://doi.org/10.1371/journal.pone.0055053.

Bradford, M., 1976. Rapid and sensitive method for quantification of microgram quantities of protein utilizing principle of protein-dye-binding. Anal. Biochem. 72, 248–254.

Brodin, T., Piovano, S., Fick, J., Klaminder, J., Heynen, M., Heynen, M., Jonsson, M., 2014. Ecological effects of pharmaceuticals in aquatic systems - impacts through behavioural alterations. Philos. Trans. R. Soc. B 369, 20130580. https://doi.org/10.1098/rstb.2013.0580.

Bueno, M.J., Aguera, A., Gomez, M.J., Hernando, M.D., Garcia-Reyes, J.F., Fernandez-Alba, A.R., 2007. Application of liquid chromatography/quadrupole-linear ion trap mass spectrometry and time-of-flight mass spectrometry to the determination of pharmaceuticals and related contaminants in wastewater. Anal. Chem. 79, 9372–9384. https://doi.org/10.1021/ac0715672.

Costagliola, C., Parmeggiani, F., Semeraro, F., Sebastiani, A., 2008. Selective serotonin reuptake inhibitors: a review of its effects on intraocular pressure. Curr. Neuropharmacol. 6, 293–310. https://doi.org/10.2174/157015908787386104.

Cowden, J., Padnos, B., Hunter, D., Macphail, R., Jensen, K., Padilla, S., 2012. Developmental exposure to valproate and ethanol alters locomotor activity and retino-tectal projection area in zebrafish embryos. Reprod. Toxicol. 33, 165–173. https://doi.org/10.1016/j.reprotox.2011.11.111.

Domingues, I., Oliveira, R., Lourenço, J., Koppe, C., Mendo, S., Soares, A.M.V.M., 2010. Biomarkers as a tool to assess effects of chromium (VI): comparison of responses in zebra fish early life stages and adults. Comp. Biochem. Physiol. C 152, 338–345. https://doi.org/10.1016/j.cbpc.2010.05.010.

Ellman, G.L., Courtney, K.D., Andres Jr., V., Featherstone, R.M., 1961. A new rapid colorimetric determination of acetylcholinesterase activity. Biochem. Pharmacol. 7, 88–95. https://doi.org/10.1016/0006-2952(61)90145-9.

Fent, K., Weston, A.A., Caminada, D., 2006. Ecotoxicology of human pharmaceuticals. Aquat. Toxicol. 76, 122–159. https://doi.org/10.1016/j.aquatox.2005.09.009.

Ford, A.T., Fong, P.P., 2015. The effects of antidepressants appear to be rapid and at environmentally relevant concentrations. Environ. Toxicol. Chem. 35, 794–798. https://doi.org/10.1002/etc.3087.

Gunnarsson, L., Jauhiainen, A., Kristiansson, E., Nerman, O., Larsson, D.G.J., 2008. Evolutionary conservation of human drug targets in organisms used for environmental risk assessments. Environ. Sci. Technol. 42, 5807–5813. https://doi.org/10.1021/es8005173.

Hallare, a.V., Schirling, M., Luckenbach, T., Köhler, H.-R., Triebskorn, R., 2005. Combined effects of temperature and cadmium on developmental parameters and biomarker responses in zebrafish (*Danio rerio*) embryos. J. Therm. Biol. 30, 7–17. https://doi.org/10.1016/j.jtherbio.2004.06.002.

Heberer, T., Heberer, T., 2002. Occurrence, fate, and removal of pharmaceutical residues in the aquatic environment: a review of recent research data. Toxicol. Lett. 131, 5–17. https://doi.org/10.1016/S0378-4274(02)00041-3.

Henriques, J.F., Almeida, A.R., Andrade, T., Koba, O., Golovko, O., Soares, A.M.V.M., Oliveira, M., Domingues, I., 2015. Effects of the lipid regulator drug gemfibrozil: a toxicological and behavioral perspective. Aquat. Toxicol. https://doi.org/10.1016/j.aquatox.2015.09.017.

Henry, T.B., Black, M.C., 2008. Acute and chronic toxicity of fluoxetine (selective serotonin reuptake inhibitor) in western Mosquitofish. Arch. Environ. Contam. Toxicol. 54, 325–330. https://doi.org/10.1007/s00244-007-9018-0.

Hernando, M.D., Mezcua, M., Fernández-Alba, A.R., Barceló, D., 2006. Environmental risk assessment of pharmaceutical residues in wastewater effluents, surface waters and sediments. Talanta 69, 334–342. https://doi.org/10.1016/j.talanta.2005.09.037.

Irons, T.D., MacPhail, R.C., Hunter, D.L., Padilla, S., 2010. Acute neuroactive drug exposures alter locomotor activity in larval zebrafish. Neurotoxicol. Teratol. 32, 84–90. https://doi.org/10.1016/j.ntt.2009.04.066.

ISO, 2007. 15088: Water Quality - Determination of the Acute Toxicity of Waste to Zebrafish Eggs (*Danio rerio*). Int. Stand.

Jesus, F.T., Oliveira, R., Silva, A., Catarino, A.L., Soares, A.M.V.M., Nogueira, A.J. a, Domingues, I., 2013. Lethal and sub lethal effects of the biocide chlorhexidine on aquatic organisms. Ecotoxicology 22, 1348–1358. https://doi.org/10.1007/s10646-013-1121-6.

Kimmel, C.B., Ballard, W.W., Kimmel, S.R., Ullmann, B., Schilling, T.F., 1995 Jul. Stages of embryonic development of the zebrafish. Dev. Dyn. 203, 253–310. https://doi.org/10.1002/aja.1002030302.

Klüver, 2015. Fish embryo toxicity test: identification of compounds with weak toxicity and analysis of behavioral effects to improve prediction of acute toxicity for neurotoxic compounds. Environ. Sci. Technol. 49, 7002–7011. https://doi.org/10.1021/acs.est.5b01910.

Kolpin, D.W., Furlong, E.T., Meyer, M.T., Thurman, E.M., Zaugg, S.D., Barber, L.B., Buxton, H.T., 2002. Pharmaceuticals, hormones, and other organic wastewater contaminants in U.S. streams, 1999–2000: a national reconnaissance. Environ. Sci. Technol. 36, 1202–1211. https://doi.org/10.1021/es011055j.

Kristofco, L.A., Haddad, S.P., Chambliss, C.K., Brooks, B.W., 2018. Differential uptake of and sensitivity to diphenhydramine in embryonic and larval zebrafish. Environ. Toxicol. Chem. 37, 1175–1181. https://doi.org/10.1002/etc.4068.

Lister, A., Regan, C., Van Zwol, J., Van Der Kraak, G., 2009. Inhibition of egg production in zebrafish by fluoxetine and municipal effluents: a mechanistic evaluation. Aquat. Toxicol. 95, 320–329. https://doi.org/10.1016/j.aquatox.2009.04.011.

Martínez Bueno, M.J., Agüera, A., Gómez, M.J., Hernando, M.D., García-Reyes, J.F., Fernández-Alba, A.R., 2007. Application of liquid chromatography/quadrupole-linear ion trap mass spectrometry and time-of-flight mass spectrometry to the determination of pharmaceuticals and related contaminants in wastewater. Anal. Chem. 79 (24), 9372–9384. https://doi.org/10.1021/ac0715672.

Maximino, C., da Silva, A.W.B., Gouveia, A., Herculano, A.M., 2011. Pharmacological analysis of zebrafish (*Danio rerio*) scototaxis. Prog. Neuro-Psychopharmacol. Biol. Psychiatry 35, 624–631. https://doi.org/10.1016/j.pnpbp.2011.01.006.

Metcalfe, C.D., Miao, X.-S., Koenig, B.G., Struger, J., 2003. Distribution of acidic and neutral drugs in surface waters near sewage treatment plants in the lower Great Lakes, Canada. Environ. Toxicol. Chem. 22, 2881–2889. https://doi.org/10.1897/02-627.

OECD, 2013. Test No. 236: Fish Embryo Acute Toxicity (FET) Test. OECD Guidel. Test. Chem. Sect. 2. OECD Publ., pp. 1–22. https://doi.org/10.1787/9789264203709-en.

Oliveira, R., Grisolia, C.K., Monteiro, M.S., Soares, A.M., Domingues, I., 2016. Multilevel assessment of ivermectin effects using different zebrafish life stages. Comp. Biochem. Physiol. C 187, 50–61. https://doi.org/10.1016/j.cbpc.2016.04.004.

Padilla, S., Hunter, D.L., Padnos, B., Frady, S., MacPhail, R.C., 2011. Assessing locomotor activity in larval zebrafish: influence of extrinsic and intrinsic variables. Neurotoxicol. Teratol. 33, 624–630. https://doi.org/10.1016/j.ntt.2011.08.005.

Prieto, M.J., Gutierrez, H.C., Arévalo, R.A., Chiaramoni, N.S., del Valle Alonso, S., 2012. Effect of risperidone and fluoxetine on the movement and neurochemical changes of zebrafish. Open J. Med. Chem. 2, 129–138. https://doi.org/10.4236/ojmc.2012.24016.

Sabbioni, C., Bugamelli, F., Varani, G., Mercolini, L., Musenga, A., Saracino, M.A., Fanali, S., Raggi, M.A., 2004. A rapid HPLC-DAD method for the analysis of fluoxetine and norfluoxetine in plasma from overdose patients. J. Pharm. Biomed. Anal. 36, 351–356. https://doi.org/10.1016/j.jpba.2004.06.008.

Scholz, S., Fischer, S., Gündel, U., 2008. The zebrafish embryo model in environmental risk assessment - applications beyond acute toxicity testing. Environ. Sci. Pollut. Res. Int. 15, 394–404. https://doi.org/10.1007/s11356-008-0018-z.

Schoots, A.F.M., Meijer, R.C., Denucb, J.M., 1983. Dopaminergic regulation of hatching in fish embryos. Dev. Biol. 63, 59–63. https://doi.org/10.1016/0012-1606(83)90200-2.

SPSS, 2004. Sigma Stat for Windows (Version 3.10).

Stewart, A.M., Grossman, L., Nguyen, M., Maximino, C., Rosemberg, D.B., Echevarria, D.J., Kalueff, A.V., 2014. Aquatic toxicology of fluoxetine: understanding the knowns and the unknowns. Aquat. Toxicol. https://doi.org/10.1016/j.aquatox.2014.08.014.

Tierney, K.B., 2011. Behavioural assessments of neurotoxic effects and neurodegeneration in zebrafish. Biochim. Biophys. Acta Mol. basis Dis. 1812, 381–389. https://doi.org/10.1016/j.bbadis.2010.10.011.

USEPA, 2018. Pesticide Ecotoxicity Database, Formerly: Environmental Effects Database (EEDB). Environ Fate Eff Div US EPA.

Voelker, D., Vess, C., Tillmann, M., Nagel, R., Otto, G.W., Geisler, R., Schirmer, K., Scholz, S., 2007. Differential gene expression as a toxicant-sensitive endpoint in zebrafish embryos and larvae. Aquat. Toxicol. 81, 355–364. https://doi.org/10.1016/j.aquatox.2006.12.013.

Weinberger, J., Klaper, R., 2014. Environmental concentrations of the selective serotonin reuptake inhibitor fluoxetine impact specific behaviors involved in reproduction, feeding and predator avoidance in the fish *Pimephales promelas* (fathead minnow). Aquat. Toxicol. 151, 77–83. https://doi.org/10.1016/j.aquatox.2013.10.012.

Weis, J.S., 2014. Delayed behavioral effects of early life toxicant exposures in aquatic biota. Toxics 2, 165–187. https://doi.org/10.3390/toxics2020165.

Ecotoxicology and Environmental Safety 164 (2018) 297–304

Contents lists available at ScienceDirect

Ecotoxicology and Environmental Safety

journal homepage: www.elsevier.com/locate/ecoenv

Chronic effects of carbamazepine on zebrafish: Behavioral, reproductive and biochemical endpoints

Niedja da Silva Santos[a], Rhaul Oliveira[b,c,d], Carolina Almeida Lisboa[b], Joana Mona e Pinto[b], Diego Sousa-Moura[b], Níchollas Serafim Camargo[e], Vitória Perillo[b], Miguel Oliveira[a,*], Cesar Koppe Grisolia[b], Inês Domingues[a]

[a] Departamento de Biologia e CESAM, Universidade de Aveiro, Campus Universitário de Santiago, 3810-193 Aveiro, Portugal
[b] Laboratório de Genética Toxicológica, Departamento de Genética e Morfologia, Instituto de Ciências Biológicas, Universidade de Brasília, 70910-900 Brasília, Distrito Federal, Brasil
[c] Faculdade de Tecnologia, Universidade Estadual de Campinas, UNICAMP, 13484-332 Limeira, São Paulo, Brazil
[d] Programa de Pós-graduação em Toxicologia e Análises Toxicológicas, Faculdade de Ciências Farmacêuticas, Universidade de São Paulo, FCF – USP, 05508-000 São Paulo, Brazil
[e] Laboratório de Nanobiotecnologia, Departamento de Genética e Morfologia, Instituto de Ciências Biológicas, Universidade de Brasília, AsaNorte, 70910-900 Brasília, Distrito Federal, Brazil

ARTICLE INFO

Keywords:
Human pharmaceutical
Danio rerio
Behavior
Biochemical biomarkers
Histology

ABSTRACT

Carbamazepine (Cbz), one of the most prescribed pharmaceuticals in the world is often detected in surface waters and sediments. However, few studies addressed its chronic effects in fish. In the present study, *Danio rerio* adults were exposed for 63 days to Cbz (0 - control, 10 μg L^{-1} - concentration found in effluents, and 10,000 μg L^{-1} – 5% of LC_{50} at 72 h). Assessed endpoints were: feeding behavior, growth rate, number of eggs produced and their viability, histological alterations in female gonads, and biochemical biomarkers associated with antioxidant defenses (catalase - CAT, and glutathione *S*-transferase – GST activities), neurotransmission (acetylcholinesterase activity - AChE) and metabolism (lactate dehydrogenase - LDH). Cbz exposure increased the total time for food intake but did not affect *D. rerio* growth. Although the total number of eggs was not affected by Cbz exposure, the eggs viability was significantly impaired. Exposure to Cbz caused alterations in the female gonads follicular stages. In terms of biochemical endpoints, CAT activity in liver and gills, was sensitive to the pharmaceutical exposure presenting a decreased activity. AChE activity was induced in the head (both concentrations) and muscle (10,000 μg L^{-1}). GST activity was increased in gills (both concentrations) but inhibited in the intestine. Concerning LDH, enzymatic activity was increased in the liver and decreased in muscle and gills. Several of the above-mentioned effects can be directly linked with effects at population level (e.g. feeding behavior) and occurred at environmental concentrations (the lowest concentration tested), thus serious concerns regarding risks posed by Cbz residues to fish populations arise with this study.

1. Introduction

Pharmaceuticals are currently considered emerging contaminants of concern (Santos et al., 2010) mainly due to their increased production, consumption and presence in the environment allied with a biological active nature and potential noxious effects in the living organisms (Palacios-Rosas and Castro-Pastrana, 2017). Most of these compounds and their metabolites are not efficiently removed or biodegraded in the sewage treatment plants (Martins et al., 2012). Once in the environment pharmaceuticals residues may undergo bioaccumulation (Deblonde et al., 2011) and/or act on aquatic organisms, especially fish which have highly conserved physiological features compared to humans (Kreke and Dietrich, 2008; LaLone et al., 2013), for whom drugs have been designed. Carbamazepine (Cbz) is an anticonvulsant prescribed for the treatment of psychomotor epilepsy, bipolar disorder, and trigeminal neuralgia (Calcagno et al., 2016). It is known to interact with potassium and sodium channels and several signaling pathways (Ayano, 2016) and to modulate voltage gated sodium channels that will decrease the neuronal activity (Galus et al., 2014). In the liver, the main biotransformation organ, Cbz is converted into Cbz 10,11- epoxide and other derivatives (Villanueva et al., 2018). Cbz has a high distribution and abundance in the aquatic environment (Oropesa et al., 2016; Pires

* Corresponding author.
E-mail address: migueloliveira@ua.pt (M. Oliveira).

https://doi.org/10.1016/j.ecoenv.2018.08.015
Received 28 May 2018; Received in revised form 19 July 2018; Accepted 2 August 2018

et al., 2016), being found in wastewater treatment plants effluents, surface waters, and soils (Oliveira et al., 2015). Only 10% of Cbz is removed in wastewater treatment plants (Chen et al., 2014), presenting a low degradation rate in the environment (Pires et al., 2016) with a permanency time in the aquatic environment of around 82 days (Brandão et al., 2013). It can also be bioaccumulated and bioconcentrated (Oropesa et al., 2016).

Carbamazepine has been widely detected in waste waters and surface waters. For instance, a study performed in Republic of Korea monitored influents and effluents from municipal, hospital, livestock and pharmaceutical waste water treatment plants. Maximum concentrations of Cbz found in these effluents were 21.0, 14.4, 10.2 and 150 $\mu g\,L^{-1}$ respectively (Sim et al., 2011). In the "EU Wide Monitoring Survey of Polar Persistent Pollutants in European River Waters", Cbz was one of the most frequently detected contaminants in the 122 river analyzed with a highest maximum concentration found of 12 $\mu g\,L^{-1}$ (Loos et al., 2009).

Although some studies have been performed in the last years to understand lethal and sublethal effects of Cbz on aquatic organisms like algae, cladocerans and fish (Parker, 2015; Oropesa et al., 2016) there is still a lack of knowledge concerning chronic effects (Deblonde et al., 2011). The reported chronic effects in fish include decreased embryo production, irregularities in oocytes, somatic stromal tissue and decreased plasma sex steroids in adult zebrafish (*Danio rerio*) (Galus et al., 2013); decreased motility and sperm velocity and decreased superoxide dismutase, glutathione peroxidase and glutathione reductase activity and lipid peroxidation in sperm of the common carp (*Cyprinus carpio*; Li et al., 2010a); lipid peroxidation in the brain and decreased superoxide dismutase and glutathione reductase, with glutathione peroxidase and CAT presenting a non-linear response over time with an increase followed by a decrease in their activities (Li et al., 2010b).

Therefore, the aim of the study was to perform a multi-level evaluation of the chronic effects of Cbz on adult zebrafish focusing on growth, reproduction, feeding behavior, biochemistry in gills, liver and intestine, genotoxicity on erythrocytes and histopathology in female gonads. The working hypothesis is that chronic exposure to carbamazepine will induce biochemical alterations leading to behavioral and reproductive effects.

2. Materials and methods

2.1. Test chemicals and chemical analysis

Carbamazepine (Cbz) (CAS 298-46-4) was purchased from Sigma-Aldrich. All other reagents were analytical grade.

A stock solution was prepared by dissolving 200 mg of Cbz in 4 L of culture water; dissolution of the compound was promoted by sonicating the solution for 30 min. Test solutions were obtained by dilution of the stock with culture water. Carbamazepine samples were analyzed to confirm the stability of Cbz under the experimental conditions. Thus, 5 L aquaria containing 10,000 $\mu g\,L^{-1}$ of test solution, the highest concentration tested, were kept under conditions similar to the experimental tanks with fish (light and temperature) and daily, 100 ml of water from each aquarium were collected for High Performance Liquid Chromatography (HPLC Shimadzu-Prominence) following the method described by Demirkaya and Kadioğlu (2005) (See details in Suppl. Material, Fig. S1, Tables S1 and S2).

2.2. Test organisms

Sexually mature fish zebrafish (*D. rerio*), of six months, were purchased from ZAIA (Brasilia) and acclimated for 40 days to laboratory conditions. The fish average weight was of 0.51 (± 0.013) g for females and 0.34 (± 0.008) g for males. Culture water was obtained by reverse osmosis and the conductivity adjusted to 550 (± 100) μS, by adding salt "Aquarium Systems" (USA). Water temperature was kept at 26.0 (± 1) °C, pH at 7.5 (± 0.5), and dissolved oxygen equal or above 99% saturation. A 12:12 h (light: dark) photoperiod cycle was maintained. Fish were fed twice a day with commercially diet (TetraMin fish food, EUA).

2.3. Experimental design

The test procedure generally followed OECD guideline 215 (OECD, 2000) and was performed under conditions similar to acclimation.

Males and females were randomly distributed into nine experimental tanks, containing 5 L of the test solution (nominal concentrations: 0, 10 or 10,000 $\mu g\,L^{-1}$ of Cbz). Three replicates (with 10 fish each) were used per treatment. The lowest Cbz concentration tested, 10 $\mu g\,L^{-1}$, was selected based on a concentration reported in a wastewater treatment plant in lake Paranoá (Gunthert et al., 2014) - 11.3 $\mu g\,L^{-1}$. The highest concentration, 10,000 $\mu g\,L^{-1}$, corresponds to approximately 5% of Cbz lethal concentration value (LC_{50}) after 72 h of exposure (Van den Brandhof and Montforts, 2010). Animals were exposed for 63 days and fed once a day with a quantity of TetraMin fish food (EUA) corresponding to 2% of the fish weight in the aquarium. Test media was renewed every three days. Water quality parameters were kept within the ranges described in Section 2.2.

Fish weight (Section 2.3.1) and feeding behavior (Section 2.3.2) were evaluated at days 21, 42 and 63 of exposure. At days 23, 27, 35, 42, 47, 54 and 61, fish were allowed to reproduce to assess reproductive output (number of eggs and its viability). Zebrafish reproductive behavior can be observed, in their natural environment, at dawn. Thus, to obtain eggs, before the lights turned on in the lab fish were transferred from the exposure vessels to aquaria with culture water, marbles and plants and left in these conditions for mating for two hours after the lights turned on. Fish were then returned to the exposure aquaria, marbles (which were used to avoid predation of the eggs by fish) were removed and eggs carefully collected with the help of a net and washed in culture water. Approximately 2.5 h after egg collection they were examined under a stereomicroscope to determine their total number and condition (fertilized/viable or not). Eggs were considered fertilized and viable if they were in the expected developmental stage for that observation time (blastula stage according to Kimmel et al., 1995).

At the 63rd day of exposure, fish were sacrificed, peripheral blood collected and smears prepared for micronuclei and other nuclear abnormalities assessment (12 animals; Section 2.3.3). Head, gills, liver, muscle, and intestine of each fish were isolated and frozen in microtubes containing phosphate buffer, pH 7.4 for biochemical analyses (21animals; Section 2.3.4). These samples were stored at −80 °C until analysis. Nine female organisms per treatment were used for histology. Animals were sacrificed on ice, the whole-body fixed with Davidson solution during 24 h and preserved in 70% ethanol for histological analysis (Section 2.3.5).

2.3.1. Fish weight determination

The weight of each fish was determined by transferring it, with the help of a net, to a glass beaker containing approximately 60 ml culture water placed in a digital scale (0.001 g). Before weighing the fish were fasted for 24 h.

2.3.2. Feeding behavior

Feeding behavior was assessed by transferring from each tank 5 fish to an aquarium containing culture water and by adding 6 granules of TetraMin, based on the methods described by Domingues et al. (2016). The time taken until the first feeding action and for the total intake of food (up to a maximum of 20 min - min) was recorded.

2.3.3. Micronuclei and others nuclear abnormalities assessment

The assessment of micronuclei and other nuclear abnormalities generally followed the methodology established by Hooftman and de Raat (1982) for fish erythrocytes. Approximately 20 μL of peripheral

blood were collected with a heparinized pipette tip and a smear immediately performed. The slides were fixed in methanol for 20 min, allowed to dry and stained in Giemsa (20%). The stained slides were observed under an optic microscope with a magnification of 1000 x and the cells analyzed to detect the presence of micronuclei and other nuclear abnormalities such as binucleated cells, blebbed nuclei, lobed nuclei and notched nuclei (Carrasco et al., 1990; Fenech et al., 2003) on a total of 1000 cells per slide.

2.3.4. Biochemical determinations

On the analysis day, samples were thawed, homogenized by an ultrasonic cell disruptor (Bronson Ultrassonic Sonifier 450, Danbury, US) and centrifuged (4 °C, 10,000g, 20 min) to isolate the post-mitochondrial supernatant (PMS). All the enzymatic activities were measured using a microplate reader (Spectra Max M2 - Molecular Devices) and expressed as unit (U). A U corresponds to a nanomol of substrate hydrolyzed per min per milligram of protein. The protein content of the samples was determined by the Bradford method (1976) using γ-globulin as standard.

AChE activity was determined in the muscle and head, using acetylcholine as substrate and measuring the conjugation product between thiocholine (a product of the degradation of acetylthiocholine) and 5,5-dithiobis-2-nitrobenzoic acid (DTNB) (absorbance increase), at 414 nm (nm), every 40 s (sec), for 5 min, based on the method of Ellman et al. (1961). Activity was determined using 50 µL of PMS and 250 µL of reaction mixture (acetylthiocholine (7.5 mM), DTNB (10 mM) in potassium-phosphate buffer (0.1 M, pH 7.2)).

CAT activity was determined in PMS of gills and liver by monitoring at 240 nm the decrease in absorbance (every 40 s, for 5 min) due to degradation of H_2O_2, as described by Claiborne (1985). A PMS volume of 50 µL for gills or 20 µL for liver was mixed with respectively 250 µL or 130 µL of reaction mixture (666 µL H_2O_2 (30 mM) in 200 ml of potassium phosphate buffer (0.05 M, pH 7.0)).

GST activity was determined in gills, liver and intestine according to the methodology described by Habig and Jakoby (1981) adapted to microplate by Frasco and Guilhermino (2002). The GST activity was measured at 340 nm, monitoring the increase in absorbance in 40 s intervals for 5 min. To determine the GST activity in the liver and intestine 50 µL of PMS were mixed with 150 µL of reaction mixture (reduced glutathione (10 mM) and 1-chloro- 2.4-dinitrobenzene (60 mM) in potassium-phosphate buffer (0.05 M, pH 6.5)), whereas for gills 50 µL of PMS were mixed with 250 µL of reaction mixture.

LDH activity was measured in gills, liver and muscle according to the methodology described by Vassault (1983), adapted to microplate by Diamantino et al. (2001). In the liver and intestine, 15 µL of PMS, 25 µL of buffer Tris-NaCl (0.1 M, pH 7.2) and 125 µL of nicotinamide adenine dinucleotide reduced (NADH) (300 µM) were added to 20 µL of pyruvate (4.5 mM). For gills and muscle, the test was performed with 25 µL of PMS, 25 µL of buffer Tris-NaCl (0.1 M, pH 7,2), 250 µL NADH (300 µM) and 40 µL pyruvate (4.5 mM). Reading was performed at 340 nm at intervals of 40 s for 5 min, following a decrease of absorbance resulting from oxidation of NADH.

2.3.5. Ovarian follicle analysis

For histology, standard procedures of paraffin inclusion, alcoholic dehydration, xylol diaphanization were followed. Paraffin embedded zebrafish were sectioned in the median plane, sectioned in 3 – 6 µm sections, stained with hematoxylin and eosin staining and examined individually using a Zeiss Axioskop 2 optical microscope (Carl Zeiss, Hallbergmoos, Germany). Ovarian of females were analyzed for follicle stages, classified as defined on Menke Aswin et al. (2011) as oogonia, pre-vitellogenic follicle, vitellogenic follicle and pre ovulatory follicle.

2.4. Statistical analysis

Growth rate was calculated and presented as “pseudo” specific growth rate (r) according to the equation (OECD, 2000):

$$r: \frac{\log_e w2 - \log_e \bar{w}1}{t2 - t1} \times 100$$

where:

$\log_e \bar{w}1$ = average of the logarithms of the values w1 for the fish in the tank at the start of the experiment;
$\log_e w2$ = logarithm of the weight of an individual fish at the end of the experiment;
t1, t2 = time (days) at start and end of study period.

The Sigma plot 12.5 statistical package (Sigma Stat) was used for all statistical analyses. The data from growth, feeding behavior, reproduction, genotoxicity, biochemical endpoints and follicular composition were analyzed for normality and homoscedasticity. When normality and homoscedasticity of data were verified the one-way ANOVA was performed followed by the multiple comparison Dunnett's test to assess differences towards control; otherwise the non-parametric Kruskall-Wallis (or one-way ANOVA on ranks) was done followed by the multiple comparison Dunn's test. All statistical analyses were performed with a significance level of 0.05.

3. Results

No mortality was found during the experimental assay at any of the tested conditions (controls or Cbz exposed fish).

3.1. Chemical analysis

The chemical analysis demonstrated that Cbz presented a high stability in the test medium over a seven days period (Table S1), an indication that changing media every three days maintains the animals at the desired concentration. The concentrations of Cbz in the analyzed stock solutions presented a maximum variation of 13.16% of the nominal concentration. (Table S2).

3.2. Growth rate

The “Pseudo” specific growth rates of fish during the exposure period (63 days) were not significantly affected by Cbz ($p > 0.05$, Fig. S2). A similar trend was found after 21 and 42 days of exposure (data not shown).

3.3. Feeding behavior

Cbz exposure had no effect on the time fish took for first feeding action (Fig. 1, grey bars represent data from the 63rd day). However, it induced an increase in the time fish needed to completely ingest food. This trend was found in the assessments at day 21 and 42 (Fig S3) and 63 (Fig. 1, white bars), where fish exceeded the maximum time pre-established for total ingestion (20 min).

3.4. Reproduction

During the 63 days of exposure, 7 breeding events were conducted to assess the reproductive output. Egg production and viability did not differ between the several breeding events ($p > 0.05$) and thus data were pooled together. Fig. 2 depicts the total number of eggs in all breeding episodes and the percentage of viable eggs per treatment. The total number of eggs produced during the experiment was not significantly different among treatments ($p > 0.05$). However, a significant decrease ($p < 0.001$) in the viability of the eggs after Cbz exposure (10 and 10,000 µg L^{-1}) was found.

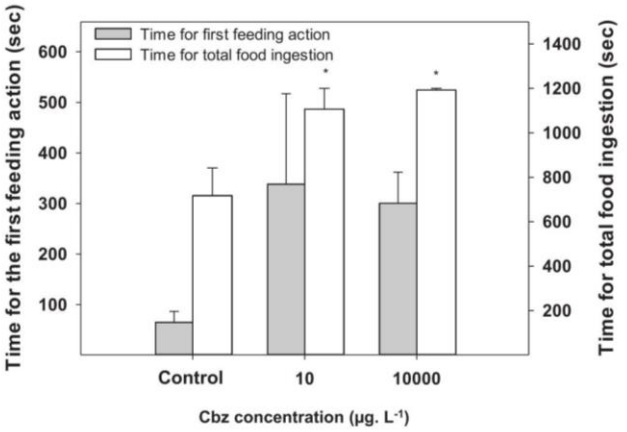

Fig. 1. Feeding behavior of adult *Danio rerio* after 63 days of exposure to carbamazepine (Cbz). The results are shown as time for first feeding action (grey bars) and time for total food ingestion (white bars). Asterisks (*) represent significant differences to the control (Dunnett's test; $p < 0.05$).

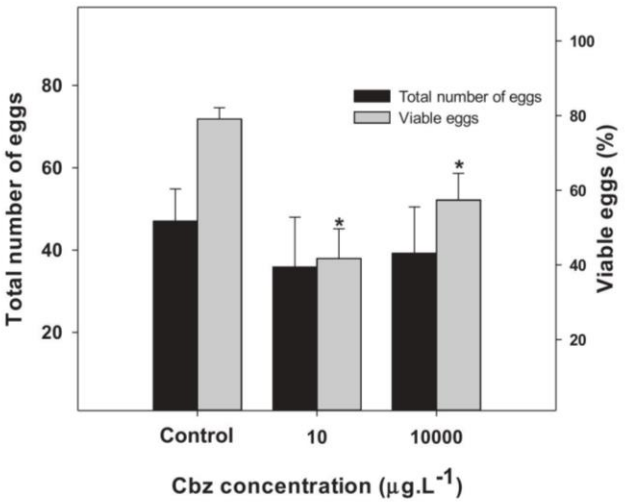

Fig. 2. Total production of eggs (black bars) and number of viable eggs (grey bars) from *Danio rerio* exposed to carbamazepine (Cbz). Results are expressed as mean ± standard error. Asterisks (*) represent significant differences towards the control (Dunnett's test; $p < 0.05$).

3.5. Micronucleus and others nuclear abnormalities assessment

No micronuclei were found in any of the treatments. The incidence of other nuclear abnormalities after Cbz exposure was not statistically different from the control treatment.

3.6. Effects of Cbz on biochemical markers

The effects of Cbz on AChE, CAT, GST and LDH activities of *D. rerio* are presented in Fig. 3. AChE activity (Fig. 3A) was increased after Cbz exposure ($p < 0.05$) both in the muscle (10,000 µg L^{-1}) and head (10 and 10,000 µg L^{-1}).

CAT activity (Fig. 3B) was inhibited by Cbz, both in the liver ($p < 0.01$) and gills ($p < 0.05$). In the liver, the two Cbz concentrations elicited the same degree of CAT inhibition whereas in the gills, a concentration dependent inhibition was observed.

GST activity was assessed in the liver, intestine and gill (Fig. 3C). Gills presented higher basal levels (100 U) when compared with the other tissues. GST response to Cbz exposure was organ dependent:

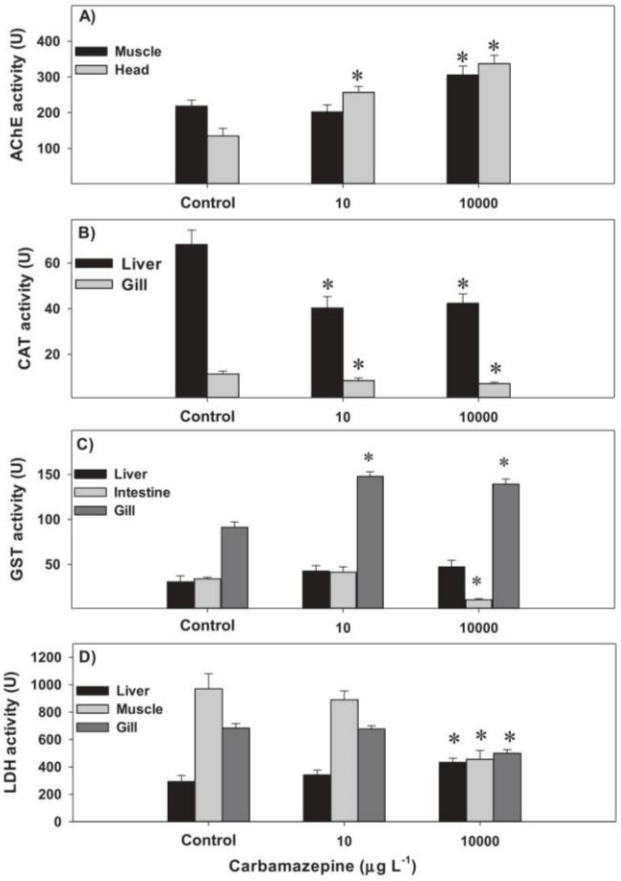

Fig. 3. Enzymatic activities of adult *Danio rerio* after 63 days exposure to carbamazepine. A – Acetylcholinesterase (AChE) activity, B – Catalase (CAT) activity; C – Glutathione S-transferase (GST) activity and D – Lactate Dehydrogenase (LDH) activity. Results are expressed as mean value ± standard error. Asterisks denote significant differences to control treatment (Dunnett's test after 1-way ANOVA except for CAT in the gills, GST in the liver and LDH in the muscle where the Dunn's test was used after the Kruskall-Wallis test). "U" - 1 nanomol of substrate per min per mg of protein.

increased activities were observed in the gills, at both tested concentrations (approximately 50%, regardless of the Cbz concentration; $p < 0.001$). In the intestine, an inhibition was found after exposure to the highest Cbz concentration ($p < 0.001$).

LDH basal levels were higher in the muscle, followed by gills and liver. A significant effect of Cbz on LDH activity was found, in all tissues, after exposure to the highest tested concentration. However, the pattern of response was different (Fig. 3D). In the liver, an increase of enzymatic activity was found ($p < 0.001$) whereas in muscle ($p < 0.001$) and gills ($p < 0.001$) an inhibition was observed (Fig. 3D).

3.7. Gonad histology

Female gonad histological analysis results are depicted in Fig. 4. The proportion of pre-vitellogenic follicles tend to be higher in the control whereas more mature type of follicles prevail in organisms exposed to the highest concentration of Cbz ($p = 0.040$).

4. Discussion

The occurrence of pharmaceuticals residues in the aquatic environment has been raising concerns regarding their potential chronic

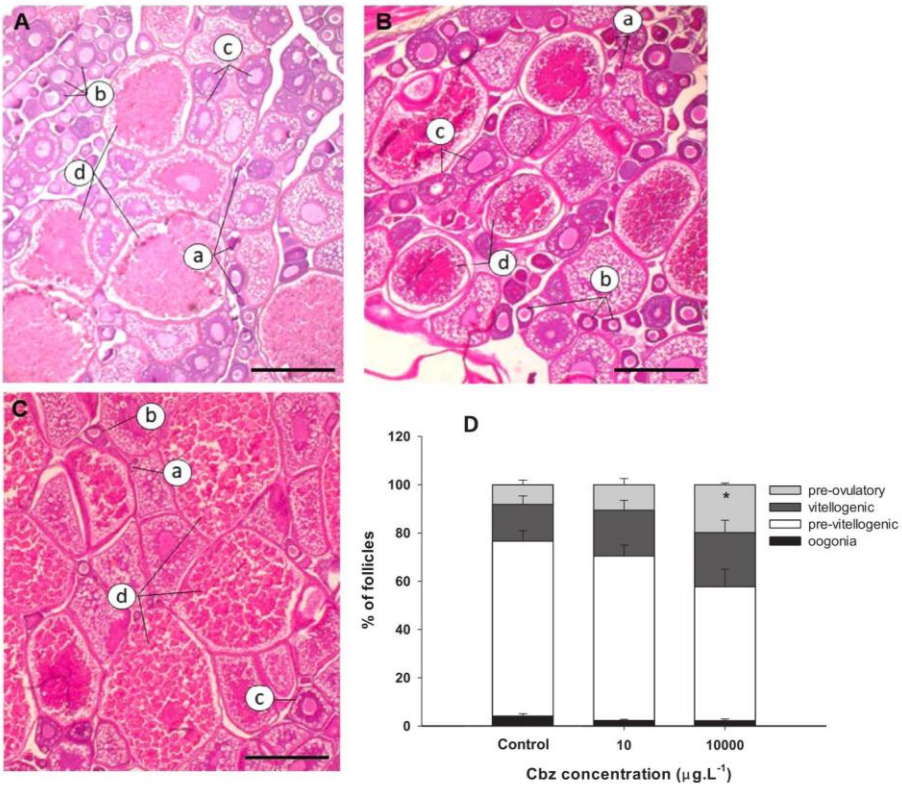

Fig. 4. Histopathological analyses of ovarian tissues of *Danio rerio* exposed for 63 days to carbamazepine (Cbz). Photomicrographs refer to female gonads of control fish (A), fish exposed to 10 µg L^{-1} (B) and 10,000 µg L^{-1} (C). The scale corresponds to 50 µm. Black lines indicate Oogonium (a), pre-vitellogenic follicle (b), vitellogenic follicle (c) or pre-ovulatory follicle (d). Graph D shows the percentage of each follicle class within the ovarian tissue. Asterisks denote significant differences towards control, Dunnett's test, $p < 0.05$.

effects to non-target organisms, considering that even very low concentrations of pharmaceuticals may exert toxicity through unexpected modes of action in non-target organisms (Malarvizhi et al., 2012).

In this study, the tested concentrations of Cbz did not induce significant alterations on fish growth over a 63 days period, corroborating the findings of the study of Madureira et al. (2012) where adult zebrafish were exposed for a shorter period (21 days) to Cbz (1780 µg L^{-1}). However, growth decrease has been reported for *O. mykiss* after 42 days exposure to 2000 µg L^{-1} of Cbz (Li et al., 2010d).

Behavior parameters have been considered a valuable tool in the assessment of the effects of chemicals. Changes in feeding and swimming behavior may have ecological consequences altering prey-predator relationship and decreasing competitive advantage (Domingues et al., 2016). In the present study, the time needed for the total food ingestion increased in fish exposed to Cbz. A similar result was reported for adult *Oryzias latipes* after 9 days exposure to 6150 µg L^{-1} of Cbz (Nassef et al., 2010). The authors of the mentioned study advanced that although the mechanisms responsible for the altered behavior are still unknown, they may be linked to changes in the levels of the neuromodulator serotonin, which has been reported to interfere with hormonal and neuronal mechanisms and play regulatory and endocrine functions. Moreover, altered levels of serotonin have been associated with changes in appetite, immune system and reproduction (Fent et al., 2006; Santos et al., 2010), influencing swimming speed and feeding behavior (Nassef et al., 2010; Lillesaar, 2011). Cbz has been reported to increase the extracellular levels of serotonin (Ambrósio et al., 2002; Yan et al., 1992) although some studies reported a variable response pattern according to the levels of Cbz: e.g. according to Okada et al. (1998) a therapeutic dose (25 mg kg^{-1}.day^{-1}) of Cbz increased the serotonergic function in rat hippocampus after 21 days whereas a supratherapeutic concentration (100 mg kg^{-1}.day^{-1}) reduced it. The effects on the feeding behavior may also be related with the levels of the hormone pro-opiomelanocortin, which acts as a regulator of feeding and energy balance and has been reported to be affected (increase in mRNA levels) in *Salmo salar* after 5 days treatment with 7.85 µg L^{-1} of Cbz (Hampel et al., 2014).

In terms of genotoxicity, the exposure of adult *D. rerio* to Cbz did not increase the incidence of micronuclei or other nuclear abnormalities. A previous study assessing DNA strand breaks reported a decrease in DNA integrity after 3 and 7 days of exposure to 0.31 µg L^{-1} Cbz and a decrease in DNA damage after 15 days exposure (Rocco et al., 2011). Reduction of DNA damage suggests reparation or recovery mechanisms and may justify the absence of genotoxicity verified in this work (Bolognesi and Hayashi, 2011). Inhibitory effect on cell division and subsequent hindrance in the passage of the affected cells into peripheral circulation, allied with the fact that circulating abnormal cells tend to be removed from the organism faster than undamaged ones (Oliveira et al., 2007) may be involved in the observed response.

AChE activity is inhibited by neurotoxic compounds and thus it is frequently used as a biomarker for environmental pollution by this type of chemicals (Pfeifer et al., 2005). However, in the present study, an increased activity after Cbz exposure was observed. Increases in AChE activity have been associated with apoptotic processes ongoing in the organism (Zhang et al., 2002, 2012) and with the production of free radicals and oxidative stress (Ferreira et al., 2012). AChE activity increase causes a fast degradation of the transmitter acetylcholine and a subsequent down stimulation of acetylcholine receptors affecting the cognitive functions of the organisms (Tõugu and Kesvatera, 1996).

Reactive oxygen species are produced at low concentrations by living organisms as result of normal metabolic processes but, in the presence of environmental pollutants, high concentrations can be generated with adverse effects on cellular components such as lipids, proteins, carbohydrates, and DNA. Therefore, the equilibrium of the redox state is fundamental for the proper functioning of organisms (Birben et al., 2012). A group of antioxidant enzymes (e.g. superoxide dismutase, CAT and glutathione peroxidase) and non-enzymatic antioxidants (e.g. reduced glutathione) play a fundamental role in controlling the levels of reactive oxygen species and thus in maintaining

the balance between oxidant/antioxidant states (Birben et al., 2012). CAT acts as first line of enzymatic defense against reactive oxygen species, degrading hydrogen peroxide into water and oxygen (Birben et al., 2012). In the present study, CAT activity was inhibited by Cbz both in liver and gills, suggesting an imbalance in the antioxidant status. Previously reported effects of Cbz on fish CAT activity include increased activity in *O. mykiss* after 7 days exposure to 2000 μg L^{-1}, followed by a decrease after 21 and 42 days of exposure (Li et al., 2010b). The authors proposed that the initial increase in CAT activity could be a stress response to neutralize reactive oxygen species formation and the reduction after prolonged exposure could be due to lipid peroxidation and the direct attack of reactive oxygen species to proteins. The present study results suggest that in a prolonged exposure, CAT may not able to cope with the level of pro-oxidants induced by Cbz. However, activation of other defense pathways responsible for the reduction of hydrogen peroxide, such as the glutathione peroxidase may also be involved in the protection of cells.

GST belongs to the Phase II of the detoxification mechanism and is implicated in the conjugation of xenobiotics with glutathione, increasing their solubility and excretion (Vernouillet et al., 2010). In the present study, GST response was tissue-dependent. GST activity was increased in the gills, an organ involved in physiological functions such as exchange of respiratory gases, osmoregulation, excretion of nitrogen residues and maintenance of acid-base balance (Rombough, 2002). In the intestine, organ important for nutrient digestion and absorption, a GST activity inhibition was found, probably associated with decreased levels of reduced glutathione, a co-factor of antioxidant enzymes that also plays an important role as non-enzymatic antioxidant defense against reactive oxygen species, or associated with an enzyme inhibition caused by high levels of reactive oxygen species. The gills were the organ most responsive to Cbz in terms of GST activity which may be explained by its direct contact with waterborne Cbz and its role in respiration, osmoregulation and in acid base balance (Li et al., 2009). To the author knowledge, this is the first report of chronic effects exposure of Cbz on *D. rerio* GST activity in different tissues.

LDH is widely distributed and used as a marker of organ or tissue damage, as it reflects the metabolic activity of a tissue and morphological and structural alterations that have a high association with pathological processes (Osman et al., 2010). In the present study, LDH activity was differentially affected in the tested organs, increasing in the liver and being inhibited in the muscle and gills. Increased LDH activity has been reported in the gills, liver and muscle of *C. carpio* exposed for 35 days to 5700 μg L^{-1} of Cbz (Malarvizhi et al., 2012) and interpreted a result of metabolic changes induced by Cbz. Increased LDH activity has also been reported in the plasma of *O. mykiss*, after 7 days of exposure to Cbz (1, 200 and 2000 μg L^{-1}) (Li et al., 2010d). In the present study, results obtained in the liver samples agree with the above mentioned studies suggesting changes in anaerobic metabolism or in the histological structure of the hepatic and extrahepatic tissues with potential damages in the tissue (Li et al., 2010a).

Histological results revealed a concentration dependent ovary composition, with a significant increase in the relative content of mature stages of follicles oocytes. These results are in line with other studies where non-steroidal pharmaceuticals interfered with the reproductive homeostasis of aquatic organisms (Madureira et al., 2011; Galus et al., 2014). The observed induction of pre-ovulatory follicle in high concentrations of Cbz may explain the absence of effect on the total number of produced eggs. Exposure to Cbz increased the occurrence of atreitic oocytes, often reported as a toxic effect on reproduction caused by estrogenic compounds (Diniz et al., 2005; Van der Ven et al., 2007). Follicular atresia, a normal degenerative process in fish ovaries has been associated with spontaneous pathological alterations in ovarian morphology (Rossteuscher et al., 2008). Cbz treatments although not altering the number of eggs produced, significantly impaired their viability. This observation corroborates other studies, with shorter exposure periods, reporting effects of Cbz on fish reproduction. In a study performed during 6 weeks, Galus et al. (2013) found a decrease in egg production in zebrafish after exposure to 0.5 and 10 μg L^{-1} of Cbz, associating this effect to reduction of the excitability of neurons leading to a reduction of neuronal stimulation in reproductive organs and synthesis of gonadal steroids. In *C. carpio*, Li et al. (2010a) observed decreased motility and velocity of sperm after 2 h exposure to 2000 and 20,000 μg L^{-1} Cbz. Aggressive behavior of males *D. rerio* during breeding was also pointed as factor for fertility decrease rate after 6 weeks exposure to 10 μg L^{-1} of Cbz (Galus et al., 2014). Thus, a decrease in sperm and oocytes quality, may explain the decrease in fertilized eggs viability observed in the present study. The decrease in the rate of viable eggs is an important parameter supporting ecological consequences of chronic exposure of aquatic organisms to Cbz, since it may lead to a reduction in population growth.

5. Conclusions

Generally, data obtained suggest that oxidative stress may occur in prolonged Cbz exposure with antioxidant defenses overwhelmed in some of the tissues analyzed. Oxidative stress may be also responsible for the induction of AChE verified leading to a cognitive impairment which was not evaluated in this study. Future behavioral studies should be conducted to validate this possibility. The feeding impairment observed suggests that Cbz is acting as an appetite suppressant and reinforcing its potential role as a serotonin releasing agent or serotonin reuptake inhibitor. Effects observed on reproduction (advance in oocytes maturation and reduction of eggs viability) require further investigation to assess if they are linked with the general suppression of neuronal activity with consequent behavioral impairment or if Cbz disrupts any endocrine function in fish.

Some of the above mentioned effects occurred at 10 μg L^{-1} which is a concentration reported in effluents and thus of great ecological relevance. Further studies should address other relevant exposure scenarios such as the co-exposure to abiotic stressors (such as oxygen depletion, pH or temperature variation) and the mixture with other relevant pharmaceuticals.

Acknowledgements

Brazilian Ministry of Education and Ministry of Science and Technology of Brazil for the scholarship provided to RO (CNPq BJT-A/PNPD CAPES); DSM for CAPES Ph.D. scholarship. CKG for CNPq research grant 305741/2015-2; TSA for FAPDF research grant (1250/2016), NFO and RCS for CNPq scholarship. Thanks are due for the financial support to CESAM (UID/AMB/50017 - POCI-01–0145-FEDER-007638), to FCT/MCTES through national funds (PIDDAC), and the co-funding by the FEDER, within the PT2020 Partnership Agreement and Compete 2020. MO had financial support of the program Investigator FCT, co-funded by the Human Potential Operational Program and European Social Fund (IF/00335–2015). ID was funded through a Post-Doc grant (SFRH/BPD/90521/2012) by the Portuguese Science and Technology Foundation (FCT).

Ethical standards

All experimental procedures involving fish were performed following the International Guiding Principles for Biomedical Research Involving Animals (EU 2010/63) and are in accordance with Brazilian laws on animal safety. The study was approved by the ethics committee at the University of Brasilia (protocol no 100226/2014). Animal handling was performed with accredited researchers.

Conflict of interest

The authors declare that they have no conflict of interest.

Appendix A. Supporting information

Supplementary data associated with this article can be found in the online version at doi:10.1016/j.ecoenv.2018.08.015.

References

Ambrósio, A.F., Soares-da-Silva, P., Carvalho, C.M., Carvalho, A.P., 2002. Mechanisms of action of carbamazepine and its derivatives, oxcarbazepine, BIA 2-093, and BIA 2-024. Neurochem. Res. 27, 121–130.

Ayano, G., 2016. Bipolar disorders and carbamazepine: pharmacokinetics, pharmacodynamics, therapeutic effects and indications of carbamazepine: review of articles. J. Neuropsychopharmacol. Ment. Health 1 (4).

Birben, E., Murat, U., Md, S., Sackesen, C., Erzurum, S., Kalayci, O., 2012. Oxidative stress and antioxidant defense. WAO J. 5, 9–19.

Bolognesi, C., Hayashi, M., 2011. Micronucleus assay in aquatic animals. Mutagenesis 26, 205–213.

Bradford, M.M., 1976. A rapid and sensitive method for the quantitation of microgram quantities of protein utilizing the principle of protein-dye binding. Anal. Biochem. 72, 248–254.

Brandão, F.P., Rodrigues, S., Castro, B.B., Gonçalves, F., Antunes, S.C., Nunes, B., 2013. Short-term effects of neuroactive pharmaceutical drugs on a fish species: biochemical and behavioural effects. Aquat. Toxicol. 144–145, 218–229.

Calcagno, E., Durando, P., Valdés, M.E., Franchioni, L., Bistoni, M., de los, Á., 2016. Effects of carbamazepine on cortisol levels and behavioral responses to stress in the fish *Jenynsia multidentata*. Physiol. Behav. 158, 68–75.

Carrasco, K.R., Tilbury, K.L., Myers, M.S., 1990. Assessment of the piscine micronucleus test as an in situ biological indicator of chemical contaminant effects. Can. J. Fish. Aquat. Sci. 47, 2123–2136.

Chen, H., Zha, J., Liang, X., Li, J., Wang, Z., 2014. Effects of the human antiepileptic drug carbamazepine on the behavior, biomarkers, and heat shock proteins in the Asian clam *Corbicula fluminea*. Aquat. Toxicol. 155, 1–8.

Claiborne, A.L., 1985. Catalase activity. CRC Handb. Methods Oxyg. Radic. Res. 1, 283–284.

Deblonde, T., Cossu-Leguille, C., Hartemann, P., 2011. Emerging pollutants in wastewater: a review of the literature. Int. J. Hyg. Environ. Health 214, 442–448.

Demirkaya, F., Kadioğlu, Y., 2005. Determination of Carbamazepine Using RP-HPLC Method in Pharmaceutical Preparations. Fabad. J. Pharm. Sci. 30, 78–82.

Diamantino, T.C., Almeida, E., Soares, A.M.V.M., Guilhermino, L., 2001. Lactate dehydrogenase activity as an effect criterion in toxicity tests with *Daphnia magna* straus. Chemosphere 45, 553–560.

Diniz, M.S., Peres, I., Magalhães-Antoine, I., Falla, J., Pihan, J.C., 2005. Estrogenic effects in crucian carp (*Carassius carassius*) exposed to treated sewage effluent. Ecotoxicol. Environ. Saf. 62, 427–435.

Domingues, I., Oliveira, R., Soares, A.M.V.M., Amorim, M.J.B., 2016. Effects of ivermectin on *Danio rerio*: a multiple endpoint approach: behaviour, weight and subcellular markers. Ecotoxicology 25, 491–499.

Ellman, G.L., Courtney, K.D., Andres, V., Featherstone, R.M., 1961. A new and rapid colorimetric determination of acetylcholinesterase activity. Biochem. Pharmacol. 7, 88–95.

Fenech, M., Chang, W.P., Kirsch-Volders, M., Holland, N., Bonassi, S., Zeiger, E., 2003. HUMN project: detailed description of the scoring criteria for the cytokinesis-block micronucleus assay using isolated human lymphocyte cultures. Mutat. Res. - Genet. Toxicol. Environ. Mutagen. 534, 65–75.

Fent, K., Weston, A.A., Caminada, D., 2006. Ecotoxicology of human pharmaceuticals. Aquat. Toxicol. 76, 122–159.

Ferreira, G.K., Carvalho-Silva, M., Gonçalves, C.L., Vieira, J.S., Scaini, G., Ghedim, F.V., Deroza, P.F., Zugno, A.I., Pereira, T.C.B., Oliveira, G.M.T., Kist, L.W., Bogo, M.R., Schuck, P.F., Ferreira, G.C., Streck, E.L., 2012. L-Tyrosine administration increases acetylcholinesterase activity in rats. Neurochem. Int. 61 (8), 1370–1374.

Frasco, M.F., Guilhermino, L., 2002. Effects of dimethoate and beta-naphthoflavone on selected biomarkers of *Poecilia reticulata*. Fish. Physiol. Biochem. 26, 149–156.

Galus, M., Kirischian, N., Higgins, S., Purdy, J., Chow, J., Rangaranjan, S., Li, H., Metcalfe, C., Wilson, J.Y., 2013. Chronic, low concentration exposure to pharmaceuticals impacts multiple organ systems in zebrafish. Aquat. Toxicol. 132–133, 200–211.

Galus, M., Rangarajan, S., Lai, A., Shaya, L., Balshine, S., Wilson, J.Y., 2014. Effects of chronic, parental pharmaceutical exposure on zebrafish (*Danio rerio*) offspring. Aquat. Toxicol. 151, 124–134.

Gunthert, F.W., Freitas, V., Neder, K., Obermayer, S., Faltermaier, S., Tocha, C., 2014. Developing the urban water system towards using the Paranoá lake in Brasília as receptor and water resource. In: Integrated Water Resource Management in Brazil. IWA Publishing, pp. 109–124.

Habig, W.H., Jakoby, W.B., 1981. Assays for differentiation of glutathione-S-transferases. Methods Enzymol. 77, 398–405.

Hampel, M., Bron, J.E., Taggart, J.B., Leaver, M.J., 2014. The antidepressant drug carbamazepine induces differential transcriptome expression in the brain of Atlantic salmon, *Salmo salar*. Aquat. Toxicol. 151, 114–123.

Hooftman, R.N., de Raat, W.K., 1982. Induction of nuclear anomalies (micronuclei) in the peripheral blood erythrocytes of the eastern mudminnow *Umbra pygmaea* by ethyl methanesulphonate. Mutat. Res. Lett. 104, 147–152.

Kimmel, C.B., Ballard, W.W., Kimmel, S.R., Ullmann, B., Schilling, T.F., 1995. Stages of embryonic development of the zebrafish. Dev. Dyn. 203, 253–310.

Kreke, N., Dietrich, D.R., 2008. Physiological endpoints for potential SSRI interactions in fish. Crit. Rev. Toxicol. 38, 215–247.

LaLone, C.A., Villeneuve, D.L., Burgoon, L.D., Russom, C.L., Helgen, H.W., Berninger, J.P., Tietge, J.E., Severson, M.N., Cavallin, J.E., Ankley, G.T., 2013. Molecular target sequence similarity as a basis for species extrapolation to assess the ecological risk of chemicals with known modes of action. Aquat. Toxicol. 144–145, 141–154.

Li, Z.H., Li, P., Rodina, M., Randak, T., 2010a. Effect of human pharmaceutical carbamazepine on the quality parameters and oxidative stress in common carp (*Cyprinus carpio*) spermatozoa. Chemosphere 80, 530–534.

Li, Z.H., Zlabek, V., Velisek, J., Grabic, R., Machova, J., Randak, T., 2010c. Modulation of antioxidant defence system in brain of rainbow trout (*Oncorhynchus mykiss*) after chronic carbamazepine treatment. Comp. Biochem. Physiol. - C Toxicol. Pharmacol. 151, 137–141.

Li, Z.H., Zlabek, V., Velisek, J., Grabic, R., Machovaa, J., Randaka, T., 2010d. Physiological condition status and muscle-based biomarkers in rainbow trout (*Oncorhynchus mykiss*), after long-term exposure to carbamazepine. J. Appl. Toxicol. 30, 197–203.

Li, Z.H., Velisek, J., Zlabek, V., Grabic, R., Machova, J., Kolarova, J., Randak, T., 2010b. Hepatic antioxidant status and hematological parameters in rainbow trout, *Oncorhynchus mykiss*, after chronic exposure to carbamazepine. Chem. Biol. Interact. 183, 98–104.

Li, Z.H., Zlabek, V., Velisek, J., Grabic, R., Machova, J., Randak, T., 2009. Responses of antioxidant status and Na^+–K^+-ATPase activity in gill of rainbow trout, *Oncorhynchus mykiss*, chronically treated with carbamazepine. Chemosphere 77, 1476–1481.

Lillesaar, C., 2011. The serotonergic system in fish. J. Chem. Neuroanat. 41 (4), 294–308.

Loos, R., Gawlik, B.M., Locoro, G., Rimaviciute, E., Contini, S., Bidoglio, G., 2009. EU-wide survey of polar organic persistent pollutants in European river waters. Environ. Pollut. 157, 561–568. https://doi.org/10.1016/j.envpol.2008.09.020.

Madureira, T.V., Rocha, M.J., Cruzeiro, C., Galante, M.H., Monteiro, R.A.F., Rocha, E., 2011. The toxicity potential of pharmaceuticals found in the Douro River estuary (Portugal): assessing impacts on gonadal maturation with a histopathological and stereological study of zebrafish ovary and testis after sub-acute exposures. Aquat. Toxicol. 105, 292–299.

Madureira, T.V., Rocha, M.J., Cruzeiro, C., Rodrigues, I., Monteiro, R.A.F., Rocha, E., 2012. The toxicity potential of pharmaceuticals found in the Douro River estuary (Portugal): evaluation of impacts on fish liver, by histopathology, stereology, vitellogenin and CYP1A immunohistochemistry, after sub-acute exposures of the zebrafish model. Environ. Toxicol. Pharmacol. 34, 34–45.

Malarvizhi, A., Kavitha, C., Saravanan, M., Ramesh, M., 2012. Carbamazepine (CBZ) induced enzymatic stress in gill, liver and muscle of a common carp, *Cyprinus carpio*. J. King Saud. Univ. - Sci. 24, 179–186.

Martins, N., Pereira, R., Abrantes, N., Pereira, J., Gonçalves, F., Marques, C.R., 2012. Ecotoxicological effects of ciprofloxacin on freshwater species: data integration and derivation of toxicity thresholds for risk assessment. Ecotoxicology 21, 1167–1176.

Menke Aswin, L., et al., 2011. Normal anatomy and histology of the adult zebrafish. Toxicol. Pathol. 39.5, 759–775.

Nassef, M., Matsumoto, S., Seki, M., Khalil, F., Kang, I.J., Shimasaki, Y., Oshima, Y., Honjo, T., 2010. Acute effects of triclosan, diclofenac and carbamazepine on feeding performance of Japanese medaka fish (*Oryzias latipes*). Chemosphere 80, 1095–1100.

OECD (Organization for Economic Co-operation and Development), 2000. No. 215 adopted: Fish, juvenile growth test. OECD Guidel. Test. Chem. 301. pp. 16.

Okada, M., Hirano, T., Mizuno, K., Kawata, Y., Wada, K., Murakami, T., Tasaki, H., Kaneko, S., 1998. Effects of carbamazepine on hippocampal serotonergic system. Epilepsy Res. 31, 187–198.

Oliveira, M., Cardoso, D.N., Soares, A.M.V.M., Loureiro, S., 2015. Effects of short-term exposure to fluoxetine and carbamazepine to the collembolan *Folsomia candida*. Chemosphere 120, 86–91.

Oliveira, M., Pacheco, M., Santos, M.A., 2007. Cytochrome P4501A, genotoxic and stress responses in golden grey mullet (*Liza aurata*) following short-term exposure to phenanthrene. Chemosphere 66 (7), 1284–1291.

Oropesa, A.L., Floro, A.M., Palma, P., 2016. Assessment of the effects of the carbamazepine on the endogenous endocrine system of *Daphnia magna*. Environ. Sci. Pollut. Res. 1–11.

Osman, A., Reheem, A., Baset, M.A. El, AbuelFadl, K., Rab, A., 2010. Enzymatic and histopathologic biomarkers as indicators of aquatic pollution in fishes. Nat. Sci. 2, 1302–1311.

Palacios-Rosas, E., Castro-Pastrana, L.I., 2017. Pharmaceuticals reaching the environment: concepts, evidence, and concerns (pp. 21-41). In: Gómez-Oliván, L. (Ed.), Ecopharmacovigilance. The Handbook of Environmental Chemistry 66 Springer, Cham.

Parker, M.O., 2015. Adult vertebrate behavioural aquatic toxicology: reliability and validity. Aquat. Toxicol. 1–7.

Pfeifer, S., Schiedek, D., Dippner, J.W., 2005. Effect of temperature and salinity on acetylcholinesterase activity, a common pollution biomarker, in *Mytilus sp.* from the south-western Baltic Sea. J. Exp. Mar. Bio. Ecol. 320, 93–103.

Pires, A., Almeida, Â., Correia, J., Calisto, V., Schneider, R.J., Esteves, V.I., AMVM, Soares, Figueira, E., Freitas, R., 2016. Long-term exposure to caffeine and carbamazepine: impacts on the regenerative capacity of the polychaete *Diopatra neapolitana*. Chemosphere 146, 565–573.

Rocco, L., Izzo, A., Zito, G., Peluso, C., 2011. Genotoxicity in zebrafish (*Danio rerio*) exposed to two pharmacological products from an impacted italian river. J. Environ. Anal. Toxicol. 1, 1–7.

Rombough, P., 2002. Gills are needed for ionoregulation before they are needed for O_2 uptake in developing zebrafish, *Danio rerio*. J. Exp. Biol. 205, 1787–1794.

Rossteuscher, S., Schmidt-Posthaus, H., Schaefers, C., Teigeler, M., Segner, H., 2008. Background pathology of the ovary in a laboratory population of zebrafish *Danio*

rerio. Dis. Aquat. Org. 79, 169–172.
Santos, L.H.M.L.M., Araújo, A.N., Fachini, A., Pena, A., Delerue-Matos, C., Montenegro, M.C.B.S.M., 2010. Ecotoxicological aspects related to the presence of pharmaceuticals in the aquatic environment. J. Hazard. Mater. 175, 45–95.
Sim, W.-J., Lee, J.-W., Lee, E.-S., Shin, S.-K., Hwang, S.-R., Oh, J.-E., 2011. Occurrence and distribution of pharmaceuticals in wastewater from households, livestock farms, hospitals and pharmaceutical manufactures. Chemosphere 82, 179–186.
Tõugu, V., Kesvatera, T., 1996. Role of ionic interactions in cholinesterase catalysis. Biochim. Biophys. Acta 1298, 12–30.
Van den Brandhof, E.J., Montforts, M., 2010. Fish embryo toxicity of carbamazepine, diclofenac and metoprolol. Ecotoxicol. Environ. Saf. 73, 1862–1866.
Van der Ven, L.T.M., van den Brandhof, E.-J., Vos, J.H., Wester, P.W., 2007. Effects of the estrogen agonist 17β-estradiol and antagonist tamoxifen in a partial life-cycle assay with zebrafish (*Danio rerio*). Environ. Toxicol. Chem. 26, 92–99.
Vassault, A., 1983. Lactate dehydrogenase. In: 3rd ed. In: Bergmeye, H.U., Bergmeyer, J., Gra, I.M. (Eds.), Methods of enzymatic analysis III. Verlag Chemie, Weinheim, pp. 118–126.
Vernouillet, G., Eullaffroy, P., Lajeunesse, A., Blaise, C., Gagné, F., Juneau, P., 2010. Toxic effects and bioaccumulation of carbamazepine evaluated by biomarkers measured in organisms of different trophic levels. Chemosphere 80, 1062–1068.
Villanueva, V., Ojeda, J., Rocamora, R.A., Serrano-Castro, P.J., Parra, J., Rodríguez-Uranga, J.J., Viteri, C., 2018. EPICON consensus: recommendations for proper management of switching to eslicarbazepine acetate in epilepsy. Neurología (English Edition) 33, 290–300.
Yan, Q.S., Mishra, P.K., Burger, R.L., Bettendorf, A.F., Jobe, P.C., Dailey, J.W., 1992. Evidence that carbamazepine and antiepilepsirine may produce a component of their anticonvulsant effects by activating serotonergic neurons in genetically epilepsy-prone rats. J. Pharmacol. Exp. Ther. 261, 652–659.
Zhang, B., Yang, L., Yu, L., Lin, B., Hou, Y., Wu, J., Huang, Q., Han, Y., Guo, L., Ouyang, Q., Zhang, B., Lu, L., Zhang, X., 2012. Acetylcholinesterase is associated with apoptosis in β cells and contributes to insulin-dependent diabetes mellitus pathogenesis. Acta Biochim. Biophys. Sin. (Shanghai). 44, 207–216.
Zhang, X.J., Yang, L., Zhao, Q., Caen, J.P., He, H.Y., Jin, Q.H., Guo, L.H., Alemany, M., Zhang, L.Y., Shi, Y.F., 2002. Induction of acetylcholinesterase expression during apoptosis in various cell types. Cell Death Differ. 9, 790–800.

Chemosphere 222 (2019) 175–183

Contents lists available at ScienceDirect

Chemosphere

journal homepage: www.elsevier.com/locate/chemosphere

Exposure to dilute concentrations of bupropion affects zebrafish early life stages

Mariana Bernardes Franco [a, f], Thayres S. Andrade [a, b], Diego Sousa-Moura [a], Muriel Lopes da Silva [a], Irvin Bryan Machado Ferraz [a], Níchollas Serafim Camargo [a, f], Inês Domingues [e], Rhaul Oliveira [a, c, d, *], Cesar Koppe Grisolia [a]

[a] Laboratório de Genética Toxicológica, Departamento de Genética e Morfologia, Instituto de Ciências Biológicas, Universidade de Brasília, UnB, 70910-900, Brasília, Distrito Federal, Brazil
[b] Universidade Federal do Ceará, UFC, Campus de Crateús, 63700-000, Crateús, Ceará, Brazil
[c] Faculdade de Tecnologia, Universidade Estadual de Campinas, UNICAMP, 13484-332, Limeira, São Paulo, Brazil
[d] Programa de Pós-graduação em Toxicologia e Análises Toxicológicas, Faculdade de Ciências Farmacêuticas, Universidade de São Paulo, USP, 05508-000, Butantã, São Paulo, Brazil
[e] Departamento de Biologia & CESAM, Universidade de Aveiro, Campus Universitário de Santiago, 3810-193, Aveiro, Portugal
[f] Faculdade da Ceilândia, Universidade de Brasília, 72220-90, Brasília, Distrito Federal, Brazil

HIGHLIGHTS

- Bupropion toxicity was assessed using zebrafish early life-stages.
- The bupropion168 h-LC50 was 50346 μg/L.
- Bupropion induced lack of equilibrium, non-hatching and developmental alterations.
- Bupropion affects biochemical markers from different metabolic pathways.
- Bupropion affects the locomotor activity of embryos in a biphasic manner.

ARTICLE INFO

Article history:
Received 26 November 2018
Received in revised form
21 January 2019
Accepted 24 January 2019
Available online 25 January 2019

Handling Editor: David Volz

Keywords:
Danio rerio
Fish embryo toxicity test
Enzymatic biomarkers
Behavior
Antidepressants
Emerging pollutants

ABSTRACT

Psychiatric pharmaceuticals are one of the most prescribed active substances globally. Bupropion (BPP) is an antidepressant that acts via inhibition of norepinephrine and dopamine reuptake. It has been found in various water matrices, and thus its effects on aquatic organisms must be studied. The present study aimed to evaluate the acute toxic effects of BPP on zebrafish (*Danio rerio*) early life stages. For developmental analysis, organisms were exposed for 168 h to concentrations ranging from 0 to 82000 μg/L. Two other experiments were performed by exposing embryos to a wide range of concentrations (from 0 to 50000 μg/L) in order to evaluate BPP effects on embryonic behavior, using the Zebrabox and testing at the biochemical level (acetylcholinesterase, glutathione-S-transferase, lactate dehydrogenase and catalase). Developmental analysis indicated that BPP had low acute toxicity with a calculated 168 h-LC50 of 50346 μg/L. Concentrations equal to or above 44800 μg/L elicited several effects such as hatching delay, edemas and tail deformities. However, concentrations from 7300 μg/L upwards elicited equilibrium alteration. Behavioral analysis showed that BPP affected zebrafish locomotor behavior by decreasing activity at 0.6 μg/L, increasing activity at 8.8 and 158 μg/L, and decreasing activity at 50000 μg/L. Biochemical analysis showed an increase of AChE activity at 158 and 2812 μg/L, an increase in GST at the highest concentrations, CAT alteration and increase of LDH at 0.6, 2812 and 50000 μg/L. We can conclude that BPP affects zebrafish early life stages at environmental concentrations.

* Corresponding author. Laboratório de Ecotoxicologia e Genotoxicidade, Faculdade de Tecnologia, Universidade Estadual de Campinas, UNICAMP, 13484-332, Limeira, São Paulo, Brazil.
E-mail addresses: marianaffranco@yahoo.com.br (M.B. Franco), thayres@gmail.com (T.S. Andrade), diegosousa.12@gmail.com (D. Sousa-Moura), muriel-lopes@hotmail.com (M. Lopes da Silva), bryanmachadoferraz@yahoo.com.br (I.B. Machado Ferraz), nico.serafim@hotmail.com (N.S. Camargo), inesd@ua.pt (I. Domingues), rhaul.oliveira@gmail.com, rhaul@ft.unicamp.br (R. Oliveira), grisolia@unb.br (C.K. Grisolia).

https://doi.org/10.1016/j.chemosphere.2019.01.141
0045-6535/

1. Introduction

Psychiatric pharmaceuticals are one of the most prescribed active substances globally. They are substances often reported as contaminants in aquatic systems with potential to affects non-target organisms (Bottoni et al., 2010; Wu et al., 2015; Yuan et al., 2013; Zenker et al., 2014). Bupropion (BPP) is a monocyclic phenylaminoketone structurally related to the phenylisopropylamines, with significant antidepressant effects (Conners et al., 1996). This psychiatric pharmaceutical is approved for use in the treatment of major depressive disorder and as an aid to smoking cessation in over 50 countries, with over 40 million patients receiving treatment (Fava et al., 2005).

Similarly, to other pharmaceuticals, BPP occurs in the environment in the range of ng/L to μg/L (Calisto and Esteves, 2009). Several studies analyzing samples of various water matrices (drinking water, groundwater, surface water and wastewater) reported BPP concentrations varying from below 10–4300 ng/L (Ferrer and Thurman, 2012; Painter et al., 2010; Schultz and Furlong, 2008; Writer et al., 2013). Although levels found in the environment are often very low, pharmaceuticals are designed to target specific metabolic and biological pathways that can be conserved in aquatic organisms, and therefore some of them may disrupt key processes in non-target organisms (Dong et al., 2013; Webb et al., 2003). BPP acts by inhibiting the norepinephrine and dopamine reuptake and has no significant serotonergic or direct effects on postsynaptic receptors in humans (Fava et al., 2005; Stahl et al., 2004).

Despite the scarcity of information, there is evidence that psychiatric pharmaceuticals can modulate fish behavior, interfering with their swimming, feeding, predation, and reproduction (Blaser et al., 2010; Brandão et al., 2013; Brodin et al., 2013), particularly at larval stage. Zebrafish have been used in toxicological studies to analyze the effects of neurotoxins and neuroprotectants on the developing nervous system (Guo, 2009). This model has many advantages, such as well-known morphological, biochemical, genetic and physiological information at all stages of life, which makes the zebrafish use ideal for identifying adverse effects of chemical exposure (Hill et al., 2005). Recently, Santos et al. (2018) demonstrated that carbamazepine, a psychiatric pharmaceutical used in epilepsy treatment, affects the reproductive, enzymatic and behavioral parameters of zebrafish adults exposed to concentrations as low as 10 μg/L. Another study performed by Farias et al. (2019) used zebrafish early life-stages to assess the toxicity of the antidepressant fluoxetine. The study results showed the adverse effects of fluoxetine on development, acetylcholinesterase and locomotor activity of zebrafish early life-stages in concentrations varying from 0.88 μg/L to 5550 μg/L.

Dong et al. (2013) proposed a simple prioritization approach to identify pharmaceuticals that pose a potential risk to human and aquatic organisms. BPP is in position 7 of this risk-prioritizing ranking. Thus, the present study aimed to evaluate BPP acute toxic effects on zebrafish early life-stages employing a multiparametric approach. Effects on different levels of organization were assessed, including mortality, development, biochemical markers. We address the hypothesis that BPP can affect zebrafish embryonic development in different organizational levels.

2. Material and methods

2.1. Chemical and HPLC analysis

BPP hydrochloride was obtained from pharmaceutical industry (Amapá – Brazil, CAS Number: 31677-93-7, empirical formula: $C_{13}H_{18}ClNO \cdot HCl$). BPP stability in test solutions was assessed daily in a period of seven days, the maximum test duration period. Stability of BPP in the dilution water kept at the same climatic conditions as the tests (SL-24 Solab Científica) was evaluated by HLPC following the method described by Ulu and Tuncel (2012) (see details in Suppl. Material-SM1, Fig. S1; Table S1).

2.2. Zebrafish maintenance and embryo collection

The zebrafish embryos were provided by the facility established at the Department of Genetics and Morphology, University of Brasília, Brazil. Zebrafish adults were kept in a ZebTEC (Tecniplast, Italy) recirculating system and maintained in aquariums with reverse osmosis and activated carbon filtered water. The temperature was maintained at 26.0 ± 1 °C, ammonia <0.01 mg/L, conductivity at 750 ± 50 μS/cm, pH at 7.5 ± 0.5 and dissolved oxygen equal to or above 95% saturation. Fish were raised in a 12:12 h (light:dark) photoperiod cycle. These conditions and water parameters were maintained in all the performed tests.

Zebrafish eggs were obtained by breeding of fish in the Ispawn breeding system (Tecniplast). The day prior to breeding, males and females were sequentially added to the system and kept separated by a divider, in a proportion of two males for one female. Early in the morning, the divider was removed and the spawning platform was lifted to initiate the spawning. The eggs were collected immediately after natural mating, rinsed in water, and checked under a stereomicroscope (Stereoscopic Zoom Microscope – Stemi 2000, Zeiss, Germany). The unfertilized eggs (<20%) and those with cleavage irregularities or injuries were discarded.

2.3. Fish Embryo Toxicity (FET) test

The Fish Embryo Toxicity test were based on the OECD guideline Protocol 236 "Fish Embryo Toxicity" (FET) test (OECD, 2013) with adaptations described by Farias et al. (2018). Zebrafish embryos were exposed to six different concentrations 0, 4000, 7300, 13400, 24500, 44800 and 82000 μg/L of BPP. Those were chosen based on results of previous range finding tests prepared by successive dilutions of stock solution. Since the chemical analysis indicated that BPP is degraded over the course of days, the solutions were renewed every 48 h.

The test was performed using 72 eggs per treatment, divided in 3 replicates in 24-well microplates. Twenty wells were filled-up with 2 mL of the test solution and four wells with water (internal plate control, as required in the OECD guideline). Each well received one egg. The test was initiated immediately after fertilization and it was continued for 168 h in a climate chamber (SL-24 Solab Científica, Brazil). Embryos and larvae were observed daily under a stereomicroscope. Developmental parameters were evaluated in embryos over the test period using a magnification of × 70 for eggs and × 40 for hatched embryos. Before hatching, the following parameters were evaluated: egg coagulation, otolith formation, general delay on development, eye and body pigmentation, somites formation, heartbeat, oedemas, detachment of the tail-bud from the yolk sac, yolk sac absorption, tail malformation and hatching. After hatching, spine malformation and equilibrium were also evaluated (represented by embryos side-lying in the bottom of the microplate well). All parameters were assessed and quantified as observed or not observed.

2.4. Behavior analysis

In order to analyze locomotor and enzymatic responses of zebrafish, a wide range of concentrations comprising more realistic scenarios and also sub-acute doses (<168 h-LC50) were chosen, namely 0.0, 0.6, 8.8, 158, 2812 and 50000 μg/L.

Prior to the behavior assay, zebrafish embryos were exposed in similar conditions as described in section 2.3 "Fish Embryo Toxicity (FET) test". At 168 h the embryos were removed from the exposure dishes and placed in 96 well plates (one per well). Locomotion was evaluated for 16 embryos per treatment in triplicate including the control.

Embryonic movement was tracked using the Zebrabox (ZEB 478 Viewpoint) tracking system equipped with a 25 frame per second infrared camera over a period of 20 min. Movement analysis of all replicates were performed in the same day (168 h) one followed by the other. The temperature was maintained stable at 26 ± 1 °C. Movement was stimulated by applying light: dark intervals according to what was previously described in Irons et al. (2010). Briefly, the test consisted of acclimatizing the embryos in the light for 5 min, followed by a 10 min dark period and another 5 min light. Typically, zebrafish larvae show less locomotion during light periods and more during dark.

For each replicate, the distances travelled and time spent moving in 1 min intervals were recorded separately for each dark and light period. The behavioral endpoints measured included the total swimming time, the total swimming distance moved during each measurement period, and percentage of slow and fast movements of the organisms. The relative slow movement (%) is the ratio between slow and total distance moved in each measurement period. The relative fast movement (%) is the ratio between fast and the total distance moved in each measurement period. A threshold of 5 mm/s was used to separate slow and fast movements).

2.5. Biochemical biomarkers analysis

Tests were performed in 1 L beakers filled up with 500 mL of test solutions and 500 eggs in order to collect a high number of embryos samples for enzymatic assays.

After 168 h of incubation, 10 pools of 15 hatched embryos per concentration were collected into microtubes with 0.5 mL of K-phosphate buffer (0.1 M, pH 7.4), frozen in liquid nitrogen and immediately stored at −80 °C until the day of analysis. Prior to enzymatic activity determinations, samples were defrosted on ice, homogenized using a sonicator (Ultrasonic Cleaner 2840D-Odontobrás) and centrifuged (Centrifuge Hettich – Mikro 220R) for 20 min at 10,000 x *g* and then a post-mitochondrial supernatant (PMS) was isolated for enzymatic determinations. Enzymatic activities were determined in quadruplicate and expressed as micromoles of substrate hydrolyzed per minute per mg of protein (U). The protein concentration of samples was quantified using the Bradford's Method at 595 nm and γ-globulin as standard (Bradford, 1976). All reactions were performed spectrophotometrically (SpectraMax M2 microplate reader) and in quadruplicate.

AChE activity was determined using acetylthiocholine (ASCh) as substrate, measuring the conjugation product between thiocoline (result of the degradation of ASCh) and 5,5-dithiobis-2-nitrobenzoic acid (DTNB) (absorbance increase) at 414 nm, every 20 s, during 5 min, according to the method previously described by Ellman et al. (1961). For the enzymatic determination, 40 μl of PMS and 250 μl of reaction mixture, was used (acetylcholine and propionylcholine (75 mM) and DTNB (10 mM)) in K-phosphate buffer (0.1 M, pH 7.2). Acetylcholinesterase activities were expressed as micromoles of substrate hydrolyzed per minute per mg of protein (U).

GST activity was determined using a thioether as substrate and measuring the conjugation product between glutathione and 1-Chloro-2,4-dinitrobenzene (CDNB) (absorbance increase) at 340 nm, every 40 s, for 5 min, according to the method of Habig et al. (1981). Activity determinations were made using 50 μl of PMS, 250 μl of reaction mixture (glutathione (10 mM) and CDNB (10 mM)) in K-phosphate buffer (0.1 M, pH 6.5).

CAT activity was determined using a H_2O_2 as substrate and measuring the decrease of absorbance due to degradation of H_2O_2 at 240 nm, every 40 s, during 5 min, according to the method of Aebi (1984). Activity determinations were made using 25 μl of PMS, 275 μl of reaction mixture (H_2O_2 (30 mM)) K-phosphate buffer (0.05 M, pH 7.0).

LDH activity was determined using a pyruvate as substrate and measuring the reduction of Pyruvate and the oxidation of NADH at 340 nm, every 40 s, during 5 min, according to the method by Vassault (1983). Activity determinations were made using 40 μl of PMS, 260 μl of reaction mixture (NADH (0.24 mM) and pyruvate (10 mM)) Tris-NaCl buffer (0.1 M, pH 7.2).

2.6. Statistical analysis

All levels of lethal and effective concentrations (LCs and ECs) were calculated by fitting dose-response curves using the package drc (Ritz and Streibig, 2005). A one-way ANOVA was used to detect the differences between the groups for normally distributed data sets. When data did not pass the Kolmogorov–Smirnov normality test and the Levene's homogeneity of variance test, a Kruskal–Wallis test was used. If significant results were found, the Dunnett's or Dunn's test (for parametric or non-parametric tests, respectively) was used to detect significant differences between the tested concentrations and the control ($p < 0.05$) using Sigmaplot 12.5 statistical package (SYSTAT, n.d.).

3. Results

3.1. Chemical and HPLC analysis

The HPLC analysis showed that BPP is degraded over the course of days. At 48 h a decrease of 20% was observed in solutions with 1000 μg/L, kept in the same climatic conditions as the toxicity tests (Suppl. Material-SM1, Fig. S1; Table S1). Thus, to ensure the presence of the BPP molecule during the entire exposure period, the BPP solution was renewed every 48 h.

3.2. Fish Embryo Toxicity (FET) test

The FET analysis allows the evaluation of several parameters such as mortality, hatching, loss of equilibrium and developmental alterations. Fig. 1 shows an overview of FET analysis after 72 h of exposure, 100% of the organisms exposed to 82000 μg/L of BPP died, lethal and effective concentrations, for mortality and developmental abnormalities respectively, are shown in Table 1.

The observed effects on embryonic development were edema, tail formation, yolk sac, pigmentation and swimming bladder inflation alterations (Fig. 2). The percentages of hatching are shown in Table 2. In the control group, after 72 and 96 h, 96.7% and 100% of the individuals hatched, respectively. However, organisms exposed to 44800 μg/L did not hatch after 72 h of exposure and presented 11.8%, 30% and 58.3% hatching rate after 96, 120, and 168 h of exposure respectively.

After 96 h of exposure to BPP, an equilibrium alteration characterized by organisms' side-lying at the bottom of the microplate well and lack of response to mechanical stimuli was observed (Fig. 3). The EC 10, 20 and 50 of the lack of equilibrium was calculated and presented in Table 1. After 168 h, the EC50 for lack of equilibrium was 7715 μg/L.

3.3. Behavior analysis

The results of behavior analyses can be observed in Fig. 4.

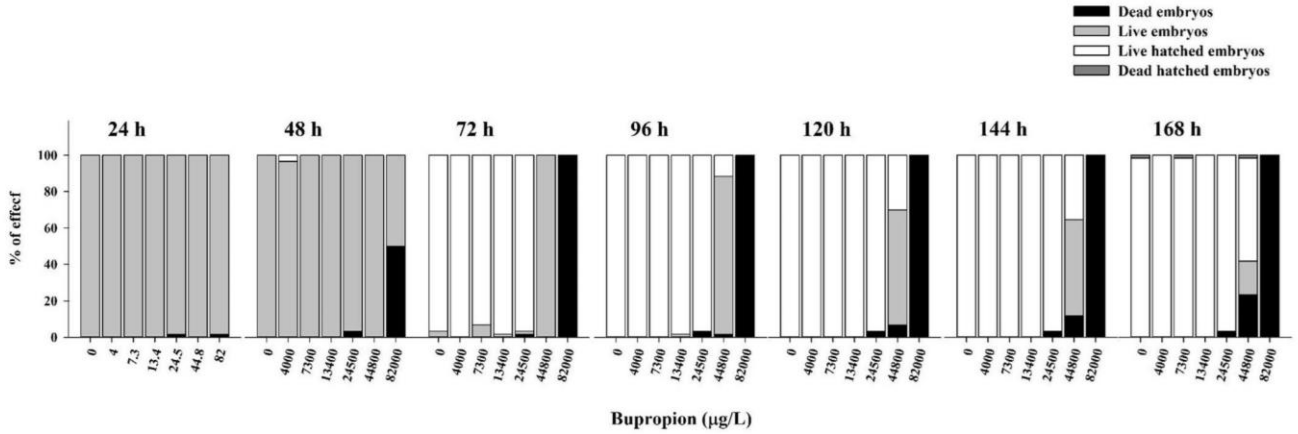

Fig. 1. Overview of effects of bupropion hydrochloride on zebrafish early-life stages during 168 h of exposure. The proportion of dead, alive and hatched organisms is represented by the different bars colors.

Table 1
Effects of bupropion hydrochloride on zebrafish embryos development after 168 h of exposure (mean values ± standard deviation between brackets). The values are presented in µg/L.

Time	L(E)C10	L(E)C20	L(E)C50
Mortality			
48 h	5130 (438)	61577 (3770)	84134 (5052)
72 h	49271 (2505)	52622 (2530)	58886 (2883)
96 h	45788 (2151)	49838 (2109)	57609 (2447)
120 h	43231 (1980)	47437 (1898)	55597 (2276)
144 h	41213 (1934)	45516 (1795)	53939 (2145)
168 h	33809 (2241)	39161 (2039)	50346 (2153)
Hatching			
72 h	20363 (1412)	23852 (1317)	31254 (1435)
96 h	28062 (1810)	30803 (1654)	36123 (1470)
120 h	29443 (2048)	32869 (1802)	39676 (1483)
144 h	29938 (2091)	33540 (1823)	40728 (1496)
168 h	33295 (2133)	37512 (1815)	45994 (1653)
Equilibrium			
96 h	9493 (661)	11055 (600)	14345 (616)
120 h	4760 (420)	5911 (409)	8560 (449)
144 h	5037 (351)	5817 (315)	7438 (305)
168 h	5878 (337)	6499 (271)	7715 (252)
Delay			
24 h	40717 (3904)	52075 (3680)	79305 (5775)
Cardiac edema			
72 h	40939 (16610)	42714 (9181)	45929 (5185)
96 h	30048 (2358)	34386 (1953)	43303 (1789)
120 h	28763 (2041)	32075 (1794)	38642 (1483)
144 h	21190 (11044)	22004 (8494)	23467 (3642)
168 h	14838 (1060)	17178 (969)	22064 (930)
Yolk sac absorption			
120 h	41184 (5021)	43823 (1687)	48733 (5989)
Tail malformations			
96 h	41644 (8782)	43778 (3007)	47682 (8606)
120 h	34607 (2963)	42450 (3052)	60192 (8042)
144 h	25787 (1909)	29853 (1714)	38343 (1681)
168 h	22969 (1436)	26209 (1341)	32843 (1416)
Non inflated swimming blader			
96 h	9493 (661)	11056 (600)	14346 (0616)
120 h	4760 (421)	5911 (409)	8561 (0449)
168 h	7629 (1538)	7866 (267)	8288 (478)

Regarding the total swimming time in the dark, the behavior test showed that zebrafish larvae exposed to a concentration of 0.6 µg/L of BPP presented a total swimming time slightly, but significantly lower than the control group, and larvae exposed to 50000 µg/L presented a total swimming time close to zero, indicating almost total paralysis.

Regarding the total distance moved in the dark, larvae exposed to 0.6 µg/L of the drug showed a significantly lower total distance moved than the control group. Likewise, organisms exposed to the highest concentration of 50000 µg/L presented a total distance moved that was significantly lower, very close to zero movement, when compared to the control group. However, organisms exposed to intermediate concentrations (8.8 and 158 µg/L) of BPP had a significantly higher total distance moved when compared to the control. Both parameters showed no dose response effect.

The percentage of slow and fast movements were also analyzed in the behavior assay. When compared to the control group, zebrafish exposed to 8.8 and 158 µg/L of BPP had a significantly higher percentage of fast movement in the dark, however, zebrafish exposed to 50000 µg/L had a significantly lower percentage of fast movement in the same test period. Regarding the percentage of slow movement in the dark, fish exposed to 8.8 and 158 µg/L of BPP had significantly lower values when compared to the control, and fish exposed to 50000 µg/L had a significantly higher value when compared to the control. Both parameters showed no dose response effect. The parameter percentage of slow and fast movements in the light did not showed statistical differences between the control and the exposed groups.

3.4. Biochemical biomarkers analysis

BPP also affected the enzymatic activity of exposed organisms. After 168 h of exposure, AChE activity was higher in zebrafish at concentrations of 158 and 2812 µg/L, when compared to the control group. However, no statistical difference was observed in AChE activity of zebrafish exposed to 50000 µg/L of BPP, showing no dose-response effect. The enzyme GST presented increased activity in zebrafish exposed to BPP 2812 and 50000 µg/L than in the control group, presenting a dose-response effect. CAT activity was significantly higher in zebrafish exposed to 158 µg/L of BPP when compared to the control, but did not differ in zebrafish exposed to 2812 and 50000 µg/L of the pharmaceutical. The LDH assay presented a statistical difference in fish exposed to 0.6, 2812 and 50000 µg/L of BPP in comparison to the control, despite the absence of dose-response effect (Fig. 5).

4. Discussion

Exposure to BPP showed effect on the survival, development, behavior and enzymatic activities of zebrafish early life stages.

Fig. 2. Zebrafish embryo abnormalities due to bupropion hydrochloride exposure during 48 h (A–B), 96 h (C–D), 144 h (E–G) and 168 h (H–J). ed - oedema, pig - weakly pigmented body, tl - tail malformation, ys - delay in yolk absorption and sb - delay in swimming bladder inflation. Legend of each picture: hours of exposure bupropion hydrochloride concentration (µg/L) between brackets followed by magnification used.

Table 2
Effects of bupropion hydrochloride on zebrafish embryos hatching for organisms exposed for 168 h (mean values ± standard deviation between brackets).

BPP (µg/L)	48 h	72 h	96 h	120 h	144 h	168 h
0.0	0 (0)	96.7 (10.4)	100 (0)	100 (0)	100 (0)	100 (0)
4000	3.3 (3.3)	100 (0)	100 (0)	100 (0)	100 (0)	100 (0)
7300	0 (0)	93.3 (4.4)	100 (0)	100 (0)	100 (0)	100 (0)
13400	0 (0)	98.3 (1.7)	98.3 (1.7)	100 (0)	100 (0)	100 (0)
24500	0 (0)	98.3 (1.7)	100 (0)	100 (0)	100 (0)	100 (0)
44800	0 (0)	0 (0)	11.8 (1.6)	30 (5.8)	35.5 (13.1)	58.3 (10.1)
82000	0 (0)	–	–	–	–	–

"-" hatching not evaluated due to mortality of all exposed organisms.

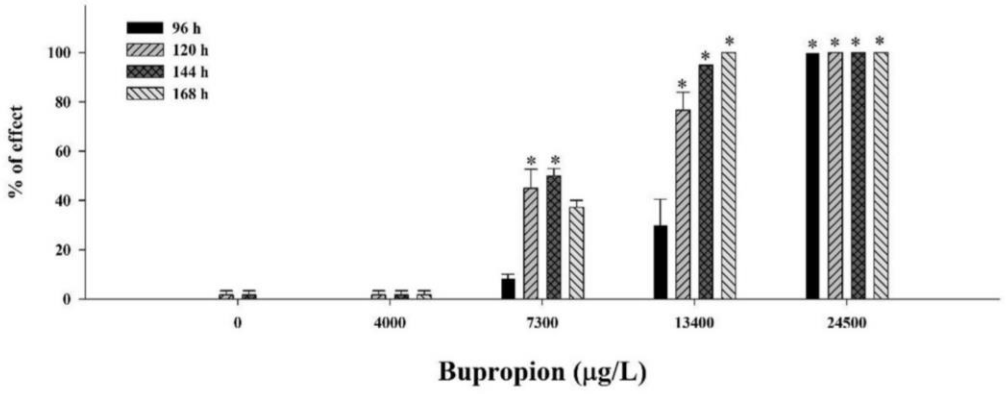

Fig. 3. Effects of bupropion hydrochloride on equilibrium of hatched zebrafish larvae from 96 h to 168 h of exposure. Values represented per mean ± the standard error of the mean. '*' denotes significantly different form control group (Dunn's or Dunnet test, $p < 0.05$).

Toxic effects of BPP on mortality, within the first 24 h, and hatching alteration within the first 72 h of exposure, suggest that this antidepressant can cross the pores of the chorion and interact with the organisms in the pre-hatching phase. The movement of the embryos inside the chorion and the action of hatching enzyme that degrade the inner zone of the chorion are fundamental for hatching (Henn, 2011). Therefore, the inhibition of hatching, observed may be related to the effects of BPP on the locomotor activity of the organisms.

After hatching, which normally occurs around 50 h post

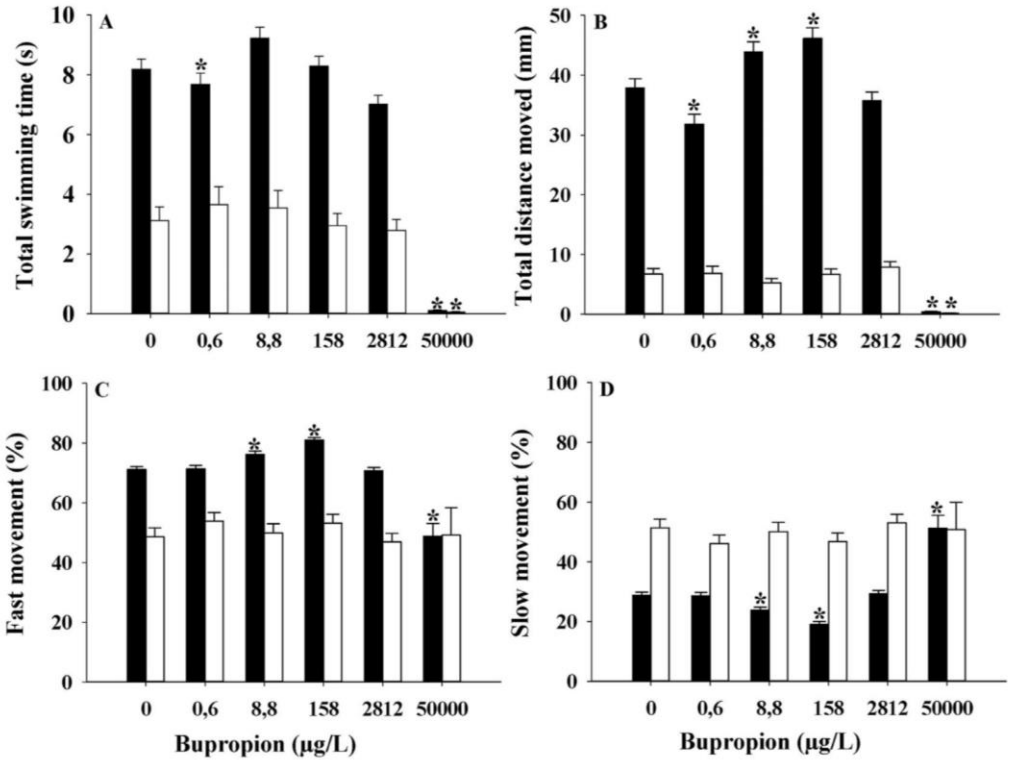

Fig. 4. Locomotor behavior zebrafish larvae after 168 of exposure to bupropion in the dark (black bars) light (white bars): A – Total swimming time; B – Total distance moved; C – Percentage of large distance moved and; D – Percentage of small distance moved. Values represented per mean ± the standard error of the mean. '*' denotes significantly different form control group (Dunn's or Dunnet test, $p < 0.05$).

fertilization (hpf), we observed equilibrium alterations in individuals exposed to low concentrations of BPP at 120 and 144 h of exposure. Additionally, alterations in swimming bladder inflation were observed (168 h EC50 of 8288 µg/L). In many individuals, we observed total paralysis. For fish embryos in natural ecosystems, paralysis can have consequences such as failure in food capture and reproduction and higher susceptibility to predation (Painter et al., 2010). After 168 h, the EC50 for que lack of equilibrium was 7715 µg/L, a concentration 6.5 times lower than the mortality parameter (LC50) for the same period, indicating the sensitivity of the equilibrium used as a parameter.

In addition, it is important to emphasize the relation between swim bladder inflation and equilibrium, observed in the present study. Teleost fish, such a zebrafish, control the volume of gas in the swim bladder, and thus they attain neutral buoyancy at any depth. This way they do not need much energy to swim to hold vertical station in the water column (Lindsey et al., 2010). Lindsey et al. (2010) demonstrated the importance of swim bladder to reduce the body density in zebrafish. Authors observed a relationship between fish volume and mass, and suggested that in the zebrafish development it is necessary a larger swim bladder volume to maintain neutral buoyancy. Therefore, in our study, alterations observed in swimming bladder inflation is probably related to the equilibrium alteration.

To refine the effects of BPP on equilibrium and locomotion of zebrafish, we performed behavior assays, using a range of concentrations covering both environmental and higher concentrations as tested in the FET assay. Regarding low concentrations tested (up to 2812 µg/L) the results showed that behavior at these concentrations levels does not respond in a dose dependent pattern, indicating a slightly decrease for locomotor activity at very low concentrations, an increase at low concentrations, and a severe decrease at high concentrations (50000 µg/L). Other studies investigating the effects of BPP in zebrafish, also observed behavioral alterations. Richendorfer and Creton (2018) showed that zebrafish exposed to 0.1 µM of BPP (27.62 µg/L) from 0 to 120 h had increased swim speeds and decreased rest, indicating an increase in the larva activity at this concentration. This finding is similar to our study, which showed an increase in the total distance moved in organisms exposed to 8.8 µg/L and 158 µg/L of the drug. Also at the behavioral level, acute administration of BPP has been shown to increases activity in rodents (Wilkinson et al., 2006; Wilkinson and Bevins, 2007).

These effects related to the movement, equilibrium and locomotion of zebrafish, observed in the present work, are in line with the mode of action of BPP. This antidepressant inhibits reuptake of norepinephrine and dopamine, producing an increase in these neurotransmitters in the extra-cellular region. Norepinephrine is related to the control of sleep and wakefulness, attention and feeding behavior, while dopamine is related regulation of movement, learning and memory, motivated behavior, and hormonal signaling (Painter et al., 2010). Loss of brain stem dopaminergic neurons leads to movement disorders in humans, nonhuman primates, rodents, and fish (Bretaud et al., 2004; Dauer and Przedborski, 2003; Lam et al., 2005; McKinley et al., 2005; Thirumalai and Cline, 2008).

On the other hand, the extracellular dopamine, in increased levels, may be harmful to dopaminergic neurons because this dopamine can be auto-oxidized to the neurotoxicant 6-hydroxydopamine (6-OHDA), which has been shown to cause cellular stress (Holtz et al., 2006; Holtz and O'Malley, 2003). Therefore, BPP, which increases extracellular dopamine, can

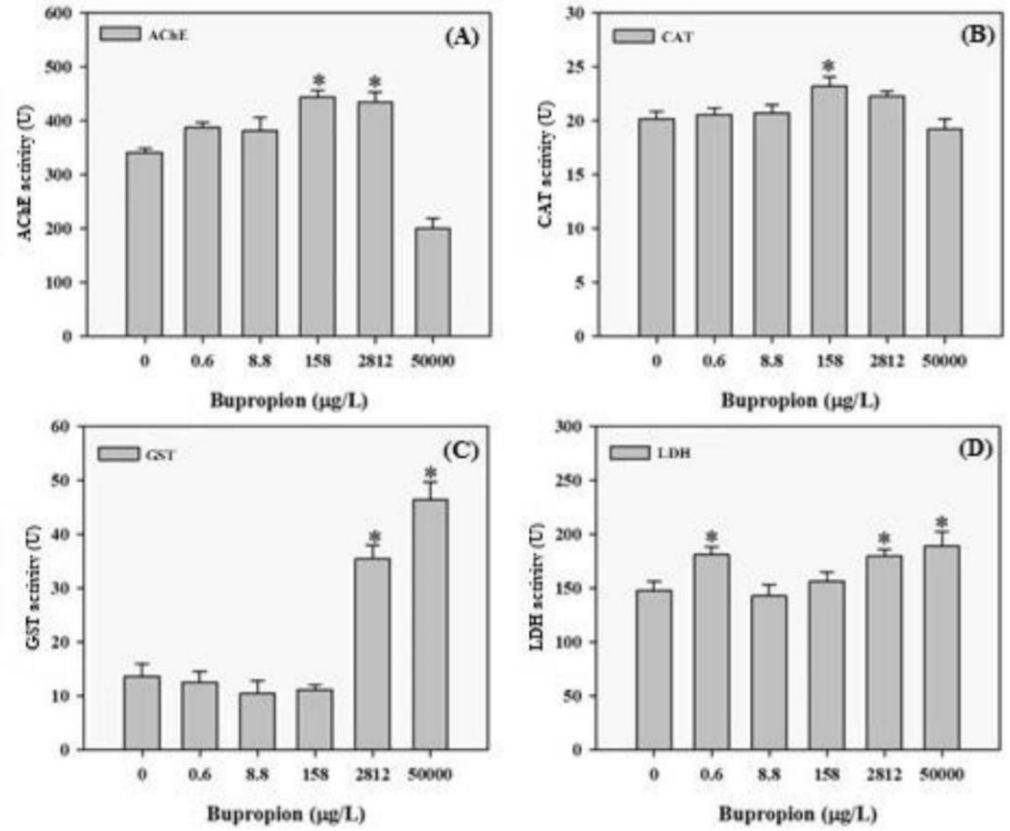

Fig. 5. Bupropion effects in zebrafish embryos enzymatic activities after 168 h of exposure: (A) AChE - acetylcholinesterase, (B) CAT – catalase; (C) GST - glutathione S-transferase and (D) LDH - lactate dehydrogenase. Values represented per mean ± the standard error of the mean. '*' denotes significantly different form control group (Dunn's or Dunnet test, $p < 0.05$).

potentially disrupt the homeostasis of the dopaminergic system (Jang et al., 2011). This auto oxidation can explain findings in the present study, showing decrease in the equilibrium and locomotion at high doses. However, low doses of BPP may not have caused this auto oxidation, but only a slight increase in extracellular dopamine, which explains the increase in the total distance moved of zebrafish exposed to low concentrations of BPP.

It is well known that the reduction of the crossed glycinergic transmission can cause an increased burst rate. Low concentrations of dopamine increase burst frequency, but high concentrations decrease it. Several authors pointed out that the mechanism of the presynaptic depression of crossed glycinergic inhibition caused by dopamine may be acting at low levels (Svensson et al., 2003). Regarding high concentrations, authors mentioned that the mechanism that can be acting is that dopamine can cause a reduction in the calcium ions in the glutamatergic neurons. This calcium reduction in these neurons leads to a reduction of the afterhyperpolarisation (sAHP). This decrease of the sAHP can cause a reduced spike frequency adaptation, and therefore also longer bursts and slower swimming (Svensson et al., 2003). These mechanisms can also be related to the findings of the present study, we observed that fast movements were more travelled during the dark period, while slow movements, during the light period. The statistical differences between the control and exposed group, however, were observed only during the dark period. Zebrafish larvae exposed to intermediate concentrations (8.8 and 158 µg/L) of bupropion travelled more in fast movements that may indicate a sign of hyperactivity in these concentrations. On the other hand, organisms exposed to 50000 µg/L swam significantly more in slow movements when compared to control, probably due to the total paralyses observed at this concentration.

In addition to FET and behavior assay, we also analyzed enzymatic activity of AChE, CAT, GST and LDH. The increased activity of AChE of larvae under exposure to 158 µg/L is in line with our behavior results, which indicated an increased total distance moved and percentage of large distance, since cholinesterase's activities are directly related to behavioral changes (Scott and Sloman, 2004). Those authors suggest that a biochemical response such as increase or inhibition of AChE activity is correlated to changes in the locomotor behavior of zebrafish embryos (Andrade, 2015). Besides, BPP, in addition to blocking dopamine and norepinephrine re-uptake, also acts as a nicotinic acetylcholine receptor (nAChR) antagonist, interfering with the movement and locomotor activity of the organism (Slemmer et al., 2000; Wilkinson and Bevins, 2007).

Our results also showed a pronounced increase in the activity of the GST enzyme and a slight increase in CAT activity in exposed organisms. Hu et al. (2000) pointed out that BPP causes mild increases of serum liver enzymes in adults of zebrafish. Therefore, the increase of these enzymes in exposed zebrafish embryos observed in the present study is probably also linked to a mild increase of serum liver enzymes. In addition, GST plays an important role in the detoxification process of xenobiotic in fish (Oliveira et al., 2009). An increase of GST have been observed in zebrafish embryos exposed to different pharmaceutical (Oliveira et al., 2009). Thus, the obtained results suggest GST activity as important biomarkers to take

in account in the evaluation of fish abilities to protects against pollutants such as BPP.

Finally, the LDH activity, measured in this study, had also an increase in exposed zebrafish early life stages. Since it is an intracellular enzyme, the increase of LDH can indicate tissue damage with the consequent release of the enzyme. The damage can vary from a slight cellular damage to severe cellular necrosis. The increase in LDH activity observed at the highest tested concentrations is probably linked to cell death, as effects on embryonic survival were observed in the FET assay in similar concentrations. Jang et al. (2011) also observed that BPP at 100 μg/mL induced cell death, with early and late apoptotic characteristics.

The present study showed that low concentrations of BPP could affect the biochemical reactions and the behavior of zebrafish. Since the BPP was already found in the environment at concentrations up to 4.3 μg/L (wastewater effluent), this antidepressant can disrupt the aquatic life homeostasis. To survive in the ecosystem, a larva must be able to respond quickly and swim rapidly, and any deviation in the normal signaling may have lethal consequences (Painter et al., 2010). Moreover, pharmaceuticals can accumulate in the tissues, having toxic effects. BPP, which has a Kow >3, was found in brains of exposed fish at higher concentrations than those suggested by water concentrations of the respective compounds (Schultz et al., 2011). Therefore, for the effective protection of aquatic ecosystems, it is necessary to carry out more analysis of drug effects, to increase policies for biomonitoring of drug concentrations, and development and use more effective technologies in the treatments in WWTPs. Besides, more effort should be invested in the research and development of pharmaceuticals with less environmental impact.

5. Conclusion

We can conclude that the exposure to the antidepressant BPP can affects zebrafish early life stages. Besides developmental endpoints measured in the FET test, we also explored sub-lethal effects of BPP exposure in a concentration range where developmental effects were not observed. Behavior (measured as locomotor activity) and enzymes activities of zebrafish were affected at concentrations close to the ones detected in the environment. These results elucidate the importance of toxicity evaluations of pharmaceuticals by applying an approach that includes multiple parameters in order to comprise more realistic exposure scenarios.

Ethical standards

The experiments are in accordance with the current laws of the country in which they were performed. The study was approved by the ethics committee at the University of Brasilia (reference no 100226/2014).

Conflicts of interest

The authors declare that they have no conflict of interest.

Acknowledgements

The authors acknowledge the Brazilian Ministry of Education, and Ministry of Science and Technology of Brazil for the scholarship provided to RO (CNPq BJT-A, CAPES PNPD, FAPESP grant no. 2018/03108-0); DSM acknowledge CAPES for the PhD scholarship. CKG is grateful to CNPq grant “Bolsas de Produtividade”. This work was also supported by CESAM (UID/AMB/50017 - POCI-01-0145-FEDER-007638), FCT/MCTES through national funds (PIDDAC), and the cofunding by the FEDER, within the PT2020 Partnership Agreement and Compete 2020. Support was also given by FCT to ID (Post-Doc grant SFRH/BPD/90521/2012) and Federal District Research Foundation (FAP-DF; water quality call - 05/2016).

Appendix A. Supplementary data

Supplementary data to this article can be found online at https://doi.org/10.1016/j.chemosphere.2019.01.141.

References

Aebi, H., 1984. [13] Catalase in vitro. Methods Enzymol. 105, 121–126. https://doi.org/10.1016/S0076-6879(84)05016-3.

Andrade, T. de S., 2015. Effects of environmental factors on the toxicity of pesticides to zebrafish embryos.

Blaser, R.E., Chadwick, L., McGinnis, G.C., 2010. Behavioral measures of anxiety in zebrafish (Danio rerio). Behav. Brain Res. 208, 56–62. https://doi.org/https://doi.org/10.1016/j.bbr.2009.11.009.

Bottoni, P., Caroli, S., Caracciolo, A.B., 2010. Pharmaceuticals as priority water contaminants. Toxicol. Environ. Chem. 92, 549–565. https://doi.org/10.1080/02772241003614320.

Bradford, M.M., 1976. A rapid and sensitive method for the quantitation of microgram quantities of protein utilizing the principle of protein-dye binding. Anal. Biochem. 72, 248–254. https://doi.org/https://doi.org/10.1016/0003-2697(76)90527-3.

Brandão, F.P., Rodrigues, S., Castro, B.B., Gonçalves, F., Antunes, S.C., Nunes, B., 2013. Short-term effects of neuroactive pharmaceutical drugs on a fish species: Biochemical and behavioural effects. Aquat. Toxicol. 144–145, 218–229. https://doi.org/https://doi.org/10.1016/j.aquatox.2013.10.005.

Bretaud, S., Lee, S., Guo, S., 2004. Sensitivity of zebrafish to environmental toxins implicated in Parkinson's disease. Neurotoxicol. Teratol. 26, 857–864. https://doi.org/https://doi.org/10.1016/j.ntt.2004.06.014.

Brodin, T., Fick, J., Jonsson, M., Klaminder, J., 2013. Dilute Concentrations of a Psychiatric Drug Alter Behavior of Fish from Natural Populations. Science (80-.) 339, 814–815.

Calisto, V., Esteves, V.I., 2009. Psychiatric pharmaceuticals in the environment. Chemosphere. https://doi.org/10.1016/j.chemosphere.2009.09.021.

Conners, C.K., Casat, C.D., Gualtieri, C.T., Weller, E., Reader, M., Reiss, A., Weller, R.A., Khayrallah, M., Ascher, J., 1996. Bupropion Hydrochloride in Attention Deficit Disorder with Hyperactivity. J. Am. Acad. Child Adolesc. Psychiatry 35, 1314–1321. https://doi.org/https://doi.org/10.1097/00004583-199610000-00018.

Dauer, W., Przedborski, S., 2003. Parkinson's Disease: Mechanisms and Models. Neuron 39, 889–909. https://doi.org/https://doi.org/10.1016/S0896-6273(03)00568-3.

Dong, Z., Senn, D.B., Moran, R.E., Shine, J.P., 2013. Prioritizing environmental risk of prescription pharmaceuticals. Regul. Toxicol. Pharmacol. 65, 60–67. https://doi.org/https://doi.org/10.1016/j.yrtph.2012.07.003.

Ellman, G.L., Courtney, K.D., Andres, V., Feather-stone, R.M., 1961. A new and rapid colorimetric determination of acetylcholinesterase activity. Biochem. Pharmacol. 7, 88–95. https://doi.org/10.1016/0006-2952(61)90145-9.

Farias, N.O., Oliveira, R., Sousa-Moura, D., de Oliveira, R.C.S., Rodrigues, M.A.C., Andrade, T.S., Domingues, I., Camargo, N.S., Muehlmann, L.A., Grisolia, C.K., 2019. Exposure to low concentration of fluoxetine affects development, behaviour and acetylcholinesterase activity of zebrafish embryos. Comp. Biochem. Physiol. Part C Toxicol. Pharmacol. 215, 1–8. https://doi.org/https://doi.org/10.1016/j.cbpc.2018.08.009.

Fava, M., Rush, A.J., Thase, M.E., Clayton, A., Stahl, S.M., Pradko, J.F., Johnston, J.A., 2005. 15 years of clinical experience with bupropion HCl: from bupropion to bupropion SR to bupropion XL. Prim. Care Companion J. Clin. Psychiatry 7, 106–113.

Ferrer, I., Thurman, E.M., 2012. Analysis of 100 pharmaceuticals and their degradates in water samples by liquid chromatography/quadrupole time-of-flight mass spectrometry. J. Chromatogr. A 1259, 148–157. https://doi.org/https://doi.org/10.1016/j.chroma.2012.03.059.

Guo, S., 2009. Using zebrafish to assess the impact of drugs on neural development and function. Expert Opin. Drug Discov. 4, 715–726. https://doi.org/10.1517/17460440902988464.

Habig, W.H., Jakoby, W.B. in E., 1981. [51] Assays for differentiation of glutathione S-Transferases. In: Detoxication and Drug Metabolism: Conjugation and Related Systems. Academic Press, pp. 398–405. https://doi.org/https://doi.org/10.1016/S0076-6879(81)77053-8.

Henn, K., 2011. Limits of the fish embryo toxicity test with Danio rerio as an alternative to the acute fish toxicity test. University of Heidelberg. https://doi.org/10.11588/heidok.00012998.

Hill, A.J., Teraoka, H., Heideman, W., Peterson, R.E., 2005. Zebrafish as a Model Vertebrate for Investigating Chemical Toxicity. Toxicol. Sci. 86, 6–19. https://doi.org/https://doi.org/10.1093/toxsci/kfi110.

Holtz, W.A., O'Malley, K.L., 2003. Parkinsonian Mimetics Induce Aspects of Unfolded Protein Response in Death of Dopaminergic Neurons. J. Biol. Chem. 278, 19367–19377. https://doi.org/10.1074/jbc.M211821200.

Holtz, W.A., Turetzky, J.M., Jong, Y.-J.I., O'Malley, K.L., 2006. Oxidative stress-triggered unfolded protein response is upstream of intrinsic cell death evoked by parkinsonian mimetics. J. Neurochem. 99, 54–69. https://doi.org/10.1111/j.1471-4159.2006.04025.x.

Hu, K.-Q., Tiyyagura, L., Kanel, G., Redeker, A, G., 2000. Case report: Acute Hepatitis Induced by Bupropion, Digestive Diseases and Sciences. https://doi.org/10.1023/A:1005553405313.

Irons, T.D., MacPhail, R.C., Hunter, D.L., Padilla, S., 2010. Acute neuroactive drug exposures alter locomotor activity in larval zebrafish. Neurotoxicol. Teratol. 32, 84–90. https://doi.org/https://doi.org/10.1016/j.ntt.2009.04.066.

Jang, E.-H., Park, C.-S., Kang, J.-H., 2011. Bupropion, an atypical antidepressant, induces endoplasmic reticulum stress and caspase-dependent cytotoxicity in SH-SY5Y cells. Toxicology 285, 1–7. https://doi.org/https://doi.org/10.1016/j.tox.2011.02.006.

Lam, C.S., Korzh, V., Strahle, U., 2005. Zebrafish embryos are susceptible to the dopaminergic neurotoxin MPTP. Eur. J. Neurosci. 21, 1758–1762. https://doi.org/10.1111/j.1460-9568.2005.03988.x.

Lindsey, B.W., Smith, F.M., Croll, R.P., 2010. From Inflation to Flotation: Contribution of the Swimbladder to Whole-Body Density and Swimming Depth During Development of the Zebrafish (Danio rerio). Zebrafish (1), 85–96. https://doi.org/10.1089/zeb.2009.0616.

McKinley, E.T., Baranowski, T.C., Blavo, D.O., Cato, C., Doan, T.N., Rubinstein, A.L., 2005. Neuroprotection of MPTP-induced toxicity in zebrafish dopaminergic neurons. Mol. Brain Res. 141, 128–137. https://doi.org/https://doi.org/10.1016/j.molbrainres.2005.08.014.

OECD, 2013. Test No. 236: Fish Embryo Acute Toxicity (FET) Test. OECD Guidel. Test. Chem. Sect. 2. OECD Publ, Paris. https://doi.org/10.1787/9789264203709-en.

Oliveira, R., Domingues, I., Grisolia, C.K., Soares, A.M.V.M., 2009. Effects of triclosan on zebrafish early-life stages and adults. Environ. Sci. Pollut. Res. 16, 679–688. https://doi.org/10.1007/s11356-009-0119-3.

Painter, M.M., Buerkley, M.A., Julius, M.L., Vajda, A.M., Norris, D.O., Barber, L.B., Furlong, E.T., Schultz, M.M., Schoenfuss, H.L., 2010. Antidepressants at environmentally relevant concentrations affect predator avoidance behavior of larval fathead minnows (Pimephales promelas). Environ. Toxicol. Chem. 28, 2677–2684. https://doi.org/10.1897/08-556.1.

Richendrfer, H., Creton, R., 2018. Cluster analysis profiling of behaviors in zebrafish larvae treated with antidepressants and pesticides. Neurotoxicol. Teratol. 69, 54–62. https://doi.org/https://doi.org/10.1016/j.ntt.2017.10.009.

Ritz, C., Streibig, J.C., 2005. Bioassay Analysis Using R. J. Stat. Software 1 (5).

Santos, N.S., Oliveira, R., Lisboa, C.A., Mona e Pinto, J., Sousa-Moura, D., Camargo, N.S., Perillo, V., Oliveira, M., Grisolia, C.K., Domingues, I., 2018. Chronic effects of carbamazepine on zebrafish: Behavioral, reproductive and biochemical endpoints. Ecotoxicol. Environ. Saf. 164, 297–304. https://doi.org/https://doi.org/10.1016/j.ecoenv.2018.08.015.

Schultz, M.M., Furlong, E.T., 2008. Trace Analysis of Antidepressant Pharmaceuticals and Their Select Degradates in Aquatic Matrixes by LC/ESI/MS/MS. Anal. Chem. 80, 1756–1762. https://doi.org/10.1021/ac702154e.

Schultz, M.M., Painter, M.M., Bartell, S.E., Logue, A., Furlong, E.T., Werner, S.L., Schoenfuss, H.L., 2011. Selective uptake and biological consequences of environmentally relevant antidepressant pharmaceutical exposures on male fathead minnows. Aquat. Toxicol. 104, 38–47. https://doi.org/10.1016/j.aquatox.2011.03.011.

Scott, G.R., Sloman, K.A., 2004. The effects of environmental pollutants on complex fish behaviour: integrating behavioural and physiological indicators of toxicity. Aquat. Toxicol. 68, 369–392. https://doi.org/https://doi.org/10.1016/j.aquatox.2004.03.016.

Slemmer, J.E., Martin, B.R., Damaj, M.I., 2000. Bupropion is a nicotinic antagonist. J. Pharmacol. Exp. Ther. 295, 321–327.

Stahl, S.M., Pradko, J.F., Haight, B.R., Modell, J.G., Rockett, C.B., Learned-Coughlin, S., 2004. A Review of the Neuropharmacology of Bupropion, a Dual Norepinephrine and Dopamine Reuptake Inhibitor. Prim. Care Companion J. Clin. Psychiatry 6, 159–166.

Svensson, E., Woolley, J., Wikström, M., Grillner, S., 2003. Endogenous dopaminergic modulation of the lamprey spinal locomotor network. Brain Res. 970, 1–8. https://doi.org/https://doi.org/10.1016/S0006-8993(02)04216-6.

SYSTAT, n.d. SigmaPlot, Systat Software, Inc., San Jose California USA, www.sigmaplot.com.

Thirumalai, V., Cline, H.T., 2008. Endogenous dopamine suppresses initiation of swimming in prefeeding zebrafish larvae. J. Neurophysiol. 100, 1635–1648. https://doi.org/10.1152/jn.90568.2008.

Ulu, S.T., Tuncel, M., 2012. Determination of Bupropion Using Liquid Chromatography with Fluorescence Detection in Pharmaceutical Preparations, Human Plasma and Human Urine. J. Chromatogr. Sci. 50, 433–439.

Vassault, A., 1983. Lactate dehydrogenase. In: Bergmeyer, H.O. (Ed.), Methods of Enzymatic Analysis, Vol III, Enzymes: Oxireductases, Transferases. Academic Press, New York, pp. 118–126.

Webb, S., Ternes, T., Gibert, M., Olejniczak, K., 2003. Indirect human exposure to pharmaceuticals via drinking water. Toxicol. Lett. 142, 157–167. https://doi.org/https://doi.org/10.1016/S0378-4274(03)00071-7.

Wilkinson, J.L., Bevins, R.A., 2007. Bupropion hydrochloride produces conditioned hyperactivity in rats. Physiol. Behav. 90, 790–796. https://doi.org/https://doi.org/10.1016/j.physbeh.2007.01.003.

Wilkinson, J.L., Palmatier, M.I., Bevins, R.A., 2006. Preexposure to Nicotine Alters the Subsequent Locomotor Stimulant Effects of Bupropion in Rats. Nicotine Tob. Res. 8, 141–146.

Writer, J.H., Ferrer, I., Barber, L.B., Thurman, E.M., 2013. Widespread occurrence of neuro-active pharmaceuticals and metabolites in 24 Minnesota rivers and wastewaters. Sci. Total Environ. 461–462, 519–527. https://doi.org/https://doi.org/10.1016/j.scitotenv.2013.04.099.

Wu, M., Xiang, J., Que, C., Chen, F., Xu, G., 2015. Occurrence and fate of psychiatric pharmaceuticals in the urban water system of Shanghai, China. Chemosphere 138, 486–493. https://doi.org/https://doi.org/10.1016/j.chemosphere.2015.07.002.

Yuan, S., Jiang, X., Xia, X., Zhang, H., Zheng, S., 2013. Detection, occurrence and fate of 22 psychiatric pharmaceuticals in psychiatric hospital and municipal wastewater treatment plants in Beijing, China. Chemosphere 90, 2520–2525. https://doi.org/https://doi.org/10.1016/j.chemosphere.2012.10.089.

Zenker, A., Cicero, M.R., Prestinaci, F., Bottoni, P., Carere, M., 2014. Bioaccumulation and biomagnification potential of pharmaceuticals with a focus to the aquatic environment. J. Environ. Manag. 133, 378–387. https://doi.org/https://doi.org/10.1016/j.jenvman.2013.12.017.

Journal of Environmental Chemical Engineering 6 (2018) 2846–2854

Contents lists available at ScienceDirect

Journal of Environmental Chemical Engineering

journal homepage: www.elsevier.com/locate/jece

Study of YVO_4 as a photocatalyst: Correlation between synthetic route and ecotoxicity

Carlos Martins Aiube[a], Tatiane Martins Lobo[a], Diego Sousa-Moura[b], Irvin Bryan Machado Ferraz[b], Marly Eiko Osugi[a], Cesar Koppe Grisolia[b], Rhaul Oliveira[c,d], Ingrid Távora Weber[a,e,*]

[a] Instituto de Química, Universidade de Brasília – UnB, Campus Darcy Ribeiro, 70910-900, Brasília, DF, Brazil
[b] Departamento de Genética e Morfologia, Instituto de Ciências Biológicas, Universidade de Brasília – UnB, Campus Darcy Ribeiro, 70910-900, Brasília, DF, Brazil
[c] Faculdade de Tecnologia, Universidade Estadual de Campinas – UNICAMP, 13484-332, Limeira, SP, Brazil
[d] Programa de Pós-graduação em Toxicologia e Análises Toxicológicas, Faculdade de Ciências Farmacêuticas, Universidade de São Paulo, FCF – USP, 05508-000, São Paulo, SP, Brazil
[e] Programa de Pós-graduação em Ciência de Materiais, Departamento de Química Fundamental, Universidade Federal de Pernambuco – UFPE, Av. Prof. Luiz Freire, Cidade Universitária, 50740-540, Recife, PE, Brazil

ARTICLE INFO

Keywords:
Yttrium orthovanadate
Combustion route
Hydrothermal route
Rhodamine B
FET

ABSTRACT

Yttrium orthovanadate (YVO_4) powders were synthesized by two different routes: the combustion route (C sample), and the hydrothermal route (H samples). In all samples, oxygen vacancies were observed by Raman, UV–vis diffuse reflectance and photoluminescence (PL) spectroscopy; however they were more significant in C sample. Photocatalytic discoloration of Rhodamine B solutions ranged from 40 to 64% and C and H4 samples presented the highest efficiencies. Although both samples showed similar photocatalytic efficiency, C sample is 11 times more efficient in producing reactive oxygen species than H4 sample, and an interesting effect of the treated solutions was observed in the Fish Embryotoxicity Test, carried out in *D. rerio*. The C-treated solution was more toxic than the untreated solution, while the H4-treated solution did not show toxicity enhancement. C-treated solution caused a significant mortality of *D. rerio* embryos beginning at the 4th day of exposure and reached total mortality at the 6th day. Thus, the synthetic route employed in the preparation of C and H4 samples leads to different toxic effects in the treated solutions. These results pointed out that microstructural characteristics and synthetic parameters are not only important for obtaining highly active materials, but they also impact on the toxicity of the effluents.

1. Introduction

Microstructural characteristics of the catalyst play an important role in heterogeneous photocatalytic reactions. It is well known that particle size, morphology, crystallinity, and presence of synthetic residues influence the efficiency of heterogeneous photocatalytic reactions. As a consequence of the many studies on this, there is a vast literature regarding the effect of synthetic route on photocatalytic activity. For instance, Giraldi et al. [1,2] has shown that the increase of crystallinity of ZnO nanoparticles achieved with post-annealing treatments enhanced their photocatalytic activity; as well, they reported on how synthetic residues can inhibit the photocatalytic activity even when crystalline particles are used. Jana et al. [3] studied CdS/ZnO nanocomposites and observed a relation between composite morphology (controlled by synthesis) and photocatalytic and antibacterial activity. Even a mixture of phases of the same semiconductor can present higher activity than pure phases, as shown by Zhang et al. [4] in the synthesis of TiO_2 nanotube arrays by electrochemical anodization. In addition, He et al. [5] showed that the deposition of Au nanoparticles onto ZnO increased the photo-induced generation of reactive oxygen species (ROS), such as hydroxyl radical, superoxide and singlet oxygen, and the production of excitons.

Besides that, structural defects of semiconductors, such as oxygen vacancies, can also play a key role in their functionality. For example, these can mediate electron-hole recombination or may introduce deep trapping states within the band gap of the semiconductors, which confines the photoinduced electrons and affects the photocatalytic performance [6]. As a result, changes in band gap and photocatalytic activity can be significant when these defects implements disorder in as many crystal lattices as possible (not only in semiconductor's surface)

* Corresponding author at: Instituto de Química, Universidade de Brasília – UnB, Campus Darcy Ribeiro, 70910-900, Brasília, DF, Brazil.
E-mail addresses: ingrid@ufpe.br, itweber@unb.br (I.T. Weber).

https://doi.org/10.1016/j.jece.2018.04.011
Received 23 November 2017; Received in revised form 2 April 2018; Accepted 6 April 2018
Available online 07 April 2018

[7], or creates permitted levels in the electronic structure [8]. For example, oxygen vacancies can drive photocatalytic activity towards visible light, as shown by Zhang et al. for ZnO nanoparticles [9] or improve photoactivity in the UV range, as shown by Yang et al. [10] for YVO_4 nanoparticles.

Another important aspect in photocatalytic reactions aiming environmental issues is toxicity. Some authors have studied the toxic effects of photocatalytic treated effluents [11–13] and the toxicity of the catalyst (especially when they are nanoscaled) [14,15]. However, only a few studies correlate the synthetic route of photocatalysts and microstructural characteristics with this kind of effect, since these features are generally ignored when evaluating photocatalytic processes. In this work, we discuss the photocatalytic activity of YVO_4, synthesized by two routes, focusing on differences of ecotoxicology of Rhodamine B treated solutions, using a Fish Embryotoxicity Test (FET) with zebrafish (*Danio rerio*) as biosensors.

2. Materials and methods

2.1. Synthesis of YVO_4

YVO_4 was synthesized by two routes: combustion and hydrothermal (adapted from the literature [16,17]).

For the combustion route (C sample), 3.76 g (9.81 mmols) of $Y(NO_3)_3{\cdot}6H_2O$ (Sigma-Aldrich, 99.9% purity), 1.15 g (9.81 mmols) of NH_4VO_3 (IMEX, 99.9% purity), and 1.77 g (29.43 mmols) of urea (Sigma-Aldrich, 98% purity) were dissolved in 20 mL of distilled water after magnetic stirring and heating at 100 °C for 1 h (for partial evaporation of the solvent). After this time, the mixture was treated initially at 550 °C for 15 min (to achieve combustion), being observed a flame and the emission of gases such as NO_x (dark brown) and possibly NH_3 (pungent scent). A post-annealing at 900 °C for 8 h was required for elimination of synthetic residues and proper crystallization of the desired phase.

For the hydrothermal route, 0.50 g (1.305 mmols) of $Y(NO_3)_3{\cdot}6H_2O$ and 1.53 g (13.05 mmols) NH_4VO_3 were dissolved in 10–15 mL of distilled water inside a 50 mL glass beaker and heated at 60–70 °C for 30 min under magnetic stirring with a watch glass covering the system. The pH was adjusted at 9–10, employing an aqueous solution of NaOH (BioXtra, Sigma-Aldrich, > 98.0% purity, anhydrous pellets) at 2 mols L^{-1}, and vigorously stirred during 1 h at same temperature as before. The mixture was transferred to a Teflon autoclave reactor, sealed and heated at 150 °C for 4 or 24 h (H4 and H24 samples, respectively). After this period, the autoclaves were statically cooled to room temperature, opened and the product (a white and thin solid) was filtered, washed 3 times with distilled water, and then dried in a hot air oven at 60 °C for 1 h. No post annealing treatment was performed in this case.

2.2. Microstructural characterization of YVO_4

The crystalline phase was identified by X-ray diffraction (XRD, Bruker D8 Focus, with Cu Kα radiation of $\lambda = 0.1540619$ nm between 2θ range = 15–60°). The specific surface area (S_{BET}) was estimated through adsorption-desorption isotherms of N_2 at −196 °C (Quantachrome Instruments, NOVA 2200e). The Raman spectra (Renishaw spectrophotometer, inVia Raman Microscope, Ar laser source operating at 20 mW and 514.5 nm) were recorded to evaluate the short-range ordering. The optic properties were studied through UV–vis (Varian Cary 5000 UV–vis NIR, diffuse reflectance mode, $BaSO_4$ as a reference, wavelength range = 200–800 nm) and photoluminescence (PL) spectra (Thermo Fischer Scientific Lumina spectrophotometer, Xe 450 W lamp adjusted for $\lambda_{excitation} = 325$ nm, step-rate = 60 nm min^{-1}). Scanning electron microscope (SEM, JEOL-JSM 7001-F) images were obtained for evaluation of morphology.

2.3. Photocatalytic tests

Photocatalytic efficiency was evaluated by discoloration of an aqueous solution of Rhodamine B (RhB, Sigma, > 95% purity) at 2.5 mg L^{-1}. For this purpose, 18.75 mg of a YVO_4 sample was added in 75 mL of the RhB solution, and the suspension was irradiated with a UV-C high pressure Hg lamp (125 W; $\lambda = 255$ nm; without the bulb) for 7 h, under stirring. Aliquots (5.0 mL) were collected first after 30 min, and, then after every 1 h. After sampling, the catalyst was separated from the solution by centrifugation at 10000 r.p.m and dye quantification was performed by UV–vis spectroscopy (Varian Cary 5000 UV–vis NIR), measuring the maximum absorbance at 554 nm. A test was also performed in the absence of the catalyst to check photolysis of RhB. Dark tests were performed as well, under the same conditions as the photocatalytic tests to evaluate dye adsorption on the catalysts' surface. The assays were performed in triplicate. Afterwards, 15.0 mL of the remaining treated solution was analyzed through Total Organic Carbon (TOC, Shimadzu LCPH/CPN) after prior removal of the catalyst.

2.4. Determination of reactive oxygen species production

The efficiency of YVO_4 samples in generating reactive oxygen species (ROS) through photocatalysis was monitored by the hydroxylation of terephthalic acid (TA), resulting in the fluorescent probe 2-hydroxyterephthalic acid (2-OH-TA, emission at 425 nm) [18]. For this purpose, suspensions made of 18.75 mg of the mentioned samples and 75 mL of an aqueous solution containing $3{\cdot}10^{-3}$ mols L^{-1} of TA (Sigma Aldrich, 98.0% purity) and $1{\cdot}10^{-2}$ mols L^{-1} of NaOH were prepared and submitted to the same light irradiation of photocatalytic tests for 2 h. Before exposure to light irradiation, the suspensions were stirred in the dark for 30 min. Then, an aliquot of 5 mL of was sampled and centrifuged every 30 min. For observing the formation of 2-OH-TA, the emission spectra of aliquots were acquired (Horiba spectrophotometer, model Fluorolog) under $\lambda_{excitation} = 315$ nm. A test was also performed in the absence of catalyst to check the effect of photolysis.

2.5. Detection of synthetic residues

Thermogravimetric and differential thermal analysis (TGA/DTA) for C catalysts were performed using a Shimadzu Simultaneous TGA/DTA Analyzer DTG-60AH, in the 25–1000 °C temperature range, using a platinum crucible with ca. 10.0 mg of sample, under synthetic air atmosphere (30 mL min^{-1}) and with a heating rate of 10 °C min^{-1}.

Suspensions formed by mixing 18.75 mg of C-sample and 75 mL of distilled water were submitted to the same conditions used in the photocatalytic test. Then they were analyzed for nitrite ions (one possible by-product of urea's oxidation) using the Griess test [19], after prior removal of the solid. Five standard solutions of 5.0 mL with concentrations ranging between of 1.0 to 5.0 μg L^{-1} of nitrite ions were prepared by mixing an appropriate dilution of a stock solution of 1.0 mol L^{-1} of $NaNO_2$ (ACS reagent, > 97.0% purity) with a solution (Griess reagent) of 2.0 wt.% sulfanilamide (Sigma-Aldrich, 99% purity), 0.2 wt.% N-(1-naphthyl)ethylenediamine dihydrochloride (NEED, ACS reagent, > 99% purity) and 10.0 wt.% of HCl, taking absorbance at 540 nm to construct a calibration curve. The sample was mixed with the Griess reagent in the volume proportion of 1:8 sample to reagent ratio.

2.6. Fish embryotoxicity test

Toxicity of the RhB solutions was studied with a 144 h (six days) fish embryotoxicity test based on the OECD guideline FET [20]. *D. rerio* (zebrafish) were raised in a recirculating system (ZebTec − Tecniplast) and maintained under routine approved animal welfare protocols at the aquatic facility of University of Brasilia (Brazil). The water parameters were strictly controlled; temperature was kept at 26.0 ± 1 °C, conductivity at 650 ± 100 μS cm^{-1}, pH at 7.0 ± 0.5 and dissolved

oxygen equal or above 95% saturation. Groups of twenty organisms, with an average weight 0.6 ± 0.1 g and size 2.5 ± 0.5 cm, were maintained in tanks (8 L) with reverse osmosis and activated carbon filtered water under a photoperiod cycle of 12:12 h (light:dark). Adults were fed two times daily with live brine shrimp nauplii, *Artemia* sp., and dry fish flake mix (TetraMin® flake). Embryos were routinely bred from bulk spawning of stock fish in a spawning platform in 2:1 male to female ratio (iSPAWN, Tecniplast). Eggs were collected immediately after natural mating, rinsed in water, and checked under a stereomicroscope (Stereoscopic Zoom Microscope − SMZ 1500, Nikon Corporation). The unfertilized eggs and those with cleavage irregularities or injuries were discarded.

Zebrafish embryos were exposed to three aqueous solutions of RhB to evaluate toxicity before and after two photocatalytic treatments: initial solution (2.5 mg L^{-1}), C-treated and H4-treated solutions. Also, a negative control was analyzed as well. The tests were performed in triplicate for all the described solutions in sterilized 24-well microplates where 20 wells were filled with 2 mL of a test solution and four wells with water (internal plate control). These microplates were kept in the dark (to avoid discoloration) inside a climate chamber (SL-24 Solab Científica). Physicochemical parameters of the solutions were monitored and were in the same range as of the negative control (average values: pH = 6.4 ± 0.3; conductivity = 152.6 ± 14.4 µS cm^{-1}; TOC = 5.4 ± 0.3 mg L^{-1} and dissolved oxygen above 80%). Embryos and larvae were observed daily under a stereomicroscope. Developmental parameters were evaluated on embryos over the test period. Before hatching, the following were evaluated: egg coagulation, otolith formation, general delay in development, eye and body pigmentation, somite formation, heartbeat, oedemas, detachment of the tail-bud from the yolk sac, yolk-sac absorption and hatching. After hatching, spine malformation and posture were also evaluated. All parameters were quantified as observed or not observed. An ANOVA test was performed to compare different replications under the same conditions for characteristics that might possess statistically significant differences. If the ANOVA test demonstrated the latter, the Tukey test was performed in pairwise comparisons. A 95% confidence level was selected for all statistical comparisons.

3. Results and discussion

Fig. 1 shows the diffraction patterns of the samples. The phases obtained by both synthetic methods are consistent with a tetragonal zircon type structure (space group $I4_1/amd$, JCPDS 17-0341) [21].

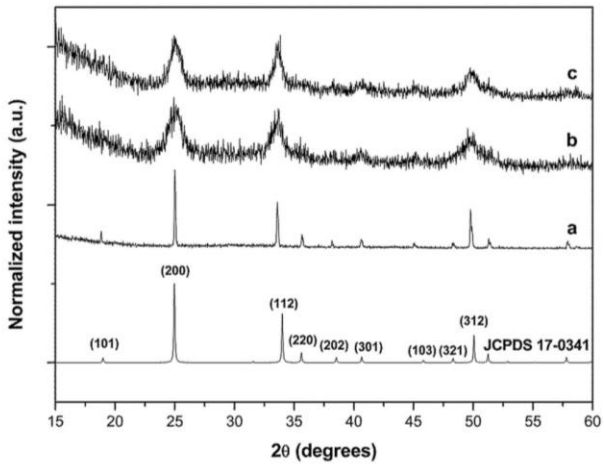

Fig. 1. X-ray diffraction patterns of YVO_4 synthesized powders: a) C; b) H4; c) H24 samples. JCPDS crystallographic data typical for YVO_4 with zircon type structure was used for comparison with the prepared samples.

Table 1
Microstructural characterization of YVO_4 synthesized powders.

Samples	Relative Crystallinity (%)	Crystallite size (nm)	S_{BET} ($m^2 g^{-1}$)	Ratio $I_3/(I_3 + I_2 + I_1)$[a]	Band Gap (eV)
C	100	74.5	5.6	0.33	3.38
H4	8.4	6.4	254	0.19	3.21
H24	10.9	8.3	205	0	3.72

[a] Calculated with UV–vis data.

Before annealing, the C sample is poorly crystalline and not single-phased, thus requiring the post-annealing in agreement with Singh et al. [16] in their description for similar systems. After annealing, the C sample presented narrower reflection peaks than the H samples. The crystallite size of the particles was calculated employing Scherrer's equation [22], using K = 0.94 and the full width at half maximum (FWHM) of the (200) diffraction peak. This is shown alongside specific surface area values in Table 1. Relative crystallinity was determined by the ratio between the FWHM of the (200) diffraction peaks of the samples, establishing the C sample as the crystalline reference (Table 1). It is noticeable that the H samples possess significantly lower crystallinity and higher values of S_{BET} than C samples. Also, it can be observed in the H samples that crystallite size and crystallinity are poorly affected by the reaction time.

SEM images for all samples are shown in Fig. 2. It is possible to observe that the morphology of the as-synthesized H powders is quite different from that observed for the C sample. The particles in the C sample (near 5 µm) are bigger and form agglomerations (probably due to sintering processes from the calcining stage). On the other hand, the hydrothermal samples exhibit aggregates (diameter near 20 nm) with irregular shapes. The images corroborate the XRD data and S_{BET} values

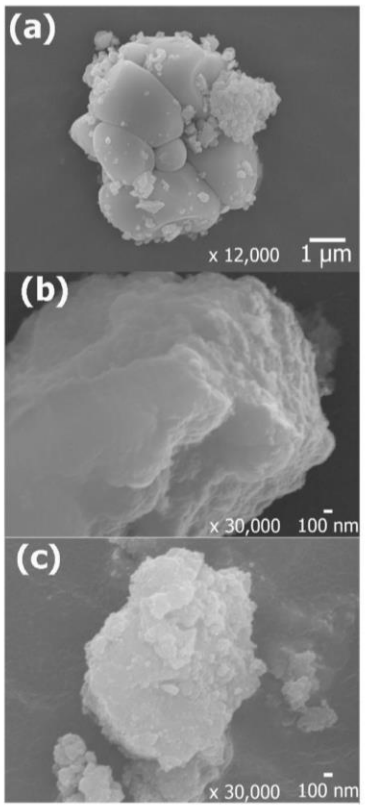

Fig. 2. SEM images of YVO_4 synthesized powders: a) C; b) H4; c) H24 samples.

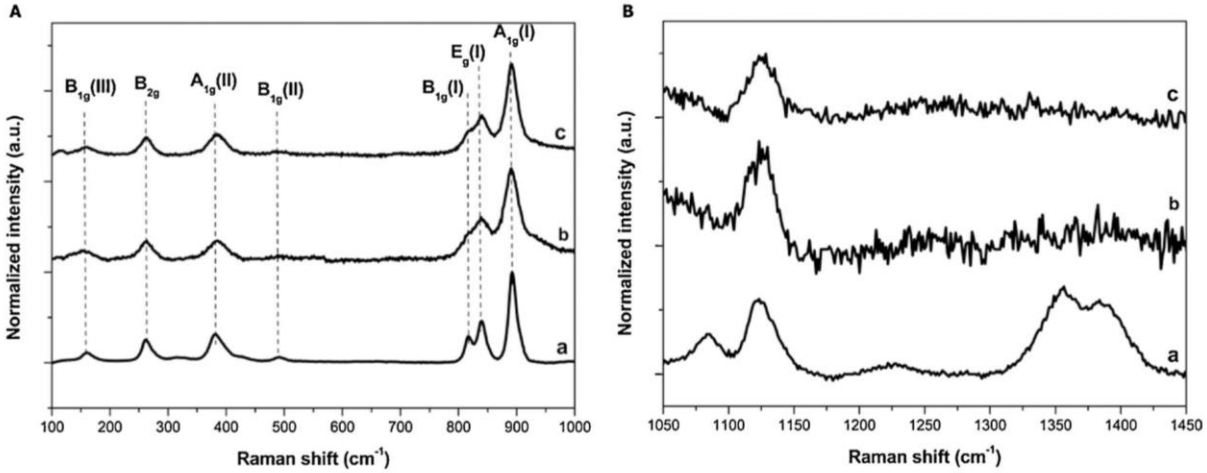

Fig. 3. (A) Raman spectra of YVO_4 synthesized powders between 100 and 1000 cm^{-1}: a) C; b) H4; c) H24 samples. (B) Raman spectra of YVO_4 synthesized powders between 1050 and 1450 cm^{-1}: a) C sample; b) H4 sample; c) H24 sample.

obtained, once crystalline solids (C sample) tend to have lower specific surface area then amorphous solids (hydrothermal samples).

Fig. 3 shows the Raman spectra of the samples. According to literature, YVO_4 belongs to D_{4h}^{19} space group and possess 36 normal vibrational modes, having as reducible representation [23]:

$$\Gamma_R = 2A_{1g} + A_{2g} + 4B_{1g} + B_{2g} + 5E_g + A_{1u} + 4A_{2u} + B_{1u} + 2B_{2u} + 5\text{-}E_u$$

The A_{1g}, B_{1g}, B_{2g} and E_g modes are Raman active. Peaks shown in Fig. 3A, except the B_{1g} mode placed at 160 cm^{-1}, belong to the internal modes of the tetrahedral groups VO_4. This B_{1g} mode corresponds to an external mode [23]. The position of these peaks is consistent with those reported in literature [10,23,24]. The C sample spectrum is better resolved than those for the hydrothermal samples, suggesting a higher short range ordering of YO_8 dodecahedrons and VO_4 tetrahedrons. It is also observable in the H samples an overlap of E_g (I) and B_{1g} (I) peaks around 800–850 cm^{-1}, suggesting local distortions of the VO_4 tetrahedrons [10,25]. These observations are consistent with the fact that the H samples are less crystalline than the C sample. Above 1000 cm^{-1} (Fig. 3B), no intrinsic signal of YVO_4 is expected, however up to four bands were observed at this region for all samples. These peaks are commonly attributed to oxygen vacancies in the crystal lattices of YVO_4 nanoparticles [26,27]. The C sample has four distinguishable peaks, in contrast with the hydrothermal samples that only present one at 1123 cm^{-1}. This suggests that, despite higher crystallinity and short range ordering, C samples possess a greater variety of oxygen vacancy types when compared to the others. This might be due to the synthetic method employed; the combustion method employs short reaction time (about 15 min) and causes the liberation of gases (NO_x and NH_3), favoring the formation of oxygen vacancies.

UV–vis diffuse reflectance spectroscopy was used to further investigate the optical characteristics of the samples and the spectra are displayed in Fig. 4. As can be observed, all samples possess an absorption edge around 350–360 nm, which then leads to maximum absorption in the UV range. For C sample, it is possible to distinguish two bands in the UV range: around 237 and 304 nm, ascribed to charge transfer transitions between O^{2-} and V ions ($^1T_2 \longleftarrow {}^1A_1$ and $^1T_1 \longleftarrow {}^1A_1$, respectively), which are typically observed in VO_4^{3-} derived systems [8,28,29]. For the other samples, the absorption increases progressively in the same range, not allowing an unambiguous assignment of bands at first look. Also, it is possible to observe for C and H4 samples a broadening between 360 and 600 nm, which is unusual for orthovanadate systems. Because of these observations, deconvolution procedures were employed, fitting the UV–vis data in terms of Gaussian functions. As a result, for the hydrothermal samples, the $^1T_2 \longleftarrow {}^1A_1$ transition is considerably blue-shifted (centered near 200 nm), which can be due to quantum size effects common for nanoparticles with diameters smaller than 100 nm [25]. This band is surface-sensitive and dependent of VO_4^{3-} ions concentration in the particles [28]. The feature above 350 nm for C and H4 samples is composed of a band commonly attributed in literature as a defect-originated transition [8,30,31]. This phenomenon in the visible range raises from lattice defects associated to oxygen vacancies that can emerge from V ions in lower valence states (V^{4+} or V^{3+}) that occupy sites typical for V^{5+} or Y^{3+} ions [8,31]. Yang et al. [8] made a spectroscopic investigation of the effect of structural defects in YVO_4 samples, showing how the defect-related transition in the visible range correlates with the presence of paramagnetic V^{4+}, proven by EPR. Also, they accessed qualitatively the concentration of defects using the ratio $I_3/(I_3 + I_2 + I_1)$ of the integrated intensities of the three transitions observed (I_1, for the $^1T_1 \longleftarrow {}^1A_1$ transition, I_2 for the $^1T_2 \longleftarrow {}^1A_1$ transition and I_3 for the defect-related transition, respectively), and correlating this parameter with luminescent and structural properties. The same ratio was calculated in this work, and the values are displayed in Table 1. C sample has the highest value, indicating that it might be the sample with most oxygen vacancies, while H24 sample has a ratio value near zero, indicating a low concentration of these defects [8]. Although the method evidences differences between the samples' defect content, XPS analysis should be performed to fully distinguish the concentration among them.

As mentioned above, the spectral feature observed can affect the band gap value of the YVO_4 powders. The optical band gap was calculated using the Tauc method [32], in which a Tauc plot is done according to the following equation: $[\alpha \cdot h\upsilon]^{\frac{1}{n}} = A(E_g - h\upsilon)$, where α is the absorption coefficient of the material, replaced in this method by the Kubelka-Munk function F(R) (where $F(R) = (1\text{-}\%R)^2/2\cdot\%R$), and%R is obtained by the diffuse reflectance data in reflectance mode), E_g is the optical band gap, hυ is energy, A is a proportionality constant and 1/n is a coefficient dependent on the type of transition responsible to the absorption edge observed in the UV–vis data. After obtaining the Tauc plot, an extrapolation to zero of the linear portion where the curvature of the graph first changes (insets in Fig. 4) gives the values displayed in Table 1. From literature, it is known that the band-to-band transition for YVO_4 is direct and allowed (n = 1/2), offering a band gap of 3.8 eV for the bulk material [29]. For C and H4 samples, the values are lower than those expected for bulk YVO_4, being probably a consequence of the oxygen vacancies which creates permitted levels into the band gap [8,9,33]. For H24 sample, the band gap is close to 3.8 eV, evidencing the possible lowest defect content among all samples.

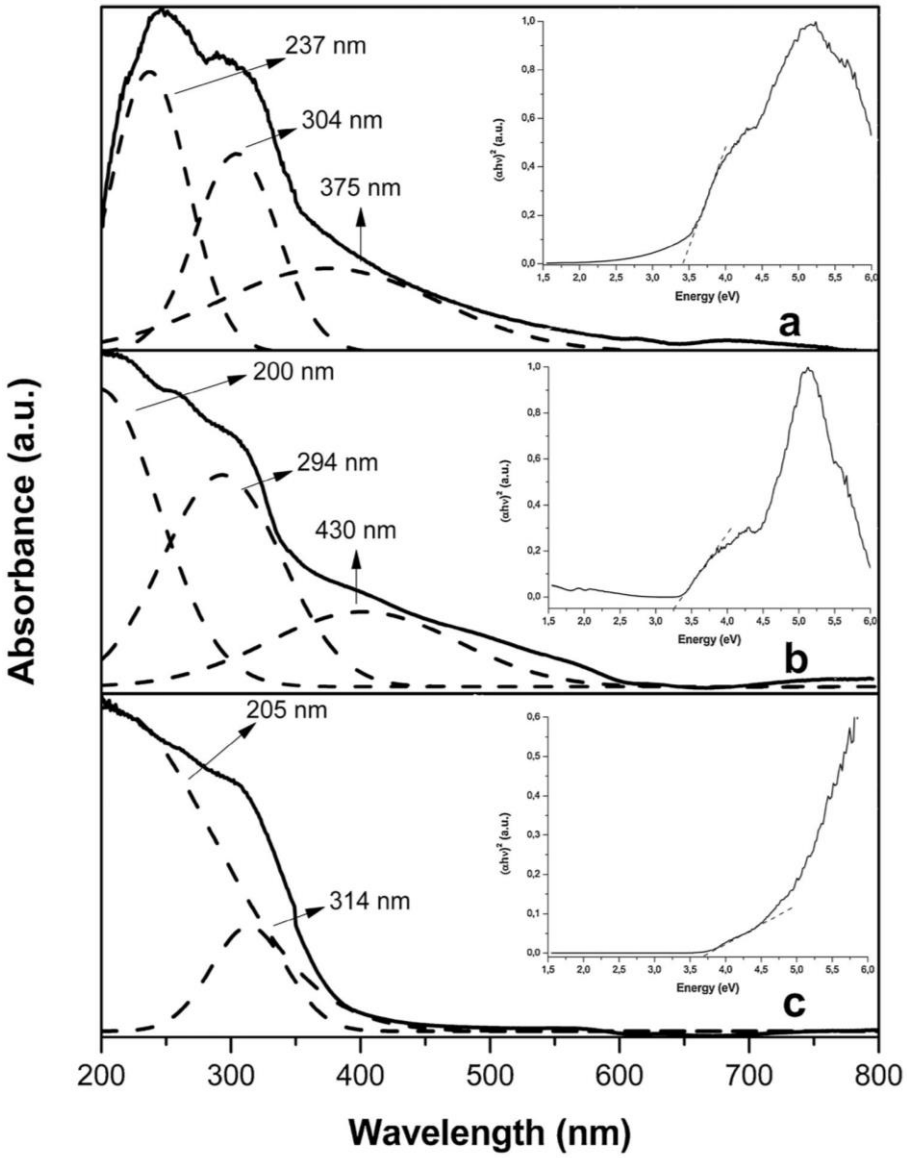

Fig. 4. Diffuse reflectance spectra of YVO_4 synthesized powders: a) C; b) H4; c) H24 samples. The positions of the transitions described in the text are informed in each spectrum. The Tauc plots used to calculate optical band gap for each sample are displayed as insets.

Another important optic property is fluorescence emission, which can reveal important information of the electronic structure of materials. Fig. 5 displays the PL spectra of the samples. Photoluminescence of structurally homogeneous orthovanadate crystals, at room, is not expected, so structural defects could be the main cause of the observed PL. This type of optical behavior was already described for YVO_4 [10,34] and other systems, such as ZnO [35], SnO_2 [36] and $BaTiO_3$ [37]. According to Yang et al. [10] and Qian et al. [34], lattice defects distorts the coordination polyhedrons for V^{5+} and Y^{3+} ions, causing unusual emissions in the visible range. In our samples, it is possible that it originates from oxygen vacancies, identified by Raman and UV–vis diffuse reflectance spectroscopy. It is worth of note that the C sample had a much more intense PL than the hydrothermal samples. According to Nobe et al. [30], the PL intensity due to these defects is proportional to their content. Since the same amount of solid was analyzed for all samples, the C sample might present greater oxygen vacancy content, in agreement with the previous spectroscopic data. The inset in Fig. 5 shows that there is a red shift and a decrease of PL intensities for the H samples according to reaction time.

Before testing the photocatalytic activity of the prepared YVO_4 powders, adsorption tests (or dark tests) were performed under the same conditions as the photocatalytic assays to evaluate possible contributions of a direct or indirect mechanism on the degradation of the RhB solutions. The quantity of adsorbed dye on the catalysts surface and the time to reach equilibrium are presented in Table 2. As can be noticed, the C sample presents the highest adsorption percentage, suggesting that there could have been a considerable contribution of the direct mechanism in the sample's photocatalytic efficiency when compared to the other ones. If it is considered that oxygen vacancies can act as adsorption sites, we could correlate the presence of these defects with the trend observed for adsorption: the higher their content, the higher the percentage of dye adsorbed.

Fig. 6 shows the discoloration profile of Rhodamine B (RhB) by the samples subjected to UV radiation (254 nm) during 7 h. A photolysis curve is also shown. Table 3 presents the results of discoloration obtained by UV–vis spectroscopy and degradation obtained by TOC

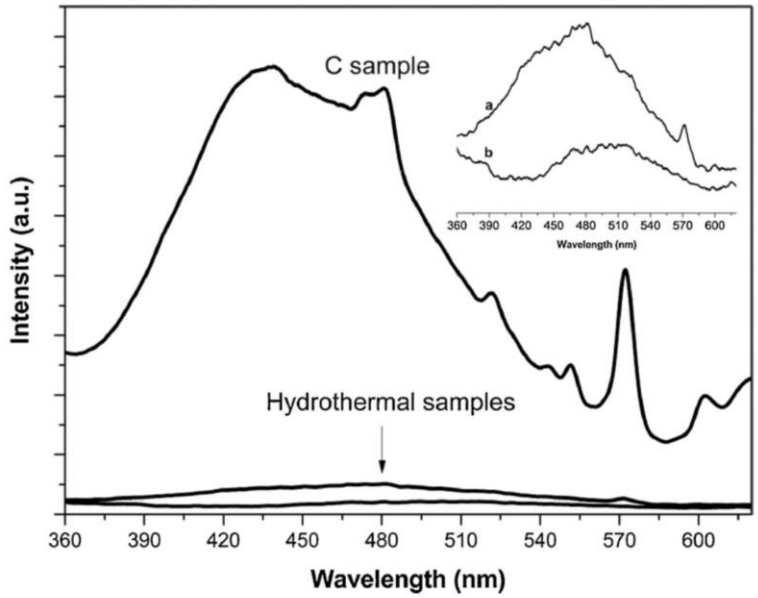

Fig. 5. PL spectra of YVO_4 synthesized powders, collected at room temperature. The most intense line (C sample) refers YVO_4 prepared by combustion route. The samples synthesized by hydrothermal route are displayed as inset and correspond respectively to: a) H4; b) H24 sample.

Table 2
Results of adsorption tests for YVO_4 synthesized powders.

Samples	Adsorbed quantity of RhB (%)	Time (h)
C	25.7	2
H4	18.4	1
H24	8.7	0.5

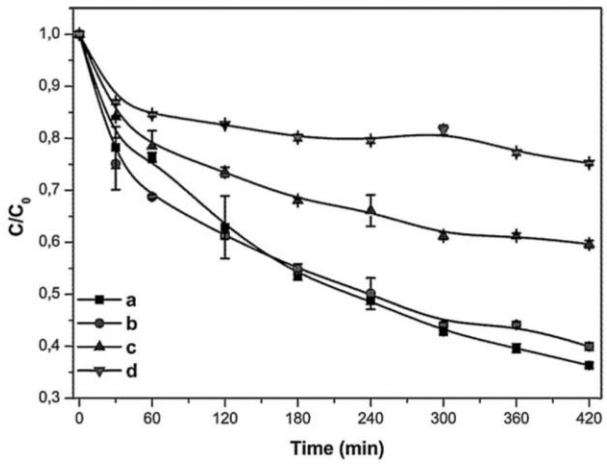

Fig. 6. Discoloration of RhB after 7 h by photocatalytic treatments: a) C sample; b) H4 sample; c) H24 sample; d) photolysis.

Table 3
Percentage of discoloration of RhB solutions treated with YVO_4 synthesized powders estimated through UV-vis spectroscopy and TOC.

Samples	Discoloration (%)	TOC reduction (%)
C	63.7 ± 0.5	56.8 ± 0.7
H4	60.1 ± 0.7	51.6 ± 1.2
H24	40.4 ± 0.7	37.0 ± 0.6
Photolysis	24.8 ± 0.4	1.4 ± 0.2

analysis. Due to proximity between results of both analyses, we concluded that both discoloration and mineralization are achieved when using YVO_4 samples. However, the photolysis did not follow this trend. Also, the photocatalytic efficiencies increases as does the ratio $I_3/(I_3 + I_2 + I_1)$, suggesting that the C samples possessed the highest photocatalytic activity possibly due to the content of oxygen vacancies, in a similar manner as what Yang et al. [10] have exposed in their work. On the other hand, sample H4 had a higher photocatalytic activity than H24, comparable with the C sample. Again, the presence of oxygen vacancies can be the reason of H4 sample's photocatalytic activity, since it is the main difference between it and H24 sample. As well as for adsorption sites (pointed out by the dark tests), it is described in literature that these defects can serve as an oxidative trigger once the exciton is formed, oxidizing organic substrates or producing reactive oxygen species (ROS), besides of narrowing the band gap and prolonging the lifetime of the exciton [9,10,33], giving an idea of the depth of its importance in photocatalytic applications. Also, it was not possible to perceive any correlation between the S_{BET} values and photocatalysis, since the defects seems to operate a major role. Moreover, according to Yang et al. [10] and Mohamed et al. [17], synthetic routes similar to the ones performed in this work does not change significantly porosity with time of hydrothermal treatment/calcination of YVO_4 powders. Also, it was demonstrated by Giraldi et al. [1,2] for ZnO and by An et al. [38] for YVO_4 that the degree of crystallinity and synthetic impurities can play a more important role in photocatalytic efficiencies than only specific surface area.

Given the importance of oxygen vacancies in the photocatalytic activity of the prepared samples, ROS-generating experiments were performed in similar conditions as the photocatalytic assays, employing the formation of 2-OH-TA as a probe to ROS production. The formation of 2-OH-TA occurs due to oxidation of TA by hydroxyl radicals that originates in the medium due to photochemical processes [39]. For this reason, a photolysis test was also performed by means of comparison. The results are displayed in Fig. 7. As can be observed by the trend lines (in all cases, $R^2 > 0.95$) and the values of their slopes, all photocatalysts promotes hydroxyl radical formation in the presence of UV light. When employing semiconductors, these radicals may be produced mainly by two routes: (i) water oxidation in the valence band by h^+ charge carrier; (ii) decomposition of other ROS such as superoxide

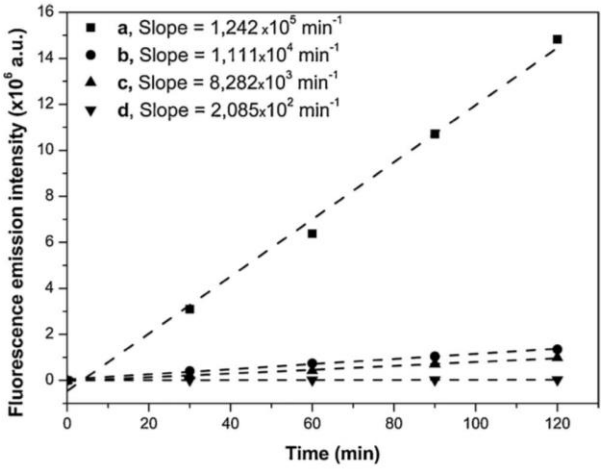

Fig. 7. Change of the fluorescence emission at 425 nm of 2-hydroxyterephthalic acid after 2 h of irradiation: a) C sample; b) H4 sample; c) H24 sample; d) photolysis.

radicals originated by O_2 reduction in the conduction band by e^- charge carrier [40]. Thus, this test is important to indicate qualitatively the capability of the samples for ROS production, independently of the mechanism of hydroxyl radical generation. It is noticeable that the C sample has the highest rate of 2-OH-TA formation, being 11 times more efficient than H4 sample. Also, the rate decreases in the same manner as the ratio $I_3/(I_3 + I_2 + I_1)$ and the PL emission of the samples, suggesting that the changes in oxygen vacancy's content affects the efficiency of ROS production, explaining the photocatalytic trend observed previously.

As exposed previously, oxygen vacancies in the YVO_4 samples are closely related to their photocatalytic performance, and that certain contents of defects can result in higher photocatalytic efficiency thanks to the production of ROS. In other words, the engineering of lattice defects can contribute to attain desirable photoactivities. However, when the concern surrounds environmental applications, the suitability of a photocatalyst must also take into account the impact that the treated effluent can have. In our work, the toxicity of treated solutions of RhB were evaluated with FET to assure if the two best photocatalytic treatments here proposed can indeed remedy any toxic effect of the initial solution. Fig. 8 shows the effects of exposure to three aqueous RhB solutions on *D. rerio* embryos and larvae development between 24 and 144 h (6 days), designated as untreated solution (2.5 mg L^{-1}), treated with C sample (C-treated solution) and treated with H4 sample (H4-treated solution), respectively. The untreated solution did not show any sign of acute toxicity to larvae. Surprisingly, the C-treated solution caused a significant mortality to the *D. rerio* embryos beginning at 96 h of exposure (65 ± 5%) and reaching total mortality at 144 h. The H4-treated solution was barely toxic to the larvae (less than 10% of the embryos died). The mortality rate for the C-treated solution was observed to be statistically different from all the solutions ($P < 0.05$, Tukey test). In addition, no malformation was observed in any of the three solutions. Concerning the developmental parameters, the only observable effects were the accumulation of the dye in the yolk sac and the inhibition of egg hatching in both C and H4 treatments, at 48 h of exposure (Figs. 8 and 9). No statistical difference was observed for dye absorption until the fourth day for the C-treated solution ($P < 0.05$). This was probably due to the mortality in this treatment that began at the same time as the change in statistics. Also, statistical difference was only observed for the inhibition of egg hatching in the C treated solution ($P < 0.05$), and not among the other solutions.

Altogether, the FET results suggest that, at the tested concentration, RhB (2.5 mg L^{-1}) was not acutely toxic for embryos and did not provoke alterations of embryo development. However, after photocatalytic treatment of RhB solutions, an increase in toxicity was observed specially for C-treated sample. Since physicochemical properties such as pH, conductivity, TOC and dissolved oxygen of the treated solutions were similar of those of the negative control (as mentioned in Section 2.6), and that these conditions are consistent with a healthy medium for this aquatic specie [41,42], the evidences suggest that the C sample might produce a toxic final effluent due to chemical changes, possibly by synthetic residues present in the photocatalyst, particles in suspension that can interact with the biosensors, or by the treatment itself, that can generate toxic chemical species.

One possible by-product, due to the oxidation of urea, is nitrite ions, whose toxicity has been well described for *D. rerio* [43]. Thermogravimetric analyses (not shown here) do not show any mass loss associated to nitrogenized compounds or organic residues above 200 °C. The presence of nitrite ions above the detection limit of it (0.742 μg L^{-1}) was not identified by the Griess test. According to literature, toxicity due to nitrite ions for *D. rerio* varies between 60,000 and 436,000 μg L^{-1} [43]. This discards the possibility of nitrite having caused the mortality.

There is not much evidence in literature about the toxicity of Y and V derived oxides for *D. rerio*. According to Harper et al. [44], the exposure of *D. rerio* embryos to dispersions of rare-earth oxide nanoparticles can provoke malformations. For instance, exposure to Y_2O_3 nanoparticles, with mean size of 150 nm, for 5 days (120 h), significantly increased the incidence of jaw malformations at 0.01 mg mL^{-1}, and the incidence of jaw and heart malformations of embryos exposed to 0.25 mg mL^{-1}, accounting for 20% of mortality at the end of the assay. None of the malformations described in the literature were observed here, demonstrating either that the centrifugation step employed was successful in the removal of the catalyst or that this oxide by itself does not offer any considerable toxic effect. Thus, the higher toxicity observed for C-treated samples should be correlated to the photocatalytic treatment.

The particular feature that turns C sample different from other YVO_4 powders prepared in this study is possibly the content of oxygen vacancies, which are related to produce ROS more efficiently. Hence, the presence of lattice defects might be associated with the mortality observed for *D. rerio*. In other words, despite giving good photoactivity, the amount of oxygen vacancies in the C sample can cause undesirable environmental impacts in treated solutions, demonstrating that the C sample is not the best option for environmental applications. On the other hand, H4 sample, which has shown to have less significance in its microstructure due to the presence of oxygen vacancies, was almost as efficient for discoloring RhB as the C sample, giving no toxicity at all to the final effluent. Summarizing, H4 sample is a better candidate for photocatalysis than the C sample once it does not generate negative impacts in treated solutions (photocatalytic reactions might take another route when mediated by H4). Possibly, the appropriate amount of oxygen vacancies may facilitate the generation of reactive species by suppressing the charge carriers recombination (demonstrated by 2-OH-TA formation), but an excess can play the aforementioned negative role. Although future analysis are needed to ensure the origin of the mortality rendered by the C sample, such as oxidative stress biomarkers for *D. rerio* or identifying final by-products in the treated solutions, it is clear the existence of a correlation between the microstructural characteristics of the prepared solids and the toxicity of final effluents. Thus, this work opens a scarce and important discussion for future studies in heterogeneous photocatalysis, pointing out the need for investigation of the effects of microstructural aspects of semiconductors on their suitability for environmental applications.

4. Conclusion

Both combustion and hydrothermal methods were efficient in the synthesis of YVO_4. No considerable crystallographic and

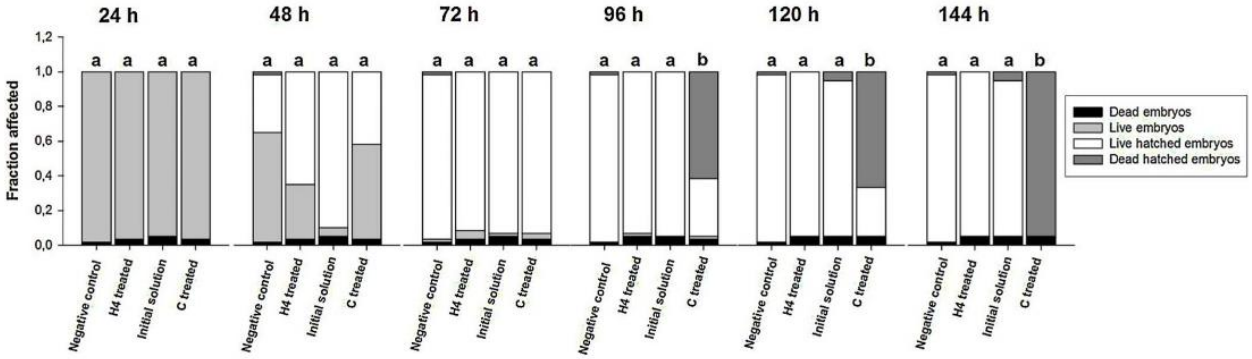

Fig. 8. Profile of zebrafish embryo/larvae stages after exposures to aqueous solutions of RhB between 24 and 144 h. Different letters above the bars of each day indicates significant statistical difference of the mortality profile between solutions (Tukey test, $P < 0.05$).

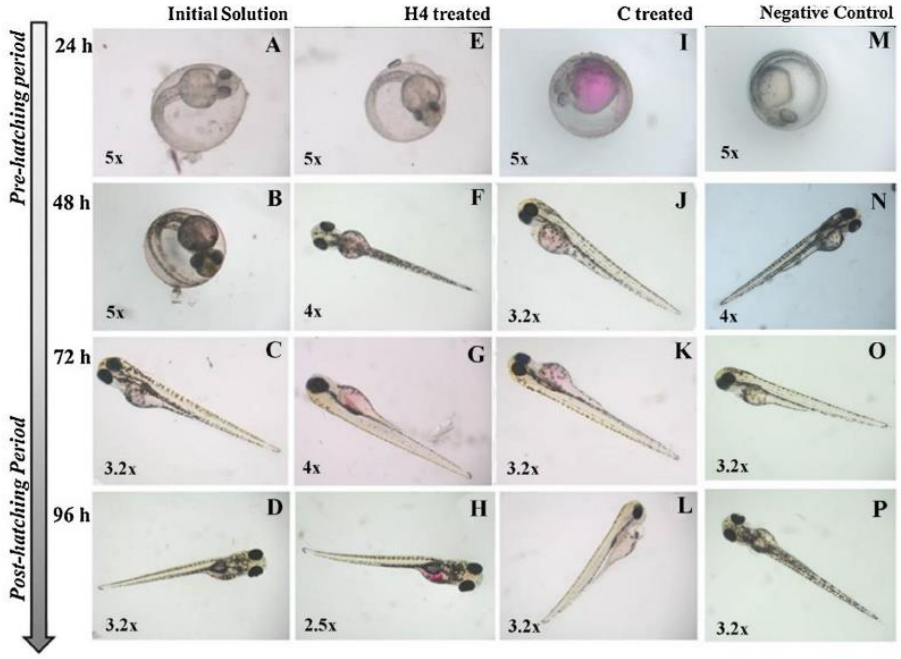

Fig. 9. Evolution of zebrafish embryo/larvae alterations observed throughout FET after exposures to: initial solution (A–D); H4-teated solution (E–H); C-treated solution (I–L). Observed features were compared to the negative control (M–P). The approximation employed is informed at the bottom-left in each photograph.

microstructural differences between the powders synthesized by either method were observed. Samples prepared by combustion method presented higher content of oxygen vacancies when compared to the H samples, as demonstrated by spectroscopic techniques. Photocatalytic efficiency of samples C and H4 was quite similar and mainly due to the presence of the cited lattice defects, as also shown by the ROS-generating experiments. Despite of this, the FET showed that the C treatment leads to a higher toxicity of the final effluent, making H4 sample the most efficient for degradation of RhB. It is important to point out that such toxicity was noticeable only at the fourth day of assay, and was related to inhibition of egg hatching and mortality of *D. rerio* embryos after hatching. Thus, it can be perceived that characteristics such as oxygen vacancies, when surpassing a certain concentration can have potentially negative environmental effects at expenses of improving photoactivity. This result draws attention to an important discussion on the roles of synthetic route of semiconductors in the treatment of liquid effluents.

Ethical standards

The biological experiments are in accordance with the current laws of the country in which they were performed. The study was approved by the Ethics Committee, of the University of Brasilia (reference no 100226/2014).

The English text of this paper has been revised by Sidney Pratt, Canadian, MAT (The Johns Hopkins University), RSAdip – TESL (Cambridge University).

Conflict of interest

There is no conflict of interests between the authors present in this study.

Acknowledgments

The authors acknowledge the Brazilian Ministry of Education, Ministry of Science and Technology of Brazil, CAPES and CNPq for the scholarships provided. We would also like to acknowledge Prof. Dr.

Iêda Maria Garcia dos Santos from the Federal University of Paraíba, for contributing with the Raman spectroscopy analysis, Prof. Dr. Julio Lemos de Macedo from the University of Brasília, for the support during this manuscripts writing, and the Microscopy Laboratory of the Institute of Biological Sciences from the University of Brasília.

References

[1] T.R. Giraldi, G.V.F. Santos, V.R. Mendonca, C. Ribeiro, I.T. Weber, Annealing effects on the photocatalytic activity of ZnO nanoparticles, J. Nanosci. Nanotechnol. 11 (2011) 3635–3640.
[2] T.R. Giraldi, G.V.F. Santos, V.R. De Mendonca, C. Ribeiro, I.T. Weber, Effect of synthesis parameters on the structural characteristics and photocatalytic activity of ZnO, Mater. Chem. Phys. 136 (2012) 505–511.
[3] T.K. Jana, S.K. Maji, A. Pal, R.P. Maiti, T.K. Dolai, K. Chatterjee, Photocatalytic and antibacterial activity of cadmium sulphide/zinc oxide nanocomposite with varied morphology, J. Colloid Interface Sci. 480 (2016) 9–16.
[4] M. Zhang, G. Yao, Y. Cheng, Y. Xu, L. Yang, J. Lv, et al., Temperature-dependent differences in wettability and photocatalysis of TiO_2 nanotube arrays thin films, Appl. Surf. Sci. 356 (2015) 546–552.
[5] W. He, H.-K. Kim, W.G. Wamer, D. Melka, J.H. Callahan, J.-J. Yin, Photogenerated charge carriers and reactive oxygen species in ZnO/Au hybrid nanostructures with enhanced photocatalytic and antibacterial activity, J. Am. Chem. Soc. 136 (2013) 750–757.
[6] T.K. Maji, D. Bagchi, P. Kar, D. Karmakar, S.K. Pal, Enhanced charge separation through modulation of defect-state in wide band-gap semiconductor for potential photocatalysis application: ultrafast spectroscopy and computational studies, J. Photochem. Photobiol. A: Chem. 332 (2017) 391–398.
[7] C.M. Aiube, L.R. de Melo, J.L. de Macedo, Preparation of hierarchical SnO_2 microspheres with controlled size from ion exchange resins, ChemistrySelect 2 (2017) 10186–10190.
[8] L. Yang, G. Li, M. Zhao, J. Zheng, X. Guan, L. Li, Preparation and morphology-sensitive luminescence properties of Eu^{3+}-doped YVO_4: a defect chemistry viewpoint of study, CrystEngComm 14 (2012) 3227–3235.
[9] J. Wang, Z. Wang, B. Huang, Y. Ma, Y. Liu, X. Qin, et al., Oxygen vacancy induced band-gap narrowing and enhanced visible light photocatalytic activity of ZnO, ACS Appl. Mater. Interfaces 4 (2012) 4024–4030.
[10] L. Yang, G. Li, W. Hu, M. Zhao, L. Sun, J. Zheng, et al., Control over the crystallinity and defect chemistry of YVO_4 nanocrystals for optimum photocatalytic property, Eur. J. Inorg. Chem. (2011) 2211–2220.
[11] M. Antonopoulou, I. Konstantinou, Photocatalytic treatment of metribuzin herbicide over TiO_2 aqueous suspensions: removal efficiency, identification of transformation products, reaction pathways and ecotoxicity evaluation, J. Photochem. Photobiol. A: Chem. 294 (2014) 110–120.
[12] M. Antonopoulou, D. Hela, I. Konstantinou, Photocatalytic degradation kinetics, mechanism and ecotoxicity assessment of tramadol metabolites in aqueous TiO_2 suspensions, Sci. Total Environ. 545–546 (2016) 476–485.
[13] X. Van Doorslaer, I.D. Haylamicheal, J. Dewulf, H. Van Langenhove, C.R. Janssen, K. Demeestere, Heterogeneous photocatalysis of moxifloxacin in water: chemical transformation and ecotoxicity, Chemosphere 119 (2015) S75–S80.
[14] L.K. Adams, D.Y. Lyon, P.J.J. Alvarez, Comparative toxicity of nano-scale TiO_2, SiO_2 and ZnO water suspensions, Water Res. 40 (2006) 3527–3532.
[15] H. Ma, P.L. Williams, S.A. Diamond, Ecotoxicity of manufactured ZnO nanoparticles – a review, Environ. Pollut. 172 (2013) 76–85.
[16] V. Singh, V. Natarajan, J.J. Zhu, Studies on Eu doped Ba and Zn aluminate phosphors prepared by combustion synthesis, Opt. Mater. (Amst). 29 (2007) 1447–1451.
[17] R.M. Mohamed, F.A. Harraz, I.A. Mkhalid, Hydrothermal synthesis of size-controllable yttrium orthovanadate (YVO_4) nanoparticles and its application in photocatalytic degradation of direct blue dye, J. Alloys Compd. 532 (2012) 55–60.
[18] G. Liu, P. Niu, C. Sun, S.C. Smith, Z. Chen, G.Q. (Max) Lu, et al., Unique electronic structure induced high photoreactivity of sulfur-doped graphitic C_3N_4, J. Am. Chem. Soc. 132 (2010) 11642–11648.
[19] T.A. Doane, W.R. Horwath, Spectrophotometric determination of nitrate with a single reagent, Anal. Lett. 36 (2003) 2713–2722.
[20] OECD, OECD Guidelines for the Testing of Chemicals - Fish Embryo Acute Toxicity (FET) Test (Test Guideline 236), (2013), pp. 1–22.
[21] J.A. Baglio, G. Gashurov, A refinement of the crystal structure of yttrium vanadate, Acta Crystallogr. Sect. B Struct. Crystallogr. Cryst. Chem. 24 (1968) 292–293.
[22] B.D. Cullity, Elements of X-ray Diffraction, 3rd ed., Addison-Wesley Publications, New York, 1967.
[23] Y.K. Voron'ko, A.A. Sobol', V.E. Shukshin, A.I. Zagumennyi, Y.D. Zavartsev, S.A. Kutovoi, Raman spectroscopic study of structural disordering in YVO_4 $GdVO_4$, and $CaWO_4$ crystals, Phys. Solid State 51 (2009) 1886–1893.
[24] A.A. Kaminskii, K. ichi Ueda, H.J. Eichler, Y. Kuwano, H. Kouta, S.N. Bagaev, et al., Tetragonal vanadates YVO_4 and $GdVO_4$ – New efficient $\chi^{(3)}$-materials for Raman lasers, Opt. Commun. 194 (2001) 201–206.
[25] H. Xu, H. Wang, H. Yan, Preparation and photocatalytic properties of YVO_4 nanopowders, J. Hazard. Mater. 144 (2007) 82–85.
[26] B. Jin, S. Erdei, A.S. Bhalla, F.W. Ainger, Micro-probe Raman spectroscopy of YVO_4 single crystals grown by different growth techniques for investigation of micro-inhomogeneities, Mater. Lett. 22 (1995) 281–284.
[27] S. Erdei, B. Jin, F.W. Ainger, A.S. Bhalla, Micro-probe Raman spectroscopy for detection of inhomogeneities in YVO_4 single crystals, J. Appl. Phys. 79 (1996) 2834–2838.
[28] H. Ronde, G. Blasse, The nature of the electronic transitions of the vanadate group, J. Inorg. Nucl. Chem. 40 (1978) 215–219.
[29] M.R. Dolgos, A.M. Paraskos, M.W. Stoltzfus, S.C. Yarnell, P.M. Woodward, The electronic structures of vanadate salts: cation substitution as a tool for band gap manipulation, J. Solid State Chem. 182 (2009) 1964–1971.
[30] Y. Nobe, H. Takashima, T. Katsumata, Decoloration of yttrium orthovanadate laser host crystals by annealing, Opt. Lett. 19 (1994) 1216–1218.
[31] N. Garces, K. Stevens, G. Foundos, L. Halliburton, Electron paramagnetic resonance and optical absorption study of V^{4+} centres in YVO_4, J. Phys. Condens. Matter. 16 (2004) 7095–7106.
[32] J. Tauc, Optical properties and electronic structure of amorphous Ge and Si, Mater. Res. Bull. 3 (1968) 37–46.
[33] M. Aslam, M.T. Qamar, M.T. Soomro, I.M.I. Ismail, N. Salah, T. Almeelbi, et al., The effect of sunlight induced surface defects on the photocatalytic activity of nanosized CeO_2 for the degradation of phenol and its derivatives, Appl. Catal. B: Environ. 180 (2016) 391–402.
[34] L. Qian, J. Zhu, Z. Chen, Y. Gui, Q. Gong, Y. Yuan, et al., Self-assembled heavy lanthanide orthovanadate architecture with controlled dimensionality and morphology, Chem. A: Eur. J. 15 (2009) 1233–1240.
[35] Y. Zheng, C. Chen, Y. Zhan, X. Lin, Q. Zheng, K. Wei, et al., Photocatalytic activity of Ag/ZnO heterostructure nanocatalyst: correlation between structure and property, Inorg. Chem. 46 (2007) 6675–6682.
[36] F. Gu, S.F. Wang, M.K. Lü, G.J. Zhou, D. Xu, D.R. Yuan, Photoluminescence properties of SnO_2 nanoparticles synthesized by sol-gel method, J. Phys. Chem. B 108 (2004) 8119–8123.
[37] L.V. Maneeshya, V.S. Anitha, S.S. Lekshmy, I. John Berlin, P.B. Nair, G.P. Daniel, et al., Influence of annealing temperature and oxygen atmosphere on the optical and photoluminescence properties of $BaTiO_3$ amorphous thin films prepared by sol?gel method, J. Mater. Sci. Mater. Electron. 24 (2013) 848–854.
[38] X. An, Y. Wang, J. Deng, J. Chen, R. Yu, X. Xing, One step molten salt synthesis of YVO_4 nanoparticles and their photocatalytic properties under UV-Visible light, Inorg. Chem. Commun. 44 (2014) 79–82.
[39] S.E. Page, W.A. Arnold, K. McNeill, Terephthalate as a probe for photochemically generated hydroxyl radical, J. Environ. Monit. 12 (2010) 1658–1665.
[40] J.H. Thurston, N.M. Hunter, L.J. Wayment, K.A. Cornell, Urea-derived graphitic carbon nitride (u-g-C_3N_4) films with highly enhanced antimicrobial and sporicidal activity, J.Colloid Interface Sci. 505 (2017) 910–918.
[41] R.E. Engeszer, L.B. Patterson, A.A. Rao, D.M. Parichy, Zebrafish in the wild: a review of natural history and new notes from the field, Zebrafish 4 (2007) 21–40.
[42] T.S. Andrade, J.F. Henriques, A.R. Almeida, A.M.V.M. Soares, S. Scholz, I. Domingues, Zebrafish embryo tolerance to environmental stress factors — Concentration–dose response analysis of oxygen limitation, pH, and UV-light irradiation, Environ. Toxicol. Chem. 36 (2017) 682–690.
[43] F. Lahnsteiner, The sensitivity and reproducibility of the zebrafish (Danio rerio) embryo test for the screening of waste water quality and for testing the toxicity of chemicals, Altern. to Lab. Anim. 36 (2008) 299–311.
[44] S. Harper, C. Usenko, J.E. Hutchison, B.L.S. Maddux, R.L. Tanguay, In vivo biodistribution and toxicity depends on nanomaterial composition, size surface functionalisation and route of exposure, J. Exp. Nanosci. 3 (2008) 195–206.

Journal of Ethnopharmacology 241 (2019) 112004

Contents lists available at ScienceDirect

Journal of Ethnopharmacology

journal homepage: www.elsevier.com/locate/jethpharm

Toxicological findings about an anticancer fraction with casearins described by traditional and alternative techniques as support to the Brazilian Unified Health System (SUS)

Paulo Michel Pinheiro Ferreira[a,b,*], Denise Barbosa Santos[a,b], Jurandy do Nascimento Silva[a,b], Amanda Freitas Goudinho[a], Carla Lorena Silva Ramos[a,b], Patrícia Canteri de Souza[c], Ricardo Sérgio Couto de Almeida[c], Diego Sousa Moura[d], Rhaul de Oliveira[d], Cesar Koppe Grisolia[d], Alberto José Cavalheiro[e], Ana Amélia de Carvalho Melo-Cavalcante[b], José Roberto de Oliveira Ferreira[f], Manoel Odorico de Moraes Filho[g], Claudia Pessoa[g]

[a] Department of Biophysics and Physiology, Laboratory of Experimental Cancerology, Federal University of Piauí, Teresina, Brazil
[b] Postgraduate Programs in Pharmaceutical Sciences and Biotechnology, Federal University of Piauí, Teresina, Brazil
[c] Department of Microbiology, State University of Londrina, Londrina, Brazil
[d] Department of Genetics and Morphology, Institute of Biological Sciences, University of Brasília, Brasília, Brazil
[e] Chemistry Institute, State University Júlio de Mesquita Filho, Araraquara, Brazil
[f] School of Medical Sciences, State University of Alagoas, Maceió, Brazil
[g] Department of Physiology and Pharmacology, Faculty of Medicine, Federal University of Ceará, Fortaleza, Brazil

ARTICLE INFO

Keywords:
Clerodane diterpenes
Embryotoxicity
Genotoxicity
Histological changes
Biochemical profile
Risk assessment

ABSTRACT

Ethnopharmacological relevance: Extracts, essential oils and molecules from *Casearia sylvestris* have popularly shown pharmacological actions against chronic diseases, as anxiety, inflammation, cancer and dyslipidemia. In the context of antitumoral therapy, we investigated *in vitro*, *ex vivo* and *in vivo* toxicological changes induced by a Fraction with Casearins (FC) and its component Casearin X isolated from *C. sylvestris* on animal and vegetal cells, and upon invertebrates and mammals.

Material and methods: Cytotoxicity was carried out using normal lines and absorbance and flow cytometry techniques, *Artemia salina* nauplii, *Danio rerio* embryos and meristematic cells from *Allium cepa* roots. Acute and 30 days-mice analysis were done by behavioral, hematological and histological investigations and DNA/chromosomal damages detected by alkaline Cometa and micronucleus assays.

Results: FC was cytotoxic against lung and fibroblasts cells and caused DNA breaks, loss of integrity and mitochondrial depolarization on *ex vivo* human leukocytes. It revealed 24 h-LC_{50} values of 48.8 and 36.7 μg/mL on *A. salina* nauplii and *D. rerio* embryos, reduced mitotic index of *A. cepa* roots, leading to cell cycle arrest at metaphase and anaphase and micronuclei. FC showed i.p. and oral LD_{50} values of 80.9 and 267.1 mg/kg body weight. Subacute i.p. injections induced loss of weight, swelling of hepatocytes and tubules, tubular and glomerular hemorrhage, microvesicular steatosis, lung inflammatory infiltration, augment of GPT, decrease of albumin, alkaline phosphatase, glucose, erythrocytes, and lymphocytes, and neutrophilia ($p > 0.05$). FC-treated animals at 10 mg/kg/day i.p. caused micronuclei in bone marrow and DNA strand breaks in peripheral leukocytes.

Conclusions: This research postulated suggestive side effects after use of FC-related drugs, demonstrating FC as antiproliferative and genotoxic on mammal and meristematic cells, including human leukocytes, teratogenicity upon zebrafish embryos, myelosuppression, clastogenicity, and morphological and biochemical markers indicating liver as main target for FC-induced systemic toxicity.

Abbreviations: ALP, alkaline phosphatase; BUN, blood urea nitrogen; DI, damage Index; FC, Fraction with casearins; GOT, glutamate oxaloacetate transaminase; GPT, glutamate pyruvate transaminase; MCH, mean corpuscular hemoglobin; MCV, mean corpuscular volume; MCHC, mean corpuscular hemoglobin concentration; PCE, polychromatic erythrocytes; PBMC, polymorphic blood mononuclear cells; RDW, red cell distribution width; RENISUS, *Relação Nominal de Plantas Medicinais de Interesse ao Sistema Único de Saúde*/National Relation of Medicinal Plants for Brazilian Health System

* Corresponding author. Department of Biophysics and Physiology, Laboratory of Experimental Cancerology, Federal University of Piauí, 64049-550, Teresina, Piauí, Brazil.
E-mail address: pmpf@ufpi.edu.br (P.M.P. Ferreira).

https://doi.org/10.1016/j.jep.2019.112004
Received 15 March 2019; Received in revised form 25 May 2019; Accepted 28 May 2019
Available online 29 May 2019

1. Introduction

In Brazil, the history of phytotherapy as primary health care has been motivated by social movements, national guidelines and recommendations from the World Health Organization in order to increase therapeutic resources, recover traditional knowledge, preserve biodiversity, stimulate organic agriculture and environmental protection (Damian et al., 2014).

Phytoterapy received more attention after publication of the Resolution 971/2006, which regulated the *Política Nacional de Práticas Integrativas e Complementares* (National Policy on Integrative and Complimentary Practices) and the *Política Nacional de Plantas Medicinais e Fitoterápicos* (National Policy of Medicinal Plants and Phytotherapeutics). This document introduced medicinal plants into the Brazilian Unified Health System (SUS) and assembled data regarding ethnopharmacological evidences (specially about safety and efficacy) to generate the RENISUS (*Relação Nominal de Plantas Medicinais de Interesse ao Sistema Único de Saúde*/National Relation of Medicinal Plants for Brazilian Health System) to create a guideline of medicinal plants – a list with 71 species. This list can be accessed by scientists for the development of new and folk drugs (Brasil, 2006; 2009).

RENISUS mentions *Casearia sylvestris* Sw. (Salicaceae), known as "guaçatonga", a well distributed shrub in South America (Brasil Ministério da Saúde, 2009). Extracts, essential oils and molecules from *C. sylvestris* have shown analgesic (Piovezan et al., 2017), anti-*Helicobacter pylori* (Spósito et al., 2019), antioxidant (Araújo et al., 2015), anxiolytic (Araújo et al., 2017), hypolipidemic (Schoenfelder et al., 2008; Espinosa et al., 2015), and antiulcerogenic (Basile et al., 1990; Esteves et al., 2005) actions and cardiovascular protection (Brant et al., 2014). Moreover, Brazilian Karajá Indian tribe and natives from the Shipibo-Conibo tribe (Peru) have historical habits of preparing leaf extracts to treat snake bites, wounds, diarrhea, flu and chest colds, probably due to their antifungal and antibacterial activity (Da Silva et al., 2008a; Espinosa et al., 2015; Pereira et al., 2017).

Cytotoxicity against cancer lines is one of the most important biological activity of clerodane diterpenes from *Casearia* and it has been demonstrated they induce DNA fragmentation, phosphatidylserine externalization, cell cycle arrest and reduction of ERK phosphorylation and cyclin D1 expression (Santos et al., 2010; Ferreira et al., 2010, 2014; 2016; Ferreira-Silva et al., 2017). We also displayed a promising potentiality of a fraction from *C. sylvestris* leaves whose tumor inhibition rates ranged from 33 to 67% for human carcinomas and glioblastomas and from 35 to 90% for Sarcoma 180 murine cells (Ferreira et al., 2016).

In the antineoplastic therapy, the determination of toxicity requires attention especially for patients in advanced cancer stages, when side effects overcome benefits and survival increasing is not accompanied by improvement of quality of life. In this context, about 72% of symptoms/signs of drug toxicity in humans can be defined in laboratory animals. Man-laboratory animal correlations are higher for cardiovascular, gastrointestinal and hematological alterations. Hypersensitivity, cutaneous reactions and hepatotoxicity present lower parallelism (Olson et al., 2000; Williams et al., 2002). Therefore, it remains essential to study molecular, cellular and tissue events involved in the progression/retraction of cancer and pharmacological details of cytotoxic agents, especially those that affect integrity of key organs. Herein, we investigated *in vitro*, *ex vivo* and *in vivo* toxicological changes induced by a Fraction with Casearins (FC) and its main component Casearin X isolated from *C. sylvestris* leaves on animal and vegetal cells, and upon invertebrates and mammals, providing a complete profile of possible side effects following use of FC-related drugs.

2. Materials and methods

2.1. Chemicals, isolation and structure identification

Fetal calf serum, RPMI 1640 medium, trypsin-EDTA, Ficoll-Hypaque, penicillin and streptomycin were purchased from Cultilab (Campinas, Brazil). Doxorubicin, resazurin, EDTA, Tris-HCl, Triton X-100, propidium iodide (PI), dimethylsulfoxide (DMSO), rhodamine 123, acetic carmine, and Schiff's reagent were purchased from Sigma-Aldrich Co. (St. Louis, MO, USA). NaCl, $MgSO_4$, HCl, $MgCl_2$, $CaCl_2$, KCl, $NaHCO_3$ and citrate were obtained from Vetec Química (Rio de Janeiro, Brazil).

Leaves of *C. sylvestris* were collected at Parque Estadual Carlos Botelho (São Miguel Arcanjo, São Paulo, Brazil/S 24° 7′ 53″, W 47° 56′ 57″) by researchers from the Chemistry Institute of São Paulo State University. Voucher specimens (AGS04, AGS05, AGS06, AGS13 and AGS19) were deposited at Herbarium Maria Eneida P. Kaufmann Fidalgo at Botanical Institute of São Paulo (São Paulo, Brazil). Registries in SisGen (*Sistema Nacional de Gestão do Patrimônio Genético e do Conhecimento Tradicional Associado* – National System of Management of Genetic Heritage and Associated Traditional Knowledge) were performed (#A00892A and #A33EA7A) according to the Brazilian biodiversity legislation (Federal Law No 13,123/2015).

The leaf ethanolic extract and its fractions were obtained as described by Santos et al. (2010) and Ferreira et al. (2014). Phytochemical investigations displayed that FC represents 56.5% (mg/g) of the fraction, and Casearin X is the most present compound (14.2%) (Ferreira et al., 2014).

2.2. Cells and animals' facilities

Human fibroblasts derived from lung tissue (MRC-5), mouse fibroblasts from adipose tissue (L-929), Chinese hamster lung cells (V-79) and polymorphic blood mononuclear cells (PBMC) were maintained in RPMI-1640 medium supplemented with 10% fetal bovine serum, 2 mM glutamine, 100 U/mL penicillin and 100 µg/mL streptomycin, at 37 °C in a 5% CO_2 atmosphere (Shel Lab CO_2 Incubator, USA).

Heparinized human blood samples (from healthy, non-smoker donors who had not taken any drug for at least 15 days prior to sampling, aged 18–35 years old) were collected. PBMC were isolated by the standard method of density-gradient centrifugation over Ficoll-Hypaque. All studies are in accordance with Brazilian guidelines (Law 466/2012, National Council of Health), the Declaration of Helsinki and with the Universal Declaration on Bioethics and Human Rights of UNESCO.

Artemia salina L. (Artemiidae) eggs were obtained from Maramar Pet™ from local market (Teresina, Brazil). Eggs of *A. salina* were hatched (10 mg/L) at 25 °C in artificial seawater (NaCl 77.2%, $MgSO_4$ 9.6%, $MgCl_2$ 7.1%, $CaCl_2$ 3.3%, KCl 2.1% and $NaHCO_3$ 0.6%) prepared with non-chlorinated mineral water. Incubation was performed at 25 °C with constant aeration for 24 h to allow nauplii hatching.

Danio rerio (zebrafish) organisms were maintained in aquariums with reverse osmosis and activated carbon filtered water. Fishes were maintained in an aquatic facility with controlled photoperiod (12:12 h, light:dark) and controlled water physical-chemical parameters: temperature at 26.0 ± 1 °C, ammonia < 0.01 mg/L, conductivity at 750 ± 50 µS/cm, pH at 7.5 ± 0.5, dissolved oxygen equal to or above 95% saturation. Zebrafish eggs were collected after natural mating, rinsed in water, and checked under a stereomicroscope (Stereoscopic Zoom Microscope - SMZ 1500, Nikon Corporation). Unfertilized eggs and those with cleavage irregularities or injuries were discarded (Andrade et al., 2018).

Adult female Swiss mice (*Mus musculus*) were obtained from the Universidade Federal do Piauí (UFPI), Teresina, Brazil. They were kept in well-ventilated and cages (Alesco) under standard conditions of light (12 h with alternative day and night cycles) and temperature

(22 ± 1 °C) and were housed with access to commercial rodent stock diet (Nutrilabor, Campinas, Brazil) and water *ad libitum*. All procedures were approved by the Committee on Animal Research at UFPI (#373/2017) and followed Brazilian (*Colégio Brasileiro de Experimentação Animal* - COBEA) and International rules on the care and use of experimental animals (Directive, 2010/63/EU of the European Parliament and of the Council on the protection of animals used for scientific purposes).

2.3. Evaluation of cytotoxicity on normal adherent lines by Alamar Blue assay

It was investigated the *in vitro* cytotoxic capacity on adherent lines using the Alamar Blue™ assay. MRC-5, L-929 and V-79 cells were plated in 96-well plates (3×10^5 cells/well in 100 µL of medium). After 24 h, FC dissolved in DMSO was added to each well (0.04–25 µg/mL) and the cells were incubated for 72 h. Twenty-four hours before the end of the incubation, 20 µL of resazurin stock solution (0.156 mg/mL) were added to each well (Alamar Blue™). Cell proliferation was determined at 570 and 595 nm using a multiplate reader (DTX 880 Multimode Detector, Beckman Coulter, Germany) (Ferreira et al., 2014). Control groups (negative and positive) received the same amount of DMSO 0.1%. Doxorubicin (0.005–5 µg/mL) was used as positive control.

2.4. Analysis by flow cytometry in PBMC cells

Previously, we have reported cytotoxic action of FC and its main diterpenes on human PBMC cells and additional lines (Ferreira et al., 2010, 2014). To detail such cytotoxicity, we performed biochemical assessments in primary culture of PBMC cells by flow cytometry in a 24-well plates incubated with increasing concentrations of the FC (0.3 and 0.6 µg/mL) for 24 h (Ferreira et al., 2014). Doxorubicin (0.3 µg/mL) was used as positive control. Cytometry analyzes were performed in a Guava EasyCyte Mine™ using Guava Express Plus CytoSoft 4.1 software (Guava Technologies Inc. Industrial Blvd. Hayward, CA, USA). Five thousand events were evaluated per experiment and cell debris was omitted from the analysis.

2.4.1. Membrane integrity

Cell membrane integrity was evaluated after 24 h of incubation by the exclusion of PI. Briefly, 100 µL of treated and untreated cells were incubated with PI (50 µg/mL). The cells were then incubated for 5 min at 37 °C (Darzynkiewicz et al., 1992).

2.4.2. DNA fragmentation

Briefly, 24 h-treated and untreated cells were incubated at 37 °C for 30 min in the dark, in a lysis solution containing 0.1% citrate, 0.1% Triton X-100 and 50 µg/mL PI and fluorescence was measured afterwards (Krysko et al., 2008).

2.4.3. Mitochondrial transmembrane potential

Cells were washed with PBS and incubated with rhodamine 123, a cell-permeable, cationic, fluorescent dye, at 37 °C for 15 min in the dark. Cells were incubated again in PBS at 37 °C for 30 min in the dark, and fluorescence was measured (Cury-Boaventura et al., 2003).

2.5. Analysis of DNA strand breaks in primary cultured human cells

It was used the alkaline Comet assay to detect single and double DNA damages according to the recommendations of the International Workshop on Genotoxicity Test Procedures (Singh et al., 1988; Hartmann et al., 2003). PBMC were cultured as described above in the presence of phytohemagglutinin 2% and exposed to Casearin X (0.4, 0.8 and 1.6 µg/mL) for 24 h at 37 °C with 5% CO_2. Following exposure, slides containing treated cells for the comet assay were placed in the chilled lysis solution for 16 h at 4 °C (Singh et al., 1988; Hartmann et al., 2003). The slides were removed from the lysing solution, placed on a horizontal electrophoresis tank filled with freshly prepared alkaline buffer (300 mM NaOH, 1 mM EDTA, pH > 13.00). Electrophoresis were performed at 25 V, 300 mA for 20 min. Aftewards, each slide was stained with 50 µL ethidium bromide (20 µg/mL), and a cover slip was placed on the slide. Cellular analysis (100 cells for each of the three replicate slides) were performed using a visual scoring system that categorized tail length into five classes (0, 1, 2, 3 and 4) to determine the Damage Index (DI), which is considered to be a sensitive DNA measure and based on migration length as well as the amount of DNA in the tail. Therefore, a damage index value was assigned to each comet according to its class, and the values ranged from 0 (completely undamaged) to 400 (maximum damage). The Damage Index (DI) was calculated using the formula: DI = Σ (number of cells with damage x class of damage), which ranged from 0 (ex.: 100 cells with damage 0 × 0) to 400 (ex.: 100 cells with damaged 4 × 4). Doxorubicin (0.6 µM) was used as the positive control.

2.6. Fish embryo acute toxicity (FET) test

Assays were based on the Fish Embryo Toxicity (FET) test guideline (OECD 236, 2013). Zebrafish embryos (20 eggs/well) were exposed to six concentrations in triplicate of FC (1,1.9, 5.2, 13.9, 37.3 e 100 µg/mL) in 24-well microplates filled up with 2 mL of the test solution.

Developmental parameters were evaluated in embryos over the test, using a magnification of 70x for eggs and 40x for hatched embryos. Before hatching, the following parameters were evaluated: egg coagulation, otolith formation, general delay in development, eye and body pigmentation, somite formation, heartbeat, abnormal accumulation of blood cells, oedemas, detachment of the tail-bud from the yolk sac, yolk-sac absorption and hatching. After hatching, tail malformation, swim bladder inflation, and equilibrium (embryos lying on their side at the bottom of microplate well) were also evaluated (Andrade et al., 2018). Embryo mortality in the negative control (DMSO 1%) below 10% was required for test validity. All parameters were assessed in a qualitative way (observed or not observed). Lethal concentration values (LC_{50}) were determined for 24, 28, 72, 96 e 120 h exposure (Hamilton et al., 1977).

2.7. Acute toxicity assay on brine shrimps

After 48 h, hatched *A. salina* larvae were collected (n = 10) and added to diluted FC (1, 5, 25, 50 and 100 µg/mL) with artificial seawater (Meyer et al., 1982). Negative control group was represented only by artificial seawater with DMSO 0.1%. Potassium dichromate was used at 50 µg/mL as a positive control to confirm sensitivity of the technique. All bioassays were performed in triplicate per concentration and surviving larvae were analyzed after 24 h for CL_{50} value calculation (Hamilton et al., 1977).

2.8. Evaluation of the cytotoxic and genotoxic potential on root meristematic cells of Allium cepa

In addition to the *in vitro* models with animal cells, plant cytotoxicity bioassays using *A. cepa* have been widely used to detect *in situ* genotoxic and mutagenic compounds of synthetic and natural products and have been validated by the International Chemical Safety Program (IPCS, WHO), US Environment Program (UNEP) and US Environmental Protection Agency (USEPA) as an efficient test for genetic monitoring (Bagatini et al., 2007; Misik et al., 2014; Machado et al., 2018).

Healthy cleaned onions of uniform size were washed in running water for 20 min. Five bulbs were used for each concentration of FC (1, 10, 25 and 50 µg/mL) and for controls (negative: dechlorinated water; positive: copper sulphate 0.6 µg/mL). Bulbs were placed in glass vials and the sample volume was completed every 24 h for a final volume of 5 mL at 23 ± 2 °C. Thereafter, the roots were removed and measured

with a digital pachymeter. Then, they were fixed in Carnoy solution [ethanol:acetic acid (3:1)] for 24 h. Roots were washed in distilled water and followed by hydrolysis with 1 N HCl for 10 min at 60 °C in a water bath. The roots were kept in vials containing Schiff's reagent for 120 min (Fiskesjö, 1985; Bagatini et al., 2007). A solution of 2% acetic carmine was added to sectioned materials meristematic regions and slides were prepared. Examinations were performed by optical microscope (Olympus, Tokyo, Japan) at 400x, and 5000 cells per concentration (1000 cells/slide) were analyzed to determine the Mitotic Index (MI) and chromosomal alterations (micronuclei, delays, C-metaphases, bridges and breaks).

2.9. In vivo protocols

The fraction with casearins was solubilized in DMSO 4% and dissolved in purified water immediately before intraperitoneal (i.p.) or oral administration.

2.9.1. Acute toxicity in mice

To minimize pain and suffering as well as ensuring the robustness and reproducibility of the experiments, it was adapted a methodology recommended by the acute toxic class method – Guideline 423 – described in the "Guideline for Testing of Chemicals" from OECD to evaluate the acute toxicity (OECD, 2001). Before administrations, all animals were acclimatized for 5 days. Following the administration, the animals were fed restricted for 2 h and observed at 30 min, 60 min and 24 h. Thereafter, animals were observed daily until the 14th day (ANVISA, 2013). After 60 min of administration, the hippocratic screening was performed (Lucio et al., 2000). Based on previous studies in our laboratory (results nor published), the initial dose administered to each animal was 100 mg/kg i.p. and 400 mg/kg oral. Due to the presence of deaths after administration, it was proceeded additional treatments. All doses observed the limit of 10 mL/kg of body weight. LD_{50} was estimated according to the Globally Harmonized System (GHS) and calculated based on Trimmed Sperman-Karber method (Hamilton et al., 1977).

2.9.2. Evaluation of subacute toxicity: hematological and biochemical parameters and morphological analysis

Swiss female mice with 25–30 g were randomly divided into 6 groups (n = 10 animals/group): a) negative control groups received vehicle (DMSO 4%, i.p. or oral); b) Intraperitoneal treatment: 5 and 10 mg/kg/day; c) Oral treatment: 10 and 20 mg/kg/day by gavage. Treatments were performed for 30 days, animals were weighed weekly and observed for signals of toxicity (diarrhea, hair erection, lethargy, convulsions and death).

On the 31st day, all animals were anaesthetized with ketamine (90 mgkg)-xylazine (4.5 mg/kg) for blood collection from retrorbital plexus using sterile tubes and heparinize pipettes. Hematological assessments were performed in total blood samples using an automatic analyzer of hematologic cells (SDH-3 Vet Labtest™). For biochemical analysis, blood samples were centrifuged at 2000 rpm for 5 min. Then, we examined physiological markers of liver [albumin, blood urea nitrogen (BUN), glutamate oxaloacetate transaminase (GOT) and glutamate pyruvate transaminase (GPT), alkaline phosphatase (ALP)], kidneys (creatinine), pancreas (amylase, glucose), triglycerides and total cholesterol according to Labmax Plenno Labtest™.

Afterwards, animals were euthanized to dissect out liver, kidneys, spleen, stomach, heart and lungs to obtain wet relative weights and for macroscopic analysis. Next, organs were fixed with 10% buffered formalin, processed, cut into small pieces to prepare histological sections (4–7 μm) and stained with hematoxylin and eosin (H&E). Morphological analyses were performed under light microscopy (Olympus, Tokyo, Japan).

2.9.2.1. In vivo analysis of DNA strand breaks. A total of 200 μL of peripheral blood removed from each treated animal was submitted to density-gradient centrifugation using Ficoll-Hypaque to allow isolation of PBMC. After isolation, 20 μL of mononuclear cells were transferred to tubes containing 110 μL of 0.5% low melting agarose for preparation of slides (3 slides/sample). The processes of lysis and electrophoresis and analysis of results were performed as described above (Singh et al., 1988; Hartmann et al., 2003).

2.9.2.2. Determination of chromosomal damages. The femurs were removed, carefully cleaned and proximal epiphyses were sectioned. The bone marrow was removed using 5 mL syringes previously filled with 0.5 mL of sterile fetal bovine serum. Bone marrows were centrifuged, the precipitate was homogenized, drops of cell suspension were transferred slides to prepare smears (two slides/animal), fixed and stained by the Leishman method. All analysis were blinded-experiments performed in binocular optical microscopes at magnification of 200× and 400×. We considered as micronucleus as rounded structures, with a diameter of 1/5 to 1/20 found in young erythrocytes and identified by bluish staining. A total of 1000 polychromatic erythrocytes (PCE) was quantified per slide (two slides/animal) (Schmid, 1975; Heddle, 1973).

2.10. Statistical analysis

The IC_{50}, CE_{50}, and LC_{50} values and their 95% confidence intervals were obtained by nonlinear regression using the GraphPad program (Intuitive Software for Science, San Diego, CA). *In vitro* studies were carried out in duplicate and represented independent biological evaluations. For FET results, statistical and normality analysis were conducted using the Logistic 4-parameter. LC_{50} values were calculated for each parameter by fitting logistic dose-response curves (Andrade et al., 2018). Additional outcomes were evaluated by comparing data using one-way analysis of variance (ANOVA) followed by the Newman-Keuls test (Intuitive Software for Science, San Diego, CA). All statistical analyses considered significance level of $p < 0.05$.

3. Results

3.1. Cytotoxic activity and DNA damages

In vitro antiproliferative activity of FC was investigated on 3 adherent lines by the Alamar Blue assay. As previously demonstrated for human PBMC (Ferreira et al., 2014), FC was also cytotoxic against hamster lung V-79 cells, human MRC-5 fibroblasts and mice L-929 fibroblasts cells (Table 1).

Outcomes by flow cytometry revealed that FC reduced membrane integrity (0.8 μg/mL: 65.2 ± 1.8%) and caused DNA fragmentation (0.4 and 0.8 μg/mL: 13.1 ± 1.6 and 31.8 ± 1.1%) and mitochondrial depolarization (0.8 μg/mL: 15.0 ± 0.9%) in primary cultures of

Table 1
Antiproliferative activity of the Fraction with Casearins (FC) isolated from *Casearia sylvestris* on normal lines quantified by Alamar Blue assay after 72 h exposure.

Cell line	IC_{50} (μg/mL)[a]		Coefficient of cytotoxicity[b]
	FC	Doxorubicin	
V-79	1.9 (1.4–2.4)	0.9 (0.7–1.3)	2.1
MRC-5	9.2 (5.0–17.0)	1.8 (0.8–4.1)	5.1
L-929	3.8 (3.3–4.4)	0.7 (0.5–0.9)	5.4

[a] Data are presented as IC_{50} values and 95% confidence interval for human fibroblasts derived from lung tissue (MRC-5), mouse fibroblasts from adipose tissue (L-929) and Chinese hamster lung fibroblast cells (V-79).
[b] Coefficient of cytotoxicity determined by IC_{50} in FC/IC_{50} in Dox. Doxorubicin was used as positive control.

leukocytes (PBMC) when compared to the negative control (90.1 ± 2.1, 6.7 ± 0.6 and 8.4 ± 0.8%), respectively, after 24 h exposure (Fig. 1, $p < 0.05$). On the other hand, Doxorubicin 0.3 µg/mL was more effective to induce reduction of membrane integrity for 26.8 ± 1.8% and DNA fragmentation of 61.9 ± 2.5% ($p < 0.05$).

PBMC-treated samples after 24 h exposure were evaluated by the alkaline Comet using the main compound – Casearin X – presented in the FC. Casearin X increased DNA strand breaks in all concentrations tested (Table 2), showing increasing of frequency of damage (FD) and DI when compared to the negative control ($p < 0.05$).

3.2. Findings on zebrafish eggs and A. salina larvae

Fertilized zebrafish eggs were exposed to FC until 120 h. As shown in Fig. 2, death of embryos did not occur with concentrations up to 13.9 µg/mL, but after 24 h exposure to the following concentration (37.3 µg/mL), about 60% of mortality was verified, and at 48 h of treatment, viability of embryos was not observed ($p < 0.05$). All embryos were dead at 100 µg/mL. LC_{50} values changed significantly in a concentration- and time-dependent way: 24 h-LC_{50} was 36.65 ± 0.05 µg/mL while the 120 h-LC_{50} was 27.49 ± 0.01 µg/mL. Zebrafish embryos treated with 13.9 µg/mL did not present swim bladder inflation after 120 h exposure (Fig. 2). Other sublethal or lethal malformations were not noticed in zebrafish early life stages. Negative control organisms presented a normal embryo development as described by Kimmel et al. (1995).

After 24 h of exposure on *A. salina* nauplii, FC revealed a LC_{50} value of 48.8 (42.3–56.5) µg/mL ($R^2 = 0.9086$).

3.3. Antiproliferative and clastogenic action

FC inhibited the growth of *A. cepa* roots of in all tested concentrations (34.9 ± 7.1, 20.9 ± 8.5, 30.6 ± 7.0 e 55.8 ± 4.4% for 1, 5, 25 and 50 µg/mL, respectively) in a concentration-dependent manner when compared to the negative control ($p < 0.05$). Onions treated with copper sulphate 0.6 µg/mL also caused growth inhibition (60.9 ± 3.7%, Fig. 3).

Confirming its capacity to inhibit root growth, FC also caused reduction of MI from 37.8 to 45.7% in a non-dependent concentration way when compared to the negative control (53.3 ± 0.6%). Concentrations of 25 and 50 µg/mL increased cells in metaphase and anaphase was registered ($p < 0.05$, Table 3). Similarly, such concentrations induced chromosomal alterations, including micronuclei and chromosomic lost ($p < 0.05$, Table 4).

3.4. Acute and subacute effects on physiological and morphological parameters

Intraperitoneal and oral LD_{50} values obtained for the FC were 80.9 (65.9–97.9) and 267.1 (229.9–310.4) mg/kg body weight, respectively. Following administration, the most signals of toxicity were irritability, hyperactivity, vocal frenzy, diarrhea, straub, ataxia and insensitivity to painful stimuli, specially at higher doses. One death was detected at the highest oral and i.p. doses (Table 5).

The second part of toxicity studies in mice was performed for consecutive 30 days, during which animals were treated with FC 5 and 10 mg/kg/day i.p. or 10 and 20 mg/kg/day by gavage. Animals were weighed weekly to verify gain of body weight. After 7 days (T_7), both i.p. doses (5 mg/kg/day: 28.4 ± 0.5 g) and (10 mg/kg/day: 30.6 ± 0.8 g) reduced growth of mice when compared to the negative control (33.4 ± 0.4 g) ($p < 0.05$, Fig. 4). In subsequent weeks (T_{15}, T_{22} and T_{30}), the growth of animals remained statistically lower ($p < 0.05$) until the end of the treatment in both i.p. treated groups, which causes lower gain of body weight (5 mg/kg/day: 4.4 ± 0.4 g; 10 mg/kg/day: 3.9 ± 0.6 g), while control grew 9.2 ± 0.4 g (Table 6). In a similar way, 20 mg/kg/day-treated animals also presented diminution of weight gain (2.2 ± 0.8 g; control grew 9.6 ± 0.7 g), but such reduction occurred in the last week of administration ($p < 0.05$). Neither growth nor body weight gain altered in 10 mg/kg/day oral-treated animals ($p > 0.05$).

After animals' dissection, analysis of wet relative weight of key organs (liver, kidneys, spleen, heart, and lungs) revealed increased of livers and spleens of FC-treated animals at 10 mg/kg/day i.p., while hearts showed reduction at both i.p. doses ($p < 0.05$, Table 6). Concerning oral treatments, both doses increased relative weights of stomachs in comparison with oral control group ($p < 0.05$).

3.4.1. Histopathological alterations

Microscopic analysis of livers revealed a moderate (5 mg/kg/day ip, Fig. 5C) to the intense cellular swelling of hepatocytes (10 mg/kg/day i.p.; 10 and 20 mg/kg/day oral, Fig. 5D, E and 5 F, respectively), portal and centrilobular vein congestion, accumulation of hemosiderin

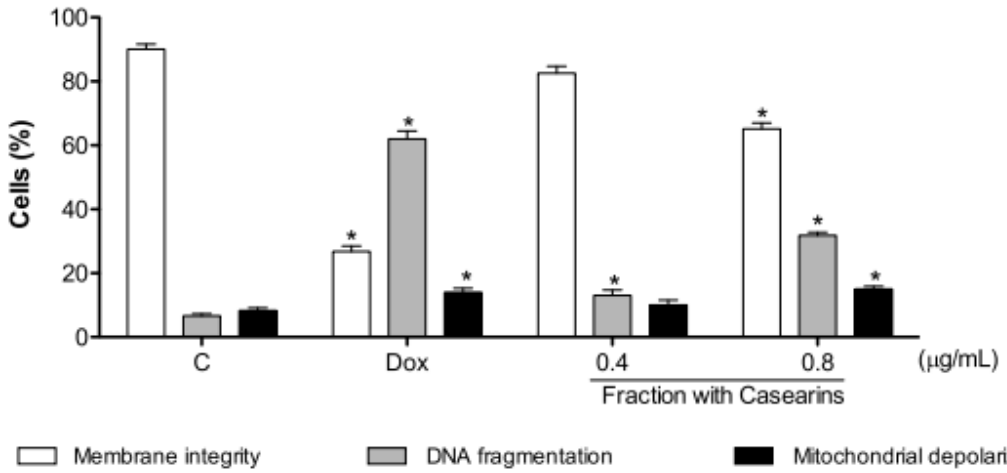

Fig. 1. Effects of the Fraction with Casearins (FC) on *ex vivo* primary cultures of polymorphic blood mononuclear cells after 24 h exposure and analysis by flow cytometry. Cell membrane integrity was evaluated by the exclusion of propidium iodide. DNA fragmentation evaluation was performed by nuclear fluorescence using propidium iodide, Triton X-100 0.1% and citrate. Mitochondrial transmembrane potential was determined by rhodamine 123 retention. Negative control (C) was treated with the vehicle used for diluting the tested substance (DMSO 1%). Doxorubicin (0.3 µg/mL) was used as positive control (Dox). Results are expressed as mean ± standard error of mean (S.E.M.) from two independent experiments. *$p < 0.05$ compared to control by ANOVA followed by Student Newman-Keuls test.

Table 2
Frequency of Damage and Damage Index caused by Casearin X isolated from the fraction of *Casearia sylvestris* leaves on primary culture of peripheral blood mononuclear cells after 24 h exposure determined by alkaline Cometa assay.

Parameter	Negative control	Doxorubicin (0.3 μg/mL)	Casearin X		
			0.4 μg/mL	0.8 μg/mL	1.6 μg/mL
Frequency of Damage (%)[a]	7.6 ± 1.5	88.3 ± 2.4*	43.5 ± 3.8*	89.5 ± 1.8*	87.8 ± 2.7*
Damage Index[b]	10.0 ± 1.0	221.7 ± 3.7*	44.3 ± 3.9*	112.8 ± 6.3*	137.5 ± 9.5*

[a] Values expressed as total damage percentages (%).
[b] Calculated using the formula: DI = Σ (number of cells with damage X class of damage), which ranged from 0 (ex.: 100 cells with damage 0 × 0) to 400 (ex.: 100 cells with damaged 4 × 4). Results are expressed as mean ± standard error of mean (S.E.M.) from two independent experiments. *$p < 0.05$ compared to control by ANOVA followed by Student Newman-Keuls test. Doxorubicin was used as positive control.

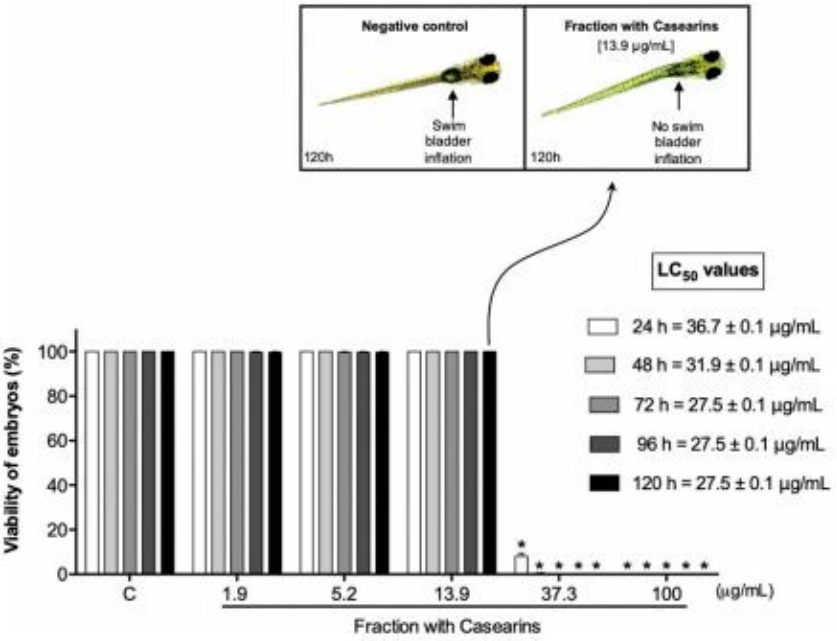

Fig. 2. Effects on viability and induction of malformations in zebrafish embryos following 120 h exposure to the Fraction with Casearins. Values were obtained fitting models to data using non-linear regression (Logistic 4-parameter). Negative control (C) was treated with the vehicle used for diluting the tested substance (DMSO 1%). *$p < 0.05$ compared to the negative control by ANOVA followed by Dunnett's test.

pigments and Kupffer cell hyperplasia (at all doses). Except for the lowest i.p. dose, other ones caused inflammatory foci in the parenchyma or stroma of liver tissues, but areas of focal necrosis and polymorphonuclear neutrophil granulocytes were found only in highest doses (10 mg/kg/day i.p. and 20 mg/kg/day oral). Disarrangement of hepatocyte cords indicating cell death followed by regeneration was extensively detected at 10 mg/kg/day i.p. Accumulation of small lipid droplets in hepatocytes' cytoplasm (microvesicular steatosis) was found in animals treated with 5 mg/kg/day i.p. and 20 mg/kg/day oral (Fig. 5C and F).

All FC-treated groups showed moderate (5 and 10 mg/kg/day i.p.; Fig. 6C and D) to the intense epithelium cellular swelling of proximal and distal tubules from kidneys (10 and 20 mg/kg/day oral, Fig. 6E and F, respectively). Moreover, tubular and glomerular hemorrhage and presence of hyaline cylinders were also detected. Extensive areas of necrosis with neutrophil granulocyte collections similar to abscesses

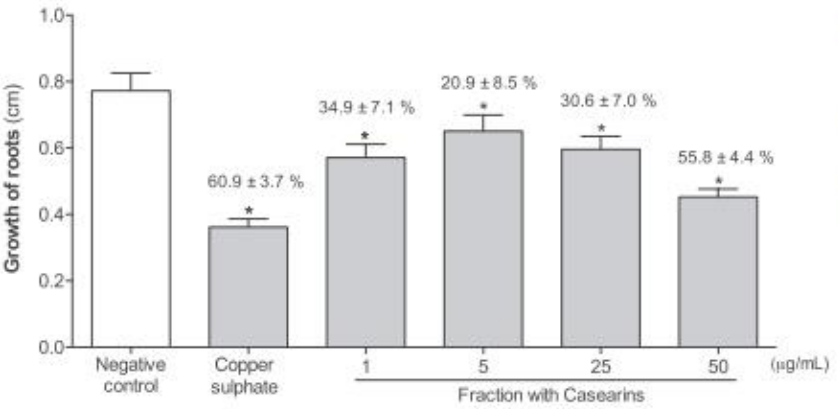

Fig. 3. Growth of *Allium cepa* roots treated with a Fraction with Casearins after 72 h exposure. Negative control was exposed to dechlorinated water and DMSO 0.5%. Copper sulphate (0.6 μg/mL) was used as positive control. Percentages of growth inhibition are described. Results are expressed as mean ± standard error of mean (S.E.M.) from two independent experiments. *$p < 0.05$ compared to control by ANOVA followed by Student Newman-Keuls test.

Table 3
Cytotoxic activity of the Fraction with Casearins on meristematic cells of *Allium cepa* roots after 72 h exposure.

Treatment	Concentration (μg/mL)	Interphase	Mitosis				Mitotic Index** (%)
			Prophase	Metaphase	Anaphase	Telophase	
Negative control	–	500.0 ± 34.7	470.8 ± 31.3	11.8 ± 1.1	3.8 ± 0.8	13.8 ± 2.9	53.3 ± 0.6
Copper sulphate	3	861.0 ± 5.6*	104.5 ± 3.0*	12.0 ± 1.9*	11.0 ± 1.5*	11.5 ± 3.2*	13.9 ± 0.6*
Fraction with Casearins	1	525.0 ± 33.5	446.6 ± 31.3	12.8 ± 2.0	5.2 ± 0.6	14.0 ± 2.8	45.7 ± 2.3*
	5	604.6 ± 39.2	365.0 ± 38.9	13.6 ± 3.1	5.2 ± 1.4	13.8 ± 2.3	38.7 ± 1.2*
	25	537.4 ± 47.0	416.0 ± 48.9	23.4 ± 2.3*	10.2 ± 1.5*	16.6 ± 2.3	39.9 ± 0.9*
	50	538.0 ± 3.4	421.4 ± 31.2	20.4 ± 2.6*	15.2 ± 1.2*	18.0 ± 1.9	37.8 ± 0.8*

Results are expressed as mean ± standard error of mean (S.E.M.) from two independent experiments. *$p < 0.05$ compared to control by ANOVA followed by Student Newman-Keuls test. Copper sulphate 3 μM was used as positive control. ** Mitotic index was calculated as follow: Prophase + Metaphase + Anaphase + Telophase/Total number of cells x 100.

Table 4
Chromosomal changes induced by the Fraction with Casearins on meristematic cells of *Allium cepa* roots after 72 h exposure.

Treatment	Concentration (μg/mL)	Chromosomal alterations					Total of chromosomal alterations
		Micronuclei	Delays	Chromosomic lost	Bridges	Breaks	
Negative control	–	7.4 ± 1.1	2.8 ± 1.4	0.4 ± 0.4	1.0 ± 0.8	1.6 ± 0.5	15.8 ± 2.4
Copper sulphate	0.6	11.5 ± 0.7*	13.0 ± 0.7*	16.3 ± 0.9*	6.3 ± 0.6*	8.0 ± 1.0*	55.0 ± 2.0*
Fraction with Casearins	1	17.0 ± 4.1	3.6 ± 1.1	2.0 ± 0.3	2.2 ± 0.4	0.0	24.0 ± 8.6
	5	23.6 ± 8.8	2.4 ± 0.5	1.0 ± 0.3	3.8 ± 2.1	0.0	24.2 ± 3.5
	25	44.2 ± 4.9*	2.4 ± 0.6	4.2 ± 1.8*	4.2 ± 1.1	0.0	55.0 ± 4.1*
	50	24.6 ± 2.9*	3.8 ± 0.9	1.8 ± 0.5	2.6 ± 0.7	3.5 ± 1.0	30.0 ± 1.7*

Results are expressed as mean ± standard error of mean (S.E.M.) from two independent experiments. *$p < 0.05$ compared to control by ANOVA followed by Student Newman-Keuls test. Copper sulphate 3 μg/mL was used as positive control.

Table 5
Acute toxic effects of Fraction with Casearins after oral intraperitoneal single dose in Swiss mice.

Group	Dose (mg/kg)	Signs of toxicity		
		Survival	Latency for death	1 h later
Negative control	–	0/3	–	Piloerection, increased respiration
Intraperitoneal	12,5	0/3	–	Piloerection, increased respiration, ataxia, contortion, straub, tremors, irritability
	25	0/3	-	Increased respiration, piloerection, tremors, ataxia, contortion
	50	0/3	-	Ataxia, vocal frenzy, increased respiration, piloerection, diarrhea, contortion
	100	1/3	24 h	Altered respiration, tremors, piloerection, diarrhea, straub, ataxia, insensitivity to painful stimuli
Oral	50	0/3	–	Piloerection, lacrimation, contortion
	100	0/3	–	Increased respiration, straub, tremors, piloertion, vocal frenzy
	200	0/3	–	Vocal frenzy, tremors, straub, piloerection, ataxia, contortion
	400	1/3	24 h	Vocal frenzy, piloerection, hyperactivity, increased respiration, ataxia, straub, diarrhea.

N = 3 animals/group. Negative control was treated with the vehicle used to dilute the fraction (DMSO 5%).

(5 mg/kg/day i.p.; Fig. 6C) and foci of nephrotoxic necrosis of tubular epithelium were also found (10 mg/kg/day i.p. and 20 mg/kg/day oral; Fig. 6D and F). Spleens did not show significant changes when compared to the control group, but all treated groups showed severe congestion of red pulps and disorder of lymphoid follicles, especially with two highest doses investigated (not showed). Although i.p. treatment has induced decreasing in their wet relative weight, microscopic examinations revealed normal tissue morphologies in a very similar way to the oral negative control and signs of cardiotoxicity were not found (not showed). Similarly, stomachs did not show macro or microscopic alterations in comparison to their respective negative controls. They demonstrated pleated intact mucosa and absence of hemorrhagic or inflammatory foci. Parietal and chief cells from gastric body presented morphologically normal characteristics, indicating secretory functions were not affected (not showed).

Lungs from untreated and treated animals showed well delimited alveolar sacs, integrity of bronchial epithelium (ciliated columnar pseudostratified), some dilated blood vessels and small hemorrhagic points probably associated with euthanasia surgical techniques (Fig. 7C, D, 7E and 7F). Treated animals by i.p. injections (5 and 10 mg/kg/day, Fig. 7C and D) exhibited some perivascular collections of inflammatory infiltrates with neutrophils.

3.4.2. Biochemical and hematological changes

Serum biochemical parameters are described in Table 7. It was noted increase of ALT and decrease of albumin, alkaline phosphatase and glucose in animals treated with FC 10 mg/kg/day i.p. ($p < 0.05$) when compared to the control. Meanwhile, total cholesterol decreased at both i.p. doses ($p < 0.05$). Animals that received FC oral 20 mg/kg/day showed alkaline phosphatase reduction.

Hematological examinations detected significant changes only after i.p. treatments (5 and 10 mg/kg/day). Such doses caused decrease of erythrocytes, hematocrit, hemoglobin and lymphocytes when compared to the control that received only DMSO 4% (Table 8, $p < 0.05$). On the other hand, there was increase of segmented leukocytes and RDW ($p < 0.05$).

3.4.3. In vivo genotoxic damages on hematological cells

In order to complement genotoxic/mutagenic investigations performed with *ex vivo* human leukocytes and *in vivo A. cepa* meristematic

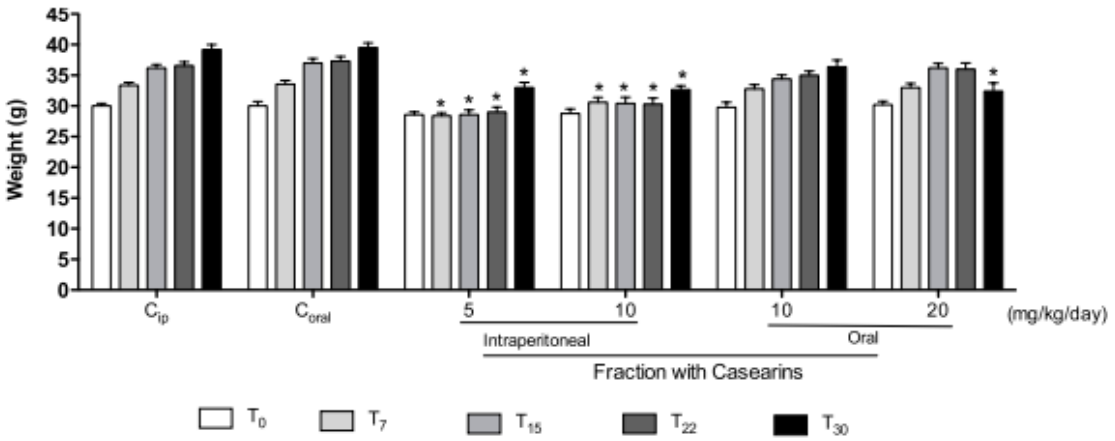

Fig. 4. Evaluation of Swiss mice growth during intraperitoneal treatment (5 and 10 mg/kg/day) or oral treatment (10 and 20 mg/kg/day) by gavage with the Fraction with Casearins (FC) isolated from *Casearia sylvestris* leaves. Animals were weekly weighed. T_0 = Time 0 (start of treatment); T_7 = seventh day; T_{15} = fifteenth day; T_{22} = twenty-second day; T_{30} = thirtieth day (end of treatment). Negative control received DMSO 4%. Results are expressed as mean ± standard error of mean (S.E.M.) of 10 animals/group. $^*p < 0.05$ compared to control by ANOVA followed by Student Newman-Keuls test.

tissues, we also analyzed DNA damage and MN in 30-days treated animals.

As detailed in Fig. 8, only FC-treated animals at 10 mg/kg/day i.p. revealed increase of DI in PBMC (17.0 ± 1.9) and micronucleated polychromatic erythrocytes (5.5 ± 0.7 MNPCE/2000 cells) when compared to the i.p. negative control (9.7 ± 1.0 and 2.2 ± 0.6 MNPCE/2000 cells, respectively) ($p < 0.05$).

4. Discussion

It remains problematical developing target medicines to affect the course of diseases since most of them have been removed from the market (Harvey, 2014; Newman and Cragg, 2016) because failure in phase I, II and/or III clinical trials due to lack of efficacy (~30–56% of failures), toxicity concerns (~30%), and commercial issues (~20–28%) (Arrowsmith and Miller, 2013), demonstrating approval about 10% (Hay et al., 2014). In general, the main objective of toxicity studies is to identify the presence of compound(s) responsible for damages, the related-changes and to link them with histopathological, hematological and serum biochemical analysis (Cullen and Miller, 2006; Ramaiah, 2007). So, Taking into consideration such dilemmas, we evaluated the toxic effects of an ethyl acetate fraction from *C. sylvestris* leaves using *in vitro* and *in vivo* traditional methods and alternative tools. Most studies were carried out using the fraction, which is composed by a mixture of casearins and represents the most folk approach in etnopharmacological uses by Brazilian population (Araújo et al., 2015, 2017; Ferreira et al., 2016).

Initially, FC showed cytotoxic action on cell cultures of normal fibroblasts from different histological sources and species, which confirmed previous results describing the antiproliferative capacity of molecules from *C. sylvestris* leaves (Da Silva et al., 2008b, 2009; Santos et al., 2010; Ferreira et al., 2010, 2014; Bou et al., 2013; Felipe et al., 2014, 2016). Although this cytotoxicity on non-transformed cells emphasizes a relatively low selectivity, it is important to note that FC was about 5-fold less toxic on fibroblasts than doxorubicin, an anthracycline widely used as primary therapeutic agent or in combination regimens for the treatment of lymphomas and solid tumors.

To understand consequences of this non-specific cytotoxicity, and based on own results showing Casearin X and FC as cytotoxic substances on primary cultures of leukocytes (Ferreira et al., 2010, 2014), we also analyzed FC-treated PBMC by cytometry. The findings (reduction of membrane integrity, DNA fragmentation, and mitochondrial depolarization) suggest FC triggers cell death of leukocytes by apoptosis (Krysko et al., 2008; Ferreira et al., 2016).

It is well known that mitotic phases are very susceptible to environmental toxins, which explain the use of early life stages to assess important toxicological and pharmacological end points. In this context, we showed, for first time, that FC induced accumulation in metaphase and anaphase and chromosomal changes (micronuclei and chromosomal lost) and reduction of cell division of meristematic cells. Taking into consideration that compounds with antiproliferative action usually cause arrest at specific stage(s) of mitosis as part of the cytotoxic mechanism due to the induction of aneugenic or clastogenic chromosome damages, this cell cycle arrest may be related to DNA breaks and repair machinery triggering (Bagatini et al., 2007; Ferreira et al., 2014; Sales et al., 2017).

Table 6
Effects of the Fraction with Casearins isolated from *Casearia sylvestris* leaves on the wet relative weight of key organs from Swiss mice intraperitoneally or orally treated for 30 days. Negative control received DMSO 4%. Oral.

Treatment	Dose (mg/kg/day)	Gain of body weight (g)	Liver	Kidneys	Spleen	Stomach	Heart	Lungs
			Relative weight (g/100 g)					
Control	–	9.2 ± 0.4	4.02 ± 0.07	1.41 ± 0.04	0.34 ± 0.02	0.82 ± 0.04	0.47 ± 0.02	0.49 ± 0.04
Fraction with Casearins	5	4.4 ± 0.4*	3.95 ± 0.29	1.27 ± 0.06	0.40 ± 0.06	0.99 ± 0.12	0.36 ± 0.01*	0.39 ± 0.03
	10	3.9 ± 0.6*	4.73 ± 0.31*	1.42 ± 0.10	0.57 ± 0.10*	0.98 ± 0.05	0.36 ± 0.01*	0.45 ± 0.05
Control	–	9.6 ± 0.7	4.05 ± 0.16	1.36 ± 0,07	0.19 ± 0.02	0.73 ± 0.07	0.41 ± 0.02	0.47 ± 0.04
Fraction with Casearins	10	6.6 ± 1.3	3.81 ± 0.12	1.30 ± 0.05	0.20 ± 0.02	1.30 ± 0.06*	0.35 ± 0.01	0.41 ± 0.03
	20	2.2 ± 0.8*	3.73 ± 0.14	1.38 ± 0.05	0.19 ± 0.02	1.11 ± 0.11*	0.45 ± 0.04	0.51 ± 0.03

Results are expressed as mean ± standard error of mean (S.E.M.) of 10 animals/group. $^*p < 0.05$ compared to control by ANOVA followed by Student Newman-Keuls test.

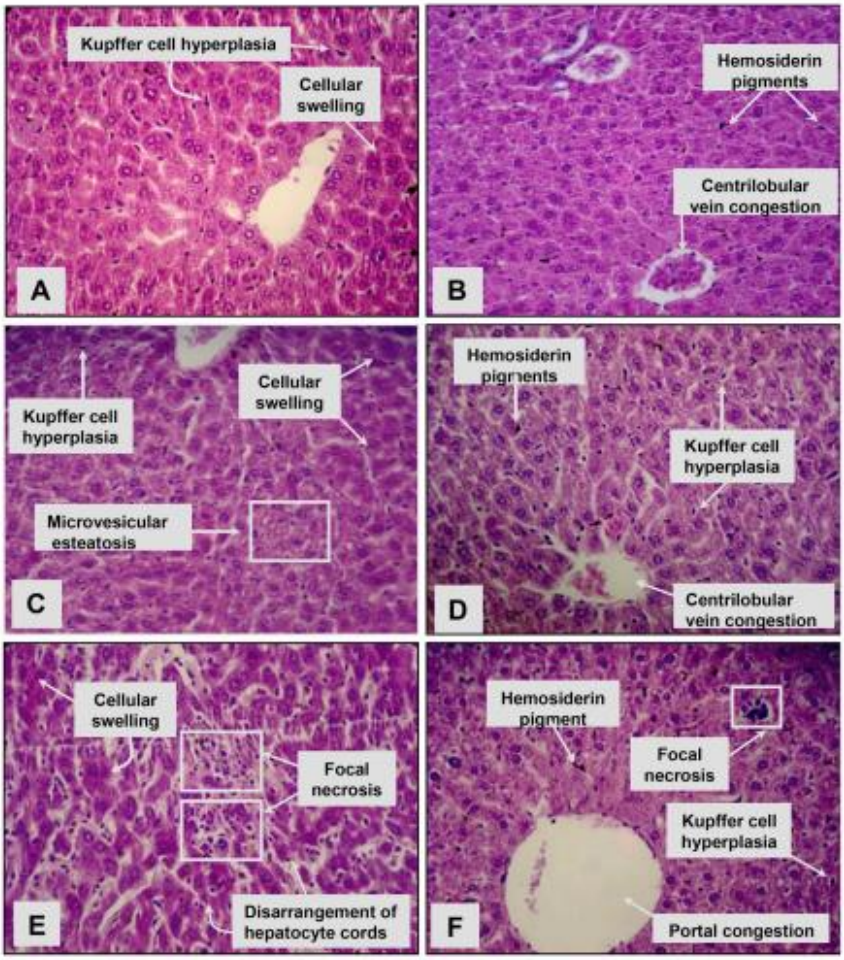

Fig. 5. Histological analysis in livers of mice treated with the Fraction with Casearins isolated from *Casearia sylvestris* leaves at doses of 5 (C) and 10 mg/kg/day i.p. (D) and 10 (E) and 20 mg/kg/day oral (F) during 30 days. Negative controls (A, B) received DMSO 4% (i.p. and oral). Hematoxylin-eosin staining. Light microscopy magnification, 400x.

Besides cytotoxic analyzes using normal mammals and proliferating meristematic cells, we used zebrafish dividing embryos to analyze development phases of this metazoan to detect early signs of teratogenicity. Zebrafish exhibits prodigious versatility as a systemic vertebrate model to identify developmental abnormalities and congenital malformations in living organisms caused by chemicals, such drugs, pesticides and hormones with less prone to legal and ethical restrictions. Studies have demonstrated *D. rerio* embryos responds to xenobiotics as mammals do because they share similarities in their development biology, metabolism, physiology (70% gene homology), and signaling pathways (Yue et al., 2015; Rivero-Wendt et al., 2016; Raghunath and Perumal, 2018).

For our surprise, more than 50% of zebrafish embryos were dead after 24 h in the presence of FC 37.3 µg/mL and so on. Coagulation of embryos, lack of somite formation, non-detachment of the tail, and lack of heartbeat were not detected, but survived embryos after 120 h exposure in lower concentration (13.9 µg/mL) did not present swim bladder inflation. Microscopic analysis also indicated FC-treated embryos with swim bladders reduced in size, whose wall seemed thinner and half-finished in the histological point of view at 120 h post fecundation (data not showed).

Swim bladders, a sac filled by gas to regulate buoyancy and acoustic sensation, are found in about half of all modern teleost fishes. Of course, they are vital organs for survival because it reduces energy required to maintain vertical position in the water column (Zeddies and Fay, 2005; Yue et al., 2015). Then, taking into consideration the onset of time- and concentration-dependent abnormalities/malformations, embryo lethality may be directly or indirectly associated with absence of swim bladder inflation in FC-treated larval embryos. It is likely that FC induces disruption of swim bladder development at initial stages during construction/assembling of tissue layers (epithelial layer, mesenchymal layer, and/or outer mesothelium) in budding step (1st phase) and/or in the growth/elongation step (2nd phase at 65–96 h post fecundation), but consequences of malformations were noted later during the inflation step, the 3rd phase involving inflation of the single-chambered swim bladder at 96–120 h post fertilization by air-gulping (Finney et al., 2006; Winata et al., 2009).

Another larval tool to analyze (eco)toxicological aspects of bioactive substances is represented by brine shrimps of *A. salina*. *Artemia* nauplii have been used to test the toxicity of a wide range of chemicals such heavy metals, engineered nanomaterials, herbicides, insecticides, pesticides, pharmaceuticals, and plant extracts (Meyer et al., 1982; Hamidi et al., 2014; Melo et al., 2018). David et al. (2001) classify as very toxic those substances whose LC_{50} values are < 100 µg/mL. The ethanolic extract from C. *sylvestris* leaves revealed a LC_{50} value of 724.76 µg/mL (Espinosa et al., 2015), which suggests FC (LC_{50} value of 48.8 µg/mL) as a sample almost 14-fold more toxic. Naturally, biossays with *A. cepa*, *D. rerio* and *A. salina* nauplii, allows reducing number and suffering of

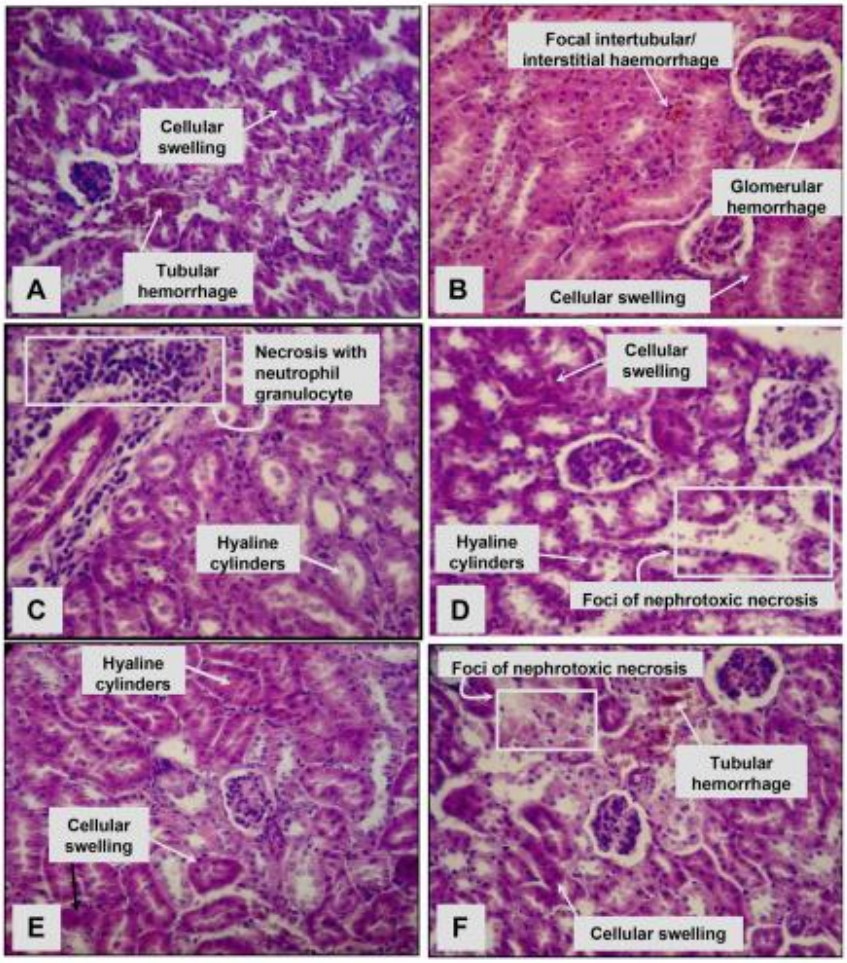

Fig. 6. Histological analysis in kidneys of mice treated with the Fraction with Casearins isolated from *Casearia sylvestris* leaves at doses of 5 (C) and 10 mg/kg/day i.p. (D) and 10 (E) and 20 mg/kg/day oral (F) during 30 days. Negative controls (A, B) received DMSO 4% (i.p. and oral). Hematoxylin-eosin staining. Light microscopy magnification, 400x.

mammals and the development of alternative methods for the use of mice and rats as predictors of toxicity.

To confirm such parallel biological response, mice were treated orally or intraperitoneally with a single dose of FC and observed for 14 days. Oral and i.p. treatments were chosen as a way to evaluate the interference of factors such as absorption, stomach and intestinal pH, enzymatic activity of digestive tract and first pass metabolism (Karalliedde et al., 2003), and revealed LD_{50} values of 267.1 and 80.9 mg/kg body weight, respectively. Such LD_{50} values are lower than those found by Basile et al. (1990), Esteves et al. (2005) and Ameni et al. (2015) for ethanolic extract (> 1842 mg/kg), essential oil (1100 mg/kg) and hydroethanolic fluid (> 2000 mg/kg) of *C. sylvestris* leaves, respectively, suggesting that FC is more toxic. Based on the Globally Harmonized System of Classification and Labelling of Chemicals guidelines (UN, 2017), FC is considered toxic if ingested, which corroborates the results suggesting FC as very toxic on *A. salina* nauplii.

For both *in vitro* and *in vivo* genotoxicity studies, PBMC are used as experimental model because they are sensitive indicators to genotoxic agents, have a relatively long life, circulate through all tissues and are easy to obtain (Albertini et al., 2000; Machado et al., 2018). Cometa assay was carried out considering alkaline conditions (pH > 13), the best version to recognize genotoxic agents, and capable of detecting DNA double-strand breaks, single-strand breaks, alkali-labile sites, DNA-DNA/DNA-protein cross-linking, and incomplete excision repair sites (Pu et al., 2015).

Although Cas X have caused similar FD in similar ways to that showed by Dox (88.3 ± 2.4%) in higher concentrations (0.8 and 1.6 μg/mL), Cas X caused lower DNA damages. In agreement with results described above, *in vivo* subacute injections of FC 10 mg/kg/day i.p. increased FD, DI and micronucleated erythrocytes.

Level 4 induced-damages by Casearin X is a signal of cytotoxic effect, being the most indicative aspect of apoptotic recognition in Comet parameters (Hartmann et al., 2003; Ferreira et al., 2014; Machado et al., 2018). So, it is plausible that FC (and its components) activates similar non-selective death pathways in normal and cancer cell lines. On the other hand, Oliveira et al. (2009) suggest that ethanolic extract (up to 25 mg/kg/day) and Caseargrewiin F (up to 2.5 mg/kg/day) from *C. sylvestris* leaves has antimutagenic and antigenotoxic action against cyclophosphamide-induced effects after 14 days exposure. Meanwhile, clastogenic potential was seen in higher doses (50 and 75 mg/kg/day of ethanolic extract and 3.8 mg/kg/day of Caseargrewiin F).

Herein, most studies clearly demonstrate genotoxic and clastogenic actions of FC, since double-stranded breaks, chromosomal lost and MI reduction represent severe DNA damage due to the loss of chromosomal continuity and the generation of chromosomal fragments (without centromere) which compromise chromosomal segregation during mitosis (Kaye et al., 2004). This is linked to generation of micronucleated polychromatic erythrocytes in root meristematic tips and bone marrow

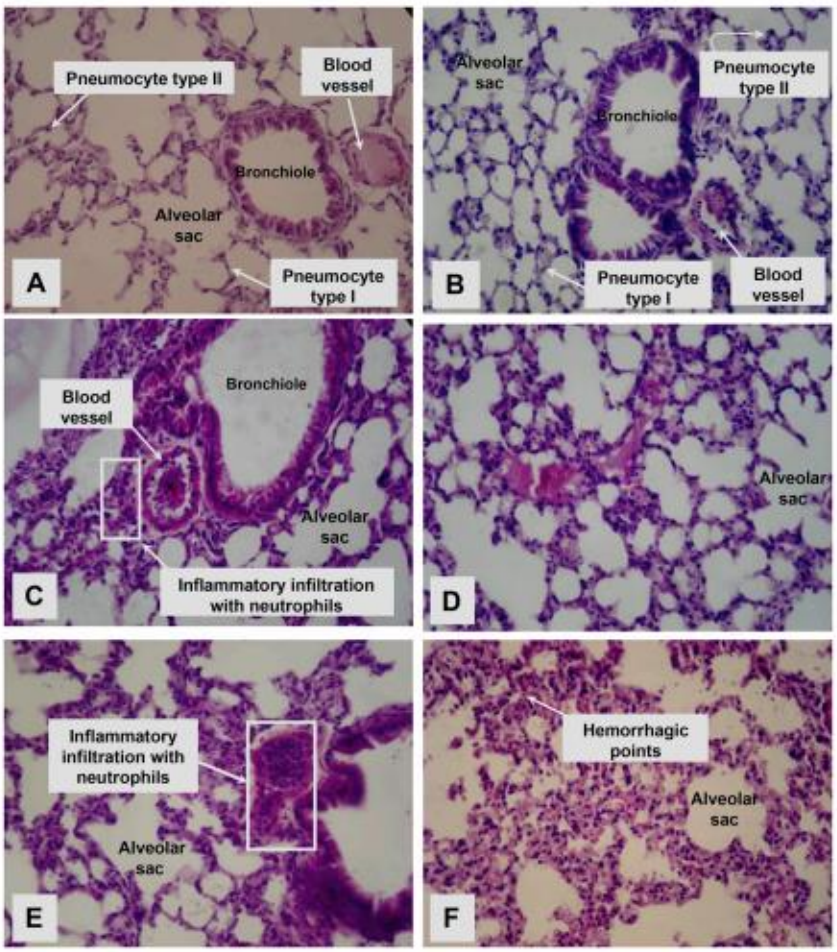

Fig. 7. Histological analysis in lungs of mice treated with the Fraction with Casearins isolated from *Casearia sylvestris* leaves at doses of 5 (C) and 10 mg/kg/day i.p. (D) and 10 (E) and 20 mg/kg/day oral (F) during 30 days. Negative controls (A, B) received DMSO 4% (i.p. and oral). Hematoxylin-eosin staining. Light microscopy magnification, 400x.

cells from FC 10 mg/kg/day i.p-treated mice. Nevertheless, a genotoxic agent is not necessarily a mutagenic substance, since DNA induced-lesions can be repaired. Additionally, these damages should not be directly extrapolated to all human somatic and germ cells, because it is not sure whether DNA injuries found in white blood cells accurately reproduce damages in target organs (Fenech, 2007). So, DNA damage is just the first stage of carcinogenic process, providing no enough data about carcinogenic potency of FC and isolated molecules (Mattioli

Table 7
Biochemical profile of Swiss mice intraperitoneally or orally treated for consecutive 30 days with the Fraction with Casearins isolated from *Casearia sylvestris* leaves. Negative control received DMSO 4%.

Biochemical parameters	Intraperitoneal treatment			Oral treatment		
	Control	Fraction with Casearins		Control	Fraction with Casearins	
		5 mg/kg/day	10 mg/kg/day		10 mg/kg/day	20 mg/kg/day
Albumin (g/dL)	1.78 ± 0.1	1.75 ± 0.1	1.57 ± 0.1*	1.95 ± 0.1	2.1 ± 0.1	2.0 ± 0.1
GOT (U/L)	140.4 ± 5.3	177.6 ± 7.7	170.2 ± 17.1	126.0 ± 5.0	145.8 ± 6.9	140.2 ± 10.7
GPT (U/L)	37.4 ± 2.9	67.0 ± 6.4	73.0 ± 14.0*	43.0 ± 6.4	47.8 ± 4.4	43.8 ± 2.1
ALP (U/L)	63.8 ± 4.5	50.4 ± 5.9	34.2 ± 4.3*	88.6 ± 8.0	88.6 ± 5.1	53.4 ± 5.5*
Total cholesterol (mg/dL)	162.6 ± 10.7	115.2 ± 12.6*	121.8 ± 9.4*	194.3 ± 9.9	177.6 ± 17.0	171.3 ± 11.8
Triglycerides (mg/dL)	161.6 ± 18.9	142.0 ± 27.8	149.8 ± 15.2	156.5 ± 11.0	176.5 ± 23.9	136.4 ± 38.7
BUN (mg/dL)	37.0 ± 3.9	37.8 ± 5.4	32.6 ± 4.7	49.7 ± 6.9	43.6 ± 5.6	38.6 ± 5.9
Creatinin (mg/dL)	0.5 ± 0.1	0.5 ± 0.1	0.4 ± 0.1	0.5 ± 0.1	0.4 ± 0.1	0.4 ± 0.1
Glucose (mg/dL)	112.5 ± 7.6	96.9 ± 8.5	78.2 ± 11.6*	133.3 ± 9.2	145.6 ± 9.4	111.7 ± 12.5
Amylase (U/dL)	619.2 ± 4.8	628.8 ± 23.3	643.9 ± 22.2	619.2 ± 15.1	582.5 ± 11.4	589.4 ± 10.0

BUN, blood urea nitrogen; GOT, glutamate oxaloacetate transaminase; GPT, glutamate pyruvate transaminase; alkaline phosphatase (ALP). Results are expressed as mean ± standard error of mean (S.E.M.) of 10 animals/group. *$p < 0.05$ compared to control by ANOVA followed by Student Newman-Keuls test.

Table 8
Hematological profile of Swiss mice intraperitoneally or orally treated for consecutive 30 days with the Fraction with Casearins isolated from *Casearia sylvestris* leaves. Negative control received DMSO 4%.

Biochemical parameters	Intraperitoneal treatment			Oral treatment		
	Control	Fraction with Casearins		Control	Fraction with Casearins	
		5 mg/kg/day	10 mg/kg/day		10 mg/kg/day	20 mg/kg/day
Erythrocytes (x 10^6/μL)	8.8 ± 0.3	7.8 ± 0.2*	7.7 ± 0.2*	9.3 ± 0.2	9.2 ± 0.1	9.5 ± 0.5
Hematocrit (%)	49.2 ± 2.2	40.9 ± 1.5*	39.1 ± 0.9*	50.0 ± 0.7	50.6 ± 0.8	50.4 ± 3.4
Hemoglobin (g/dL)	14.1 ± 0.5	11.6 ± 0.3*	11.6 ± 0.6*	14.3 ± 0.2	14.7 ± 0.2	15.1 ± 0.9
MCV (fL)	55.9 ± 1.7	52.5 ± 0.5	54.4 ± 2.3	53.6 ± 0.4	54.9 ± 0.3	55.8 ± 1.2
MHC (pg)	16.0 ± 0.4	14.9 ± 0.1	14.7 ± 0.7	15.3 ± 0.3	15.9 ± 0.2	15.9 ± 0.1
MCHC (g/dL)	28.7 ± 0.4	28.5 ± 0.5	27.9 ± 0.7	28.5 ± 0.4	29.0 ± 0.3	28.5 ± 0.5
Platelets (μL)	1.313 ± 44.7	1.200 ± 59.5	1.102 ± 66.3	1.261 ± 73.2	1.138 ± 95.7	1.241 ± 167.2
Total leukocytes (x 10^3/μL)	5.7 ± 0.4	4.5 ± 0.5	3.8 ± 1.2	6.6 ± 1.5	4.2 ± 0.5	5.6 ± 1.0
Neutrophils (%)	12.2 ± 0.9	38.4 ± 2.1*	56.2 ± 4.1*	21.8 ± 2.2	17.0 ± 1.6	25.0 ± 2.9
Lymphocytes (%)	84.8 ± 1.6	56.8 ± 2.1*	37.8 ± 2.5*	75.4 ± 1.9	79.2 ± 1.5	73.4 ± 3.5
Monocytes (%)	2.8 ± 0.7	3.8 ± 0.5	4.0 ± 0.7	2.8 ± 0.7	3.8 ± 0.6	3.8 ± 0.7
Eosinophils (%)	0.2 ± 0.2	0.2 ± 0.2	0.2 ± 0.2	0.0 ± 0.0	0.0 ± 0.0	0.0 ± 0.0
RDW (%)	13.4 ± 0.5	22.4 ± 1.9*	19.4 ± 1.3*	17.3 ± 2.1	13.7 ± 1.0	14.6 ± 1.2

MCH, mean corpuscular hemoglobin; MCV, mean corpuscular volume; MCHC, mean corpuscular hemoglobin concentration; RDW, red cell distribution width. Results are expressed as mean ± standard error of mean (S.E.M.) of 10 animals/group. *$p < 0.05$ compared to control by ANOVA followed by Student Newman-Keuls test.

et al., 2006).

It is worth mentioning that most antineoplastic agents currently employed induce DNA strand breaks in mammalian cells. The compound 5-fluorouracil, for example, spite of *in vivo* clastogenic potentiality, it is an antimetabolite widely used to treat breast adenocarcinomas and gastrointestinal cancers (Srinivas et al., 2015). Thus, it is reasonably probable that chromosomal damages on human normal/tumor lines or vegetal cells induced by FC (and main compounds) are a reflector mirror-like of its non-selective cytotoxicity.

Hematological data from 30 days-treated animals also revealed that 5 and 10 mg/kg/day i.p. reduced erythrocytes, hematocrit, hemoglobin and lymphocyte levels and increased neutrophils. Previously, we had already demonstrated that Casearin X-treated mice presented lymphocytopenia and neutrophilia after 7 days exposure (Ferreira et al., 2016). On the other hand, Ameni et al. (2015) reported that rats treated daily for 28 or 90 days with *C. sylvestris* hydroethanolic extract did not reveal changes in blood count at doses of 60, 120, and 240 mg/kg/day.

Leukocytosis with neutrophilia often occur during infections, immune-mediated inflammation, tissue necrosis and severe hemolysis. In this context, spleen is the chief responsible for renewal of peripheral blood cells and has capacity to retain and accumulate blood cells, which may increase its volume. However, if engulfment/digestion by spleen macrophages is exceeded, hepatic parenchyma and Kupper cells are also involved in blood restoration (Jagannathan-Bogdan and Zon, 2013). Thus, increase in relative weights of spleens and livers, and presence of Kupffer cell hyperplasia and hemosiderin pigments after FC subacute exposure are likely associated to hematologic renewal. Moreover, such hepatosplenomegaly could be related with hypersplenism, a condition in which coexist anemia, leukopenia and thrombocytopenia, although platelet levels were not altered. Spleens from treated animals at higher doses did not show severe morphological changes, but congestion of red pulp and noticeable vessel dilatation were detected, features pointing to the involution of white pulp and lymph nodes (Jagannathan-Bogdan and Zon, 2013), which corroborates peripheral lymphocytopenia and disorganization of lymphoid follicles.

Hepatic markers changed in both subacute i.p. groups. Live is a key detoxifier organ in the body, since it is habitually under imminent direct or undirect injuries by a variety of pharmaceutical and

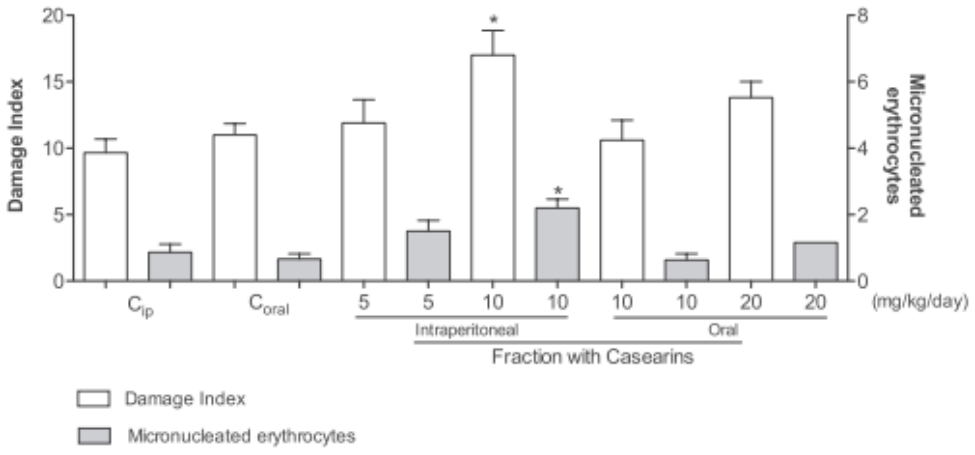

Fig. 8. *In vivo* genotoxicity upon Swiss mice treated for consecutive 30 days with the Fraction with Casearins isolated from *Casearia sylvestris* leaves. Damage index on peripheral blood mononuclear cells was determined by Cometa assay. Micronucleated polychromatic erythrocytes (MNPCE/2000 cells) were quantified in bone marrow cells. Negative control received DMSO 4%. Results are expressed as mean ± standard error of mean (S.E.M.) of 10 animals/group. *$p < 0.05$ compared to control by ANOVA followed by Student Newman-Keuls test.

environmental chemicals. Therefore, hepatotoxicity is the most common toxic manifestation (Cullen and Miller, 2006). Liver synthetizes most serum proteins, including 12 g/day of albumin. Taking into consideration its half-life from 14 to 20 days and renal elimination, albumin levels decline when hepatocellular damage lasts longer than 3 weeks (experimental protocol used here considered 4 weeks exposure). The ability to act as an amino acid reservoir makes also albumin a good indicator of nutritional *status*, as well as its primary function to keep oncotic pressure (Ramaiah, 2007; Aires, 2018). Then, FC 10 mg/kg/day i.p. possibly affected capacity of liver's synthesis and caused hypoalbuminemia.

Such hepatotoxicity was confirmed by 2-fold increase of serum GTP levels in FC 10 mg/kg/day i.p.-treated animals, and helps to reject arguments for anemia induced by hemolysis. Transaminases (GOT and GTP) are widely distributed in the body, being more abundant in hepatocytes due to their fundamental role for protein synthesis, but only GTP is considered more specific for hepatocellular injuries, although it is found in smaller amounts in kidneys, heart and skeletal muscles. On the other hand, GOT is more abundant in heart, skeletal muscles and erythrocytes (Ramaiah, 2007). GOT quantities return to normal more rapidly (some hours) than serum GPT activity (days), that makes GPT more reliable to detect acute or subacute hepatocellular injuries (Cullen and Miller, 2006). In addition, histopathological analyzes revealed presence of cellular swelling and focal necrosis with polymorphonuclear granulocytes (neutrophils, mainly) in livers from two highest established subacute i.p. and oral doses. Despite such biochemical and morphological changes, sometimes associated with disorganization of hepatocyte cords - a clear denoting of cell death followed by tissue regeneration - the maintenance of GOT levels indicate moderate liver damage since its augmentation frequently requires more severe conditions of hepatic damage, such as intense necrosis (Ramaiah, 2007).

Intraperitoneal doses also decreased cholesterol and glucose levels. Studies have reported that acute treatment with methanolic extract (Schoenfelder et al., 2008) and 28-day oral subchronic treatment with hydroalcoholic extract (Werle et al., 2009) from *C. sylvestris* leaves reduced serum triglycerides. Since cholesterol is mainly synthesized in hepatocytes from acetyl-CoA, it is more likely that reduction in serum cholesterol levels is another indication of hepatoxicity caused by FC (Ramaiah, 2007), corroborating albumin reduction, increased GPT and tissue changes (microvesicular steatosis, cell swelling, inflammatory foci and focal necrosis). Although glycemia is directly influenced by insulin levels released from pancreatic β cells, the metabolism of carbohydrates (glycogen mainly) is largely controlled by hepatic metabolism (Aires, 2018). Thus, in occasions of liver injuries, hypoglycemia might result from the inability of residual hepatocytes to generate glucose by glycogenolysis.

Former analysis in 7 days-treated animals under higher doses (up to 25 mg/kg/day) have suggested liver and kidneys as main targets for FC and Casearin X, especially for i.p. treated groups (Araújo et al., 2015; Ferreira et al., 2016). Anyway, if considerable hepatic lesions induced by xenobiotics (such as 5-FU) or after intense hepatocytes' death occur due to acute injury, such injuries are potentially reversible whether connective tissue and extracellular matrix architecture remains intact, being capable of promoting cellular regeneration, including whole hepatic lobes (Ramaiah, 2007).

Important signs of systemic toxicity are observed from the body mass reduction and increase or involution of key organs in experimental groups (Hou et al., 2018). Intraperitoneally treatment, mainly, lead to weight loss. We had already showed that 7 days-treated animals with FC and Casearin X at 25 mg/kg/day i.p. reduced body mass gain of Sarcoma 180-bearing mice (Ferreira et al., 2016). Although reduction of tumor mass associated with minimal weight loss after 2 weeks of treatment (not more than 10%) are indicative of tolerable therapeutic window for anticancer drugs, intense weight reduction is a common side effect for antineoplastic treatments with 5-FU and doxorubicin, since intestinal mucosal cells are also nonspecific targets, which induces nausea, loss of appetite, vomit and diarrhea (Carlotto et al., 2013; Rapoport, 2017). Diarrhea was present in i.p. treated animals since 10th day exposure. Associated with additional discoveries (loss of weight, increase of stomach and qualitative decline in water and food intake), they also implies some toxicity for digestive tract (Ramaiah, 2007). Moreover, terpenes are liposoluble small molecules that are habitually rapidly absorbed by enterocytes, and may provoke food intake reduction due to antinutritional events (Gemede and Ratta, 2014).

Heart was the exclusive organ which presented involution, but cardiotoxicity was not confirmed by the histological and biochemical investigations. Ultrastructural cardiac changes typically caused by antineoplastic agents, including inflammatory reaction, necrosis, interstitial fibrosis, loss of myofibrils, mitochondrial edema and vacuolization were not observed (Sara et al., 2018).

If we take into consideration that most antineoplasic drugs clinically available cause myelosuppression, hepatotoxicity, diarrhea, and alopecia, besides cardiotoxicity (myocardial ischemia, ventricular arrhythmias, and sudden death), opportunistic infections, peripheral neuropatia, nausea, vomiting, anorexia, fatigue and tiredness (Carlotto et al., 2013; Ferreira and Pessoa, 2017; Rapoport, 2017; Nurgali et al., 2018; Sara et al., 2018), we believe that preclinical anticancer properties of FC are not threatened by toxicological effects.

It is also interesting mentioning that FC has neurobiological effects, including reduction of spontaneous and exploratory locomotor activity by a GABAergic system independent way, alters levels of free radicals and nervous tissue morphology (hippocampus and striatum), and Casearin X may interact with central dopamine D1 receptors (Araújo et al., 2015, 2017), indicating that chemotherapeutics based on *C. sylvestris* might induce central side effects.

Despite of qualitative and quantitative differences between species in the functional regulation of absorption, distribution, metabolism, excretion and toxicity (ADMET) processes difficult extrapolation of preclinical experimental results to humans (Olson et al., 2000; Williams et al., 2002), we were successful to show that the use of different biological models is an early cost-effective way to 'capture' the complexity of individual (cellular) and systemic (animal) toxicity induced by promising anticancer substances, especially if we highlight that liver injury is the most common cause of drug withdrawal from the market because most of hepatic damages are poorly understood. Here, this hepatic injury was well defined and confirmed that mammals continues being an excellent tool to predict systemic toxicity, though methods using metazoan cellular models are reliable to detect early signs of cytotoxicity, genotoxicity, clastogenicity and embryotoxicity.

5. Conclusions

A fraction with casearins from *C. sylvestris* leaves revealed cytotoxicity on normal human, mouse and hamster cells, teratogenicity upon zebrafish embryos, larval toxicity on *A. salina* nauplii, antiproliferative and clastogenic action on meristematic *A. cepa* cells, caused cell death suggestive of apoptosis in leukocytes. Its main component - Casearin X - induced DNA damages on *ex vivo* and *in vivo* leukocytes. FC was considered acutely toxic if orally or intraperitoneally inoculated. Additionally, i.p. 30 days-treated animals showed myelosuppression, loss of weight, macroscopic changes in key organs, and biochemical and morphological alterations indicating liver as main target for FC-induced systemic toxicity. This fraction certainly concentrates bioactive compounds during chemical preparation steps, which explain, at least in part, higher toxicity of FC when compared to ethanolic extracts from *C. sylvestris* previously described.

Conflicts of interest

The authors declare there are no conflicts of interest.

Author's contributions

PMPF coordinated the research, managed scientific and funding supports, wrote and revised the manuscript. PMPF and DBS performed *in vivo* acute and subacute studies with mice, including histological, genotoxic and hematological techniques; JNS, AFG and CLSR carried out investigations about genotoxic and clastogenic action on meristematic cells from *Allium cepa* roots and toxicity on *Artemia salina* nauplii; PCS, RSCA, DSM, RO and CKG performed, acquired and analyzed all data about embryotoxicity on *Danio rerio*; AJC extracted plant material and isolated the compound Casearin X. AACMC analyzed results from genotoxic tests. JROF and MOMF determined biochemical changes by flow cytometry. CP managed funding supports.

Acknowledgments

We thank to the Brazilian agencies "Fundação de Amparo à Pesquisa do Estado do Piauí" [FAPEPI (Public Call 004/2011, grant number 034/2012) and "Conselho Nacional de Desenvolvimento Científico e Tecnológico" [CNPq (#484286/2011-0)] for financial support. Dr. Paulo Michel Pinheiro Ferreira is also grateful to the CNPq (#305086/2016-2) for the personal scholarship.

References

Organisation for Economic Co-operation and Development (OECD), 2001. Test No. 423: acute oral toxicity – acute toxic class method. https://www.oecd-ilibrary.org/environment/test-no-423-acute-oral-toxicity-acute-toxic-class-method_9789264071001-en, Accessed date: 15 January 2017.

Aires, M.M., 2018. Physiology, five ed. Guanabara Koogan, Rio de Janeiro.

Albertini, R.J., Anderson, D., Douglas, G.R., Hagmar, L., Hemminki, K., Merlo, F., Natarajan, A.T., Norppa, H., Shuker, D.E., Tice, R., Waters, M.D., Aitio, A., 2000. IPCS guidelines for the monitoring of genotoxic effects of carcinogens in humans. Mutat. Res. 463, 111–172. https://doi.org/10.1016/S1383-5742(00)00049-1.

Ameni, A.Z., Latorre, O.A., Torres, L.M., Górniak, S.L., 2015. Toxicity study about a medicinal plant *Casearia sylvestris*: a contribution to the Brazilian Unified Health System (SUS). J. Ethnophrmacol. 175, 9–13. https://dx.doi.org/10.1016/j.jep.2015.08.027.

Andrade, T.S., Oliveira, R., Silva, M.L., Von Zuben, M.V., Grisolia, C.K., Domingues, I., Caldas, E.D., Pic-Taylor, A., 2018. Exposure to ayahuasca induces developmental and behavioral alterations on early life stages of zebrafish. Chem. Biol. Interact. 293, 133–140. https://doi.org/10.1016/j.cbi.2018.08.001.

Agência Nacional de Vigilância Sanitária (ANVISA), 2013. Guia para condução de estudos não clínicos de toxicologia e segurança farmacológica necessários ao desenvolvimento de medicamentos. 2ª versão. ANVISA, Brasília.

Araújo, E.J.F., Oliveira, G.A.L., Sousa, L.Q., Bolzani, V.D., Cavalheiro, A.J., Tome, A.R., Peron, A.P., Santos, A.G., Citó, A.M.G.L., Pessoa, C., Freitas, R.M., Ferreira, P.M.P., 2015. Counteracting effects on free radicals and histological alterations induced by a fraction with casearins. An. Acad. Bras. Cienc. 87, 1791–1807. https://doi.org/10.1590/0001-3765201520150149.

Araújo, E.J.F., Almeida, A.A.C., Silva, O.A., Costa, I.H.F., Rezende-Júnior, L.M., Lima, F.C.A., Cavalheiro, A.J., Pessoa, C., Moraes, M.O., Ferreira, P.M.P., 2017. Behavioral effects induced by antitumor clerodane diterpenes from *Casearia sylvestris* and *in silico* interactions with neuron receptors. J. Ethnopharmacol. 198, 460–467. https://doi.org/10.1016/j.jep.2017.01.006.

Arrowsmith, J., Miller, P., 2013. Trial watch: phase II and phase III attrition rates 2011 - 2012. Nat. Rev. Drug Discov. 12, 569. https://doi.org/10.1038/nrd4090.

Bagatini, M.D., Silva, A.C.F., Tedesco, S.B., 2007. The use of Allium cepa test as a bioindicator of genotoxicity of medicinal plants infusions. Braz. J. Pharmacogn. 17, 444–447. http://doi.org/10.1590/S0102-695X2007000300019.

Basile, A.C., Sertié, J.A.A., Panizza, S., Oshiro, T.T., Azzolini, C.A., 1990. Pharmacological assay of *Casearia sylvestris*. I: preventive anti-ulcer activity and toxicity of the leaf crude extract. J. Ethnopharmacol. 30, 185–197. https://doi.org/10.1016/0378-8741(90)90007-G.

Bou, D.D., Lago, J.H., Figueiredo, C.R., Matsuo, A.L., Guadagnin, R.C., Soares, M., Sartorelli, P., 2013. Chemical composition and cytotoxicity evaluation of essential oil from leaves of *Casearia sylvestris*, its main compound α-zingiberene and derivatives. Molecules 8 (8), 9477–9487. https://doi.org/10.3390/molecules18089477.

Brant, N.M.F., Gasparotto, F.M., Araújo, V.A., Maraschin, J.C., Ribeiro, R.C.L., Lourenço, E.L.B., Junior, E.L.C., Junior, A.G., 2014. Cardiovascular protective effects of *Casearia sylvestris* Swartz in Swiss and C57BL/6 LDLr-null mice undergoing high fat diet. J. Ethnopharmacol. 154, 419–427. https://doi.org/10.1016/j.jep.2014.04.019.

Brasil, 2006. Ministério da Saúde Secretaria de Ciência, Tecnologia e Insumos Estratégicos. Departamento de Assistência Farmacêutica. Política Nacional de Plantas Medicinais e Fitoterápicos. Moderna, Brasília.

Brasil, 2009. Ministério da Saúde. RENISUS: Relação Nacional de Plantas Medicinais de Interesse ao SUS. Espécies vegetais. http://bvsms.saude.gov.br/bvs/sus/pdf/marco/ms_relacao_plantas_medicinais_sus_0603.pdf, Accessed date: 15 February 2018.

Carlotto, A., Hogsett, V.L., Maiorini, E.M., Razulism, J.G., Sonis, S.T., 2013. The economic burden of toxicities associated with cancer treatment: review of the literature and analysis of nausea and vomiting, diarrhoea, oral mucositis and fatigue. Pharmacoeconomics 31, 753–766. https://doi.org/10.1007/s40273-013-0081-2.

Cullen, J.M., Miller, R.T., 2006. The role of pathology in the identification of drug-induced hepatic toxicity. Expert Opin. Drug Metabol. Toxicol. 2, 241–247. https://doi.org/10.1517/17425255.2.2.241.

Cury-Boaventura, M.F., Pompéia, C., Curi, R., 2003. Comparative toxicity of oleic acid and linoleic acid on Jurkat cells. Clin. Nutr. 23, 721–732. https://doi.org/10.1016/j.clnu.2003.12.004.

Da Silva, S.L., Calgarotto, A.K., Chaar, J.S., Ma-Rangoni, S., 2008a. Isolation and characterization of ellagic acid derivatives isolated from *Casearia sylvestris* Sw. aqueous extract with anti-PLA_2 activity. Toxicon 52, 655–666. https://doi.org/10.1016/j.toxicon.2008.07.011.

Da Silva, S.L., Chaar, J.S., Figueiredo, P.M.S., Yano, T., 2008b. Cytotoxic evaluation of essential oil from *Casearia sylvestris* Sw on human cancer cells and erythrocytes. Acta Amazonica 38, 107–112. https://doi.org/10.1590/S0044-59672008000100012.

Da Silva, S.L., Chaar, J.S., Yano, T., 2009. Chemotherapeutic potential of two gallic acid derivative compounds from leaves of *Casearia sylvestris* Sw (Facourtiaceae). Eur. J. Pharmacol. 608, 76–83. https://doi.org/10.1016/j.ejphar.2009.02.004.

Damian, A.G., Tesser, C.D., Moretti-Pires, R.O., 2014. Phytotherapy in primary health care. Rev. Saude Publica 48, 541–553. https://doi.org/10.1590/S0102-311X2007000600021.

Darzynkiewicz, Z., Bruno, S., Del Bino, G., Gorczyca, W., Hotz, M.A., Lassota, P., Traganos, F., 1992. Features of apoptotic cells measured by flow cytometry. Cytometry 13, 795–808. https://doi.org/10.1002/cyto.990130802.

David, J.P., Silva, E.F., Moura, D.L., Guedes, M.L.S., Assunção, R.J., David, J.M., 2001. Lignans and triterpenes from cytotoxic extract of *Eriope blanchetii*. Quim. Nova 24, 730–733. https://dx.doi.org/10.1590/S0100-40422001000600004.

Espinosa, J., Medeiros, L.F., Souza, A., Göntzel, A.R.C., Röcker, B., Casali, E.A., Ethur, E.M., Wink, M.R., Torres, I.L.S., 2015. Ethanolic extract of *Casearia sylvestris* Sw exhibits *in vitro* antioxidant and antimicrobial activities and *in vivo* hypolipidemic effect in rats. Rev. Bras. Plantas Med. 17, 305–315. https://doi.org/10.1590/1983-084X/13_074.

Esteves, I., Souza, I.R., Rodrigues, M., Cardoso, L.G., Santos, L.S., Sertie, J.A., Perazzo, F.F., Lima, L.M., Schneedorf, J.M., Bastos, J.K., Carvalho, J.C., 2005. Gastric anti-ulcer and anti-inflammatory activities of the essential oil from *Casearia sylvestris* Sw. J. Ethnorpharmacol. 101, 191–196. https://doi.org/10.1016/j.jep.2005.04.020.

Felipe, K.B., Kviecinski, M.R., Da Silva, F.O., Bücker, N.F., Farias, M.S., Castro, L.S., Souza, G.V.M., Motta, N.S., Correia, J.F., Rossi, M.H., Pedrosa, R.C., 2014. Inhibition of tumor proliferation associated with cell cycle arrest caused by extract and fraction from *Casearia sylvestris* (Salicaceae). J. Ethnopharmacol. 155, 1492–1499. https://doi.org/10.1016/j.jep.2014.07.040.

Fenech, M., 2007. Cytokinesis-block micronucleus cytome assay. Nat. Protoc. 2, 1084–1104. https://doi.org/10.1038/nprot.2007.77.

Ferreira, P.M.P., Pessoa, C., 2017. Molecular biology of human epidermal receptors, signaling pathways and targeted therapy against cancers: new evidences and old challenges. Braz. J. Pharm. Sci. 53, 1–17. https://doi.org/10.1590/s2175-97902017000216076.

Ferreira, P.M.P., Santos, A.G., Tininis, A.G., Costa, P.M., Cavalheiro, A.J., Bolzani, V.S., Moraes, M.O., Costa-Lotufo, L.V., Montenegro, R.C., Pessoa, C., 2010. Casearin X exhibits cytotoxic effects in leukemia cells triggered by apoptosis. Chem. Biol. Interact. 188, 497–504. https://doi.org/10.1016/j.cbi.2010.08.008.

Ferreira, P.M.P., Militão, G.C.G., Lima, D.J.B., Costa, N.D.J., Machado, K.C., Santos, A.G., Cavalheiro, A.J., Bolzani, V.S., Silva, D.H.S., Pessoa, C., 2014. Morphological and biochemical alterations activated by antitumor clerodane diterpenes. Chem. Biol. Interact. 222, 112–125. https://doi.org/10.1016/j.cbi.2014.10.015.

Ferreira, P.M.P., Bezerra, D.P., Silva, J.N., Costa, M.P., Ferreira, J.R.O., Alencar, N.M.N., Figueiredo, I.S.T., Cavalheiro, A.J., Machado, C.M.L., Chammas, R., Alves, A.P.N.N., Moraes, M.O., Pessoa, C., 2016. Preclinical anticancer effectiveness of a fraction from *Casearia sylvestris* and its component Casearin X: *in vivo* and *ex vivo* methods and microscopy examinations. J. Ethnopharmacol. 186, 270–279. https://doi.org/10.1016/j.jep.2016.04.011.

Ferreira-Silva, G.A., Lages, C.C.L., Sartorelli, P., Hasegawa, F.R., Soares, M.G., Ionta, M., 2017. Casearin D inhibits ERK phosphorylation and induces downregulation of cyclin D1 in HepG2 cells. Toxicol. Vitro 38, 27–32. https://doi.org/10.1016/j.tiv.2016.10.011.

Finney, J.L., Robertson, G.N., McGee, C.A., Smith, F.M., Croll, R.P., 2006. Structureand autonomic innervation of the swim bladder in the zebrafish (*Danio rerio*). J. Comp. Neurol. 495, 587–606. https://doi.org/10.1002/cne.20948.

Fiskesjö, G., 1985. The *Allium* test as a standard in environmental monitoring. Hereditas 102, 99–112. https://doi.org/10.1111/j.1601-5223.1985.tb00471.x.

Gemede, H.F., Ratta, N., 2014. Antinutritional factors in plant foods: potential health benefits and adverse effects. Int. J. Nutr. Food Sci. 3, 284–289. https://doi.org/10.11648/j.ijnfs.20140304.18.

Hamidi, M.R., Jovanov, B., Panovska, T.K., 2014. Toxicological evaluation of the plant products using Brine Shrimp (*Artemia salina* L.) model. Macedonian Pharm. Bull. 60, 9–18.

Hamilton, M.A., Russo, R.C., Thurston, R.V., 1977. Trimmed Spearman-Karber method for estimating median lethal concentrations in toxicity bioassays. Environ. Sci. Technol. 12, 714–719. https://doi.org/10.1021/es60130a004.

Hartmann, A., Agurell, E., Beevers, C., Brendler-Schwaad, S., Burlinson, B., Clay, P., Collins, A.R., Smith, A., Speit, G., Thybaud, V., Tice, R.R., 2003. Recommendations for conducting the *in vivo* alkaline comet assay. Mutagenesis 18 45-5. https://doi.org/10.1093/mutage/18.1.45.

Harvey, A.L., 2014. Toxins and drug discovery. Toxicon 92, 193–200. https://doi.org/10.

1016/j.toxicon.2014.10.020.
Hay, M., Thomas, D.W., Craighead, J.L., Economides, C., Rosenthal, J., 2014. Clinical development success rates for investigational drugs. Nat. Biotechnol. 32, 40–51. https://doi.org/10.1038/nbt.2786.
Heddle, J.A.A., 1973. A rapid *in vitro* test for chromosome damage. Mutat. Res. 18, 187–190. https://doi.org/10.1016/0027-5107(73)90035-3.
Hou, L., Fan, C., Liu, C., Qu, Q., Wang, C., Shi, Y., 2018. Evaluation of repeated exposure systemic toxicity test of PVC with new plasticizer on rats via dual parenteral routes. Regenerative Biomaterials 5, 9–14. https://doi.org/10.1093/rb/rbx020.
Jagannathan-Bogdan, M., Zon, L.I., 2013. Hematopoiesis. Development 140 (12), 2463–2467. https://doi.org/10.1242/dev.083147.
Karalliedde, L.D., Edwards, P., Marris, T.C., 2003. Variables influencing the toxic response to organophosphates in humans. Food Chem. Toxicol. 41, 1–13. https://doi.org/10.1016/S0278-6915(02)00232-6.
Kaye, J.A., Melo, J.A., Cheung, S.K., Vaze, M.B., Haber, J.E., Toczyski, D.P., 2004. DNA breaks promote genomic instability by impeding proper chromosome segregation. Curr. Biol. 14, 2096–2106. https://doi.org/10.1016/j.cub.2004.10.051.
Kimmel, C.B., Ballard, W.W., Kimmel, S.R., Ullmann, B., Schilling, T.F., 1995. Stages of embryonic development of the zebrafish. Dev. Dynam. 203, 253–310. https://doi.org/10.1002/aja.1002030302.
Krysko, D.V., Berghe, T.V., D'Herde, K., Vandenabeel, P., 2008. Apoptosis and necrosis: detection, discrimination and phagocytosis. Methods 44, 205–221. https://doi.org/10.1016/j.ymeth.2007.12.001.
Lucio, E.M.R.A., Rosalen, P.L., Sharapin, N., Souza Brito, A.R.M., 2000. Avaliação toxicológica aguda e *screening* hipocrático da epiisopilosina, alcaloide secundário de *Pilocarpus microphyllus* Stapf. Rev. Bras. Farmacogn. 9/10, 23–25. https://doi.org/10.1590/S0102-695X2000000100003.
Machado, K.C., Sousa, L.Q., Lima, D.J.B., Soares, B.M., Cavalcanti, B.C., Maranhao, S.S., Noronha, J.C., Rodrigues, D.J., Militão, G.C.G., Chaves, M.H., Vieira-Júnior, G.M., Pessoa, C., Moraes, M.O., Sousa, J.M.C., Cavalcante, A.A.C.M., Ferreira, P.M.P., 2018. Marinobufagin, a molecule from poisonous frogs, causes biochemical, morphological and cell cycle changes in human neoplasms and vegetal cells. Toxicol. Lett. 285, 121–131. https://doi.org/10.1016/j.toxlet.2017.12.018.
Mattioli, F., Martelli, A., Gosmara, M., Garbero, C., Manfredi, V., Varaldo, E., Torre, G.C., Brambilla, G., 2006. DNA fragmentation and DNA repair synthesis induced in rat and human thyroid cells by chemicals carcinogenic to the rat thyroid. Mutat. Res. 609, 146–153. https://doi.org/10.1016/j.taap.2004.07.009.
Melo, R.C., Geronco, M.S., Sousa, R.W.R., Ramos, L.P.S., Araujo, F.P., Ribeiro, A.B., Ferreira, P.M.P., Osajima, J.A., Costa, M.P., 2018. Biopolymer from *Adenanthera pavonina* L. seeds: characterization, photostability, antioxidant activity, and biotoxicity evaluation. Int. J. Polym. Sci. 2018, 1–7. https://doi.org/10.1155/2018/1385830.
Meyer, B.N., Ferrigni, N.R., Putnam, J.E., Jacobsen, L.B., Nichols, D.E., McLaughlin, J.L., 1982. Brine shrimp: a convenient general bioassay for active plant constituents. Planta Med. 45, 31–34. https://doi.org/10.1055/s-2007-971236.
Misik, M., Pichler, C., Rainer, B., Filipic, M., Nersesyan, A., Knasmueller, S., 2014. Acute toxic and genotoxic activities of widely used cytostatic drugs in higher plants: possible impact on the environment. Environ. Res. 135, 196–203. https://doi.org/10.1016/j.envres.2014.09.012.
Newman, D.J., Cragg, G.M., 2016. Natural products as sources of new drugs from 1981 to 2014. J. Nat. Prod. 79, 629–661. https://dx.doi.org/10.1021/acs.jnatprod.5b01055.
Nurgali, K., Jagoe, R.T., Abalo, R., 2018. Editorial: adverse effects of cancer chemotherapy: anything new to improve tolerance and reduce sequelae? Front. Pharmacol. 9, 245–247. https://dx.doi.org/10.3389/fphar.2018.00245.
Organization for Economic Co-Operation and Development (OECD), 2013. Test No. 236: Fish Embryo Acute Toxicity (FET) Test. https://www.oecd-ilibrary.org/environment/test-no-236-fish-embryo-acute-toxicity-fet test_9789264203709-en, Accessed date: 10 December 2017.
Oliveira, A.M., dos Santos, A.G., Santos, R.A., Csipak, A.R., Olivato, C., Silva, I.C., Freitas, M.B., Bassi, C.L., Cavalheiro, A.J., Bolzani, V.S., Silva, D.H., Sakamoto-Hojo, E.T., Takahashi, C.S., Soares, C.P., 2009. Ethanolic extract of *Casearia sylvestris* and its clerodane diterpen (caseargrewiin F) protect against DNA damage at low concentrations and cause DNA damage at high concentrations in mice's blood cells. Mutagenesis 24, 501–506. https://doi.org/10.1093/mutage/gep034.
Olson, H., Betton, G., Robinson, D., Thomas, K., Monro, A., Kolaja, G., Lilly, P., Sanders, J., Sipes, G., Bracken, W., Dorato, M., Van Deun, K., Smith, P., Berger, B., Heller, A., 2000. Concordance of the toxicity of pharmaceuticals in humans and in animals. Regul. Toxicol. Pharmacol. 32, 56–67. https://doi.org/10.1006/rtph.2000.1399.
Pereira, F.G., Marquete, R., Domingos, L.T., Rocha, M.E.N., Ferreira-Pereira, A., Mansur, E., Moreira, D.L., 2017. Antifungal activities of the essential oil and its fractions rich in sesquiterpenes from leaves of *Casearia sylvestris* Sw. An. Acad. Bras. Cienc. 89, 2817–2824. https://doi.org/10.1590/0001-3765201720170339.
Piovezan, A.P., Batisti, A.P., Benevides, M.L.A.C.S., Turnes, B.L., Martins, D.F., Kanis, L., Duarte, E.C.W., Cavalheiro, A.J., Bueno, P.C.P., Seed, M.P., Norling, L.V., Cooper, D., Headland, S., Souza, P.R.P.S., Perretti, M., 2017. Hydroalcoholic crude extract of *Casearia sylvestris* Sw. reduces chronic post-ischemic pain by activation of pro-resolving pathways. J. Ethnopharmacol. 204, 179–188. https://doi.org/10.1016/j.jep.2017.03.059.
Pu, X., Wang, Z., Klaunig, J.E., 2015. Alkaline comet assay for assessing DNA damage in individual cells. Curr. Protoc. Toxicol. 65, 1–11. https://doi.org/10.1002/0471140856.tx0312s65.
Raghunath, A., Perumal, E., 2018. Analysis of lethality and malformations during zebrafish (*Danio rerio*) development. Methods Mol. Biol. 1797, 337–363. https://doi.org/10.1007/978-1-4939-7883-0_18.
Ramaiah, S.K., 2007. A toxicologist guide to the diagnostic interpretation of hepatic biochemical parameters. Food Chem. Toxicol. 45, 1551–1557. https://doi.org/10.1016/j.fct.2007.06.007.
Rapoport, B.L., 2017. Delayed chemotherapy-induced nausea and vomiting: pathogenesis, incidence, and current management. Front. Pharmacol. 8, 1–10. https://dx.doi.org/10.3389/fphar.2017.00019.
Rivero-Wendt, C.L., Oliveira, R., Monteiro, M.S., Domingues, I., Soares, A.M., Grisolia, C.K., 2016. Steroid androgen 17α-methyltestosterone induces malformations and biochemical alterations in zebrafish embryos. Environ. Toxicol. Pharmacol. 44, 107–113. https://doi.org/10.1016/j.etap.2016.04.014.
Sales, I.M.S., Barbosa, J.S., Santos, F.K.S., Silva, F.C.C., Ferreira, P.M.P., Sousa, J.M.C., Peron, A.P., 2017. Acute toxicity of grape, plum and orange synthetic food flavourings evaluated in *in vivo* test systems. Food Technol. Biotechnol. 55, 131–137. https://doi.org/10.17113/ftb.55.01.17.4770.
Santos, A.G., Ferreira, P.M.P., Vieira-Júnior, G.M., Perez, C.C., Tininis, A.G., Silva, G.H., Bolzani, V.S., Costa-Lotufo, L.V., Pessoa, C., Cavalheiro, A.J., 2010. Casearin X, its degradation product and other clerodanediterpenes from leaves of *Casearia sylvestris*: evaluation of cytotoxicity against normal and tumour human cells. Chem. Biodivers. 7, 205–215. https://doi.org/10.1002/cbdv.200800342.
Sara, J.D., Kaur, J., Khodadadi, R., Rehman, M., Lobo, R., Chakrabarti, S., Herrmann, J., Lerman, A., Grothey, A., 2018. 5-fluorouracil and cardiotoxicity: a review. Therapeutic advances in medical oncology. Ther. Adv. Med. Oncol. 10, 1–18. https://doi.org/10.1177/1758835918780140.
Schmid, W., 1975. The micronucleus test. Mutat. Res. 31, 9–15. https://doi.org/10.1016/0165-1161(75)90058-8.
Schoenfelder, T., Pich, C.T., Geremias, R., Ávila, S., Daminelli, E.M., Pedrosa, R.C., Bettiol, J., 2008. Antihyperlipidemic effect of *Casearia sylvestris* methanolic extract. Fitoterapia 79, 465–467. https://doi.org/10.1016/j.fitote.2008.03.008.
Singh, N.P., McCoy, M.T., Tice, R.R., Schneider, E.L., 1988. A simple technique for quantitation of low levels of DNA damage in individual cells. Exp. Cell Res. 175, 184–191. https://doi.org/10.1016/0014-4827(88)90265-0.
Spósito, L., Oda, F.B., Vieira, J.H., Carvalho, F.A., Ramos, M.A.S., Castro, R.C., Crevelin, E.J., Crotti, A.E.M., Santos, A.G., Silva, P.B., Chorilli, M., Bauab, T.M., 2019. *In vitro* and *in vivo* anti-*Helicobacter pylori* activity of *Casearia sylvestris* leaf derivatives. J. Ethnopharmacol. 233, 1–12. https://doi.org/10.1016/j.jep.2018.12.032.
Srinivas, U.S., Dyczkowski, J., Beißbarth, T., Gaedcke, J., Mansour, W.Y., Borgmann, K., Dobbelstein, M., 2015. 5-Fluorouracil sensitizes colorectal tumor cells towards double stranded DNA breaks by interfering with homologous recombination repair. Oncotarget 6, 12574–12586. https://doi.org/10.18632/oncotarget.3728.
United Nations (UN), 2017. A Guide to the Globally Harmonized System of Classification and Labeling of Chemicals (GHS). https://www.osha.gov/dsg/hazcom/ghsguideoct05.pdf, Accessed date: 20 November 2017.
Werle, A.L.B., Zanetti, G.D., Ceron, C.S., Manfroni, M.P., 2009. Evaluation of the activity of *Casearia sylvestris* Swartz (Flacourtiaceae) on rats serum triglyceride. Rev Bras Farmacogn 19, 400–402. https://doi.org/10.1590/S0102.
Williams, D.P., Kitteringham, N.R., Naisbitt, D.J., Pirmohamed, M., Smith, D.A., Park, B.K., 2002. Are chemically reactive metabolites responsible for adverse reactions to drugs? Curr. Drug Metabol. 3, 351–366. https://doi.org/10.2174/1389200023337423.
Winata, C.L., Korzh, S., Kondrychyn, I., Zheng, W., Korzh, V., Gong, Z., 2009. Development of zebrafish swim bladder: the requirements of hedgehog signaling in specification and organization of the three tissue layers. Dev. Biol. 331, 222–236. https://doi.org/10.1016/j.ydbio.2009.04.035.
Yue, M.S., Peterson, R.E., Heideman, W., 2015. Dioxin Inhibition of swim bladder development in zebrafish: is it secondary to heart failure? Aquat. Toxicol. 162, 10–17. https://doi.org/10.1016/j.aquatox.2015.02.016.
Zeddies, D.G., Fay, R.R., 2005. Development of the acoustically evoked behavioral response in zebrafish to pure tones. J. Exp. Biol. 208, 1363–1372. https://doi.org/10.1242/jeb.01534.

Acta Limnologica Brasiliensia

Publication of the Brazilian Association of Limnology

Original Article
Acta Limnologica Brasiliensia, 2019, vol. 31, e12
https://doi.org/10.1590/S2179-975X8118
ISSN 2179-975X on-line version

Evaluation of the embryotoxicity in zebrafish (*Danio rerio*) of the flocculant and coagulant compounds used for water remediation

Avaliação da embriotoxicidade em zebrafish (*Danio rerio*) de compostos floculantes e coagulantes usados em remediação da água

Diego Sousa Moura[1], Rafael Oliveira Duarte da Mota[2], José Francisco Gonçalves Júnior[2]*, Newton Flávio de Vasconcelos[3], Marco Aurélio Reis[3], Cesar Koppe Grisolia[1]

[1]Departamento de Genética e Morfologia, Instituto de Ciências Biológicas, Universidade de Brasília – UnB, Asa Norte, Campus Universitário Darcy Ribeiro, CEP 70910-900, Brasília, DF, Brasil

[2]Departamento de Ecologia, Instituto de Ciências Biológicas, Universidade de Brasília – UnB, Asa Norte, Campus Universitário Darcy Ribeiro, CEP 70910-900, Brasília, DF, Brasil

[3]WaterFlows Bioquimica do Brasil Company, Av. Pedro Botesi, 2636, Jardim Flamboyant, Mogi Mirim, SP, Brasil

*e-mail: jfjunior@unb.br

Cite as: Moura, D.S. et al. Evaluation of the embryotoxicity in zebrafish (*Danio rerio*) of the flocculant and coagulant compounds used for water remediation. *Acta Limnologica Brasiliensia*, 2019, vol. 31, e12.

Abstract: Aim: Leaching from mining activities reaches water bodies, causing water contamination and acidification by toxic metals. As a consequence, oxygen depletion occurs, with the disappearance of certain benthic organisms, losses in phytoplankton and zooplankton biomass, and fish mortality. Remediation of contaminated water from mining involves the use of flocculants based on acrylamide monomers and polyacrylamide and of coagulants based on aluminum. Our aim was to assess the aquatic toxicity of the flocculant WF 424 and the coagulant WF 2000 PCA. **Methods:** A flocculant anionic polymer (WF 424) and a coagulant polynuclear complex of polymerized hydro-aluminum ions (WF2000 PCA) were tested for embryotoxicity to zebrafish (*Danio rerio*, FET test - OEDC, 236, 2013). **Results:** After 96 h of exposure to WF424, there was no significant lethality, nor were there sublethal effects such as hatching delay, heartbeat alteration, and malformation in embryonic development, when compared with the control group ($p > 0.05$). The coagulant compound WF2000 PCA did not show lethal effects during 96 h of exposure, and EC50 was considered as above the highest concentration-level tested. **Conclusions:** For both compounds, no malformation, embryonic development delay or embryotoxicity were observed.

Keywords: mining tailing; contamination; wastewater; toxicity.

Resumo: Objetivo: O carreamento decorrente das atividades de mineração atinge corpos d'água, causando contaminação da água e acidificação por metais tóxicos. Como conseqüência, a depleção de oxigênio ocorre, com o desaparecimento de certos organismos bênticos, perdas na biomassa do fitoplâncton e do zooplâncton, e mortalidade de peixes. Remediação da água contaminada da mineração envolve o uso de floculantes baseados em monômeros de acrilamida e poliacrilamida e de coagulantes à base de alumínio. Nosso objetivo foi avaliar a toxicidade aquática do floculante WF 424 e do coagulante WF 2000 PCA. **Métodos:** Um polímero aniónico floculante (WF 424) e um complexo polinuclear coagulante de íons hidro-alumínio polimerizados (WF2000 PCA) foram testados quanto à embriotoxicidade para o peixe-zebra (Danio rerio, teste FET - OEDC, 236, 2013).

Resultados: Após 96 h de exposição ao WF424, não houve letalidade significativa, nem efeitos subletais como atraso na eclosão, alteração do batimento cardíaco e malformação no desenvolvimento embrionário, quando comparados com o grupo controle (p> 0,05). O composto coagulante WF2000 PCA não apresentou efeitos letais durante 96 h de exposição, e EC50 foi considerado acima do nível de concentração mais alto testado. **Conclusões:** Para ambos os compostos, nenhuma malformação, atraso no desenvolvimento embrionário ou embriotoxicidade foram observados.

Palavras-chaves: mineração de rejeito; contaminação; águas residuárias; toxicidade.

1. Introduction

Anthropogenic impacts on aquatic ecosystems are a current theme of significant importance due to the use of water resources for industrial, agricultural and urban processes (Dudgeon et al., 2006). This can lead to a reduction in water quality (Allan & Castillo, 2007; Hepp & Gonçalves Junior, 2015; Callisto et al., 2016), which affects fauna in their diversity and functionality by altering the key attributes of ecosystem integrity (Albuquerque et al., 2010; Honda & Durigan, 2017; Dias, 2017).

The extraction and beneficiation of metals have produced different type of waste, causing serious risks to the aquatic environment. Leaching from mining processes reaches water bodies, causing water contamination and acidification by toxic metals (Wright & Welbourn, 2002). Oxygen depletion and the disappearance of certain benthic organisms, decreases in phytoplankton and zooplankton biomass and changes in fish communities are indicators of water degradation caused by mining tailing. Remediation of wastewater from mining involves actions controlling the toxic load, significantly reducing contaminated sediments and allowing the restoration of aquatic biota (Wright & Welbourn, 2002).

Flocculants based on acrylamide monomers and polyacrylamide are indicated for use in water remediation contaminated by mining tailings. They are used to promote the clumping of particles in surface water, so that this clump floats to the top. Coagulants based on aluminum are used to precipitate impurities in the water in a cleaning process. Both compounds are commonly used in the cleaning of drinking water, in sewage treatments and in the remediation of accidents caused by mining tailings or dam failure (Susaya et al., 2010; Wang et al., 2015). On the other hand, coagulation/flocculation treatment processes have showed an increased toxicity of treated waters (Wang et al., 2015).

WF424 is a flocculant anionic polymer, obtained from the copolymerization of acrylamide with acrylic acid or by hydrolysis reactions of polyacrylamide. Through a hydrolysis process, the amide group is replaced by a carboxylic group. In this way, the molecule acquires negative charge in a neutral or alkaline medium. The electrostatic repulsion between the ionized groups results in the stretching of the molecule. As a synthetic process, this macromolecule can be easily obtained as hydrolyzed monomers. Also, the hydrolysis and ionization processes to acquire the compound with desirable characteristics for the intended purpose are totally under control (AWWA, 2015, B453-13 Polyacrylamide).

WF2000 PCA ($Al_n(OH)_m Cl_{3n-m}$) is a polynuclear complex of polymerized hydro-aluminum ions, with high solubility in water. Its hydrolysis provides the neutralization of electric charges in the medium and consequently promotes a more effective coagulation process when compared to the coagulants derived from monomeric salts. WF2000 PCA promotes the formation of clots by destabilizing colloidal systems in water, allowing sedimentation and consequently water clarification. The main advantages of its use in the treatment of water and effluents are related to better control of the pH of the medium, greater removal of organic and inorganic contaminants, reduction of sources of sulfate added to the treatment process and, especially, low levels of residual aluminum in the treated water, 0.01 - 0.05 mg/L (ABNT, 2016).

The study protocol for acute embryo-toxicity test (OECD, 2013), based on fertilized eggs of zebrafish (*Danio rerio*), has showed high sensitivity in the evaluation of chemical toxicity. For this reason, it was adopted by the European Union (EU 2010/63), as one of the main bioassays for the toxicological evaluation of chemical compounds for registration (REACH - *Registration, Evaluation, Authorization and Restriction of Chemicals*). There are few studies in the scientific literature showing the risks to the aquatic environment of such compounds used with the purpose of remediating water contaminated by mining tailings (Lammer et al., 2009; OECD, 2013). In this study, the zebrafish embryos were used in the understanding of the aquatic toxicity of the flocculant WF 424 and the coagulant WF 2000 PCA.

2. Materials and Methods

2.1. Chemicals tested

The flocculant WF424 was obtained from WaterFlows Bioquímica do Brasil . CAS: 31212-13-2; poly(acrylic acid-co-acrylamide). Polyacrylamides (PAMs) belong to a large family of synthetic organic polyelectrolytes and, because of their high molecular weight, they make relatively dilute solutions of PAMs highly viscous. Some important physical and chemical characteristics are: High molecular weight relative to most other polymer types, between 4 and 30 million, pH in solution 0.5% weight between 4.0 and 9.0, and residual acrylamide monomer levels no greater than 0.05 percent by weight of the active polymer content (AWWA, 2015, B453-13 Polyacrylamide).

The coagulant WF 2000 PCA was obtained from WaterFlows Bioquímica do Brasil, CAS: 1327-41-9, with the empirical formula $Al_n(OH)_mCl3_{m-n}$. The polyaluminum chloride content is from 16 to 18 percent by weight expressed as Al_2O_3. The percent basicity of the sample can be calculated using the values of alkalinity (OH %) and aluminum (Al %), with 38 percent as the minimum concentration. Other important physical and chemical characteristics are: turbidity (NTU) less than 50, pH in solution 1% in weight between 3.50 and 5.50 and density ($g.cm^{-3}$) between 1.33 and 1.40 (AWWA, 2018, B408-18 Liquid polyaluminum chloride).

2.2. Fish Embryo-toxicity Test (FET)

Zebrafish were maintained in tanks with reverse osmosis and activated carbon filtered water and raised in an facility (ZebTec - Tecniplast, Varese, Italy) with a photoperiod cycle of 12:12h (light:dark) at the laboratory of Toxicologic Genetics at University of Brasilia (Brazil). The water parameters were strictly controlled: temperature was maintained at 27.0 ± 1ºC, conductivity at 740 ± 100 µS/cm, pH at 7.0 ± 0.5 and dissolved oxygen ≥ 95% saturation. Zebrafish embryos were collected immediately after natural mating, rinsed in water, and checked under a stereomicroscope (Stereoscopic Zoom Microscope – Stemi 2000, Zeiss, Germany). The unfertilized eggs and those showing cleavage irregularities or injuries were discarded. Fish embryo toxicity test was based on the OECD guideline Protocol 236 "Fish Embryo Toxicity" (FET) test (OECD, 2013). Zebrafish embryos were exposed to seven graded concentrations of the WF2000 PCA, after pH adjustment for 7.2 with TRIS-buffer (Tris-Hydroxymethyl aminomethane CAS 77-86-1, tested alone at concentration of 183 mg/L) at levels of 0.0; 7.81; 15.62; 31.25; 62.50; 125.0; 250.0 and 500.0 mg/L, prepared by successive dilutions of stock solution. WF424 was tested at concentration levels of 0.0; 1.0; 10.0; 100.0 and 1000.0 mg/L, also prepared by successive dilutions of stock solution at pH of 7.2. The test was performed using 60 eggs per treatment, divided in 3 replicates, selected and distributed in 24-well microplates in climate chamber (SL-24 Solab Científica, Brazil), 20 wells were filled with 2 mL of the test solution and four wells with water (internal plate control, as required in the OECD guideline). The test was initiated immediately after fertilization and continued for 96 h. Embryos were observed daily under a stereomicroscope. Developmental parameters were evaluated in embryos over the test period using a magnification of × 70 for eggs and × 40 for hatched embryos. Before hatching, the following parameters were evaluated: egg coagulation, otolith formation, general delay in development, eye and body pigmentation, somites formation, heartbeat, edemas, detachment of the tail-bud from the yolk sac, yolk sac absorption and hatching. All parameters were assessed and quantified as observed or not observed. The FET-test with zebrafish embryos was approved by the Animal Ethics Committee of University of Brasilia, protocol n. 100226/2014.

2.3. Statistical analyses

A one-way ANOVA was used to detect the differences between the groups for normally distributed data sets. When data did not pass the Kolmogorov–Smirnov normality test and Levene's homogeneity of variance test, a Kruskal–Wallis test was performed. If significant results were found, either Dunnett's or Dunn's test (for parametric or non-parametric data, respectively) was used to detect significant differences between the tested concentrations and the control ($p < 0.05$). All analyses were performed using the Sigma Stat 3.5 statistical package.

3. Results

During the 96 h of test, no significant mortality was observed for the control groups considering both treatment groups. Additionally, control groups showed normal development where the hatching rate and survival rates were above 90%, as described by Kimmel et al. (1995) and recommended by the OECD 236 protocol.

After 96 h of exposure for WF424, there were no significant lethal (mortality) or sublethal effects such as hatching delay, heartbeat alteration

and malformation in embryonic development, when compared with control group ($p > 0.05$). The maximum mortality was 2% for the entire test period (Figure 1). In addition, the control group (water) presented normal development as described by Kimmel et al. (1995). The LC50 was estimated above the highest concentration tested (1000 mg/L). On the last day of exposure, it was observed that approximately 10% of the organisms exposed to the concentration of 1000 mg/L presented alteration in the balance (behavior change). However, there were no statistical differences when compared to the control group ($p > 0.05$).

An overview of the embryotoxicity test with the coagulant compound WF2000 PCA did not show lethal effects during 96 h of exposure (Figure 2).

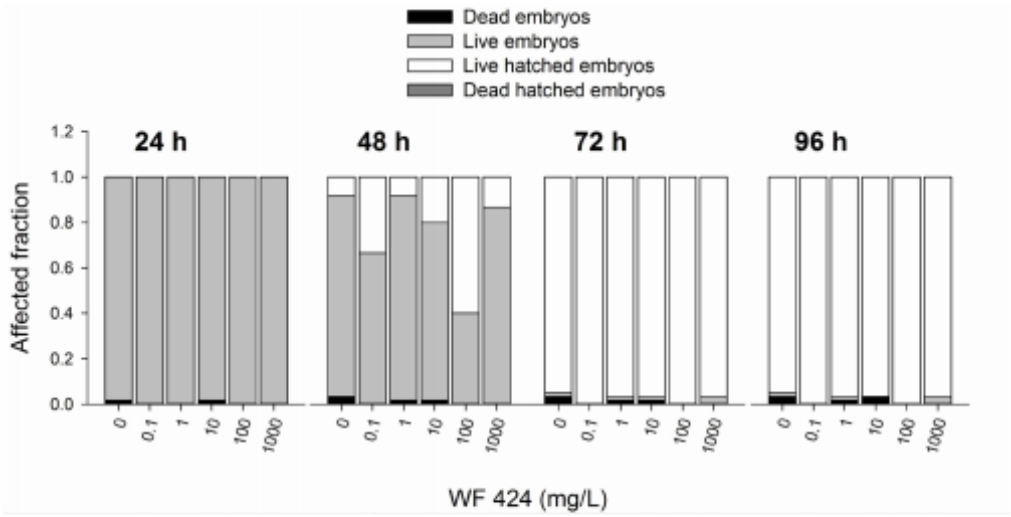

Figure 1. Overview of zebrafish embryo toxicity test after 96 h of exposure to WF424. The proportion of eggs and non-hatched embryos that died are represented by black bars; the proportion of embryos that stayed alive but did not hatch are presented as grey bars; those that hatched as white bars and the proportion of embryos that died after hatching as spotted, dark dashed grey bars.

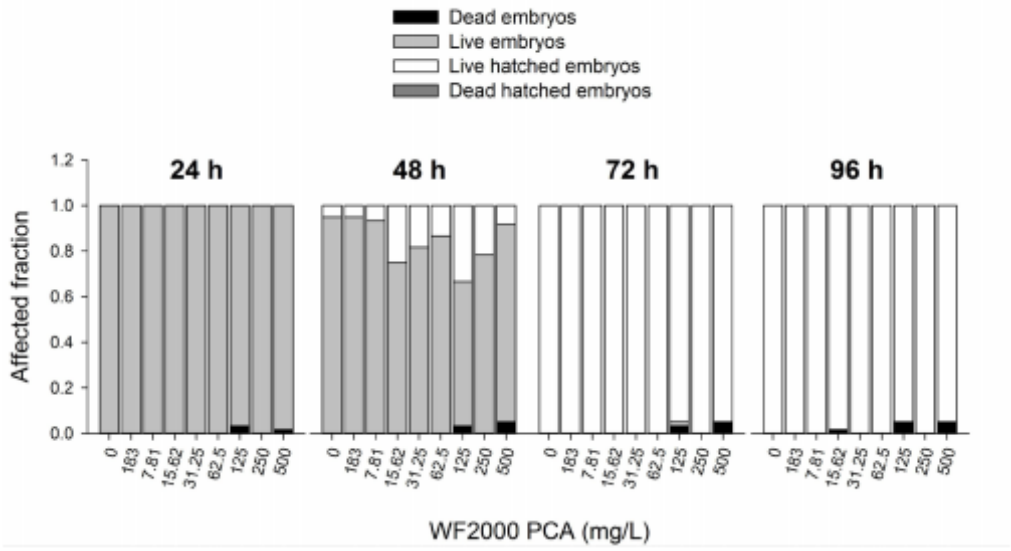

Figure 2. showing an overview of zebrafish embryo toxicity test after 96 h of exposure to WF 2000 PCA. The proportion of eggs and non-hatched embryos that died are represented by black bars; the proportion of embryos that stayed alive but did not hatch are presented as grey bars; those that hatched as white bars and the proportion of embryos that died after hatching as spotted, dark dashed grey bars.

The LC50 was determined as being above the highest tested concentration levels of 500 mg/L. It was not possible to determine the effective concentration (EC50) for any sublethal parameter analyzed, such as changes in balance, hatching, heartbeat and embryonic development. Therefore, EC50 was considered also as above the highest concentration level tested.

4. Discussion

The literature has shown that there are some sublethal and lethal effects of aluminum at different concentration ranges. García-Medina et al. (2010) studied the oxidative stress induced by aluminum in common carp lymphocytes (*Cyprinus carpio*), and they found significant effects at concentrations of 120-239 mg/L. Griffitt (2018) studied the toxicological effects of metal nanoparticles of aluminum on zebrafish adults and juveniles, and they estimated a LC50 above 10 mg/L. Lee (2014), when evaluating a zebrafish transgenic lineage (huORFZ), determined a LC90 of 34.53 mg/L for aluminum. Dave (1985) evaluated the influence of pH on aluminum toxicity, and determined a LC50 of 80-106 mg/L for zebrafish. In our results with WF 2000 PCA, the LC50 was estimated at over 500 mg/L, which demonstrated low toxicological risks to the aquatic environment. Also, no malformation or developmental delay occurred in zebrafish embryos.

In a search in the database of the US Environmental Protection Agency using the keyword polyacrylamide, we did not find studies showing lethal and sublethal effects on aquatic organisms. Acharya et al. (2010) studied physiological responses in *Daphnia magna* exposed to Linear Anionic Polyacrylamide, in which they determined the acute LC50 at 152 mg/L. In order to evaluate the acute toxicity of acrylamide to non-target organisms (macroinvertebrates and fish), through determination of LC50 values, Krautter et al. (1986) found: *Daphnia magna* = 160 mg/L; *Paratanytarsus parthenogenetica* = 410 mg/L; *Salmo gairdneri* = 110 mg/L; *Pimephales promelas* = 120 mg/L; *Lepomis macrochirus* = 100 mg/L. Finally, Hall & Mirenda (1991), evaluating the acute toxicity of 34 acrylamide polymers to *Daphnia pulex* and the fish *Pimephales promela*, observed that the chemical composition of the polymers is the main factor that controls the toxicity.

In addition, the molecular weight of the polymers should not be correlated with toxicity. This makes it difficult to establish a toxicity pattern. Thus, specific studies are required for each molecule of interest. No studies were found with zebrafish (*Danio rerio*) for comparative purposes. The determination of the EC50 for sublethal measured parameters, such as changes in balance, hatching, heartbeat and embryonic development, was not possible due to the low toxicity of the tested compound. In fact, EC50 is also above the highest tested concentration. In conclusion, results of the embryotoxicity test showed that the flocculant compound WF 424 presented low acute toxicity to zebrafish embryos (*Danio rerio*). Thus, because the LC50 (mortality) and EC50 were above 1000 mg/L, this compound does indeed represent a low risk to aquatic organisms. When compared with concentration ranges in the literature, the flocculant WF424 was tested at higher concentration levels than observed in other studies, and some toxicity occurred only at the highest exposure level of 1000 mg/L, which does not occur in the remediation processes. The coagulant compound WF2000 PCA, with a LC50 over 500 mg/L, also showed low risks to the environment. If used in accordance with the manufacturer's recommendations, neither compound causes damage to the aquatic environment.

In conclusion, these chemical compounds could have occasional toxicity at higher concentrations, differently from when used in the remediation of leaching from mining. These products can be considered as low toxicity to the zebrafish embryos. Once they can have commercial multiple uses, studies with species from different trophic levels should be carried out. Therefore, the management of the remediation processes must be under user control, especially when the water body receptor receives this effluent, and mainly when this water is used for human supply. The user must always be aware of the parameters established by the regulatory agencies. When working with remediators, we must always keep in mind the cost-benefit relationship for comparing the risks, human exposure and impacts on aquatic ecosystems.

Acknowledgements

This study was supported by the University of Brasilia, the Brazilian Research Council (CNPq, grant n. 305741/2015-2 and n. 310641/2017-9) and WaterFlows Bioquímica do Brasil. The authors declare that they have no conflict of interests.

References

ACHARYA, K., SCHULMAN, C. and YOUNG, M.H. Physiological response of daphnia magna to linear anionic polyacrylamide: Ecological implications for receiving waters. *Water, Air, and Soil Pollution*, 2010, 212, 309-317.

ALBUQUERQUE, L. B., ALONSO, A.M., AQUINO, F.G., REATTO, A., SOUSA-SILVA, J.C., LIMA, G.E.F.W. & SOUSA, E.D.S. *Restauração ecológica de matas ripárias: uma questão de sustentabilidade*. Planaltina: Embrapa, 2010. Embrapa Cerrados, no. 75.

ALLAN, J.D. and CASTILLO, M.M. *Stream ecology: structure and function of running waters*. 2nd ed. Dordrecht: Springer, 2007.

AMERICAN WATER WORKS ASSOCIATION – AWWA. *B453-13 polyacrylamide*. Denver: AWWA, 2015.

AMERICAN WATER WORKS ASSOCIATION – AWWA. *B408-18 liquid polyaluminum chloride*. Denver: AWWA, 2018.

ASSOCIAÇÃO BRASILEIRA DE NORMAS TÉCNICAS – ABNT. *NBR 16488 – polyaluminum chloride (PAC) – 2016. Drinking water and wastewater treatment purposes – Technical especification, sampling and test methods*. Rio de Janeiro: ABNT, 2016.

CALLISTO, M., GONÇALVES, J.F. and LIGEIRO, R. Water resources in the rupestrian grasslands of the espinhaço mountains. In: G. W. FERNANDES, editor. *Ecology and conservation of mountaintop grasslands in Brazil*. Cham: Springer International Publishing, 2016, pp. 87-102.

DAVE, G. The Influence of pH on the Toxicity of aluminum, cadmium, and iron to eggs and larvae of the Zebrafish, *Brachydanio rerio*. *Ecotoxicology and Environmental Safety*, 1985, 10, 253-267.

DIAS, B. Biodiversidade, porque importa! *Revista Cause*, 2017, 5, 94-100.

DUDGEON, D., ARTHINGTON, A.H., GESSNER, M.O., KAWABATA, Z., KNOWLER, D.J., LEVEQUE, C., NAIMAN, R.J., PRIEUR-RICHARD, A.H., SOTO, D., STIASSNY, M.L. and SULLIVAN, C.A. Freshwater biodiversity: importance, threats, status and conservation challenges. *Biological Reviews of the Cambridge Philosophical Society*, 2006, 81, 163-182.

EUROPEAN UNION – EU. Directive 2010/63/EU of the European Parliament of the Council of 22 September 2010 on the protection of animals used for scientific purposes. *Official Journal of the European Union*, Strasbourg, 22 sep. 2010, pp. L 276/33-L 276/79.

GARCÍA-MEDINA, S., RAZO-ESTRADA, A.C., GÓMEZ-OLIVÁN, L.M., AMAYA-CHÁVEZ, A., MADRIGAL-BUJAIDAR, E. and GALAR-MARTÍNEZ, M. Aluminum-induced oxidative stress in lymphocytes of common carp Cyprinus carpio. *Fish Physiology and Biochemistry*, 2010, 36(4), 875-882. http://dx.doi.org/10.1007/s10695-009-9363-1. PMid:19866366.

GRIFFITT, R.J. Effects of particle composition and species on toxicity of metallic nanomaterials in aquatic organisms. *Environmental Toxicology and Chemistry*, 2018, 27, 1972-1978.

HALL, W.S. and MIRENDA, R.J. Acute toxicity of wastewater treatment polymers to Daphnia pulex and the fathead minnow (Pimephales promelas) and the effects of humic acid on polymer toxicity. *Research Journal of the Water Pollution Control Federation*, 1991, 63, 895-899.

HEPP, L.U. and GONÇALVES JUNIOR, J.F. A decomposição de detritos em riachos como serviço ecossistêmico de regulação e suporte prestado pela natureza. In: L. M. PARRON, R. GARCIA JUNIOR, E. B. OLIVEIRA, G. G. BROWN, R. B. PRADO, org. *Serviços ambientais em sistemas agrícolas e florestais do bioma Mata Atlântica*. Brasília: EMBRAPA, 2015, pp. 226-233. vol. 3.

HONDA, E.A. and DURIGAN, G. A restauração de ecossistemas e a produção de água. *Hoehnea*, 2017, 44, 315-327.

KIMMEL, C.B., BALLARD, W.W., KIMMEL, S.R., ULMAN, B. and SCHILLING, T.F. Stages of embryonic development of the zebrafish. *Developmental Dynamics*, 1995, 203, 253-310.

KRAUTTER, G.R., MAST, R.W., ALEXANDER, H.C., WOLF, C.H., FRIEDMAN, M.A., KOSCHIER, F.J. and THOMPSON, C.M. Acute toxicity tests with acrylamide monomer and macroinvertebrates and fish. *Environmental Toxicology and Chemistry*, 1986, 5(4), 373-377. http://dx.doi.org/10.1002/etc.5620050406.

LAMMER, E., CARR, G.J., WENDLER, K., RAWLINGS, J.M., BELANGER, S.E. and BRAUNBECK, T. Is the fish embryo toxicity test (FET) with the zebrafish (Danio rerio) a potential alternative for the fish acute toxicity test? *Comp. Biochem. Physiol. Part C Toxicol. Pharmacol.*, 2009, 149, 196-209.

LEE, H.-C. Zebrafish transgenic line is an effective living bioindicator for detecting environmental toxicants. *PLoS One*, 2014, 9(3), e90160. http://dx.doi.org/10.1371/journal.pone.0090160.

ORGANIZAÇÃO PARA A COOPERAÇÃO E DESENVOLVIMENTO ECONÓMICO – OECD. *Test no. 236: Fish Embryo Acute Toxicity Test (FET)*. Paris: OECD, 2013, 22 p.

SUSAYA, J., KIM, K.-H. and JUNG, M.C. The impact of mining activities in alteration of ss levels in the surrounding ecosystems: an encompassing risk assessment and evaluation of remediation strategies. *Journal of Hazardous Materials*, 2010, 182, 427-438.

WANG, C., ALPATOVA, A., MCPHEDRAN, K.N. and GAMAL EL-DIN, M. Coagulation/flocculation process with polyaluminum chloride for the remediation of oil sands process-affected water: performance and mechanism study. *Journal of Environmental Management*, 2015, 160(1), 254-262. http://dx.doi.org/10.1016/j.jenvman.2015.06.025. PMid:26119332.

WRIGHT, D.A. and WELBOURN, P. *Environmental toxicology*. Cambridge: Cambridge University Press, 2002. Recovery, rehabilitation, and reclamation, pp. 520-535. https://doi.org/10.1017/CBO9780511805998.

Received: 09 December 2018
Accepted: 08 March 2019

Declaração da comissão de ética no uso animal do instituto de ciências biológicas da universidade de Brasília –UnB, protocolo nº100226/2014.

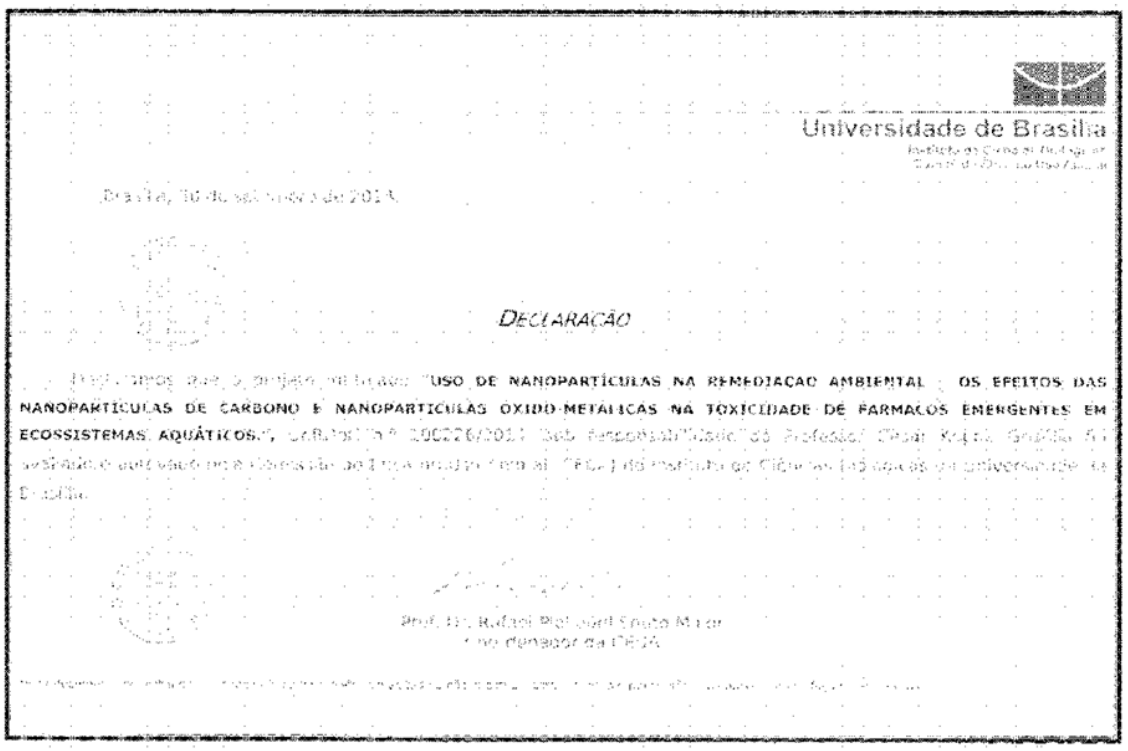

Universidade de Brasília

Brasília, [illegible] de 2014.

DECLARAÇÃO

[illegible] o projeto intitulado "USO DE NANOPARTÍCULAS NA REMEDIAÇÃO AMBIENTAL : OS EFEITOS DAS NANOPARTÍCULAS DE CARBONO E NANOPARTÍCULAS ÓXIDO-METÁLICAS NA TOXICIDADE DE FÁRMACOS EMERGENTES EM ECOSSISTEMAS AQUÁTICOS.", [illegible] sob responsabilidade do Professor [illegible] está [illegible] Comissão de Ética no Uso Animal (CEUA) do Instituto de Ciências Biológicas da Universidade de Brasília.

Prof. Dr. Rafael Rios Vicente Mello
Coordenador da CEUA